UNIVERSITY OF OKLAHOMA

GRADUATE COLLEGE

DEEPWATER SEDIMENTARY PROCESSES IN AN ACTIVE MARGIN, MAGDALENA SUBMARINE FAN, OFFSHORE COLOMBIA

A DISSERTATION

SUBMITTED TO THE GRADUATE FACULTY

in partial fulfillment of the requirements for the

Degree of

DOCTOR OF PHILOSOPHY

By

GLORIA AMPARO ROMERO OTERO
Norman, Oklahoma
2009

Downloaded from SHAREOK. Persistent Handle URL: https://hdl.handle.net/11244/319039

DEEPWATER SEDIMENTARY PROCESSES IN AN ACTIVE MARGIN, MAGDALENA SUBMARINE FAN, OFFSHORE COLOMBIA

A DISSERTATION APPROVED FOR THE
CONOCOPHILLIPS SCHOOL OF GEOLOGY AND GEOPHYSICS

BY

Dr. Roger M. Slatt, Chair

Dr. Carlos Pirmez

Dr. Kurt Marfurt

Dr. Shankar Mitra

Dr. May Yuan

© Copyright by GLORIA AMPARO ROMERO OTERO 2009
All Rights Reserved.

To my family

ACKNOWLEDGEMENTS

This work was possible thanks to the generous support of different institutions that facilitated the use of proprietary data. I would like to thank Ecopetrol for providing the seismic and Bahia–Sinú bathymetry data, the Institut de Ciències del Mar-CSIC for allowing the use of the proprietary bathymetry; and the Centro de Investigaciones Oceanográficas e Hidrográficas de Colombia *(*CIOH) for providing complementary bathymetry surveys. Additional data used during this project was financed by the US-NSF grants OCE8901848 and OCE9712079. The ConocoPhillips School of Geology and Geophysics provided the financial support through research and teaching assistantships during the project length. Seismic Micro Technology and ESRI provided the educational software licenses to the University of Oklahoma.

The faculty and staff from the ConocoPhillips School of Geology and Geophysics at the University of Oklahoma have helped me through all these years and I would like to recognize their work and dedication. Also, I would like to express my gratitude to Dr. May Yuan, Dr. Kurt Marfurt, Dr. Shankar Mitra and Dr. Carlos Pirmez for their commitment to be part of my Ph.D. committee and their helpful reviews. Especially, I would like to express my

gratitude to Dr Carlos Pirmez for his dedication and enthusiasm with the project, numerous ideas and helpful discussions.

I can not describe the profound admiration and gratitude that I have for Dr. Roger Slatt. It was an honor to work with him throughout my graduate studies, he was not only my advisor, but also my mentor during this time. I am very grateful for all his dedication, help and support. This project has only been completed thanks to him. He believed in me and on my interest to give a little contribution to the knowledge of the geology of Colombia.

Many people have crossed my life; some of them have stayed and shared the path with me. I would like to thank all my friends, there have always been somebody helping me to standup and continue my journey. I would like to thank especially Andrea Miceli and Gustavo Diaz for their support during the last months; afternoons without coffee are not the same.

I could not have accomplished this without the support of my family. They have been and will always be the inspiration and the reason to continue pursuing my dreams.

TABLE OF CONTENTS

ACKNOWLEDGMENTS…..……..……iv
LIST OF TABLES..... ix
LIST OF FIGURES x
ABSTRACT..... xxi
CHAPTER 1.....1
1.1 Objectives 1
1.2 Research Hypothesis.....2
1.3 Importance.....7
1.4 Thesis Outline 9
1.4.1 Chapter 2. Evolution of the Magdalena deepwater fan in a tectonically active setting, offshore Colombia.....9
1.4.2 Chapter 3. Active sedimentation and submarine cable breaks on the Magdalena deepwater fan, Colombia: linkages with shallow water processes as starting point for turbidite flows. 11
1.4.3 Chapter 4. Mass transport complexes on the Magdalena deepwater fan: possible timing and causal mechanisms.....12
1.4.4 Chapter 5. Integration of results.....13
1.4.5 Chapter 6. Conclusions.....13
CHAPTER 2.....14
Evolution of the Magdalena deepwater fan in a tectonically active setting, offshore Colombia 14
Abstract :.....14
2.1 Introduction 15
2.1.1 Geological Setting.....18
2.1.2 Magdalena River History.....22
2.1.3 Deepwater Fan Deposits 25
2.2 Data and Methods.....27
2.3 Area Physiography.....29
2.4 Channel levee complexes.....32
2.4.1 CLC- IV 32
2.4.2 CLC III.....40
2.4.3 CLC II.....44
2.4.4 CLC IIa and CLC IIb.....47
2.4.5 CLC-IIc.....49
2.4.6 CLC-I 56
2.4.7 Active Magdalena Fan 61
2.5 Knickpoints.....64
2.6 Magdalena River Delta Phases – Submarine Fan Migration 67
2.6.1 Phase Ea 70
2.6.2 Phase Eb 70
2.6.3 Phase D 71

2.6.4 Phase C 71
2.6.5 Phase B 72
2.6.6 Phase A 73
2.7 Discussion 74
2.7.1 Degradation Processes on the Channel Systems 74
2.7.2 Influence of Tectonics on the Magdalena Deepwater Fan 77
2.7.3 Initiation of Channel Levee Systems 93
2.8 Significance for Hydrocarbon Exploration 98
2.9 Conclusions 99
2.10 Acknowledgements 102
CHAPTER 3 103
Active sedimentation and Submarine cable breaks on the Magdalena deepwater fan, Colombia: linkages with shallow water processes as starting point for sediment gravity flows. 103
Abstract 103
3.1 Introduction 105
3.1.1 Regional Setting 109
3.1.2 Data and Methodology 112
3.2 Morphology of the active fan area 115
3.2.1 Canyons 115
3.2.2 Piggyback basins 118
3.2.3 Mass transport complexes 122
3.3 Cable breaks 124
3.4 GLORIA Image 127
3.5 Flow pathways and distribution of cable breaks 130
3.5.1 Active Magdalena Canyon 131
3.5.2 Delta west 132
3.5.3 Delta East 134
3.5.4 Aguja Canyon 136
3.6 Sediment distribution – Piston cores. 136
3.7 Piston Cores Interpretation 143
3.8 Discussion 146
3.8.1 River sediment discharge and flood stages -cable breaks 146
3.8.2 Hyperpycnites in the Magdalena Fan? 150
3.8.3 Shallow Processes 154
3.8.4 MTC-1 and Interaction of turbidity flows 162
3.8.5 Origin of the 1935b Cable break 163
3.8.6 Recurrence of sediment gravity flows 164
3.8.7 Similar depositional settings 166
3.8.8 Slope deposition 167
3.8.9 Importance 168
3.9 Summary and conclusions 169
3.10 Acknowledgements 171
CHAPTER 4 173

Detached and shelf–attached mass transport complexes on the Magdalena deepwater fan 173
Abstract 173
4.1 Introduction 174
4.1.1Regional Setting 175
4.1.2 Data and Methods 181
4.2 Location and characteristics of MTCs 183
4.2.1 Thrust deformed belts MTCs 183
4.2.2 Channel walls and levees MTCs 189
4.2.3 Interchannel lows MTCs 189
4.3 Types of MTCs 194
4.3.1 Detached MTCs 194
4.3.2 Shelf Attached MTC 198
4.3.3 Other Causal Mechanisms 200
4.3.4 Possible Timing of Events 203
4.4 Conclusions 206
4.5 Acknowledgments 207
CHAPTER 5 208
Integration of Results 208
5.1 Fan Deformation 208
5.2 Deepwater sedimentation: 211
5.3 Magdalena fan depositional styles 213
5.4 Limitations 217
5.5 Future Work 218
CHAPTER 6 221
CONCLUSIONS 221
REFERENCES 228
APPEDIX 1 241
CORE DESCRIPTION 241
Core location 241
APPENDIX 2 279
Flows calculations following Mulder and Syvitski (1995) methodology. 279
APPENDIX 3 280
Curvature on Seafloor bathymetry 280

LIST OF TABLES

Table 2.1. Morphometric measurements of main channel systems. * Due to the advanced degradation stage these values where collected at the most preserved interval. …….35

Table 2.2. Summary of Evolution of the Magdalena fan…….……...68

Table 2.3. High sinuosity values on the literature……..…89

Table 3.1. Cable Breaks Events (Modified from Heezen,1956)……..…126

Table 3. 2. Magdalena River flood concentrations, calculated for different periods of high water discharge. (Q) water discharge, (Qs) sediment load, Css average suspended particle concentration values. (Qflood) maximum flood discharge. (Cflood) maximum flood concentration in suspended particles. Cflood is always below the concentration threshold Cc =36.25 kg m^{-3} (Mulder &Syvitski, 1995). But if other conditions are considered where Cc could be as low as 5 kg m^{-3} , then the Magdalena fan is likely to produce hyperpycnal flows. (see Appendix 2) ……..…….153

Table 4.1. Classification, causal mechanisms, and source areas of MTCs (Moscardelli and Wood,2008)……..…….176

Table 4.2. Morphometry of main scarps on the deformation fronts. Location is shown in figures 4.2 and 4.3……..184

Table 4.3. Magdalena Fan MTCs classification (base on Moscardelli and Wood, 2008)……194

LIST OF FIGURES

Figure 1.1. Breen (1984) model of the effects of sedimentation on the geometry of a convergent margin. ……...2

Figure 1.2. Main morphologic features of northern Colombia and Magdalena fan area. ……..…..3

Figure 1.3. Migration of the deformation point due to the decrease in the slope of the upper plate in a convergent margin. (Breen, 1989)……. 4

Figure 1.4. Comparison of major submarine fan systems (Modified from Kendall and Haughton, 2006……..8

Figure 2.1. Bathymetry map of the Magdalena fan, southern Caribbean Sea. Location of the channel-levee complexes (CLC) and active fan. Canyons: U (Unnamed), S (Sabanilla), M (Magdalena); D (Delta front gullies), SB (Shelf Break). Regional cross sections X-X', Y-Y' shown in figure 7 and location of figures 9b, 10b, 12a, 17a and 19a. Multibeam Bathymetry –Slope of the bathymetry. Cities of Cartagena, Luruaco and Barranquilla are shown as a reference. ……..…….17

Figure 2.2. Major structural elements. Magdalena fan is characterized by the presence of two deformation belts that correspond to the Sinu fold belt initiated during the Miocene, that are separated by the main fan deposition. Deeper structures seem to be the continuation of the thrust growth out of the southwestern thrust belt. The presence of the Canoas Fault (C?) could not be confirmed with the available data……..20

Figure 2.3. Magdalena River course shifts from the Pliocene to present day location. Relative order of delta phases: E, D, C, B and A. Note the presence of the La Popa coralline limestone near Barranquilla that support the southward shift of the drainage (Reyes, 2001). Cities of Cartagena, Luruaco and Barranquilla are shown as a reference.…….……24

Figure 2.4. Architectural elements of the Magdalena fan. (Modified from Ercilla et al., 2002). Northeastern and southwestern deformation belts are the boundaries of the CLC studied. Also is important to notice the presence of MTCs located at the interchannel system lows. ……..……26

Figure 2.5. Slope variations of the fan. Upper left, division of the slope: (US) Upper Slope, (MS) Middle slope, (LS) Lower slope. Upper right, slope map

(0-5 degrees, values >5 excluded). Lower. Profiles for the western, central and eastern areas.(SB) Shelf Break. Western profile exhibit very rough morphology and lower slope angles. Central profile is very smooth by the presence of a MTC at the interchannel low. Eastern profile show the modification of the slope by the thrust deformed belt, creating piggyback basins (low angles) separated by thrust formed ridges. ……..30

Figure 2.6. A. Seismic line RMS Charles Darwin expedition CD40a in 1987 (Lower Fan) (Pirmez et al., 1990). B. Bathymetry profile through the middle slope. The CLC are older towards the west, with exception of CLC I that is the youngest complex in the fan.……..……...33

Figure 2.7.Thalweg profiles for the Magdalena fan. All the channels are referenced to the break of the slope at (60m bsl) to have a better comparison of the slope changes. Note that western thalwegs are deeper and with higher gradients at the upper slope. The profiles are ordered from young (upper) to old (lower). ……..……..…..33

Figure 2.8. Channel profiles. Measured every 5 km of thalweg length. Vertical scale depth (below sea level) Note the change in the morphology of the conduit the upper 1000 m bsl. Increase in sinuosity and lower slopes is shown by the decrease of space between the profiles in the deeper sections.…….……36

Figure 2.9. A. Thalweg profile of the remnants. Note lower profile of IVa and the convex up profile of IVb and IVc at 80km. The difference in thalweg depth corroborates that V remnant correspond to an older system. B. Main channel systems of IV in map view. Note how IVd and IVe are cannibalizing and covering the previous systems. Bathymetry map (curvature and slope) referenced to the general context Figure 2.1……..38

Figure 2.9. C. A-A' Seismic profile perpendicular to the flow direction. IVe and IVd thalwegs are covering older channel systems. Levees (Yellow), Channels (Pink), MTC (red)…….…….39

Figure 2.10. A. Thalweg profile of CLC III. The westward migration and the deepening of the thalwegs as it is getting younger. IIIa, IIIb, IIIb2, IIIb3, IIIc, IIIc1, IIId (Youngest). Note the convex up profile of IIIb and really steep gradients for the first 80km. B. Main channel systems of III in map view. Bathymetry map (Curvature and Slope). Reference to the general context in Figure 2.1. Upper slope is characterized by avulsion points. Also note how the central MTC is cutting the eastern side of the channel systems. …….…42

Figure 2.10. C. B-B' Seismic profile perpendicular to the flow direction. IIIa morphology is completely covered by later sedimentation. Eastern levee of IIId is completely modified by the erosion of Central MTC. Levees (Yellow), Channels (Pink), MTC (red). …….....43

Figure 2.11. A. CLC II in map view. Bathymetry map (Curvature and Slope). Note how younger down slope flows are modifying the morphology of the system. B. MTCs that are modifying the slope morphology (Slope of bathymetry map). ……..…45

Figure 2.11.C. C-C' Seismic profile perpendicular to the flow direction. II buried morphology describe a probably sinuous channel system completely modified by post abandonment flows. Compare the size relationship between CLC I and II on Figure 2.6 A. Levees (Yellow), Channels (Pink).…….46

Figure 2.12 A. Location of CLC IIa, IIb, and IIc. Bathymetry map (Curvature and Slope). Referenced to the general context in Figure 2.1. IIa increases sinuosity downslope, with marked bend toward the west. IIb lower sinuosity than older CLC IIa. B. D-D' Seismic profile perpendicular to the flow direction. Clearly depicts the relative age of the different systems being IIc4 the youngest, between the three. IIa and IIb thalwegs are filled and morphology seems to be modified. Levees (Yellow), Channels (Pink), MTC (red), Base of channels (blue). Arrow indicates the erosive character of the flows going downslope. ……..…..48

Figure 2.12 C. Thalweg profile for IIa and IIb. Black arrows in IIa profile are indicating areas of the channel (pink arrows) that have been modified by later flows. CLC IIb profile exhibits a concave up section that corresponds which is indication on the map. ……...50

Figure 2.13. Thalweg profile of CLC IIc. IIc1, IIc2, IIc3, IIc4, IIc5 (Youngest) (Location of the channels Figure 2.12A). IIc1 shows an abrupt change in the profile due to later establishment of IIc3. The remnants of IIc2 exhibit a convex up profile at the encountering with IIc3 (Black arrow), which is also evident at IIc3. Note the convex up profile of IIc4 (Pink arrow) about 50 km, which may indicate deformation. Notice the fairly steep gradients of IIc5. ……..51

Figure 2.14. Series of seismic profiles showing the changes in morphology of CLS IIc4. Upper slope- erosional architecture (a,b,c) and Middle to lower slope-aggradational morphology (d,e,f). HARS are observed on the channel thalweg (d,e). C and E shows evidences of later slope deformation since the channel wedge is tilted. ……..53

Figure 2.15. A. Thalweg profile for IIc4. B. Slope angle and sinuosity values for IIc4 thalweg. The overall slope tendency is to decrease down slope in the erosional upper section. But changes drastically in agradational lower section. The sinuosity values are high at the steep segments of the channel. ……..……54

Figure 2.16. Channel system IIc4. Increase in sinuosity is observed to accommodate changes in the slope. a and b are showing the slope of near by areas and b is showing the thalweg profile. Additionally a series of cut-offs loops are observed in this segment (yellow dashed lines) ……..……55

Figure 2.17. A. CLC I in map view. Bathymetry map (Curvature and Slope). Note how younger downslope flows are modifying the morphology of the northern levee/overbank. Referenced to the general context in figure 1. B. Azimuth map displaying the wave field at the southern levee/overbank of CLC I. Arrows are parallel to the two main directions…….……57

Figure 2.17.C. Seismic profiles showing the changes in morphology of CLS I down slope. HARS are observed on the channel thalweg. (Location of seismic profiles Figure 2.17A)…….....58

Figure 2.18. A. Thalweg profile for I, overall concave up, but with some local convex up sections (e.g. 40km). It is also displaying the profile of the conduits jointing the knickpoints in Figure 2.21. B. Slope and sinuosity values for I Thalweg. The overall slope tendency is to decrease in angle down slope, with some sections of steeper slopes. The sinuosity higher values coincide with these steep segments of the channel. ……..……60

Figure 2.19. A. Active Fan bathymetry map. Referenced to the general context in Figure 2.1. B. Canyon profiles measured every 5 km. Vertical scale depth (below sea level). Sabanilla canyon change its morphology once reaches the low section of the slope (piggyback basin). Magdalena canyon describes a wider channel with an entrenched thalweg. Arcuate scarps and creeping can be observed in the canyon walls. East of the Magdalena canyons channel/ gullies and mass transport complexes are observed. C. Canyon thalweg profiles. Active Magdalena canyon depicts a fairly smooth profile with some area where is convex up (Ridges sections). Sabanilla and the U canyon profiles are parallel. ……..……62

Figure 2.19. C. Canyon thalweg profiles. Active Magdalena canyon depicts a fairly smooth profile with some area where is convex up (Ridges sections). Sabanilla and the U canyon profiles are parallel……..63

Figure 2.20. Knickpoint sequence. 3D bathymetry of the western deformed belt area. A series of knickpoints on the slope are located in areas with abrupt changes (steps) followed by low gradient areas. Lobate shapes at the toe of the knickpoints. Some of these lobes present erosional cuts. IIc6 conduit seems to be connecting all the knickpoints through the slope. Upper figures are the frontal view of the knickpoints (blue arrow). It is important to notice the sinuous morphology that KP2 exhibit. The steps on the slope coincide with IIc4 higher sinuosity zones (yellow lines). Profile of the knickpoints (IIc6) is shown in Figure 2.18A…..……..66

Figure 2.21. Evolution of the Magdalena fan, A. Early to middle Pleistocene produce phase Ea (CLC IV) and Eb (CLC III), B. middle Pleistocene produce phase D., C. late Pleistocene phase Ca, Cb, C. D. Holocene produces phase B and phase A (Active fan)……...69

Figure 2.22. Degradation of the Channels A. Arcuate scarps at the walls of the channel (yellow). The channel was affected by the thrust imbricates (parallel to the ridges) becoming beheaded (Blue arrow) and creating a new channel course (red arrow). B. Major scarp (yellow arrows) located at the northern levee of CLC I. The scarp was connected to an older canyon downslope……..…….75

Figure 2.23. Major fold axis and alignment of knickpoints and channel bends on the southwestern fan. Continuous black lines are folds associated with thrust imbricates with seafloor expression. Dashed black lines are deeper fold geometries. Red dotted lines are possible faults. Knickpoint are highlighted with blue arrows……..……..76

Figure 2.24. A. Western fan underlying deformation. Thrust faults, related fold and normal faults seem to be playing an important role in the development of high sinuosity channels. ……..79

Figure 2.24. B. Central Fan, no major deformation is observed. Levees (Yellow), channels (pink), canyons (orange), channel-levee system base (blue). …….....80

Figure 2.25. A. Slope angle changes through the slope measured for each channel system. All distances are referenced to the shelf break. The dashed line indicates a decreasing the gradient with distance (basinward), but there are many points that are showing higher vales from the tendency line. The out of trend points (squared data) are referenced in Figure 2.26. B. Sinuosity changes through the slope. There is a big variability of sinuosity through the slope…….86

Figure 2.26. Slope angle vs sinuosity plot. For high slopes the sinuosity is low, as the gradient decreases the sinuosity increases generating highly sinuous channels, reached that point the sinuosity start decreasing down slope. The red box highlights points that exhibit high sinuosity values than the normal distribution. These points correspond to areas where the gradient is higher (Squared data in Figure 2.24) indicating irregularities on the slope. ……..88

Figure 2.27. Low gradient sections of the slope allow the deposition of unconfined flows that heal the slope. A. Deposits upslope of KP1, the flows are filling an interchannel low. B. Lobate features down slope of KP2. Even though frequency of the seismic is low, it is possible to observe the onlap of the lobe against the channel overbank. ……..….92

Figure 2.28.A Knickpoint evolution. Fault related folds may create areas in the slope where erosional processes generate knickpoints that migrate upslope and generating unconfined deposits down slope. Later these knickpoints are connected by an erosional conduit, which may explain the initiation of a channel levee system. ……..……93

Figure 2.28. B The diagram depicts the same process of knickpoint migration constrained within the interchannel lows.……..……..96

Figure 3.1. Bathymetry map of the Magdalena fan, southern Caribbean sea. Location of the active fan and regional structure. Contour interval is 1000 m ……..……..……106

Figure 3.2. Historic bathymetry map from Heezen 1956, indicating his interpretation of the Cable break and possible flow pathways B. High resolution multibeam bathymetry. Main differences are the presence of the northeast trending thrust ridges that are not identified in the old bathymetry and the flow paths of the canyons. However, Heezen's work illustrates the presence of several canyons at the upper slope near the river mouth. Cable breaks are represented by triangles and the lines correspond to the replaced cable. The cable breaks are distinguished depending on the river flood stage at the time of their occurrence. H1 (Red) correspond to high flood stages during July and August. H2 high flood stages presented during November to December and low flood (L) occurring during the rest of the year. ….……...108

Figure 3.3. Architectural elements of the Magdalena fan. (Modified from Ercilla et al., 2002). Northeastern and southwestern deformation belts are the boundaries of the CLC studied. Note the presence of MTCs located at the interchannel system lows. ……..…110

Figure 3.4. GLORIA image for the study area. High reflectivity is common in areas of active sedimentation or coarser material. A. Sediment waves at the abyssal plain. B. Northeastern canyon that communicate the upper slope with the abyssal plain. C. Distributary lobe feature at the toe of the thrust deformation front at the Aguja Canyon. Black triangles correspond to the cable break location and the red dots to piston cores……..……..114

Figure 3.5. Active canyons of the Magdalena slope: S) Sabanilla, U) Unnamed, M) Magdalena. East of the Magdalena Canyon are found SC) Slope channels of gullies, MTCs, and D) Diapirs. Cable breaks are represented by triangles and the extension of the line corresponds to the replaced cable. The cable breaks are distinguished depending on the flood stage of the river at the time they were presented. H1 (Red) high flood stage during July and August. H2 high flood stage during November to December and low flood (L) during the rest of the year……116

Figure 3.6. Piggyback basins and main flow path directions. (Blue) represent the gravity flows transported through the Sabanilla, U and Magdalena canyons that converge towards KP1 and continue down slope through PBB4 to the abyssal plain. (Red) represents the gravity flows that are diverged towards the east, transported through PBB1 and PBB3 to reach the abyssal plain. (Green) corresponds to the gravity flows transported by the Aguja Canyon..……117

Figure 3.7. Pathway profiles (Figure 3.6). Pathway A is composed of the Magdalena (Pink), Sabanilla (Red) and U canyons. The confluence of the Sabanilla and U canyons is depicted by a convex-up change in the profile. The knickpoints KP1 and KP3 show breaks in the slope, additional breaks in the slope (convex up sections) are found in this pathway. Pathway B profile is characterized by marked breaks in the slope that correspond to the MTC-1 scarp and knickpoints 2 and 4. Pathway C- Aguja Canyon shows a smooth convex-up profile. The major break corresponds to the area were the canyon exhibits terraces, slumps and a conspicuous sinuous bend……...121

Figure 3.8. Turbiditic flows pathways. Main Magdalena Canyon flows (M), Eastern flows (E1) and (E2). 3D display of the MTC-1. Note the Knickpoint created at the toe of the thrust ridge back limb…….……123

Figure 3.9. Location of the cable from 1930 to 1954. As a result of the rupture of the submarine cable the location was moved to deeper areas. A. Location of the cable line from 1930 to 1937. B. Location of the cable line from 1937 to 1950. C. Location of the cable line from 1950 to 1954…….125

Figure 3.10. A. GLORIA image in a gray scale. High reflectivity areas correspond to the whiter colors. B. GLORIA image in a color scale integrated with the bathymetry map. ……128

Figure 3.10. C. Detail of the GLORIA image in PBB1 (L) Lobate features. (C) Conduit of sediments feature. X-X' seismic profile through the PBB1 (Figure 3.11)……..…129

Figure 3.11. MTC-1 seismic interpretation. Corresponds to line X-X' in figure 9c. A. Uninterpreted seismic profile. B. Interpreted profile showing the multiple stacking of chaotic packages in the piggyback basin…..……..133

Figure 3.12. Lithologic description of piston cores in the Magdalena. Vema acquisition. Data obtained from the Lamont Doherty Laboratory repository. Note the only cores that have evidences of turbidites flows are V12-112 in PBB4, V12-118 in PBB1 and V12-119 at the abyssal plain. The rest of the cores are composed of fine-grained sediments, mainly mud and silty claystone (See complete description Appendix 1)…….137

Figure 3.13. Lithologic description for piston cores VM12-112, VM12-118 and VM12-119. Note the abundance of turbidites for the three cores. Location at Figure 3.12…….....138

Figure 3.14. V12-118 core description and grain size analysis from Muñoz (1966). Note the absence of pelagic drape at the top of the core. Arrows indicate possible hyperpycnal flow deposits. Core photograph LDEO Deep-sea sample repository
http://www.ldeo.columbia.edu/res/fac/CORE_REPOSITORY/RHP1.html……
…….....…140

Figure 3.15. A. The core VM12-111 do not exhibit turbidites since is located in a bypass area. B (x-x') depicts the erosive nature of the area close to the V12-111. C (y-y') exhibits horizontal and continuous reflectors that are missing on the proximal line and may correspond to turbidite flows deposited in PBB4…….……141

Figure 3.16. Grain size, sand content and sorting of the V12-118, V12-112 and V12-118. A) Sand content (%) vs grain size (phi), note the samples for the V12-112 core are out of the main trend. B) Sand content (%) vs sorting (phi), the sand rich sediment are very to poorly sorted with the exception of the V12-112 samples that are extremely poor sorted. ……145

Figure 3.17. (A) Monthly mean and standard deviation of water discharge; and (B) sediment load, in the Magdalena River at Calamar, 1975–1995.

(From Restrepo and Kjerfve,2000). (C) Cable breaks monthly distribution: 1927-1956. The seasonal distribution of sediment load indicates high values of 690 x103 t day-1 and 678 x103 t day-1during November and December. Secondary high sediment loads occur during June–July with loads reaching 443 x103 t day-1. These periods coincide with some of the cable breaks. ……....148

Figure 3.18. Cable breaks (1927-1956) and Mean Annual Discharge, Calamar Gage 1941 to 1970 (Modified from Winkley et al., 1994). The cable breaks are separated from the Magdalena River area breaks. Note the correlation between high discharge years and the rupture of the cables. ……149

Figure 3.19. Retreat of the coast line by erosional processes. Construction of jetties increases the erosion of the western arm of the Magdalena delta and builds up downstream sand bodies. Shore line retreats between 21-150 m/yr during 1939-1987 period. Black morphology lines correspond to the coastline published by Heezen and should correspond to a map from the 1930's. Lines of coastal retreat (color lines) are taken from Martinez et al. (1985). ……..…...156

Figure 3.20. Northeasterly winds throughout the year causing persistent NE to SW longshore drift. Construction of jetties increased the erosional processes of the western arm of the Magdalena delta and build up downstream sand bodies. The shelf floor depicts reworking of sediments forming linear features parallel to the wind direction. A) Slope of bathymetry and B) Azimuth of the bathymetry. 158

Figure 3.21. Landsat Orthorectified image in false color from January 11, 1989. Magdalena River plume is deflected towards the west at the dry season. In addition, a sediment plume is observed directed towards the Aguja Canyon. TM (1989/1/11 ID: ET009R52_4T19890111) USGS Tri-decadal global Landsat Orthorectified http://eros.usgs.gov/products/ satellite/landsat_ortho.php..……159

Figure 3.22. Sediment load (gray line)/nearshore wave power (bold line). The system is out of phase which allowed the formation of a delta shape at the river mouth. The cable breaks associated with the rupture of the jetty occurred during the months after a peak and at the rising of the wave power. (Modified from Restrepo et al. 2008)……....160

Figure 4.1. . Location and general structure of the area of study located offshore Colombia, Northern South America. Slope of bathymetry and GLORIA image. Major structural features include SNSM Sierra Nevada de

Santa Marta., Romeral and Bucaramanga Fault systems. (C?) Canoas Fault. Rectangles are indicating the location of Figures 4.2 and 4.3…..…177

Figure 4.2. Southwestern deformed belt. Arcuate scarps in red. GLORIA color image over slope of the bathymetry .Numbers are scarps in Table 4.2……179

Figure 4.3. Northeastern deformation belt. Major scarps are labeled with numbers characterized on table 4.2. Arcuate scarps in red. GLORIA color image over slope of the bathymetry. Numbers are scarps in Table 4.2……180

Figure 4.4. A. x-x' seismic profile of the southwestern deformed belt. MTC (green) are part of the deformed sequences generated as a result of the thrust imbricate advancement. Notice the presence of gas hydrates in the area (BSR). B. y-y' seismic profile of the southwestern Magdalena Fan. MTC (green lines) were deposited at the deformed belt toe as a result of thrust imbricate advancement. Notice the abundance of channel levee systems (blue lines represent the base of the CLS)……....182

Figure 4.5. Slope of bathymetry 3D view of the northwestern section. Highlighting the thrust ridges degradation and the presence of MTCs : sliding blocks, scarps and creeping of sediments . Vertical exaggeration 10x.……185

Figure 4.6. Bathymetry 3D view of the northeastern section. Highlighting the location of MTC-1 and thrust ridges. Sediments from the Magdalena River flow downward through the canyons conduits, and are deposited in Ridges (R) or confined piggyback basins (C). The MTC-1 deposits are deflected eastward due to the presence of the structural ridge. A morphologic depression is observed with the same fault trend related with the MTC-1 scarp. Vertical exaggeration 10x……..181

Figure 4.7. Detailed view of MTC-1 and escarpment profiles. A-A' Longitudinal profile traced along the axis of the scarp zone and MTC-1 deposits. B-B' MTC-1 strike profile. Note the trough formed at the western side of the MTC-1, corresponding to local slides or earlier morphology of the seafloor. C-C' Strike profile through the MTC-1 escarpment which is displaying the differences of bathymetry within the east and west walls.……...188

Figure 4.8. Upper slope multiple arcuate scarps and canyons due to retrogradational erosion. Also note the channel inner wall collapses at the eastern channel (Detached MTCs)……..190

Figure 4.9. Channel levee collapse scarps (Detached MTC). The scarp is linked with an abandoned channel which served as a conduit to transport the deposits downslope……..191

Figure 4.10. Channel levee collapse scarps in the Aguja Canyon (Detached MTC). Also observe the different levels of terraces on the canyon.……....191

Figure 4.11. GLORIA image (A) and bathymetry (B) for the main fan. Four MTCs filling the interchannel lows can be recognized. Also lobate forms (north of thrust ridges) are highlighted on both images……..……..….192

Figure 4.12. Types of detached MTCs (Moscardelli and Wood, 2008).....195

Figure 4.13. Earthquake activity of the margin……...197

Figure 4.14. Types of attached MTCs (Moscardelli and Wood, 2008)…...199

Figure 4.15. Global distribution of MTCs compared with modern-day seismic risk and plate boundaries. The Magdalena Fan in red triangle and ODP Site 999 location is highlighted with the blue circle. (Modified from Maslin et al., 2004)……..201

Figure 4.16.Comparision of the Isotope record in the Amazon fan and the ODP site 999 in the Colombian basin. Note the similarity of the record on both sites, which indicate that the Colombian basin present similar sea level changes to the Amazon Fan for the last 500 Ky. (Compiled from Maslin (2005) and Martinez et al. (2007). ……204

Figure 4.17. Global sea level changes and Isotopic record from the OPD site 999 compared with the Magdalena delta and submarine fan shifts. ……..…..205

Figure 5.1. Depositional styles on the Magdalena fan. ……..214

ABSTRACT

The Magdalena submarine fan, offshore Colombia, is the result of sediment accumulation in an accretionary prism initiated during the middle Miocene. It is fed by the Magdalena River, which drains the northern Andean Cordillera. Integration of multibeam bathymetry, GLORIA side scan sonar and 2D seismic profiles reveal a series of seafloor deepwater channel-levee systems and mass transport complexes (MTCs) that have evolved as a result of changes in the processes controlling the sedimentation. This study explains the fan evolution during the Pleistocene up to present times and how the tectonic setting has modified the morphology of different architectural elements and their depositional styles.

The river delta migrated westward during Pleistocene to Holocene times, generating eight phases in the submarine fan, mainly represented by channel-levee complexes, unconfined deposits and MTCs filling the interchannel lows. A major Late Pleistocene shift towards the east defined the western abandonment phase of the main fan area (Galerazamba).

The present day fan is located north of the river mouth, revealing its recent activity by deposition of sediment gravity flows which have ruptured submarine cables. Two flow pathways trend down slope through piggyback basins that are linked by knickpoints and canyons. A third flow pathway corresponding to the Aguja Canyon, located northeast of the river mouth,

also provided sediment gravity flows which ruptured submarine cables. The flow events are related to different processes on the continental shelf: 1) High flood stages of the river, 2) coastal erosion, 3) longshore drift, 4) hyperpycnal flows and 5) river mouth instability. The sedimentological characteristics of the different deposits should vary because the flow properties are different. Flows through the active Magdalena Canyon and western gullies may be related to high flood stages of the river, giving rise to hyperpycnal flows and instability of the Magdalena delta front. Meanwhile, flows from the Aguja and Sabanilla canyons are associated with longshore drift and coastal erosion.

Mass transport processes have smoothed sea bottom morphology and have been subdivided according to the following causal mechanisms: 1) detached (growth of thrust structures, instability of slope canyon and channel walls) and shelf-attached (major slope failures).

Deformation of the Magdalena Fan occurs at the proximities of the deformation fronts, where buried folds and faults modified the slope. This was recorded in the western fan by increase of sinuosity of the channel-levee systems, forced migration (avulsion) and generation of knickpoints at the higher slope section. Higher slope angles occur at the upper slope, along the northeastern section of the fan, where retrogradational erosion is linked with MTCs as a result of uplift of the inner thrust ridges and the shelf.

Depositional styles vary from the fan to the deformation fronts. Channel-levee systems, unconfined flows and MTCs are typical on the main fan, while thrust deformed areas are dominated by above-slope deposition, represented by unconfined deposits that fill the piggyback basins or are transported downslope to the abyssal plain.

This work provides new understanding of the processes involved in submarine fan evolution in an active margin setting. This knowledge has implications for both petroleum exploration and assessment of shallow hazards of submarine infrastructure in the area.

CHAPTER 1

1.1 OBJECTIVES

The modern south Caribbean seafloor, offshore Colombia, displays a series of submarine channel levee complexes, mainly formed by turbidity currents fed by the main drainage system in the area (Magdalena River). The aims of this dissertation are to analyze the distribution of the modern turbidite channels, provide an interpretation of the evolution of the channel complexes through time and evaluate the possible changes in morphology due to tectonic forces. Multibeam bathymetry, side scan sonar imagery, sediment samples (piston cores) and 2D seismic profiles were analyzed to achieve these purposes.

This dissertation involves four main topics:

1. Analysis of the sedimentary processes operating in the submarine channels in the northwestern Colombia slope.
2. Study of the influence of tectonic setting in the evolution of the Magdalena Fan through the sinuosity vs. slope relationship.
3. Characterization of the submarine fan morphology.
1. Relation of the sea bottom morphology to deeper strata using 2D seismic lines to determine stratigraphic evolution of the turbidite deposits, in particular the evolution of submarine channels.

1.2 RESEARCH HYPOTHESIS

Changes in slope angle as well as channel maturity and variation of flow characteristics such as current energy, flow volume, and sediment load, are among the factors that modify the submarine channel morphology (Babonneau et al., 2002). In an active compressional tectonic setting, the deepwater depositional system evolves as the slope angle is continuously modified. Consequently, the sedimentation style is modified. In active convergent margins major deformation events occur, leaving as a result an accretionary wedge. The geometry of the convergent margin can be

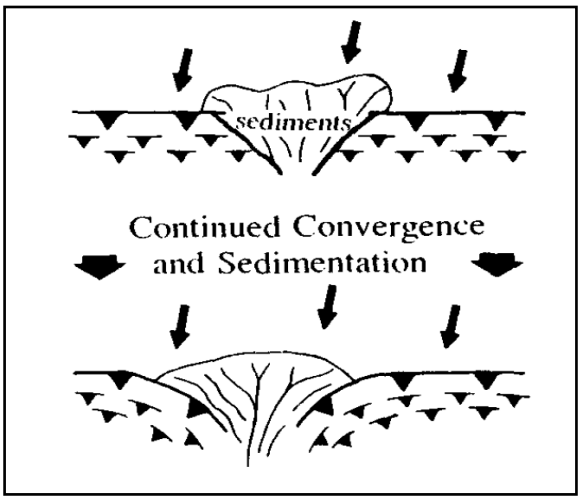


Figure 1.1. Breen (1984) model of the effects of sedimentation on the geometry of a convergent margin.

modified by high rates of sedimentation on the margin (Davis et al., 1983). Figure 1.1 illustrates how high rates of sedimentation may produce curvilinear structural trends and indentation on the convergent margin.

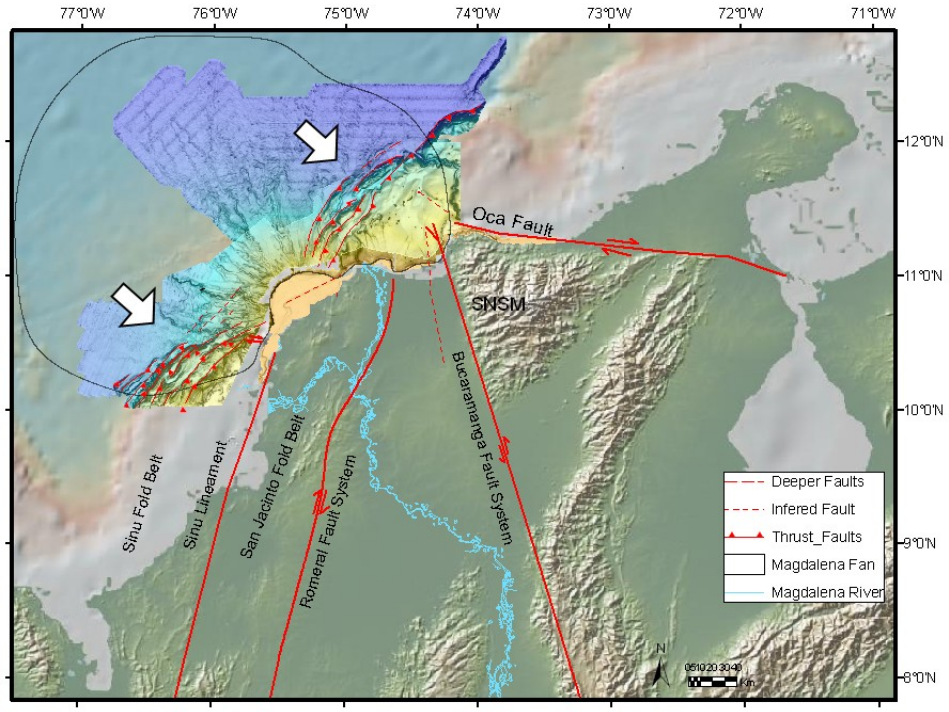


Figure 1.2. Main morphologic features of northern Colombia and Magdalena fan area.

Breen (1989) proposed that the rapid buildup of the Magdalena Fan may act as a rigid indenter in creating locally curved structural trends within the upper plate. The Magdalena Fan sediments cover the shelf margin of the Colombian basin, separating two arcuate deformation fronts (Figure 1.2 arrows). The fan started to receive sediments during the late Cenozoic Andean Orogeny (Kolla and Buffler, 1984a) and remains active today (Heezen, 1956a). The structural response has been indentation and curvature of the accretionary wedge and increase deformation inboard of the Magdalena Fan, increasing the tectonically driven uplift of the Santa Marta block in Colombia (Breen, 1989).

The deformation style of an accretionary wedge was explained by Davis et al. (1983). The accretionary wedge will deform internally until a critical taper is reached. For slopes greater than the critical taper the wedge will slide stably (Thrust faults). The presence of active sedimentation at the toe of the deformation front will reduce the wedge slope lower than the critical taper and reinitiate the internal deformation (Davis et al., 1983). If the sedimentary load persists on the slope at the same place the deformation front may become markedly curved. (Breen, 1989)

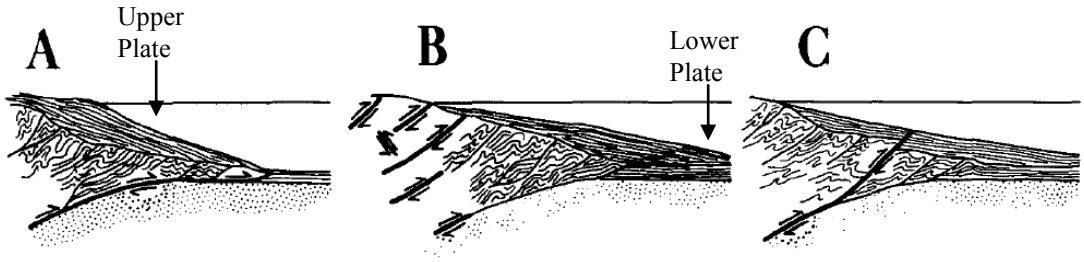


Figure 1.3. Migration of the deformation point due to the decrease in the slope of the upper plate in a convergent margin. (Breen, 1989).

The slope of the Magdalena Fan is about 2˚ on the upper fan and decreases to less than 0.5˚ on the middle and lower fan (Kolla and Buffler, 1984b). In contrast, the adjacent accretionary wedge has a slope of 2.5˚-8.5 ˚. The pattern of deformation on the northwestern Colombian margin appears to be altered in the vicinity of the Magdalena fan. The main deformation point has shifted back from the toe of the accretionary wedge towards areas on land behind the Magdalena Fan (Figure 1.3) (Breen, 1989).

The modification of the slope by the internal deformation in the Magdalena Fan should modify the channels morphology of the developed in the area of indentation (Magdalena submarine fan). Likewise, grow of the accretionary wedge areas (western and eastern areas) should affect the geometry of the channels and sediments that are deposited during the deformation.

The timing of deposition is also an important factor to evaluate in this system. The Magdalena Fan shifted in response to inland tectonic events during the Pliocene-Holocene interval, migrating towards the southwest and later to the northeast, where it is currently located, leaving a series of paleo-fans (Hoover and Bebout, 1985; Pirmez et al., 1990). If the main deformation occurred after the abandonment of the fan, the channel geometry would not reflect the slope changes and will be out of the equilibrium profile (Pirmez et al., 2000). Conversely, if deformation was acting at the time of deposition of the channel systems, the slope modification would be recorded by changes in the morphology of the channel, such as increase in sinuosity, lateral migration of the systems and erosional downcutting (Flood and Damuth, 1987; Pirmez and Flood, 1995).

The migration of the Magdalena Fan also helps to establish relative timing of the deformation events. If the two arcuate deformation areas were active during the same period of time, major deformation events should be reflected on the fan sedimentary sequence in both areas. Even though the

Magdalena Fan shifted its main deposition, some evidence of deformation should be present in the coeval structures.

The eastern fan area is currently active, hence sediment gravity flows, MTCs and slumps are common. Submarine cable breaks attest to the very recent sedimentary flow activity (Heezen, 1956a). The channel morphology of this area differs from the western channels. Straight segments and lower sinuosity are recognized in these channels and canyons. These variations in channel morphology may be indicating differences in the slope angles due to variations in the deformation style through the area or merely changes resulting from different deformational events resulting from shifting of the Magdalena River delta.

A complete study of the Magdalena submarine fan area will properly evaluate whether the system is behaving as a passive margin system, or whether it exhibit major differences in the deformed areas that would reflect its active margin tectonic setting.

Major points addressed by this dissertation include:

1. Morphometric quantification of the channels to establish the level of similarity between the channel levee systems in the submarine fan;

2. Comparison of channel morphologies to understand what processes control the style of sedimentation and evolution of the Magdalena submarine

fan leading to an understanding of the role of slope modification related to mobile substrates and tectonic events;

3. Analyze sediment distribution and turbidity flows in the modern active fan and comparison with the paleo-fan area to understand the evolution of the fan and sediment distribution on the continental slope;

4. Comparison of the modern Magdalena Fan and older sediments to find applications to subsurface exploration in similar basins;

5. Develop deepwater sedimentary model for active basins; and

6. Understand the active processes on the continental slope in order to assess geohazards.

1.3 IMPORTANCE

The Magdalena Fan is an active system with modern deposition of sediment gravity flows. Numerous submarine cable breaks have been reported since 1950 and the sea floor morphologies exhibit great variability of the architectural element morphologies. Figure 1.4 depicts importance of the Magdalena Fan when compared with other submarine fans. The Magdalena Fan is considerable in size, in an active compressional margin setting with active sediment gravity flows today. This study aims to provide a comprehensive interpretation of the evolution of the fan based on the

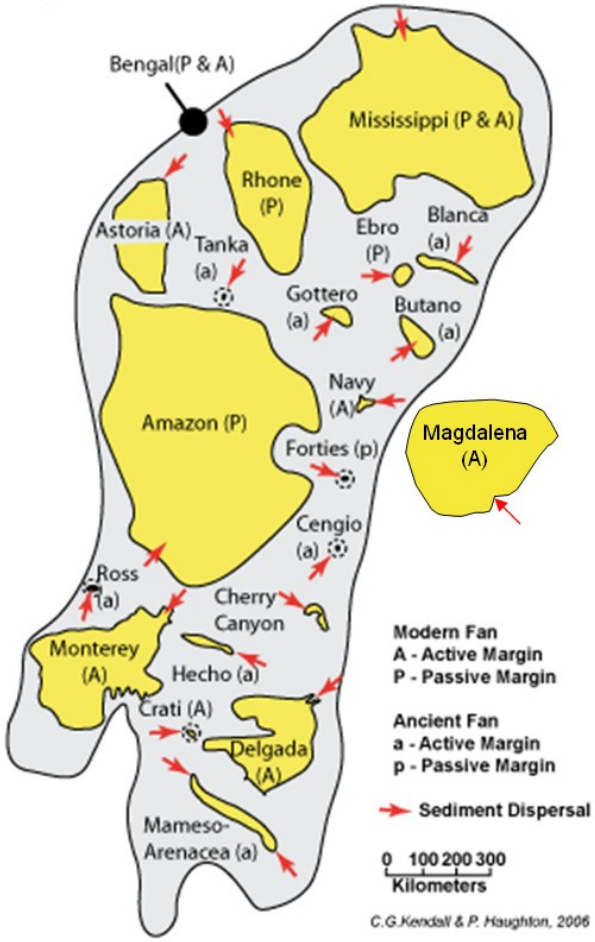


Figure 1.4. Comparison of major submarine fan systems (Modified from Kendall and Haughton, 2006)

interpretation of architectural elements and identification of the processes that control and modify the sedimentation.

The results of this study provide a better understanding of the evolution of submarine fans in active margins, depositional evolution of the continental slope offshore Colombia and in general to the generation of turbidity flow processes. In addition, the study of this area serves as an analog for

depositional models in similar tectonic settings, reservoir characterization and modeling.

The study also provides information about the sediment distribution and play concepts in the subsurface area. The promising increase in oil and gas exploration in the past year in the area makes the understanding of active slope processes and shallow hazards assessment important and urgent.

1.4 THESIS OUTLINE

Three papers (Chapters 2, 3, and 4) comprise the summary of interpretations and highlight the main findings of the study of the Magdalena submarine fan. Sections of the work explained in a particular paper were referenced with the corresponding chapter number in this dissertation. These papers were submitted to peer-reviewed scientific publication, as follows.

1.4.1 Chapter 2. Evolution of the Magdalena deepwater fan in a tectonically active setting, offshore Colombia

This manuscript addresses the evolution of the recent submarine deposits on the seafloor of the Magdalena Fan, taking into account the active tectonic setting in which it was deposited. Distribution and morphologies of the

channel complexes on the seafloor were studied using high resolution bathymetry and seismic profiles. The paper discuses how the inland tectonics controlled the location of the sediment source (Magdalena River) and induced migration of the submarine fan towards the south and northeast until it reached its current position. During Pleistocene and Holocene deposition of these channel complexes, active deformation of the continental slope occurred in some areas of the Magdalena Fan, hence allowing the study of interaction between slope modification and morphology of the fan Measurements of sinuosity, slope angles, and overall dimension of the systems were made. Additionally, the importance of knickpoint development is presented as a possible initiation point for the establishment of channel levee systems in a slope with active deformation and a relatively steep slope.

This manuscript was submitted to a SEPM Special Publication: Application of Seismic Geomorphology Principles to Continental Slope and Base-of-slope Systems: Case Studies from Seafloor and Near-Seafloor Analogues, editors: Prather B., Deptuck M., Mohring D., Van Hoorn B., Wynn R.)

1.4.2 Chapter 3. Active sedimentation and submarine cable breaks on the Magdalena deepwater fan, Colombia: linkages with shallow water processes as starting point for turbidite flows.

This chapter summarizes the recent sediment flow activity of the Magdalena Fan, characterizing the morphology of the northeastern fan, from the river mouth to the abyssal plain. Submarine cable ruptures during 1930 to 1956 demonstrate the presence of active gravity flows in the area. The use of GLORIA side scan sonar, bathymetry and seismic profiles allowed the identification of active flow pathways and distribution of the sediments. Identification of the main process that could have been associated with the initiation of flows is the main part of the discussion. High flood stages, hyperpycnal flows, coastal erosion, longshore drift, river mouth instability all seem to be playing a role in triggering gravity flows in the area. In addition, the interaction of mass transport deposits with the turbidite flows and their distribution, recurrence of the events, slope sedimentation and importance of the findings are presented in context.

This manuscript was submitted to a SEPM Special Publication: Application of Seismic Geomorphology Principles to Continental Slope and Base-of-slope Systems: Case Studies from Seafloor and Near-Seafloor Analogues, (editors: Prather B., Deptuck M., Mohring D., Van Hoorn B., Wynn R.)

1.4.3 Chapter 4. Mass transport complexes on the Magdalena deepwater fan: possible timing and causal mechanisms

An important percentage of the deep water morphology of the Magdalena Fan is a result of mass transport complexes (MTCs) distributed across the slope. This chapter is focused on the description of the different MTCs and the causal mechanisms associated with them, based on the interpretation of GLORIA side scan sonar, seismic profiles and bathymetry. These architectural elements were divided by causal mechanism into: 1) Detached MTCs triggered by either growth of thrust structures or instability of the slope canyons and channel walls, and 2) Shelf attached MTCs related to major slope failures. Additional triggers were considered for the shelf attached MTC including seismicity of the area, abandonment of the delta front and the submarine fan. Estimation of timing for the shelf-attached MTCs was based on the delta front abandonment as a result of the migration of the sediment source (Magdalena River), changes in the regional sea level and regional processes.

This manuscript was submitted to Submarine Mass Movements and Their Consequences IV. Advances in Natural and Technological Hazards Research, (editors: Mosher, D.C., Shipp, C., Moscardelli, L., Chaytor, J., Baxter, C., Lee, H., and Urgeles, R.), vol XX., Springer.

1.4.4 Chapter 5. Integration of results

This chapter summarizes important considerations derived from the study that advance the study of turbidites and the understanding of deepwater deposition in the Magdalena Fan area. The chapter integrates and discusses the results of the submarine fan deposition in terms of regional tectonics, deepwater sedimentation and depositional styles. Also included are some limitations of the data available, how these limitations affected the results and some ideas to be implemented in future studies.

1.4.5 Chapter 6. Conclusions

This chapter summarizes the main conclusions of the study.

CHAPTER 2

EVOLUTION OF THE MAGDALENA DEEPWATER FAN IN A TECTONICALLY ACTIVE SETTING, OFFSHORE COLOMBIA

ABSTRACT :

The slope morphologies of the Magdalena deepwater fan exhibit a series of channel-levee complexes, recording the evolution of the Magdalena Delta. Detailed morphological analysis of the seafloor expression of the channels and their lateral relationship allowed reconstruction of the Pleistocene fan history. The Magdalena deepwater fan was deposited on the northern offshore Colombia accretionary wedge (Caribbean Sea), initiated during the Late Miocene. The fan evolution is closely related to the Magdalena River establishment and delta migration, controlled by tectonic processes during the Pliocene to present. Major delta shifts toward the southwest (Canal del Dique) and northeast (Cienaga de Santa Marta region) created a submarine fan that migrated with the river, becoming younger towards the southwest. The main fan was abandoned during the Holocene, focusing deposition on the Barranquilla region to the northeast with modern active sedimentation. The depositional processes in the active fan area are mainly dominated by turbidity currents, possibly initiated by hyperpycnal flows, alternating with slumps/debris-flows that generated large mass transport deposits. Seven

channel–levee complexes (CLC) were imaged using multibeam bathymetry and seismic profiles.

Topographic lows between CLCs formed relatively unconfined areas for the accumulation of mass transport deposits. Morphometric measurements to define the slope angle vs. sinuosity relationships were performed on the channels in order to evaluate the interaction of deformation and sedimentation in the area. Highly sinuous channels in the western fan suggest that sinuosity changes were controlled by changes on the slope associated with deformation of the fold and thrust belt along the margin.

Upstream knickpoint migration in slope steps as a response to deformation may represent a key process explaining the initiation of deepwater channel systems on the origin of the Magdalena Fan as well as fans deposited on other tectonically active basins. This study provides new understanding of the processes involved in the Magdalena deepwater fan. Also, there are implications for the petroleum exploration and assessment of shallow hazards of submarine infrastructure of the area.

2.1 INTRODUCTION

The Magdalena submarine fan is the main physiographic feature that shapes the modern seafloor morphology of offshore northwestern Colombia. It is one of the few deep-sea fans with turbidity current activity today. The

fan consists of a series of submarine channel-levee complexes and mass transport deposits, mainly formed by transport and deposition of sediments from the Magdalena River, the main drainage system in Colombia (Figure 2.1). The fan extends about 68,000 km^2, with a volume of 180,000 km^3 and extends to over 4,000 m of water depth (Kolla and Buffler, 1984b; Wetzel, 1993; Reading and Richards, 1994). It is part of the accretionary wedge complex formed by the collision of the Caribbean –South American plates (Duque-Caro, 1979; Breen, 1989).

Previous studies on the morphology and stratigraphy of the Magdalena Fan (Kolla and Buffler, 1984a; Kolla et al., 1984b; Ercilla et al., 2002a; Estrada et al., 2005a) showed that, despite its active margin setting, the fan had features that resembled the large fan systems encountered off major rivers on passive margins, such as sinuous channel levee systems and large mass-transport deposits. Previous works by Hoover and Bebout (1985) and later by Pirmez et al. (1990) addressed the link between migration of the Magdalena River course, regional tectonics and the deepwater fan deposits. Here we present new bathymetric and seismic data that complement previous studies and allow for a more complete understanding of the fan and interpretation of its history. Seismic reflection data and detailed bathymetric coverage reveal the temporal and spatial evolution of the fan by examining the stratigraphic relationships between the various channel-levee

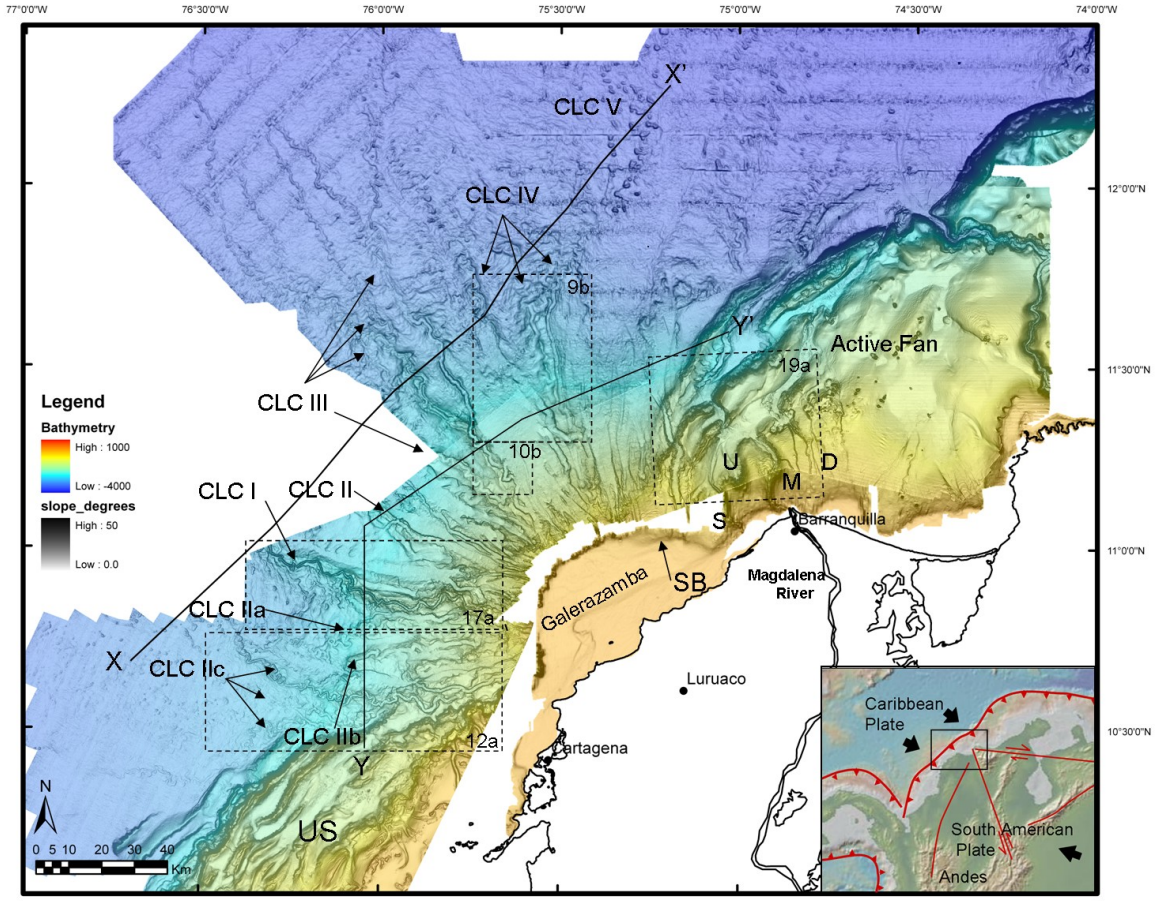


Figure 2.1. Bathymetry map of the Magdalena fan, southern Caribbean Sea. Location of the channel-levee complexes (CLC) and active fan. Canyons: U (Unnamed), S (Sabanilla), M (Magdalena); D (Delta front gullies), SB (Shelf Break). Regional cross sections X-X', Y-Y' shown in figure 7 and location of figures 9b, 10b, 12a, 17a and 19a. Multibeam Bathymetry –Slope of the bathymetry. Cities of Cartagena, Luruaco and Barranquilla are shown as a reference.

systems. Then, we relate the evolution of the fan to previous studies that discuss the evolution of the Magdalena River drainage onshore in an attempt to understand the evolution of the system from source to sink. This approach allows for constraining the models for sedimentation, tectonic interactions, and for placing constraints on the timing of fan evolution.

Finally, we attempt to link the spatial and temporal evolution of the sedimentary system to the patterns of tectonic deformation of the margin, including an analysis of the morphology of the various submarine channel-levee systems, characterizing the thalweg profiles and variations in sinuosity and slope angle. We discuss degradational processes to which the channels have been exposed after abandonment and the role of slope deformation on channel–levee morphology and knickpoint formation. Most studies of submarine fans are from passive margin settings. The Magdalena Fan is deposited in an active margin and reveals active deformation during the deposition of the channel systems, providing an opportunity to study possible differences between active and passive margin systems.

2.1.1 Geological Setting

The Magdalena submarine fan is an arcuate bathymetric feature, part of the accretionary wedge formed by the subduction zone of the Caribbean –South American plates (Duque-Caro, 1979; Kolla and Buffler, 1984b; Breen, 1989).

The Caribbean plate subducts towards the east-southeast, at a low angle beneath the South American plate and at a rate of 20 +/- 2 mm/yr (Trenkamp et al., 2002; Corredor, 2003).

The Caribbean margin of Colombia and the Magdalena Fan began receiving sediments during late Cenozoic time (Kolla and Buffler, 1984b) (Figure 2.2). In the middle of the margin, the Magdalena Fan formed a bathymetric bulge, separating two arcuate deformation fronts that delineate the fold and thrust belts east and west of the Galerazamba shelf. The fan appears largely undeformed (Breen, 1989), apparently modifying the geometry of the margin.

The main structural elements essential to the tectonic evolution of the margin are the Santa Marta massif, the San Jacinto fold belt and Sinú fold belt (Figure 2.2). The Santa Marta massif is an uplifted basement block, bounded by major strike-slip faults (Bucaramanga system to the west and Oca fault to the north). Kellogg & Bonini (1982) suggest that the majority of the offset in these two fault systems occurred during the last 10 Ma and is linked with the most important uplift of the massif. The San Jacinto fold belt represents the land portion of the accretionary complex composed of late Cretaceous to Pliocene sedimentary rocks. Deformation began during the early Paleogene and was reactivated during the late Miocene- Pliocene Andean compression (Ruiz et al., 2000). The Sinú fold belt lies west of the

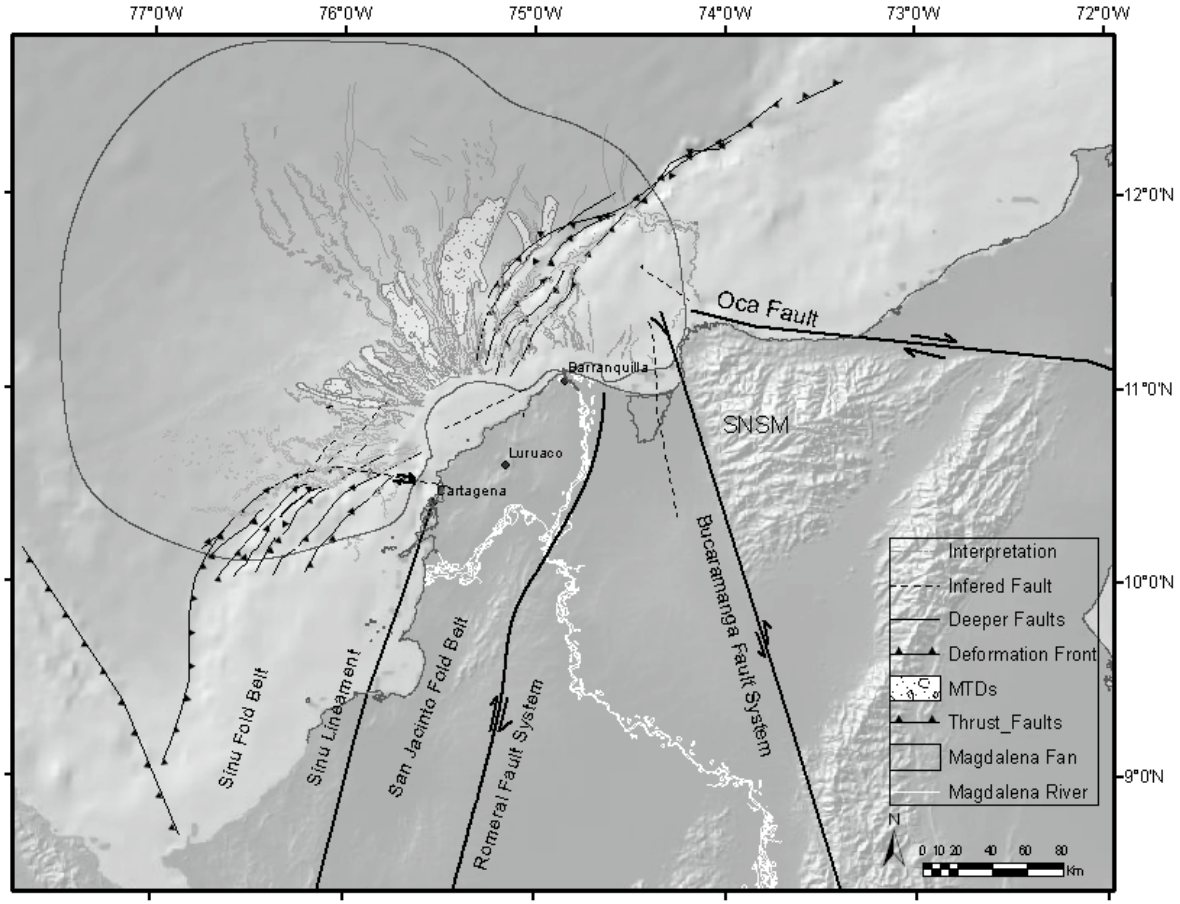


Figure 2.2. Major structural elements. Magdalena fan is characterized by the presence of two deformation belts that correspond to the Sinu fold belt initiated during the Miocene, that are separated by the main fan deposition. Deeper structures seem to be the continuation of the thrust growth out of the southwestern thrust belt. The presence of the Canoas Fault (C?) could not be confirmed with the available data

San Jacinto fold belt and is separated by the Sinú lineament (Duque-Caro, 1979) (Figure 2.2). Composed of Oligocene to Holocene sediments, it extends to the offshore area represented by a series of imbricate structures which become progressively younger towards the toe of the slope. The decollement surface seems to be related to overpressured shales deposited during Early Miocene (Vernette et al., 1992). Piggy-back basins have been preserved in the belt structures in the upper portions of the slope; they have been filled by mass transport complexes. Turbidity flows were later affected by collapse of some preexisting compressional structures (normal faulting). Sinú belt structures are aligned to the Sinú lineament and were mostly formed during the Pliocene but the prism is still active today. Pleistocene deformation is evidenced in some structures and supported by geodetic observations (Kellog and Vega,1995). Shale ridges and mud diapirism are important elements in the system. Diapirs located on the slope at the northeastern and southwestern deformation fronts, as well as onshore (Totumo Volcano) are common in the basin. Gas hydrates (BSR) and gas seepage are also present throughout the slope (Shipley, 1979; Shepard, 1973; Vernette et al., 1992).

The tectonic history of the offshore accretionary complex is still not completely resolved. Breen (1989) proposed that rapid deposition of the Magdalena Fan deposition has had a structural effect on the geometry of the convergent plate margin, creating an indentation and curvature of the

accretionary wedge. As a consequence, according to Breen (1989) the two arcuate deformation fronts were emplaced and deformation inboard of the Magdalena Fan increased, raising the tectonically driven inland uplift (e.g. Santa Marta block). Ruiz et al. (2000) presented a more complex scenario than the previous models, based on seismic interpretation, magnetic and gravity anomalies and divided northwestern Colombia into two zones separated by the Canoas Fault Zone: 1) zone of accretion (south of the Canoas fault) and 2) zone of transpression-transtension (Figure 2.2) between the Canoas and Oca-Santa Marta Fault systems. However, the presence of the Canoas Fault could not be confirmed with the available seismic profiles. Later, Flint et al. (2003) proposed an accretionary prism for the area which extends from the Uraba basin in the south and joins the northern accretionary wedge of Venezuela. High sediment supply to the offshore wedge induced a critical taper stage (Davis, 1983) and collapse of the pre-existing compressional structures. Folding and thrusting is less evident along the Proto-Magdalena (Galerazamba area) than in the deformation fronts, due to a high sedimentation rate during deformation.

2.1.2 Magdalena River History

The Magdalena River history is intimately linked with the tectonic events in northern South America. Hoorn et al. (1995) indicate a change in the northern South America drainage system during the early Miocene. Initiation

of the Eastern cordillera uplift in the late middle Miocene (between 12.9 and 11.8 Ma) generated a north and northeast flow of the river system in addition to the existing east and southern flows. Part of the drainage was directed northward along the paleo-Orinoco river to a delta in the Lake Maracaibo area. At 11.8 Ma the current directions shifted completely towards the north, changing from a meandering to an anastomosing fluvial system (Guerrero, 1993; Flynn et al., 1994). Bordine (1974) documented the paleogeography for land deposits in the lower Magdalena valley (Figure 2.3). Late Miocene – early Pliocene marginal and shallow marine deposits are the most prominent in the area. Link (1927) recognized a major ancient channel near Calamar, flowing northwestward near Luruaco, probably of late Pliocene age (based on planktonic foraminifera). The continuous northeast-southwest uplift and the presence of the Pleistocene La Popa Limestone near the ancient river mouth at Galerazamba indicate that the river was forced to shift toward the south-west (Canal del Dique) (Figure 2.3). The reef buildups were formed on the topographic highs created by shale diapirs. The uplift of the Atlantico-Turbaco Hills across the river's course caused a major east and northeast shift. Since then, the river has partially filled its estuary and has built three small, submerged delta lobes across a narrow shelf (Hoover and Bebout, 1985). It is important to mention that incipient deformation has been observed in coastal deposits by deformation of the Popa limestone along the

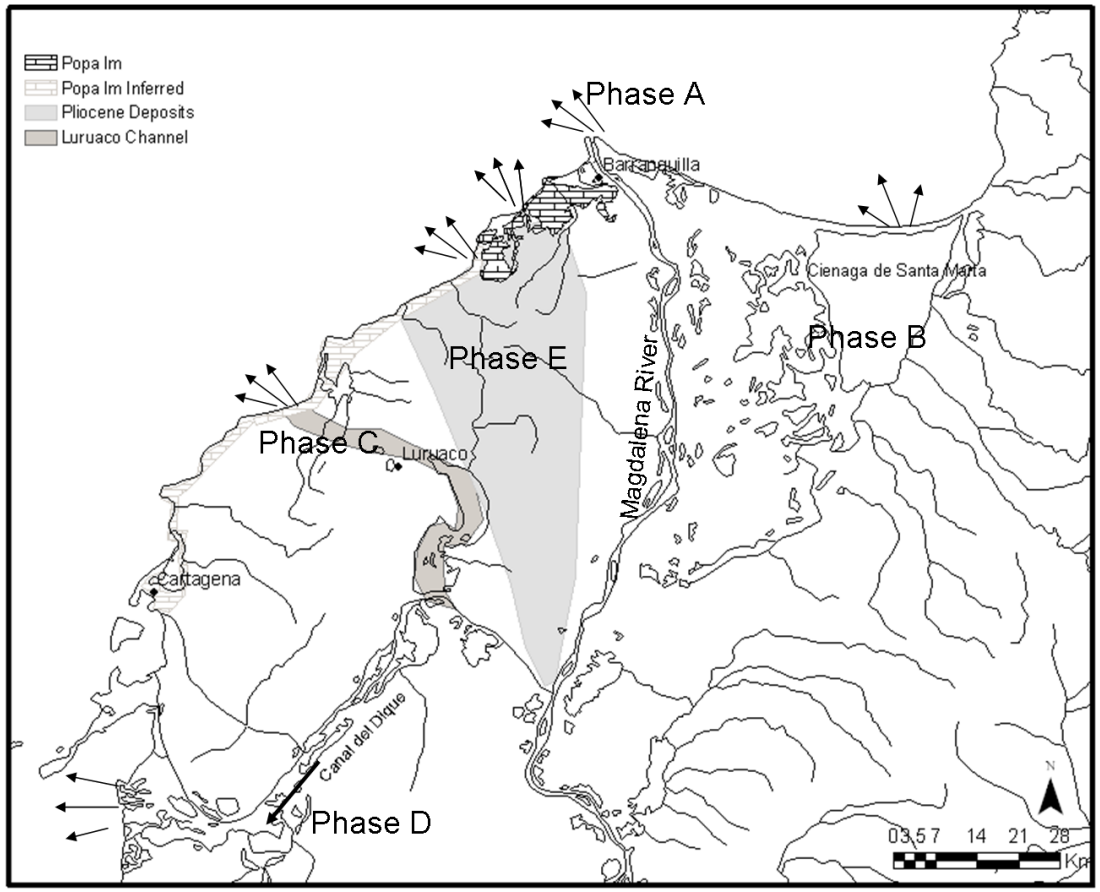


Figure 2.3. Magdalena River course shifts from the Pliocene to present day location. Relative order of delta phases: E, D, C, B and A. Note the presence of the La Popa coralline limestone near Barranquilla that support the southward shift of the drainage (Reyes, 2001). Cities of Cartagena, Luruaco and Barranquilla are shown as a reference.

coast line, particularly at the Dique canal area (Martinez and Roberson, 1997; Reyes et al., 2001).

2.1.3 Deepwater Fan Deposits

As a result of the migration and establishment of the Magdalena River northward during the Miocene, the submarine fan sedimentation was initiated. The proto-Magdalena Fan was mainly fed by the Magdalena River, but sediments of the Sinú River may also have contributed to the fan. The Magdalena Fan deposits were divided by Kolla & Buffler (1984b) into upper, middle and lower fan, based on sub-bottom profiles and piston core examination. The more recent units reveal several periods of incision and channel activity, reflecting uplift in the sediment source region, changes in sea levels and delta shifts in space and time that can be related to the Andean orogeny in the middle Pliocene (Kolla and Butter, 1984b). Modifying the earliest division of the area proposed by Ercilla et al. (2002a), the fan can be divided into: 1) deformed compressional belts and 2) main fan area. The deformed compressional belts areas include the arcuate northeast and southwest thrust belts, expressed on the sea floor as elongated ridges with strike along the margin (Figure 2.1 and 2.4). The main fan area is characterized by leveed channel complexes, large-scale mass-flow deposits, canyons and slump scars in the upper slope (Figure 2.3). The levee-channel systems are partially destroyed or buried by mass-flow

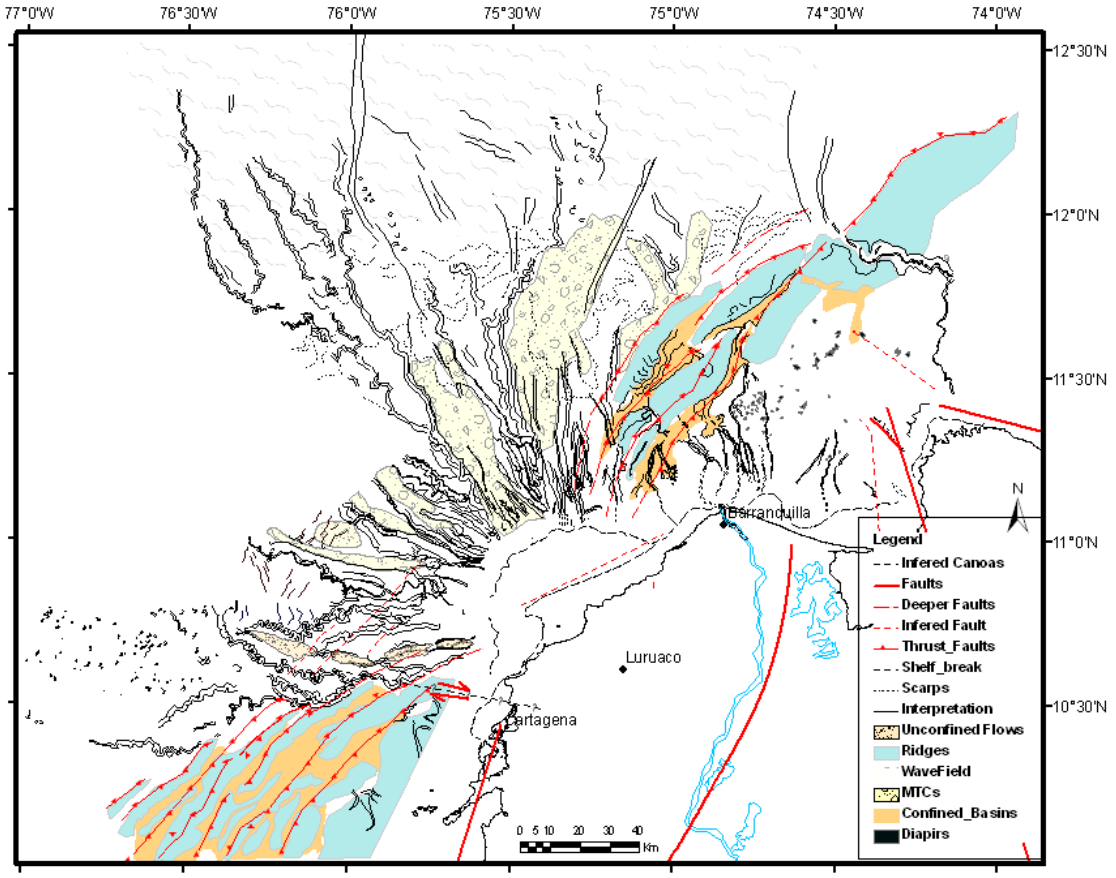


Figure 2.4. Architectural elements of the Magdalena fan. (Modified from Ercilla et al., 2002). Northeastern and southwestern deformation belts are the boundaries of the CLC studied. Also is important to notice the presence of MTCs located at the interchannel system lows.

deposits. Tectonic deformation in the main fan area is largely absent, but subtle evidence can be detected on the bathymetric and seismic data, particularly in the vicinity of the adjacent thrust belts.

2.2 DATA AND METHODS

Data available for the study include high resolution bathymetry images of the northwest Caribbean offshore Colombia (Figure 2.1). The bathymetry covers a major part of the Magdalena deepwater fan, approximately 54,000km^2 of the seafloor (Figure 2.1). Four different surveys cover the area of study. In 1997 the Spanish vessel Bio-Hesperides acquired approximately 32,500 km^2 of bathymetry data (Ercilla et al, 2002a) with the multibeam echosounder SimRad EM-12 S120. Two surveys were acquired in 2002 on behalf of Ecopetrol (14,700 km^2) and Total E&P (11,400 km^2). Data were collected using a hull—mounted, multibeam echosounder Reson SeaBat 8169 (50 KHz; for water depths between 100 and 800 m) and Simrad EM 12D (13 kHz; for water depths between 800 and 3500 m). Additional bathymetry surveys that cover the shelf area and river mouth were provided by the CIOH (Centro de Investigaciones Oceanográficas e Hidrográficas, Colombia*)* (6,000 km^2). Data were tide-corrected and processed by the contractor, and were provided in final format compatible with geographic information systems. Proximity to the Magdalena River

outflow area resulted in depth anomalies due to fresh water input which altered sound velocity ranges, but did appear to be properly corrected.

Bathymetry interpretations and quantification of the architectural elements dimensions were made using ArcGIS software (ESRI, Environmental Systems Research Institute, Inc.). Calculation of attributes such as slope and curvature were used to enhance and facilitate the interpretation. Thalweg profiles were extracted directly from the bathymetry grid for each channel studied. Thalweg profiles for each channel are referenced to the shelf break (~ 60m) to allow a better comparison of the changes in slope angle of the different systems.

Quantification of channel parameters was done measuring profiles every 5 km. Channel width was measured from the levee crest to levee crest. Levee height was calculated from the channel thalweg to the crest of the levee. Sinuosity and slope angle were measured by dividing the channel into segments for complete sinuous loops. Sinuosity is defined as the ratio between the thalweg length (channel axis) and the straight line distance between the sinuous loop end points, for a given section of the channel.

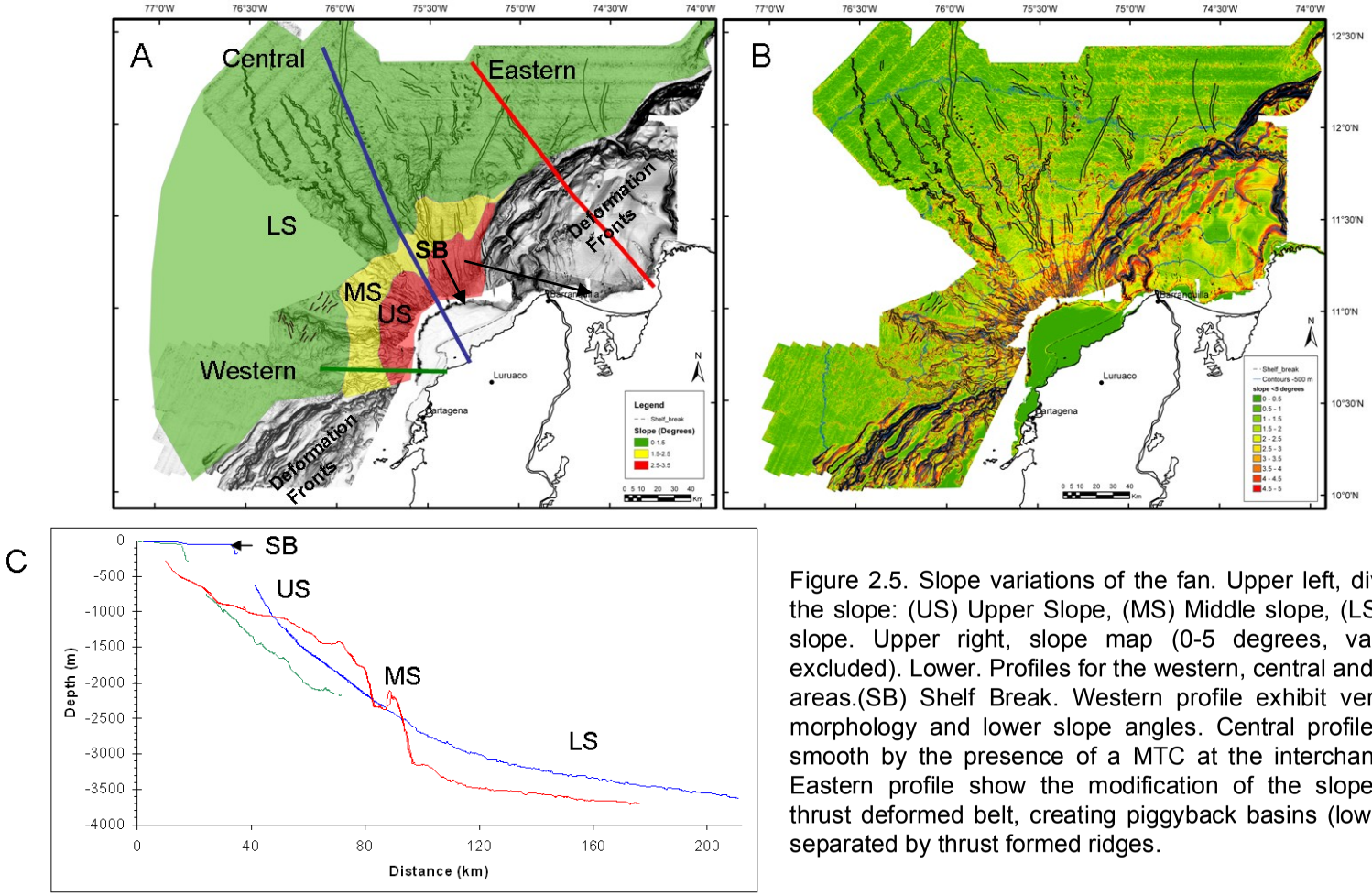
The 2D seismic lines shown in this paper illustrate the seismic expression of subsurface structure. They are part of a wider grid of seismic reflection data provided by Ecopetrol. Acquisition parameters are industry standard, nearly zero phase with SEG normal polarity. Frequencies range from 20 to 60 Hz around the level of interest. Seismic interpretation was performed in SMT

Kingdom Suite 8.1. Presence of water bottom multiples, gas hydrates, gas chimney and shale diapirs obscure the seismic signal in places. Additionally we used seismic data acquired during RMS Charles Darwin expedition CD40a in 1987 (Figure 2.1). These data were only available in paper copies and line interpretations (Pirmez et al., 1990).

2.3 AREA PHYSIOGRAPHY

The continental shelf is generally narrow (~2km), with wider sections amplified by the sediment discharge of the river mouth (e.g. 33 km in Galerazamba region, Figure 2.5c central profile) forming delta lobes (Figure 2.1). Sediment discharge was therefore directly onto the continental slope, as is happening today (Kolla and Buffler, 1984b). Ercilla et al. (2002a) characterize the central and eastern portion of the fan dividing the area into deformed and underformed zones, with a bulge shape on the basin floor towards the north of the Galerazamba region, with the presence of large mass transport deposits diminishing the slope angle.

The shelf area is very smooth; angles vary from 0 to 0.12^{o}. However, a distinct step is present at a water depth of 20 m that seems to be related to a fault system on the platform, with the slope angle increasing from 0.2 to 1 until it reaches a low angle sector (20 m deeper). The depth of the step coincides with the shelf break for the areas outside the Galerazamba region



(SB)Shelf break, (US) Upper Slope, (MS) Middle Slope (LS) Lower Slope

Figure 2.5. Slope variations of the fan. Upper left, division of the slope: (US) Upper Slope, (MS) Middle slope, (LS) Lower slope. Upper right, slope map (0-5 degrees, values >5 excluded). Lower. Profiles for the western, central and eastern areas.(SB) Shelf Break. Western profile exhibit very rough morphology and lower slope angles. Central profile is very smooth by the presence of a MTC at the interchannel low. Eastern profile show the modification of the slope by the thrust deformed belt, creating piggyback basins (low angles) separated by thrust formed ridges.

(Figure 2.5 a and b).The shelf break on average occurs at 40 m of water depth, but increases to 70 m in some areas of the Galerazamba region. The continental slope angle (Figure 2.5a) can be divided into an upper slope with angles ranging from 2.5 ^{o} to 3.5^{o}; a middle slope with values of 1.5 ^{o} to 2.5 ^{o}, and a lower slope or continental rise with angles < 1.5 ^{o}. These values exclude scarps, channel and canyon walls that locally can reach slope angles up to 50^{o}.

Slope profiles for the western, central and eastern areas show dramatic differences (Figure 2.5c) interpreted to reflect differential deformation on the fan. The central profile exhibits a concave up morphology with slope angles diminished by the presence of MTCs. The western profile is located close to the toe thrust deformed area. It exhibits gentle slopes similar to the central profile, but with pronounced erosional features. In contrast, the eastern profile shows abrupt morphology variation due to the compressional forces in the accretionary wedge (step like profile). Here, ridge-confined valleys or piggyback basins operate as conduits and basins for sediment transport and deposition. The thrust forelimb increases the angle of the slope, leaving a marked break separating slope and continental rise. In addition, it is important to observe that the eastern section is 300 m deeper (3500 m bsl) than the central and possibly the western section (no bathymetry data are available for the deep western sector).

2.4 CHANNEL LEVEE COMPLEXES

A series of submarine channel levee complexes (CLC) are present on the modern sea floor particularly in the central portion of the margin (Figure 2.1). Overlapping and compensational relationships allow us to establish the depositional order for the complexes (Figure 2.6). Seven major complexes have been recognized, each separated by interchannel lows where mass transport deposits and unconfined flows were deposited. A summary of the most representative channel characteristics is presented in Table 2.1. Figure 2.7 depicts the thalweg profiles for the different channels using the shelf break as a reference point. It is important to notice that the older eastern systems are found at deeper water depths and the younger western profiles generate gentle slopes at shallow depths, closer to the shelf. Morphology of the main systems is summarized in Figure 2.8; the profiles are measured every 5km. The closeness of the profiles indicates low slope angles or higher sinuosity where the vertical separation (depth axis) does not change much in 5 km.

2.4.1 CLC- IV

CLC-IV is the northernmost complex and is comprised of three main channel-levee systems (CLS): CLS IVa, IVb and IVc, (Figure 2.1, 2.9), extended up to 120 km from the shelf and into water depths to 3200m bsl,

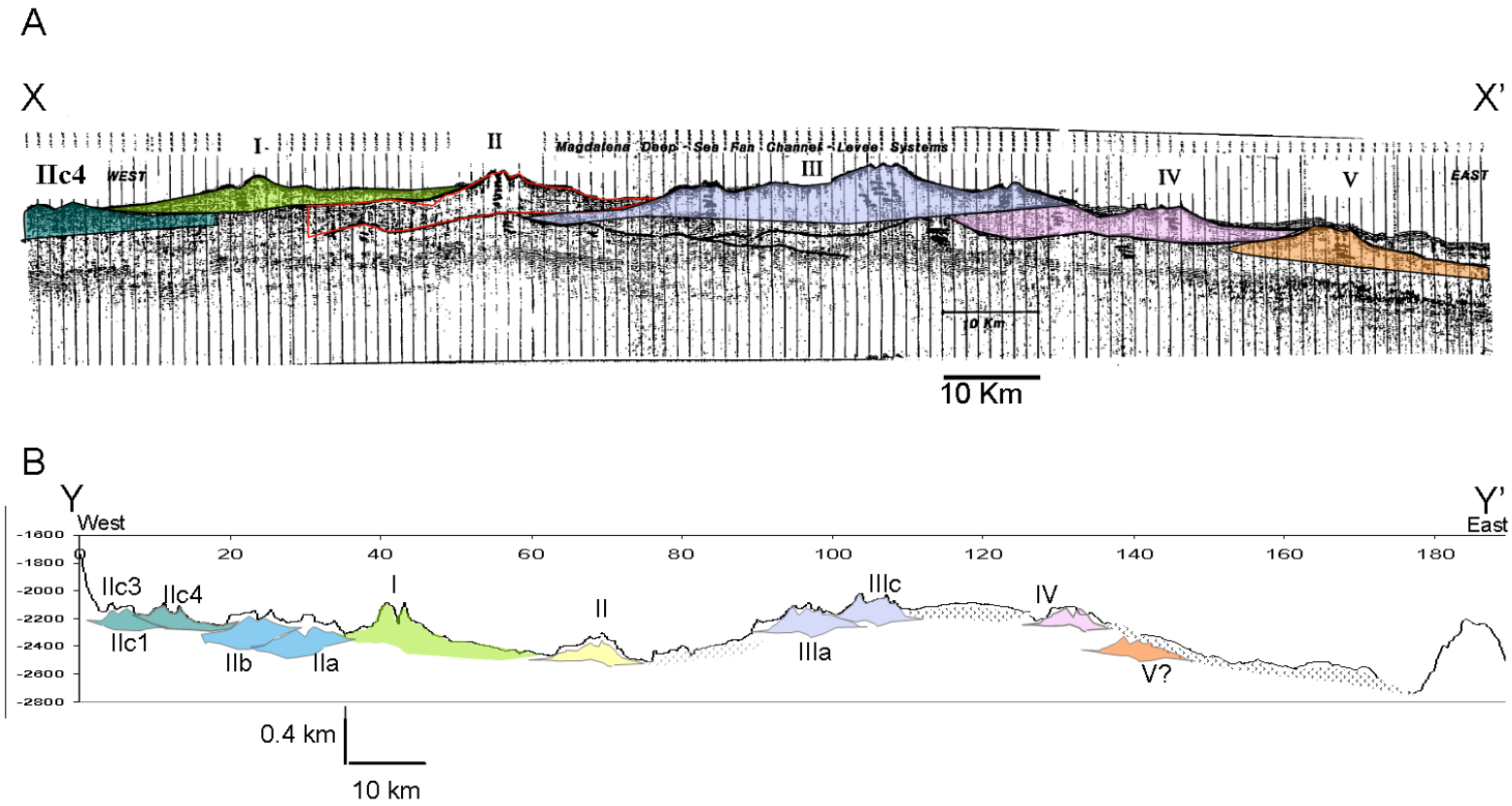


Figure 2.6. A. Seismic line RMS Charles Darwin expedition CD40a in 1987 (Lower Fan) (Pirmez et al., 1990). B. Bathymetry profile through the middle slope. The CLC are older towards the west, with exception of CLC I that is the youngest complex in the fan.

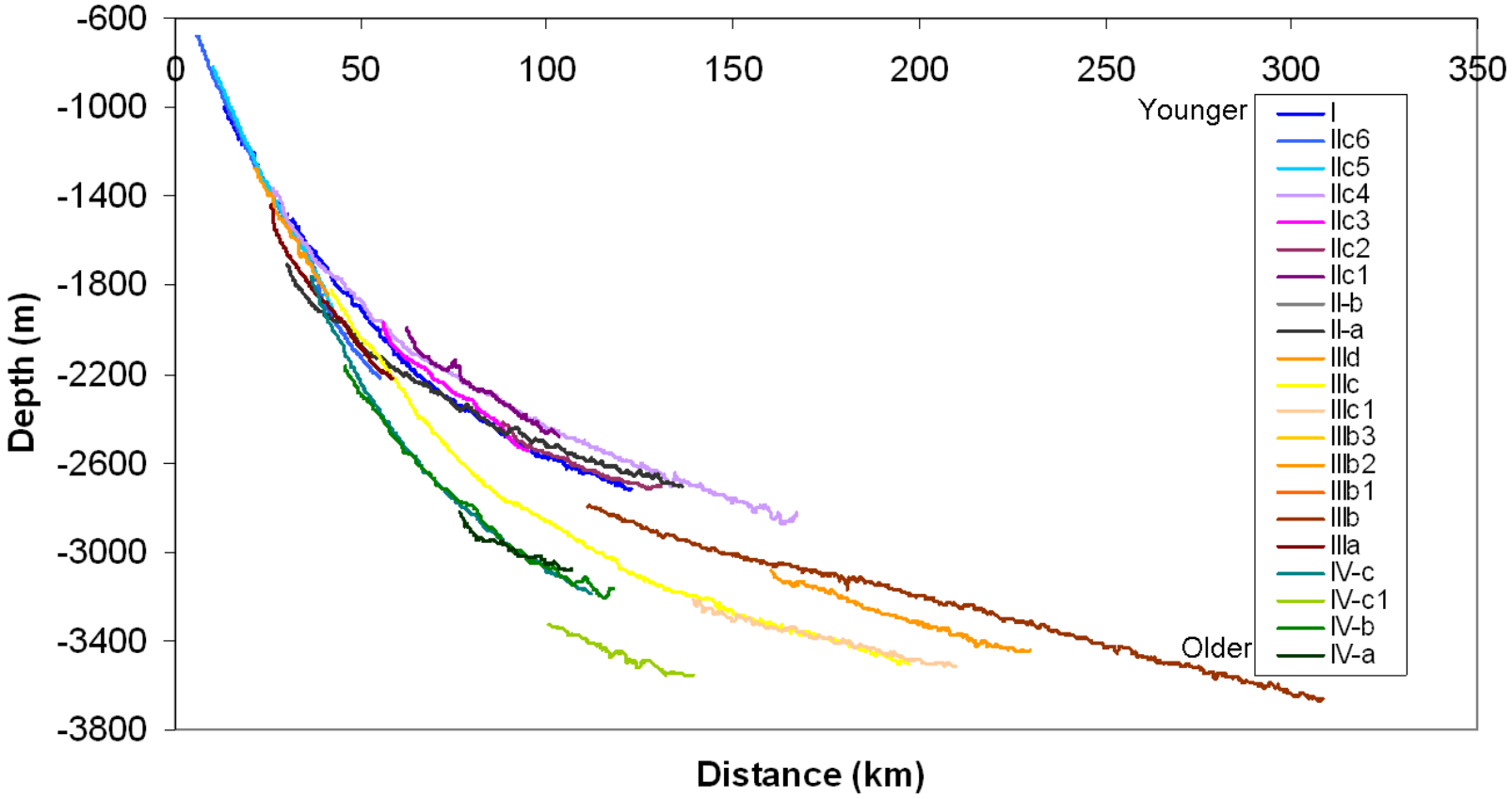


Figure 2.7.Thalweg profiles for the Magdalena fan. All the channels are referenced to the break of the slope at (60m bsl) to have a better comparison of the slope changes. Note that western thalwegs are deeper and with higher gradients at the upper slope. The profiles are ordered from young (upper) to old (lower).

Channel	Depth Range	Measured Length (km)	Ave. Width (m)	Ave. Left Levee (m)	Ave. Right Levee (m)	Max Sinuosity	Min Sinuosity
I	-1000 to 2720	110	1640	121	113	3.16	1.03
IIc5	-860 to -1920	39	1994	111	95	1.14	1.01
IIc4	-1380 to -2850	140	1390	62	67	4.08	1.14
IIId	-1276 to -1810	19	1860	41	78	1.41	1.01
IIIc	-1820 to -1350	156	1930	48	46	1.85	1.01
IVc	-1960 to -3200	75	1990	37	44		
IVb*	-2760	72	2480	48	54		
Iva*	-2958	30	1700	29	45		

Table 2.1. Morphometric measurements of main channel systems. * Due to the advanced degradation stage these values where collected at the most preserved interval.

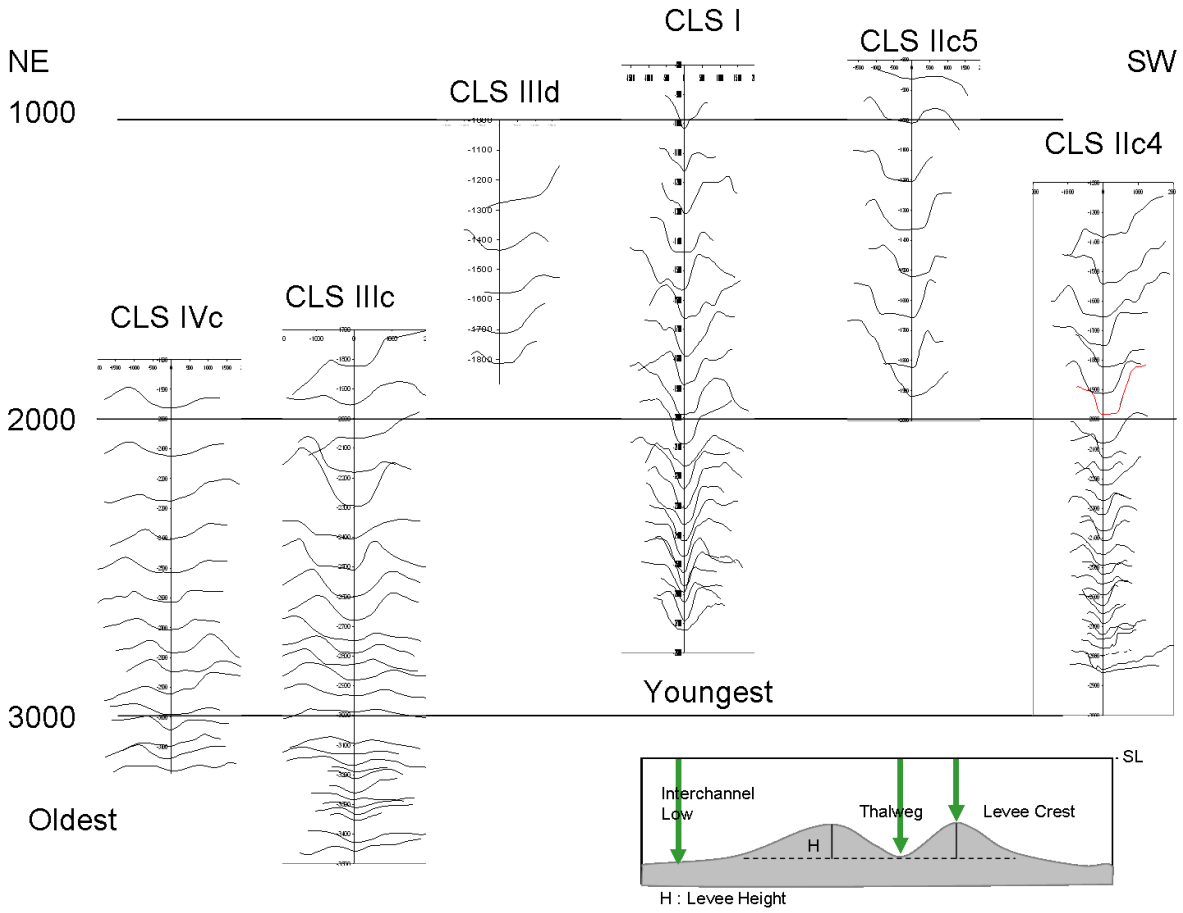


Figure 2.8. Channel profiles. Measured every 5 km of thalweg length. Vertical scale depth (below sea level) Note the change in the morphology of the conduit the upper 1000 m bsl. Increase in sinuosity and lower slopes is shown by the decrease of space between the profiles in the deeper sections.

and two younger channels IVd and IVe that eroded segments of the older channels. This channel complex is part of the channels first described by Kolla and Buffler (1984b) on the Magdalena Fan. The channel levees aggraded (up to 150 m) on the seafloor, forming a positive topographic structure (Figure 2.9b). The thalweg profile of the channels reveals a very rough morphology, except for IVc which exhibits a smooth concave up morphology (Figure 2.9a). The two younger channels IVd and IVe overlap and cannibalize the system on the upper slope.

Remnants of CLS IVa occur at 2824 m water depth (length of 30.2 km), with much reworked levees and thalwegs (Figure 2.9a). The sinuosity is moderate (1.35). The upper and lower section of the system is covered by younger channel systems.

CLS IVb occurs at 2167 m bsl, west of CLS IVa. The morphology of the levees has been highly affected by erosive processes (mainly the western levee). The measured length of the CLS IVb is 72.4 km. Sinuosity values increase down slope, from 1.10 until an avulsion point at 2790 mbsl is reached, beyond which the sinuosity is up to 1.49. The thalweg profile is very irregular (Figure 2.9a) and with higher slope angles than the CLS IVa.

CLS IVc is located at 1776 mbsl, west and parallel to CLS IVb. The preserved section of CLS is 75.6 km long. It can be divided into two sections a straight section (1.03 sinuosity) and a sinuous section (1.48 sinuosity) starting at 2780 mbsl. The change in sinuosity coincides with the avulsion

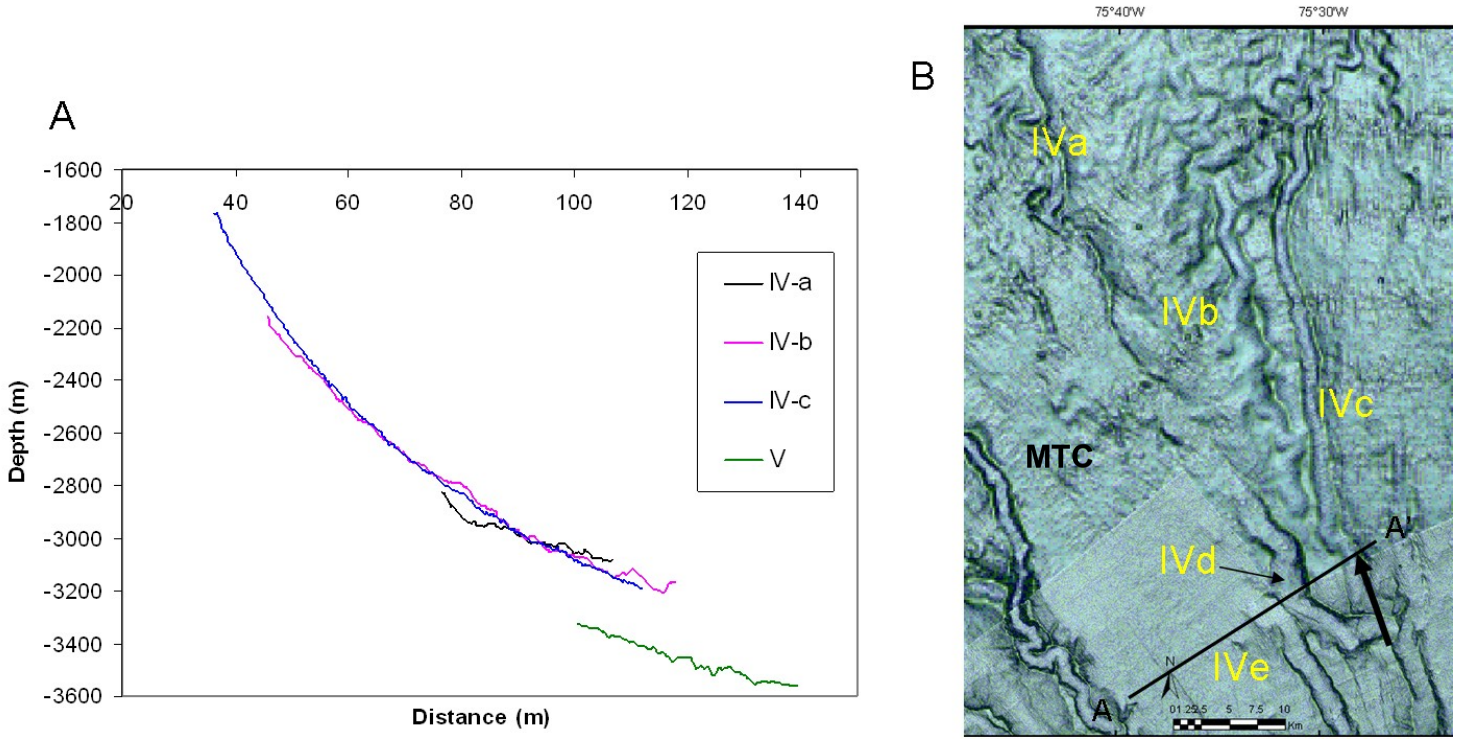


Figure 2.9. A. Thalweg profile of the remnants. Note lower profile of IVa and the convex up profile of IVb and IVc at 80km. The difference in thalweg depth corroborates that V remnant correspond to an older system. B. Main channel systems of IV in map view. Note how IVd and IVe are cannibalizing and covering the previous systems. Bathymetry map (curvature and slope) referenced to the general context Figure 2.1.

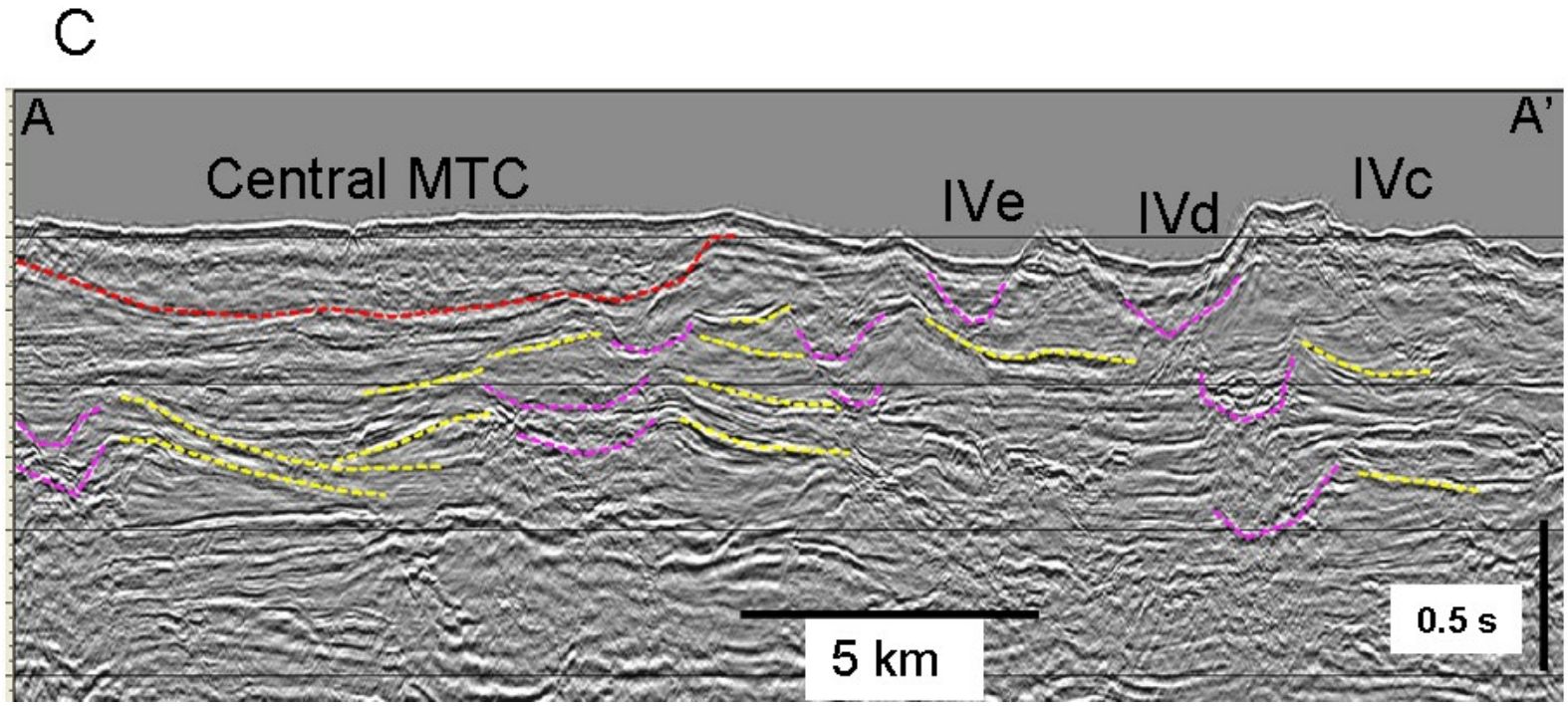


Figure 2.9. C. A-A' Seismic profile perpendicular to the flow direction. IVe and IVd thalwegs are covering older channel systems. Levees (Yellow), Channels (Pink), MTC (red).

point of CLS IVb. The thalweg profile is very smooth and concave up, and is very similar to the CLS IVb, but with higher angles upslope. Profiles normal to the axis of CLS IVc exhibit an open “U” shape (Figure 2.8). Present day relief of the levees is very smooth and reaches 70m in some areas with an average of 40m.

A younger channel system IVd cuts into the upper slope, eroding a section of VIa. This is an abandoned aggradational channel that has been exposed to erosional processes which had created flows covering sections of CLS IVa (Figure 2.9b). Seismic expression of channels IVd and IVe are shown in Figure 2.9c. The first few milliseconds correspond to very continuous reflections covering the area and partially filling channels IVe and IVd. Figure 2.9b shows more advanced erosional processes that modify the upper slope due to transport of sediments down slope through IVd and IVe.

Channels V-1 and V-2, located down dip from IVc may represent remnants of older channels not related with CLC IV, based on the extreme reworking of the thalwegs (Figure 2.1 and 2.9a).

2.4.2 CLC III

CLC III is composed by at least three main channels and four avulsions. (Figure 2.1) west of CLC IV. It extends from the upper slope to the lower slope for a distance of 57km, and water depth to 3668m. CLS IIIa is the

oldest and westernmost channel in the complex. The upper slope section of IIIa (32.8 km length) imaged by the bathymetry, exhibits high sinuosity (1.3) and appears to be linked to the CLC III (at 1370 m bsl), but is completely buried by the levees of younger channels, as can be observed in the seismic profiles (Figure 2.10). The thalweg profile exhibits angles very similar to the upper slope section of the complex (Figure 2.10a). The lower-slope section of IIIa is not covered by the bathymetric survey.

The following conduit in the CLC sequence is IIIb, which was later abandoned and replaced by IIIc. CLS IIIb occurs at 2170 mbsl, with two eastward migrating avulsion points at 3200 and 2800 mbsl (IIIb2 and IIIb3) (Figure 2.1). This part of the system is about 110 m topographically higher than the younger eastern channel system (Figure 2.10a). Sinuosity increases for IIIb, IIIb2 and IIIb3 at the avulsion point at 2800 m bsl (forming IIIb3), with values up to 2.45, coinciding with the increase in sinuosity for CLC IV.

CLS IIIc, described by Estrada et al. (2005a), is the youngest of the complex. The sinuosity increases down slope up to 1.85 and the average width of the channel is 1930m. An avulsion point is present at 3160 mbsl, which resulted in an eastward shift and abandonment of CLS IIc1. The levee relief decreases down slope and the channel becomes less entrenched, changing from a prominent “U” form to a shallower channel (Figure 2.8).

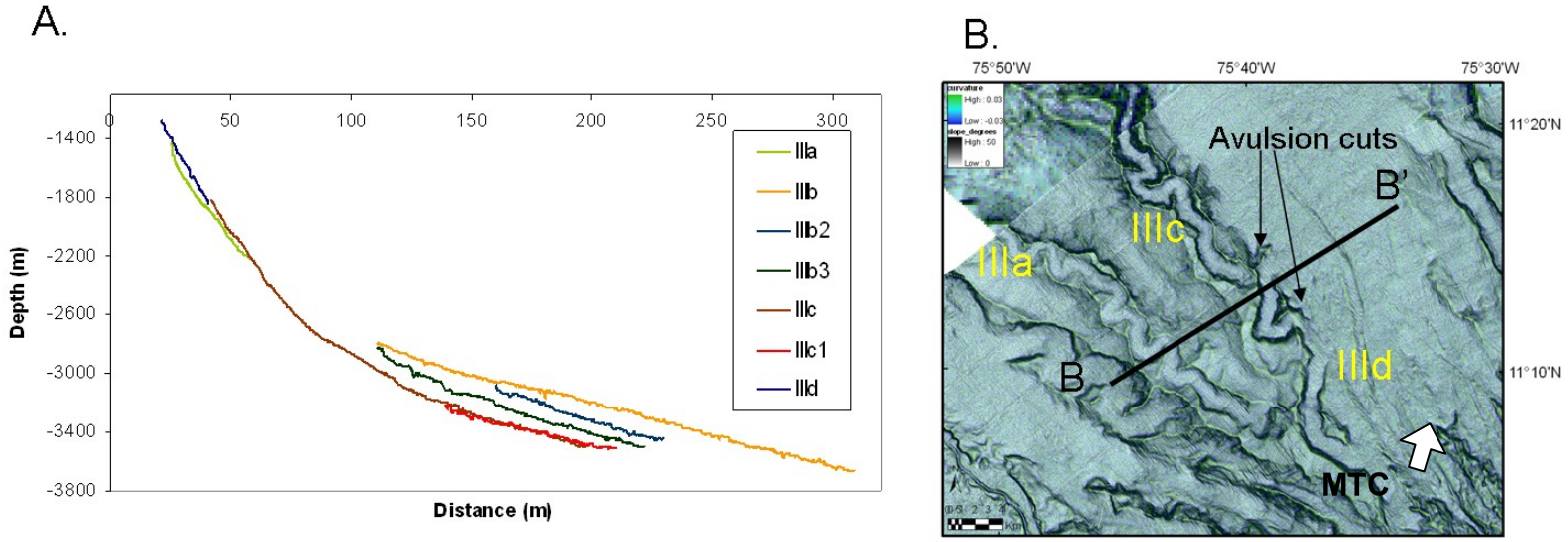


Figure 2.10. A. Thalweg profile of CLC III. The westward migration and the deepening of the thalwegs as it is getting younger. IIIa, IIIb, IIIb2, IIIb3, IIIc, IIIc1, IIId (Youngest). Note the convex up profile of IIIb and really steep gradients for the first 80km. B. Main channel systems of III in map view. Bathymetry map (Curvature and Slope). Reference to the general context in Figure 2.1. Upper slope is characterized by avulsion points. Also note how the central MTC is cutting the eastern side of the channel systems.

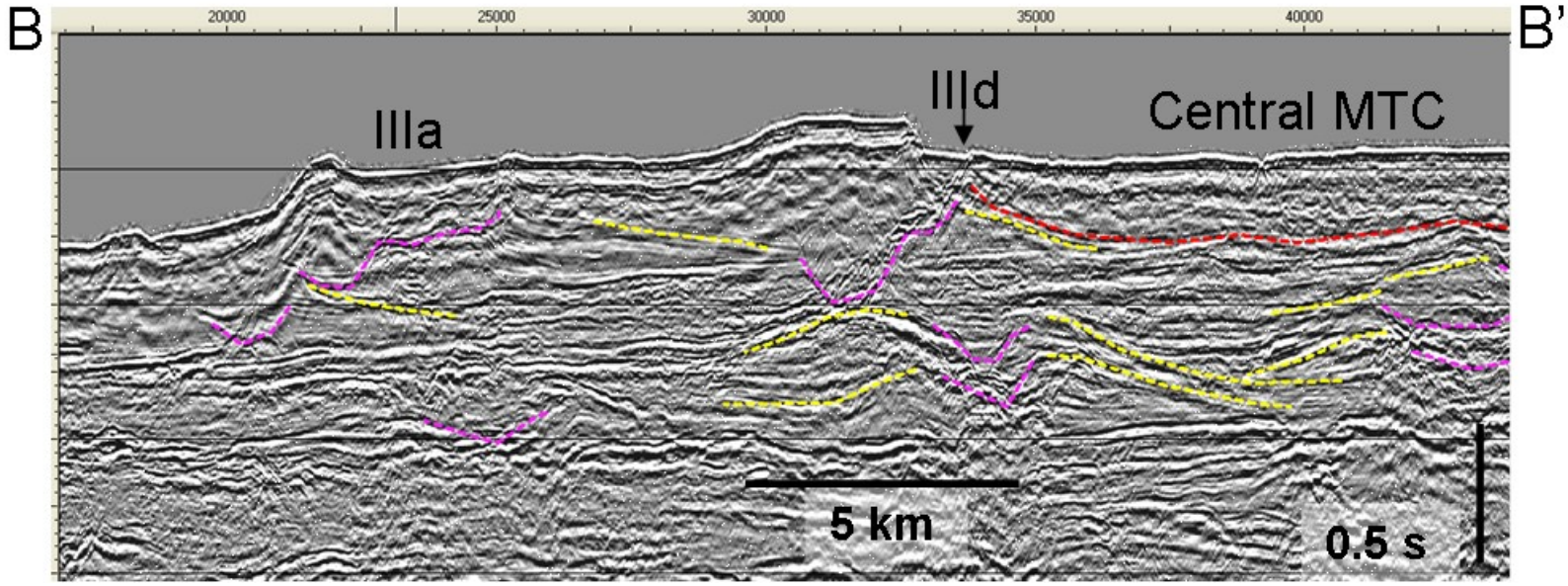


Figure 2.10. C. B-B' Seismic profile perpendicular to the flow direction. IIIa morphology is completely covered by later sedimentation. Eastern levee of IIId is completely modified by the erosion of Central MTC. Levees (Yellow), Channels (Pink), MTC (red).

Thalweg profile for this CLS is concave up with some convex areas. The higher resolution bathymetry used for this study allowed better definition of the avulsion points on the upper slope at 1588 and 1840 m bsl (Figure 2.10b), which are cutting IIIc and depositing sediments over younger conduits west of this channel. This segment, named IIId (19.3 km long) was cannibalized by the mass transport complex deposited between the interchannel lows (Ercilla et al, 2002a; Estrada et al., 2005b) (Figure 2.9c and 2.10c). The thalweg profiles show how the overall system becomes deeper towards the east. Figure 10c shows the well developed western levee, the filled thalweg of IIId and the migration of the system towards the east. This complex corresponds to Channel I, II and III of Ercilla et al.(2002a) and Estrada et al. (2005a).

2.4.3 CLC II

Towards the west on the fan, the next complex observed is CLC II (Figure 2.1). This complex is a prominent feature on the lower slope, on the CD40a seismic line (Figure 2.6). The upper slope section has been cut and/or buried by several younger mass flows and conduits (Figure 2.11a), which are covering the original morphology in this area. Thus no morphologic measurements could be made in this complex. The height and extension of the complex appear to be similar to CLC I on the lower slope

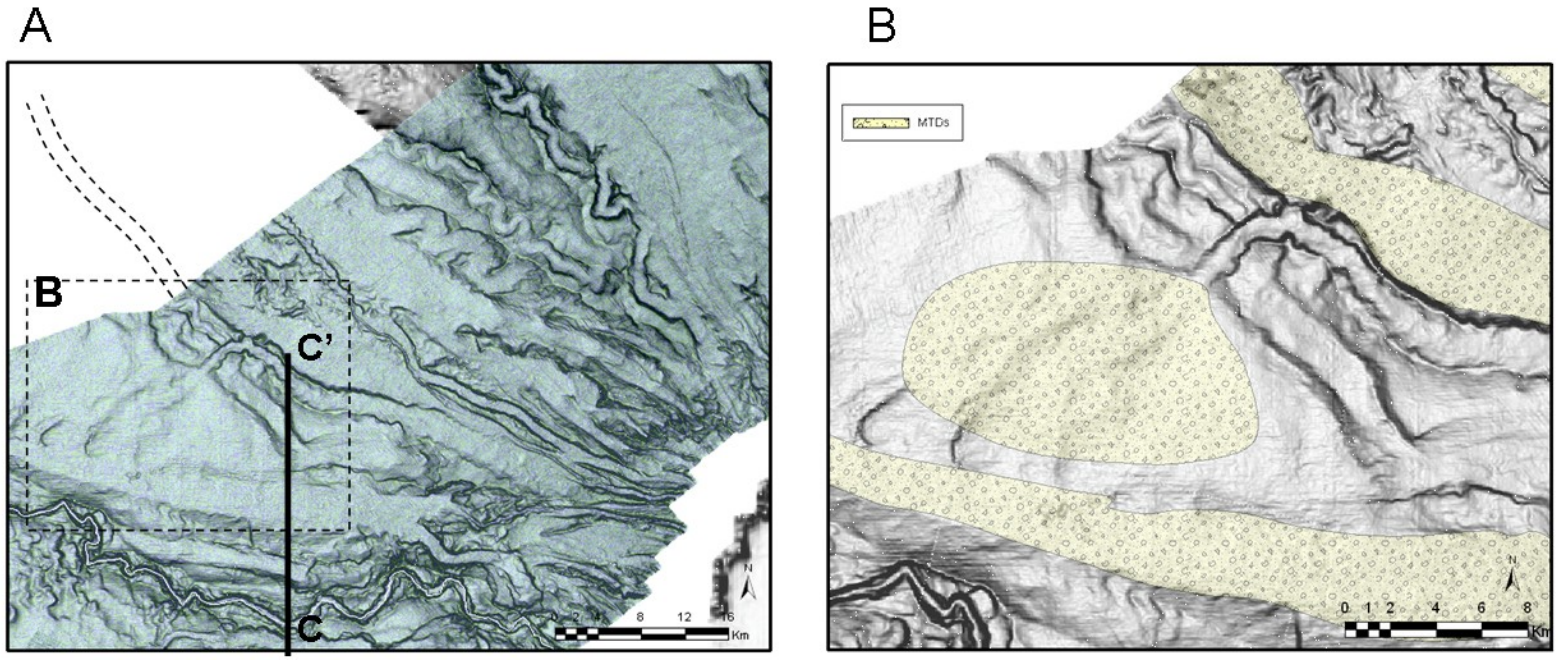


Figure 2.11. A. CLC II in map view. Bathymetry map (Curvature and Slope). Note how younger down slope flows are modifying the morphology of the system. B. MTCs that are modifying the slope morphology (Slope of bathymetry map).

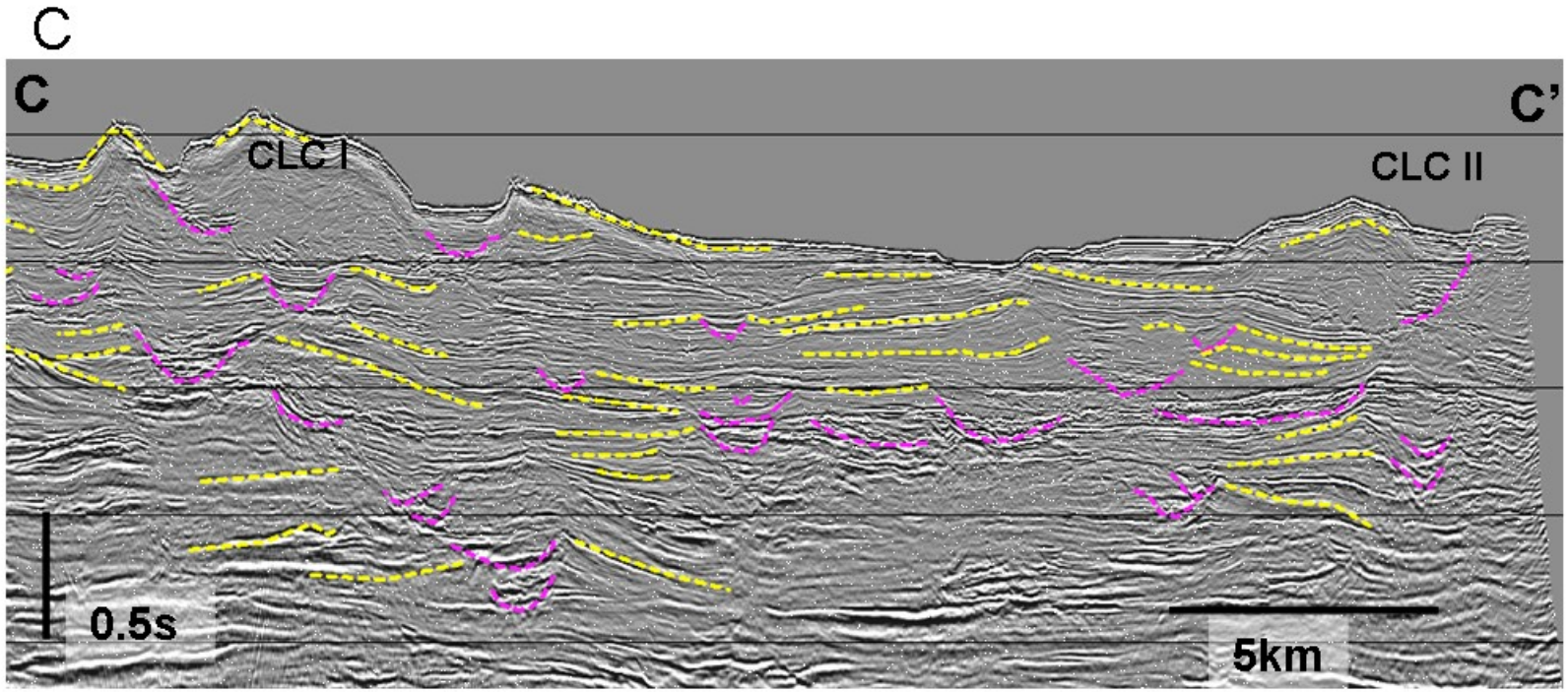


Figure 2.11.C. C-C' Seismic profile perpendicular to the flow direction. II buried morphology describe a probably sinuous channel system completely modified by post abandonment flows. Compare the size relationship between CLC I and II on Figure 2.6 A. Levees (Yellow), Channels (Pink).

(Figure 2.6), but smaller in size updip (Figure 2.11c). A prominent feature is the erosional conduit that follows the channel course but becomes diverted to the southwest, forming a lobate deposit in the interchannel complex low (Figure 2.11a,b).

2.4.4 CLC IIa and CLC IIb

As indicated in Figures 2.6 and 2.12a, younger deposition occurred to the west with CLC IIa and IIb downslope from the western side of the Galezamba shelf area. Down-cutting relationships on the seismic sections (Figure 2.12b) indicate that CLC IIa at 1700m bsl was deposited first. It developed a highly sinuous channel system (sinuosity up to 3.34) for a distance of 106.6 km mainly to the west. The middle section diverts towards the south and has an average width of 1.1km. Based on seismic interpretation, the complex is partially buried by continuous reflectors and mass transport deposits generated upslope. The morphology observed on the sea floor mimics the topographic highs at the time the channel was active (Figure 2.12b). CLC IIb can be recognized upslope at 1284m bsl. It is 45.8 km long and truncated by younger flows at 2281 mbsl. The width of the conduit varies from 2.2 km in the upper slope to 1.3 km in the lowest part of the system. CLC IIb is a very low sinuosity conduit when compared with the geometry of CLC IIa (Figure 2.12a). The higher sinuosity areas have values

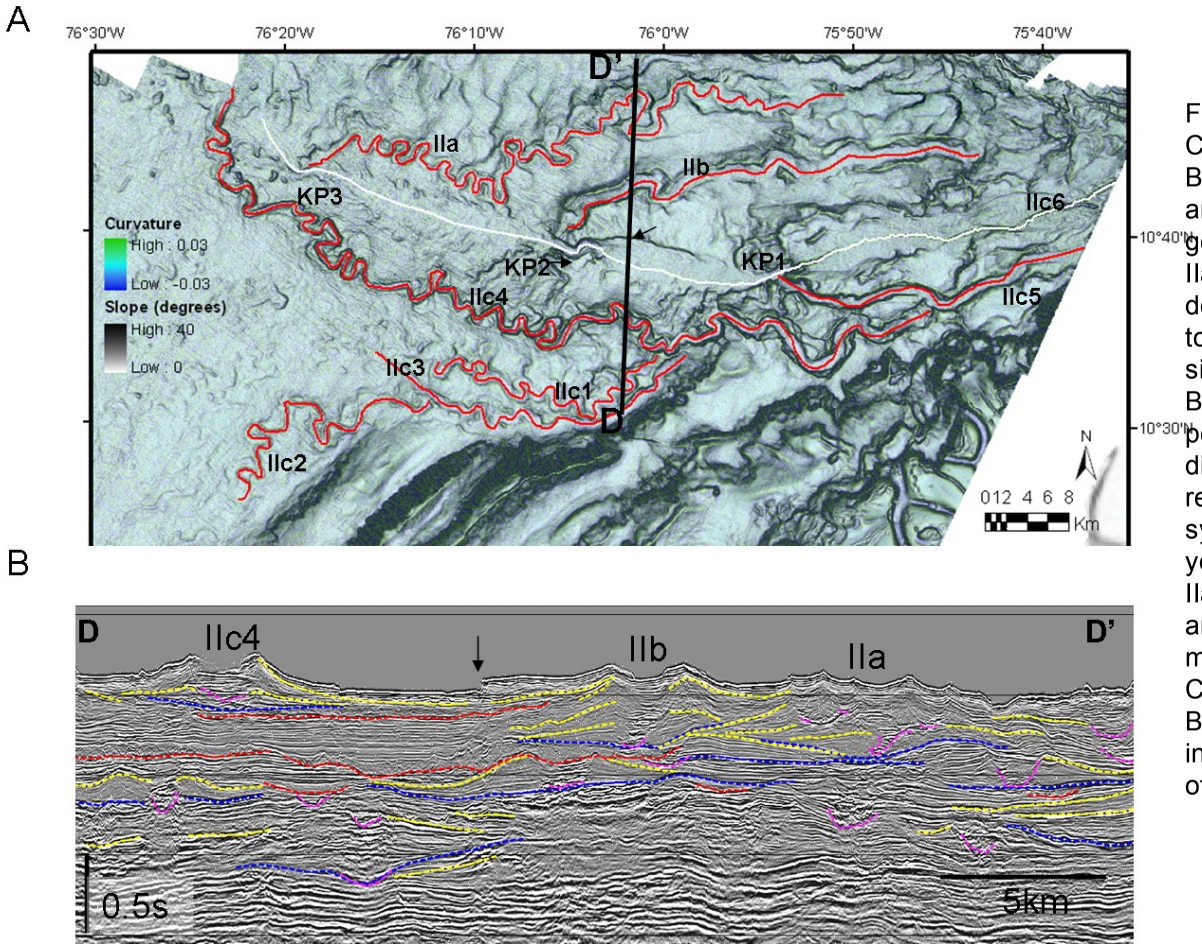


Figure 2.12 A. Location of CLC IIa, IIb, and IIc. Bathymetry map (Curvature and Slope). Referenced to the general context in Figure 2.1. IIa increases sinuosity downslope, with marked bend toward the west. IIb lower sinuosity than older CLC IIa. B. D-D' Seismic profile perpendicular to the flow direction. Clearly depicts the relative age of the different systems being IIc4 the youngest, between the three. IIa and IIb thalwegs are filled and morphology seems to be modified. Levees (Yellow), Channels (Pink), MTC (red), Base of channels (blue). Arrow indicates the erosive character of the flows going downslope.

of 1.16 and 1.46. Figure 2.12b clearly exhibits the relationship between CLC IIa and the younger CLC IIb. CLC IIb thalweg profile exhibits abrupt slope changes and some convex up sections (Figure 2.12c). Changes are particularly evident at the outer bends of CLC IIa. In comparison of the channel profile for these channels, CLC IIb has a much steeper slope than ChIIa (Figure 2.12c).

2.4.5 CLC-IIc

CLC IIc corresponds to the westernmost channel with morphologic expression on the seafloor today (Figure 2.1). The complex is recognized at the upper extension of the bathymetry survey (827 m bsl), reaching depths up to 3056 m bsl, and covering an area of 2600 km^2. The upper section of the slope is characterized by erosional canyons–channels, up to 2 km wide (Figure 2.8), which are controlled by the influence of the deformation front. CLS IIc1, IIc2, and IIc3 (Figure 2.12a) are remnants of the initial positions of the complex in the lower section of the slope. West of these CLS remnants is located CLS IIc4, the most continuous channel in the complex (Figure 2.12a).

CLS IIc1 is found at 1995 mbsl. It is 40 km long (preserved segment) and 1.1 to 0.9 km wide. CLS IIc2 is found at 2408 mbsl. The upper section is 42.7 km long, and width varies from 0.7 to 0.5 down slope. The lower

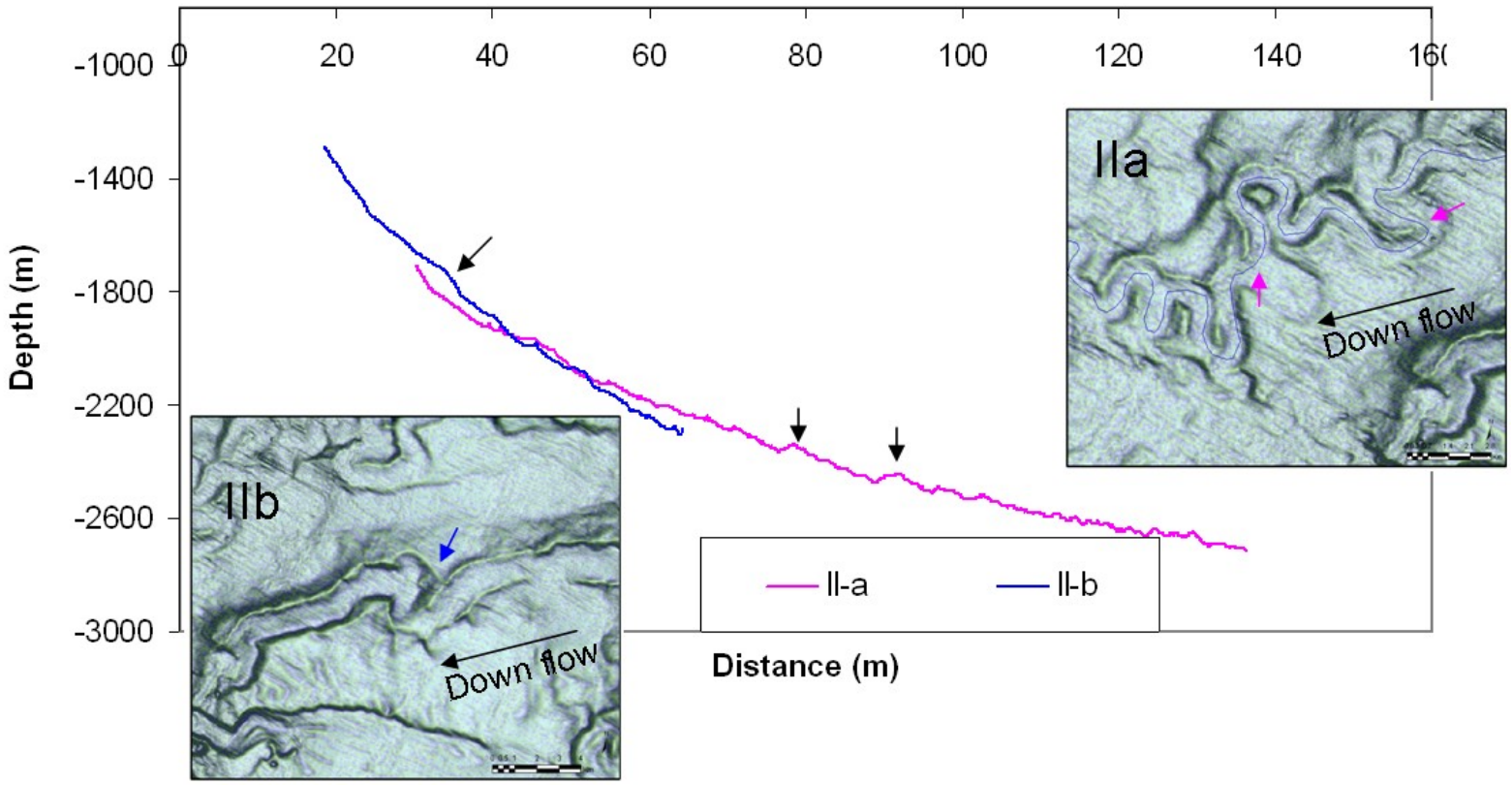


Figure 2.12 C. Thalweg profile for IIa and IIb. Black arrows in IIa profile are indicating areas of the channel (pink arrows) that have been modified by later flows. CLC IIb profile exhibits a concave up section that corresponds which is indication on the map.

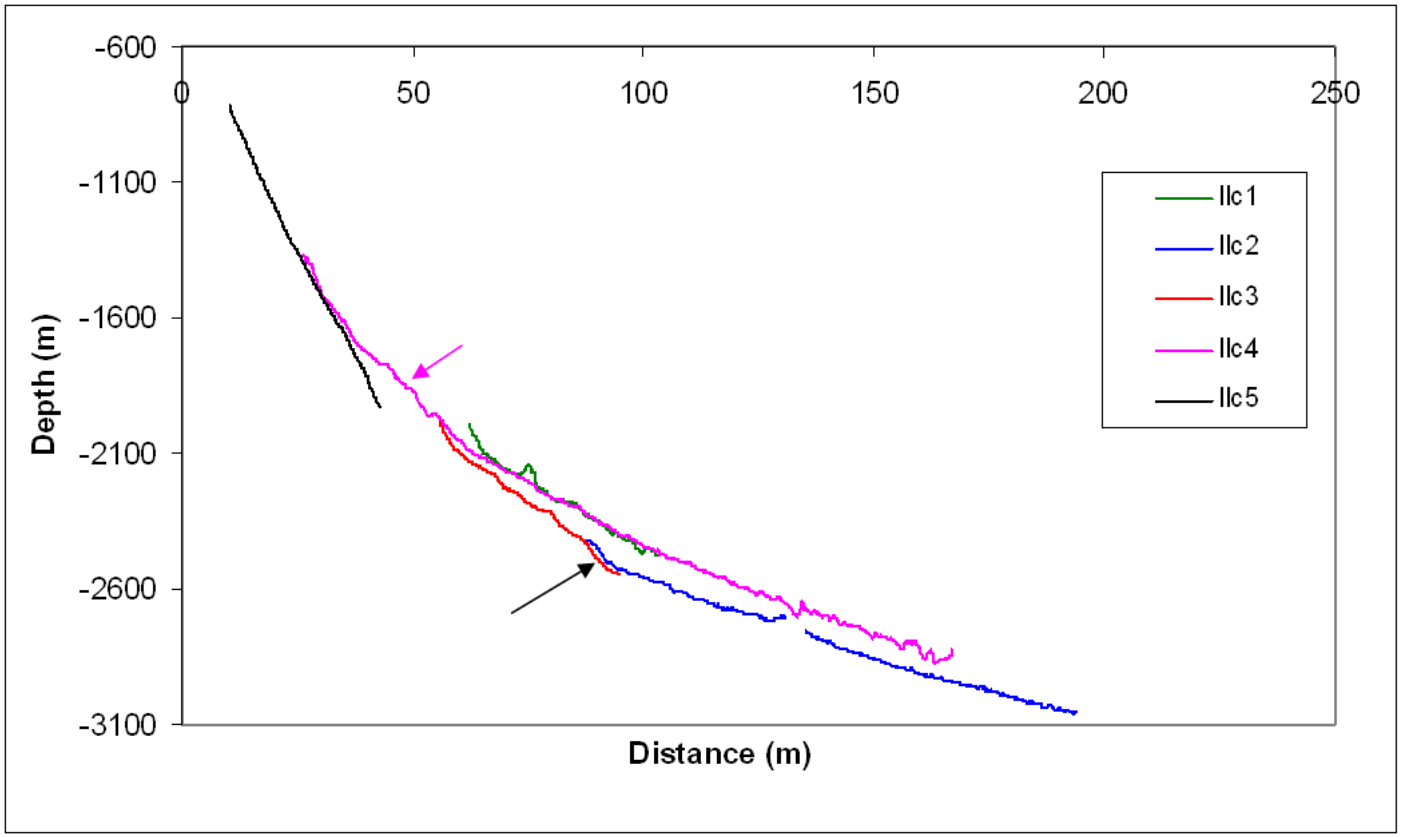


Figure 2.13. Thalweg profile of CLC IIc. IIc1, IIc2, IIc3, IIc4, IIc5 (Youngest) (Location of the channels Figure 2.12A). IIc1 shows an abrupt change in the profile due to later establishment of IIc3. The remnants of IIc2 exhibit a convex up profile at the encountering with IIc3 (Black arrow), which is also evident at IIc3. Note the convex up profile of IIc4 (Pink arrow) about 50 km, which may indicate deformation. Notice the fairly steep gradients of IIc5.

section is 62 km long and width is 0.7 km on average. Channels IIc1 and IIc2 have lower slope angles (Figure 2.13) and higher sinuosity (up to 2.8 and 3.5 respectively) than IIc3 (Figure 2.12a). The thalweg profile for IIc1 probably is more affected by the levees of the neighboring channels (IIc3 and IIc4) (Figure 2.14). CLS IIc2 thalweg profile is concave up with some irregularities with an abrupt slope change at 2440m bsl (Figure 2.13).

CLS IIc3 starts at 1960 m bsl as a fairly straight conduit (Figures 2.12a and 2.13). Increase in slope angle and sinuosity occur at 2160 m bsl. The thalweg profile shows these changes by convex up sections (Figure 2.13). A second convex up section is found at 2400 m bsl after which the thalweg becomes straight. The upper straight section of CLS IIc3 is parallel to the front limb toe of a thrust-fault ridge and is an erosional conduit (Figure 2.12a, 2.14d). The channel is affected by deformation observed in Figure 2.14e, where is part of the folded sequences.

CLS IIc4 is the most sinuous and therefore longest thalweg measured on the complex (140 km) (Table 2.2). The upper section (1300 to 2000 m bsl) of IIc4 has characteristics of an erosional channel –canyon with steep walls, U shape profile and 1.4 km width on average (Figure 2.8, 2.14 a,b,c). Despite the erosional nature of the canyon/channel, sinuosity values are up to 1.7(Figure 2.15). The lower section (2000 to 2800 bsl, 60km) channel becomes aggradational with development of levees (65m in height from the thalweg) (Figure 2.14 d,e,f) and higher sinuosity (up to 4) (Figure 2.15) with

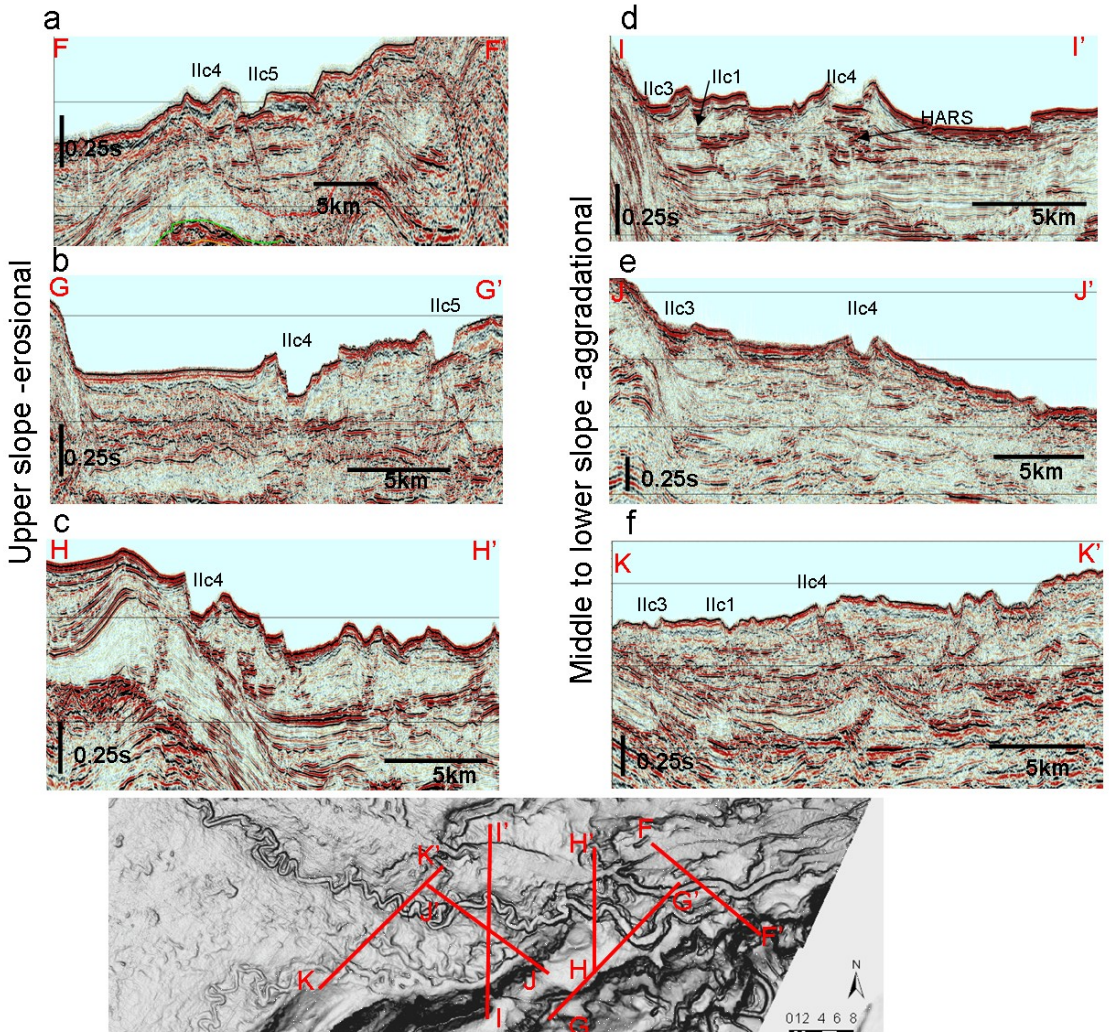


Figure 2.14. Series of seismic profiles showing the changes in morphology of CLS IIc4. Upper slope- erosional architecture (a,b,c) and Middle to lower slope-aggradational morphology (d,e,f). HARS are observed on the channel thalweg (d,e). C and E shows evidences of later slope deformation since the channel wedge is tilted

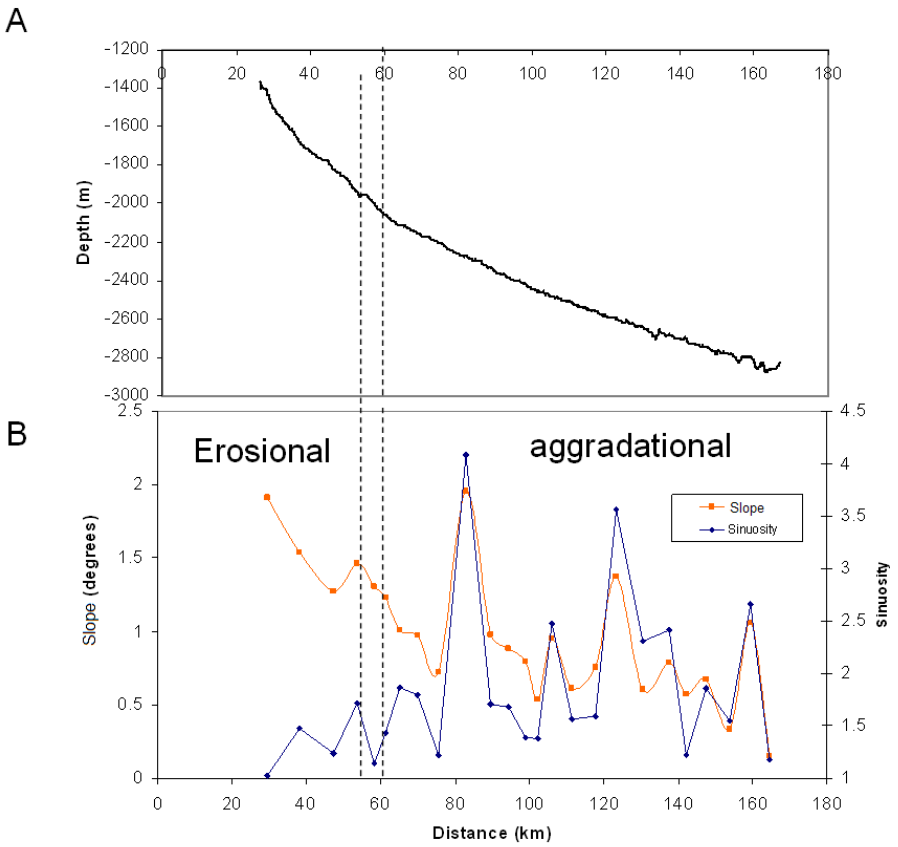


Figure 2.15. A. Thalweg profile for IIc4. B. Slope angle and sinuosity values for IIc4 thalweg. The overall slope tendency is to decrease down slope in the erosional upper section. But changes drastically in agradational lower section. The sinuosity values are high at the steep segments of the channel.

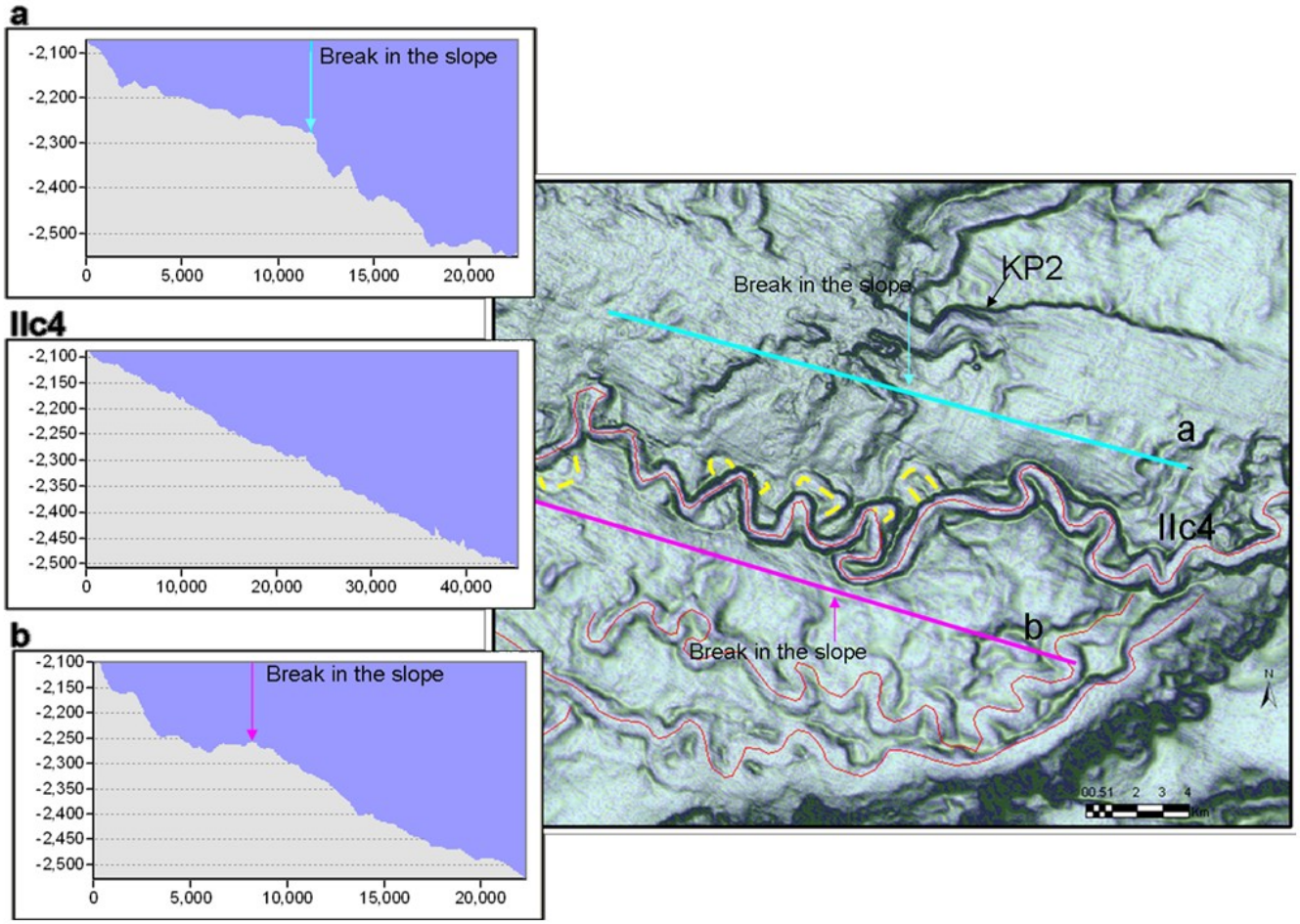


Figure 2.16. Channel system IIc4. Increase in sinuosity is observed to accommodate changes in the slope. a and b are showing the slope of near by areas and b is showing the thalweg profile. Additionally a series of cut-offs loops are observed in this segment (yellow dashed

several cutoff loops (Figure 2.16). The deeper section of the channel (~3000 bsl) broadens and appears to have migrated toward the north, abandoning the main channel. This CLS is similar to the Pleistocene Borneo channel described by Posamentier (2000). The thalweg profile is mainly concave up (Figure 2.15a), with some erosional cuts at the lower section and some bends of the channel. Around 1700mbsl the profile is convex up, which corresponds to the erosional section of the system (Figure 2.15a). High-amplitude reflections (HARs) are found at the channel thalwegs (Figure 2.14d). Channel wedges are tilted indicating post-depositional deformation (Figure 2.14e).

CLS IIc5 is a younger avulsion of the system (Figure 2.12a). It is a 32.8 km long erosional channel /canyon that cut IIc4 and that is covered by younger deposits downslope. It has a “U” shape with steep walls of 100m height and approximately 2 km width (Figure 2.8, 2.14a and 2.14b). The conduit sinuosity reaches values of 1.14. The thalweg prolife is very steep and convex up in the lower section (Figure 2.13).

2.4.6 CLC-I

CLC I is the youngest levee complex on the modern seafloor based on the overlapping relationships on seismic and seafloor morphologies (Figure 2.6, 2.17). It represents a prominent feature on the slope with levee heights up to

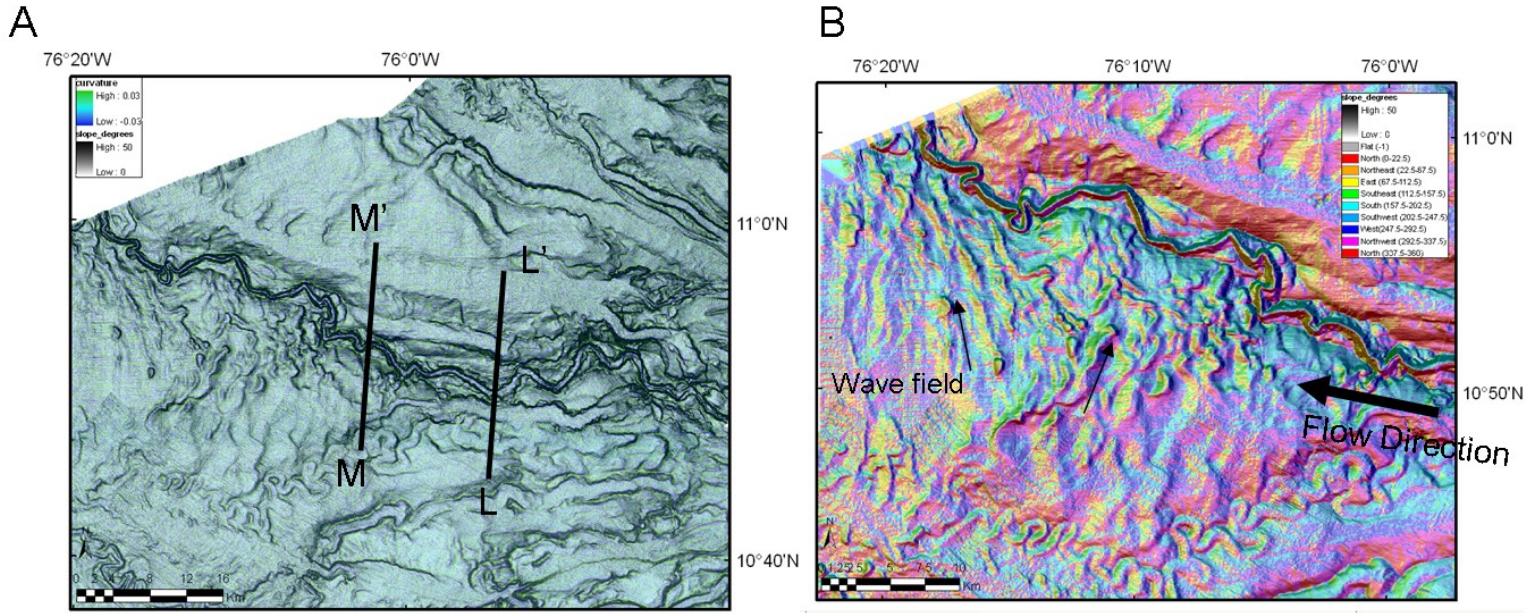


Figure 2.17. A. CLC I in map view. Bathymetry map (Curvature and Slope). Note how younger downslope flows are modifying the morphology of the northern levee/overbank. Referenced to the general context in figure 1. B. Azimuth map displaying the wave field at the southern levee/overbank of CLC I. Arrows are parallel to the two main directions.

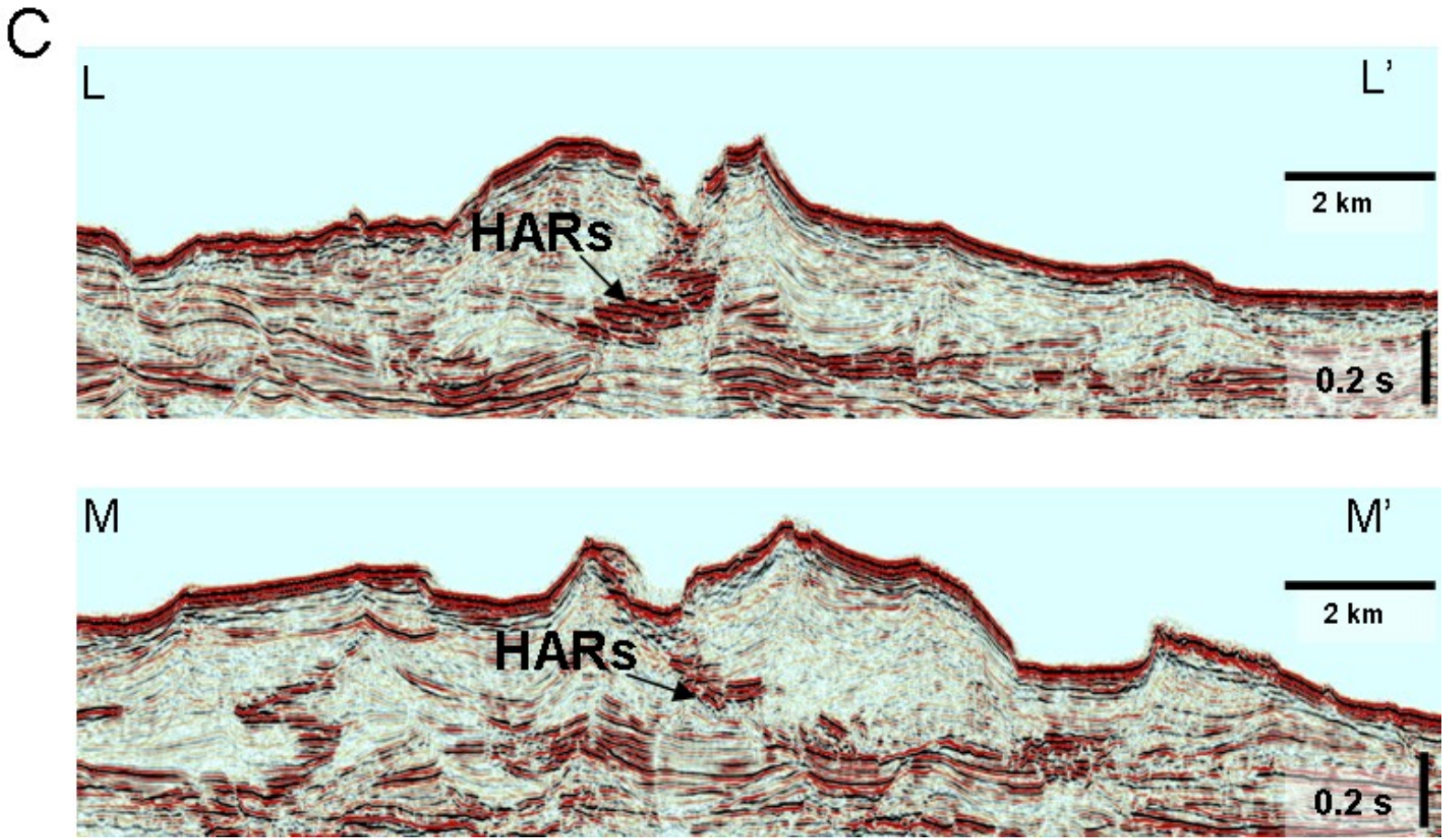


Figure 2.17.C. Seismic profiles showing the changes in morphology of CLS I down slope. HARS are observed on the channel thalweg. (Location of seismic profiles Figure 2.17A).

120m. The thalweg profile is concave up with steeper slopes on the bends of the channel making the profile irregular (Figure 2.18a). The shape of the channel is a “V” form on the upper slope (900 to 1300 mbsl), then broadens down slope to a “U” form down to 2100 mbsl were it becomes narrower (Figure 2.8). Average width is1.6 km. Seismic profiles indicate a wider thalweg for younger stages of channel growth, with the presence of HARs (Figure 2.17 c). The overall slope angles decrease down slope, but local highs correspond to high sinuosity values (Figure 2.18b). The average sinuosity is 1.4 with values up to 3.6. The southwestern overbank of the complex exhibits sediment waves (Figure 2.17b). The azimuth map shows a conjugation of wave systems towards the southeast and south probably generated by turbiditic flows overtopping the outer bend levees by flowstripping (Piper and Normark 1983; Imran et al, 1999; Posamentier, 2003).

The northeastern overbank is covered by mass transport deposits that fill the interchannel lows (Figure 2.17a). The levee height reaches up to 175m (average values of 120m). This is at least three times higher compared with the other levees in the fan. This system shows intrachannel terraces which are more common in the upper section of the channel (1000-2000m bsl, Figure 2.8). This is the only complex on the fan that is composed of a single system. The only possible avulsion point is located close to the edge of the

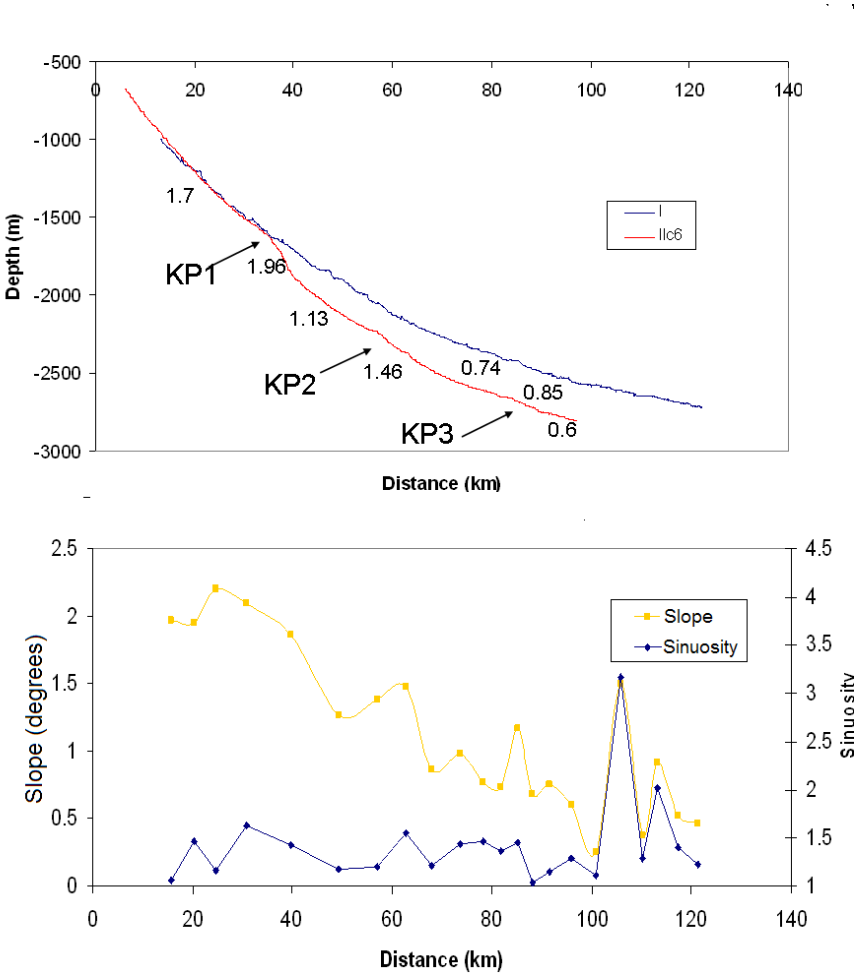


Figure 2.18. A. Thalweg profile for I, overall concave up, but with some local convex up sections (e.g. 40km). It is also displaying the profile of the conduits jointing the knickpoints in Figure 2.21. B. Slope and sinuosity values for I Thalweg. The overall slope tendency is to decrease in angle down slope, with some sections of steeper slopes. The sinuosity higher values coincide with these steep segments of the channel.

survey, although downslope avulsion beyond the area mapped may be possible.

2.4.7 Active Magdalena Fan

In active fan (eastern area) sediments are transported into the slope and abyssal plain through a series of canyons that are in communication with the Magdalena River mouth. (Canyons U,S,M,D, Figure 2.1, 2.4, 2.19a). The Magdalena Canyon is a prominent feature on the slope directly connected with the current Magdalena River. The canyon presents a maximum incision of 260m, is 2.5 km wide on average, and has a sinuosity index of 1.22. The general form is a wide V-shaped canyon with some areas of higher confinement (Figure 2.19b). The vertical profile shows more irregularities the first 10km up slope and a smoother profile downslope (Figure 2.19c). Collapse scours are common on the northeastern wall of the channel. The channel extends down slope about 30 km before it reaches a step in the slope where it converges with the U and Sabanilla canyons to continue down slope (Figure 2.19b). The U canyon is located 10 km seaward of the shelf break and is not connected to any present drainage. It is a tributary network of small gullies, which develop a channel-like feature at the change in slope. It is 1.2 km wide with maximum incision of 80 m. Sabanilla canyon is the westernmost canyon. It is a narrower feature (1.4 to 0.6 km wide) with 120m of maximum incision. The head of the canyon is connected to the

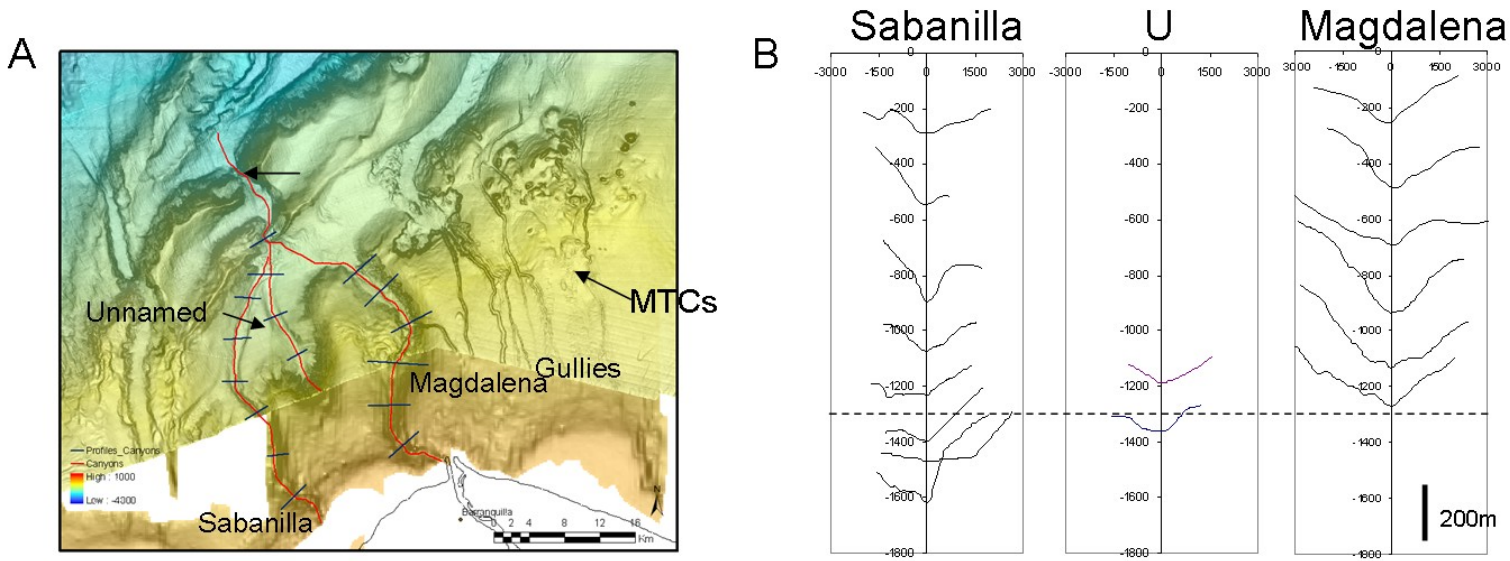


Figure 2.19. A. Active Fan bathymetry map. Referenced to the general context in Figure 2.1. B. Canyon profiles measured every 5 km. Vertical scale depth (below sea level). Sabanilla canyon change its morphology once reaches the low section of the slope (piggyback basin). Magdalena canyon describes a wider channel with an entrenched thalweg. Arcuate scarps and creeping can be observed in the canyon walls. East of the Magdalena canyons channel/ gullies and mass transport complexes are observed. C. Canyon thalweg profiles. Active Magdalena canyon depicts a fairly smooth profile with some area where is convex up (Ridges sections). Sabanilla and the U canyon profiles are parallel.

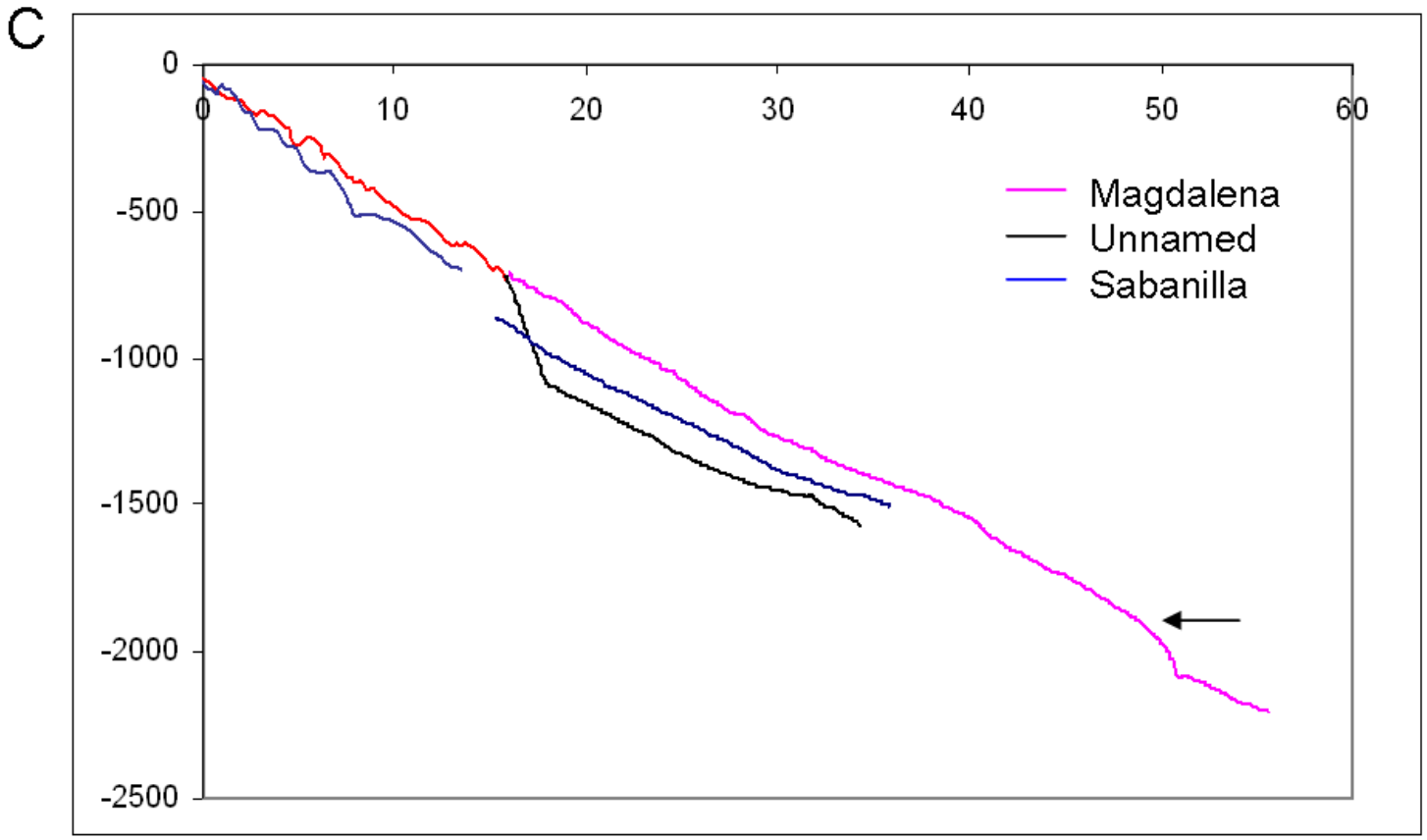


Figure 2.19. C. Canyon thalweg profiles. Active Magdalena canyon depicts a fairly smooth profile with some area where is convex up (Ridges sections). Sabanilla and the U canyon profiles are parallel.

shelf break and extends 20 km seaward before it connects with the other canyons. The “V” canyon geometry is lost once it reaches the step on the slope (Figure 2.19b).

East of the river mouth a series of slope channels or gullies are recognized (Figure 2.19a) (sensu Posamentier et al, 2003) which connect down slope to the Magdalena Canyon or a slump feature to the west. Mass transport deposits also occur. Numerous submarine cable breaks in the Magdalena River mouth area were reported in the 1950’s (Heezen, 1956a) indicating active sediment gravity flows moving through the canyons. Detailed description of active deposition on the Magdalena Fan is presented in Chapter 3.

2.5 KNICKPOINTS

A Knickpoint is defined as a steep gradient section between lower gradient sections; therefore correspond to a disruption in the equilibrium profile, first defined for fluvial systems (Howard et al., 1994). The western upper slope (between IIc and IIb) (Figure 2.12a and 2.20) displays a series of knickpoints (KP) at areas with a change in slope separated by lower slope steps (Figure 2.18a and 2.20). KP -1 is located 38 km downslope from the shelf break at 1650 mbsl, where it intersects CLS IIc5. KP1 is an erosional feature 1.1 km wide and at 130 m in height. Upslope from the knick point it

is possible to follow a channel or gully (IIc6) cutting a section of the slope covered by unconfined flows, slope angles of 1.7° (Figure 2.18a). IIc6 (Figure 2.12a) is a fairly young conduit that cut the slope until it encountered KP1. The slope profile defines an increase in the slope angles and a convex up morphology downslope (Figure 2.18a).

Downslope of KP1 is a lower slope angle area (1.13°) (Figure 2.18a), down to KP2 at 2290 mbsl (at 16 km from KP1) (Figure 2.20). KP2 is 1.2 km wide, with 90m height. An important characteristic of this knickpoint is the presence of sinuous bends in the area of higher slope angles (1.46°) (Figure 2.20). KP3 is found at 2720 mbsl (23.4 km from KP2 base), with a height of 60 m and variable width from 0.4 up to 0.8 m. This is a less entrenched feature with a minor slope angle change to 0.85 ° (Figure 2.20).

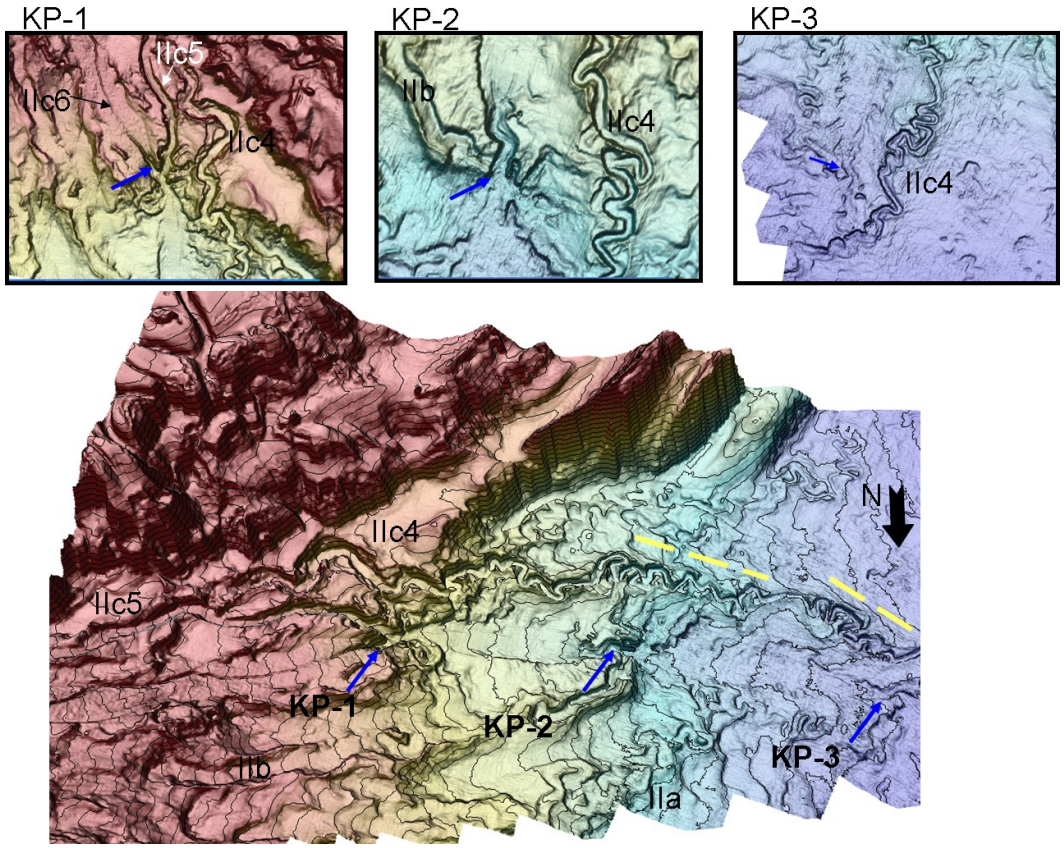


Figure 2.20. Knickpoint sequence. 3D bathymetry of the western deformed belt area. A series of knickpoints on the slope are located in areas with abrupt changes (steps) followed by low gradient areas. Lobate shapes at the toe of the knickpoints. Some of these lobes present erosional cuts. IIc6 conduit seems to be connecting all the knickpoints through the slope. Upper figures are the frontal view of the knickpoints (blue arrow). It is important to notice the sinuous morphology that KP2 exhibit. The steps on the slope coincide with IIc4 higher sinuosity zones (yellow lines). Profile of the knickpoints (IIc6) is shown in Figure 2.18A.

2.6 MAGDALENA RIVER DELTA PHASES – SUBMARINE FAN MIGRATION

The seafloor morphology and the apparent migration of the river course through time confirm a close relationship between the Magdalena River and the fan. Sedimentation rates increased during the last 2-4 Ma in many continental margins (Hay et al, 1988; Pelzhen et al, 2001) including the offshore Caribbean sector (Bordine, 1974; Duque-Caro, 1984). The Magdalena Fan is mainly fed by the sediments transported in the Magdalena River load, therefore the sediment depocenters shift laterally as the source of sediments and/or their feeder channels change course with time. In this paper the nomenclature proposed by Pirmez et al. (1990) was used which described the present day sea floor expression of the channel levee complexes with the associated river/delta phases (Table 2.2). Beside the evidence found in the outcropping deposits onshore, the shelf morphology reveals the past locations of the river mouth. The delta formed by the river creates a series of lobes widening the shelf, such as at the Galerazamba area (Figure 2.1).

At least eight different positions of the river mouth have been recognized for the Plio-Pleistocene time interval (Table 2.2, Figure 2.3). Late Miocene through Pliocene phases (Sucre & Plato and Phase E) are buried in the slope area, but are the most prominent land features. The area south

Phase	River / Delta	Channels	Time	Migration
A	Barranquilla - Boca Vieja	U,S,M,F	Late Holocene -Present	West
B			Early Holocene (to -5kybp)	East
C	North of Cartagena	I	Late Pleistocene	East
	North of Cartagena	IIb	?Late Pleistocene	East
	North of Cartagena	IIa	?Late Pleistocene	East
D	South of Cartagena Dique Canal		Mid Pleistocene	West
	North of Cartagena	II	?	West
Eb	Galerazamba	III	? Mid Pleistocene	West
Ea	Pto Colombia	IV, V	Early Pleistocene	West
E	Luruaco	>V (Buried)	? Late Pliocene	West
	Sucre& Plato		Late Mio-Pliocene	

Table 2.2. Summary of Evolution of the Magdalena fan.

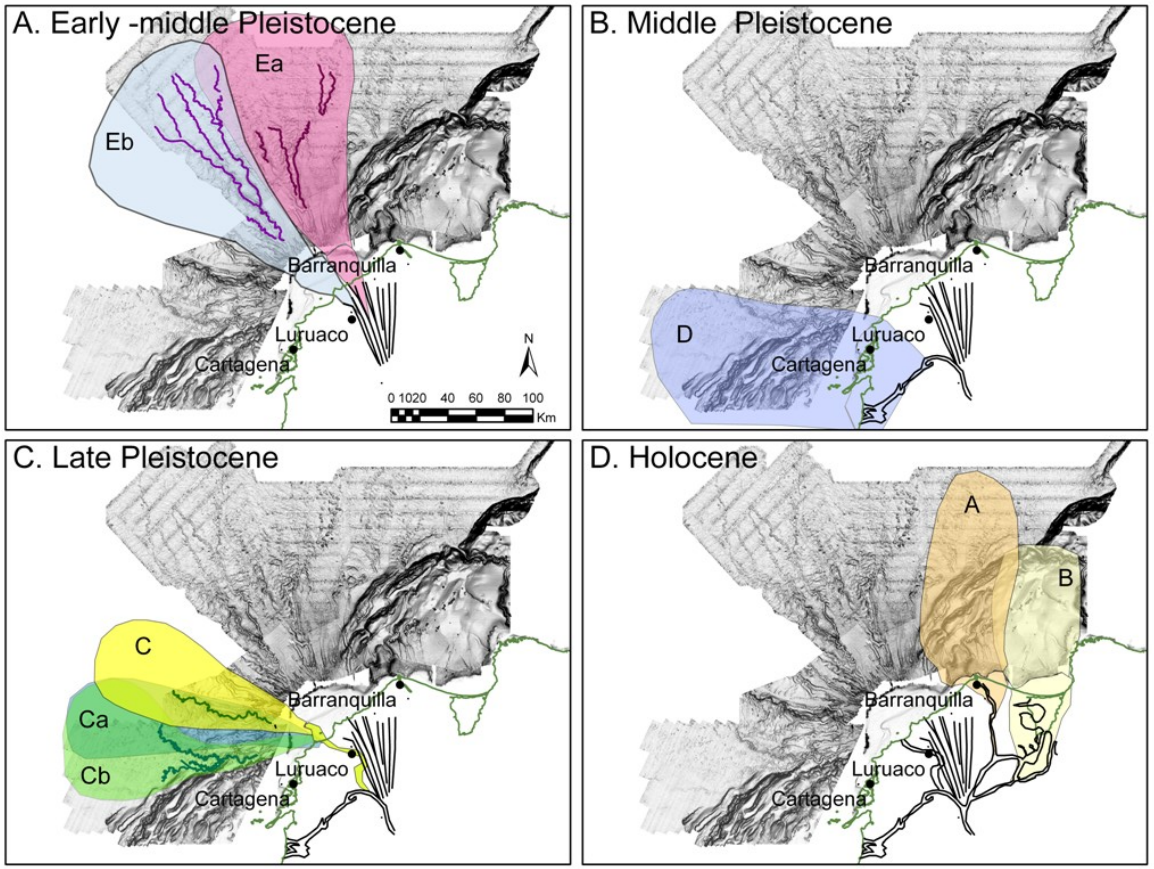


Figure 2.21. Evolution of the Magdalena fan, A. Early to middle Pleistocene produce phase Ea (CLC IV) and Eb (CLC III), B. middle Pleistocene produce phase D., C. late Pleistocene phase Ca,Cb,C, . D. Holocene produces phase B and phase A (Active fan).

of the present Magdalena River, comprised of marginal shallow marine sediments (Figure 2.3) (Bordine, 1974).

2.6.1 Phase Ea

The Early Pleistocene river mouth (Phase Ea) was located near Puerto Colombia, west of the present river location. It generated deposits that correspond to channel levee systems (CLC) IV and V. It is the oldest phase which has an apparent expression on the seafloor morphology (Figure 2.21a).

2.6.2 Phase Eb

During the middle Pleistocene (Phase Eb) the river mouth migrated to the southwest, towards the Galerazamba region, generating CLC III (Figure 2.21a).

Further westward, migration of the river mouth resulted in CLC II deposits. It is not possible with the available information to define whether these deposits correspond to a delta phase before the main shift to the southwest (D?) or the early stage of phase C (Before deposition of CLC IIa).

2.6.3 Phase D

Phase D is the product of continued migration of the river towards the south to the Canal del Dique. Mid Pleistocene sediments were deposited in the thrust belt area (Figure 2.21b), which corresponds to the southernmost position reached by the river. This phase generated deposits that were progressively deformed by the growth of the deformation front. It is possible that the nearby Sinú River delta exerted strong influence on the deposits generated at this phase. No CLS are recognized at the sea floor in this area in part due to the high input of recent sediments by the Sinú River (Pujos & Javelaud, 1991). This major shift is supported not only by the remnants of a paleo channel onshore, but also by establishment of the La Popa formation coraline limestone, which would require low influx of terrigenous sediments in the northern coastal area (Bordine, 1974; Reyes et al., 2001).

2.6.4 Phase C

During the Late Pleistocene, the river mouth switched north of Cartagena to develop Phase C, depositing fans that are overlapping and generating CLC IIa, IIb, IIc and I, from older to younger, with CLC I being the most recent on the entire submarine fan (Figure 2.21c). This area of the fan presents a dynamic interaction between deformation and sedimentation, which can be evidenced by the abrupt changes of orientation and sinuosity of the

channels and thalweg profiles. In CLC IIc4 highly sinuous segments and a series of cutoff loops are present where the slope has higher angles (Figure 2.16). The channel accommodated the change in slope by bending the course of the channel, trying to maintain the equilibrium profile (Pirmez et al., 2000; Deptuck et al.,2007). CLC-I presents higher slope angles at the bends of the channel and the sinuosity morphology is similar to the younger erosional cuts north of the channel at the upper slope (Figure 2.12, 2.16).

2.6.5 Phase B

Due to late stages of deformation during the late Pleistocene, the river course was modified as a response of the Atlantico-Turbaco Hills Uplift, causing a major depositional shift towards the east and northeast (Hoover and Bebout, 1985) (Figure 2.21d). This shift generated phase B, depositing sediments in the Cienaga de Santa Marta area, and creating an expansion of the continental shelf. The Sierra Nevada de Santa Marta drainage system should have been an important source of sediments for this area as well. A major decrease in carbonate concentration in the Colombian basin at 6000 year b,p. (Prell, 1978), may be related to the shift of the Magdalena River towards the east during this time.

2.6.6 Phase A

During the Holocene phase A the river began to migrate westward once again (Figure 2.21d). During the last century the river has switched positions initially to the Boca Vieja and Sabanilla canyon, then to its present position (Heezen, 1956; Bordine, 1974) generating a delta lobes in the shelf area (Figure 2.1). This late Pleistocene and Holocene Magdalena River to the west did not build large leveed channels. Deposition was dominated by slumps/ debris-flow fill into the slope valleys in the thrust-dominated region and overflowing to the abyssal plain. Several canyons are driving the present day sediment load down slope (Heezen, 1956; Hoover and Bebout, 1985). With almost no development of a shelf, the sediment load is transported down slope through canyons and gullies and emplaced as gravity flow deposits filling the basins on the submarine fold and thrust belt. Additional sediments were remobilized and deposited through this canyon by the longshore current that fluctuates NE-SW and SW-NE under the effect of the intertropical convergence zone (ITCZ) (Pujos et al, 1986) that seems to have been established with the closing of the Panama Isthmus 2.4Ma.

2.7 DISCUSSION

2.7.1 Degradation Processes on the Channel Systems

After abandonment of the river delta, submarine fan channel systems are exposed to degradational processes such as: 1) erosion of the CLS by mass transport deposits; 2) Collapse of channel walls and levees; 3) modification of levee morphology.

Erosion of a CLS by mass transport is a common process on the fan. Several MTCs are generated on the upper slope, which erode the antecedent deposits while traveling down the slope and finally filling interchannel lows. Some of these events in the eastern fan (CLC III and IV) were identified by Ercilla et al. (2002a) and Estrada (2005) (Figure 2.1 and 2.4). The western fan section (CLC II, IIa, IIb, IIc and I) exhibits MTCs at the interchannel lows as well, but at a smaller scale (Figure 2.4). Collapse of the channel walls and levees is an important process in some of the systems. The channel displayed on Figure 2.22a depicts collapse scarps at both margins. Figure 2.22b indicates collapse of the CLC I levee walls, such as to form a canyon downslope with parallel and similar sinuosity of CLC I.

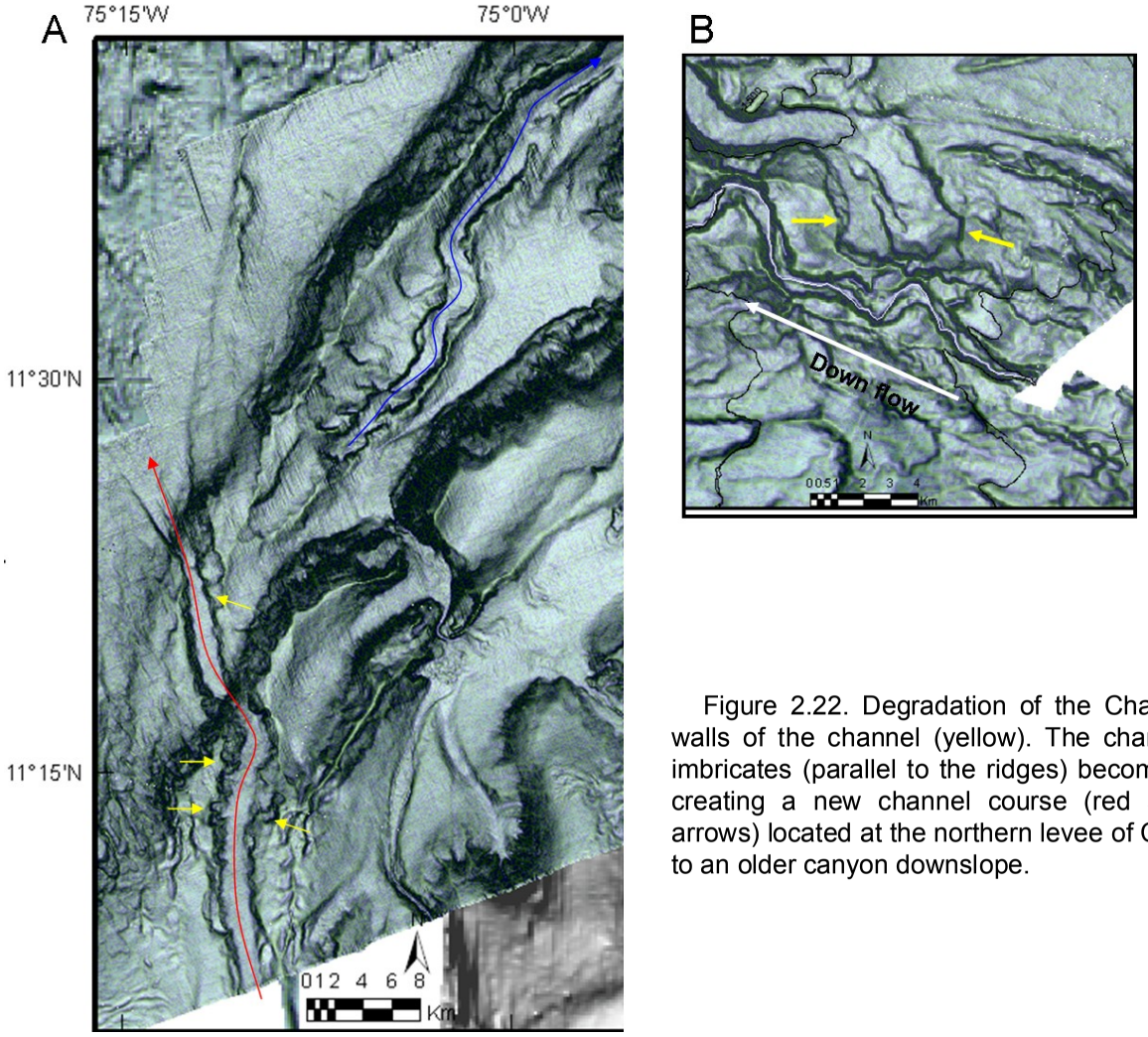


Figure 2.22. Degradation of the Channels A. Arcuate scarps at the walls of the channel (yellow). The channel was affected by the thrust imbricates (parallel to the ridges) becoming beheaded (Blue arrow) and creating a new channel course (red arrow). B. Major scarp (yellow arrows) located at the northern levee of CLC I . The scarp was connected to an older canyon downslope.

Modification of original levee morphology occurred in the older systems at the eastern part of the fan (Figure 2.8). Older channels are reworked by opportunistic mass transport flows traveling down the slope, taking advantage of the abandoned channel course and modifying the pre-existing morphology. The height of the levees is very variable and the thalweg profiles are very rough, as shown by CLC II (Figure 2.8). Seismic profiles (Figure 2.6a and 2.11c) exhibit well developed levees similar to CLC III or CLC I, with lateral migration of the thalweg (probably high sinuosity) at depth. But the sea floor morphology is very different, characterized by low sinuosity, remnants of levees, and loss of channel character upslope (Figure 2.11a).

A similar process is observed in CLC IIb. The geometries of the channel bends seem to be modified by younger flows that were channelized through the abandoned course (Figures 2.12a, 2.b and 2.c). As a result of these changes in the morphology, the channel could increase in dimension or straighten leading to erroneous assumptions about the size and capacity of the flows if evaluating channels in the subsurface. On the lower slope, modification of the morphologies could be associated with reworking of the channels by ocean bottom currents (Ercilla et al., 2002b).

2.7.2 Influence of Tectonics on the Magdalena Deepwater Fan

2.7.2.1 Sedimentation vs. Structural Setting

Slope angle is one of the factors that regulates the channel morphology, as well as channel maturity and variation of flow characteristics such as current energy, flow volume, and sediment load (Babonneau et al., 2002). Turbiditic systems in active tectonic settings evolve as the slope angle is continuously modified by major compressional events. Consequently, sedimentation style is modified as well. Compressional structures orthogonal to channels seem to cause large changes in the channel profiles as has been observed in the thrust front of the Barbados accretionary prism (Huyghe et al, 2004) and the growth fold in the western Niger delta (Heiniö and Davies, 2007).

The western compressional belt structures are almost orthogonal to the CLS axis (Figure 2.23a). Interaction of the deformation and the channels seems to be present during different phases of evolution of the fan. Some of the evidence can be identified directly by changes in sinuosity and slope angle of the channel systems (e.g. Figures 2.15 and 2.16) or on the adjacent slope by formation of knickpoints and steps (Figure 2.12, 2.16 and 2.20).

Some of the thrust imbricates and fold geometries with expression on the sea floor extend into the slope, underlying and deforming the fan sediments (Figure 2.23a and 2.24a). Some of these structures are actively

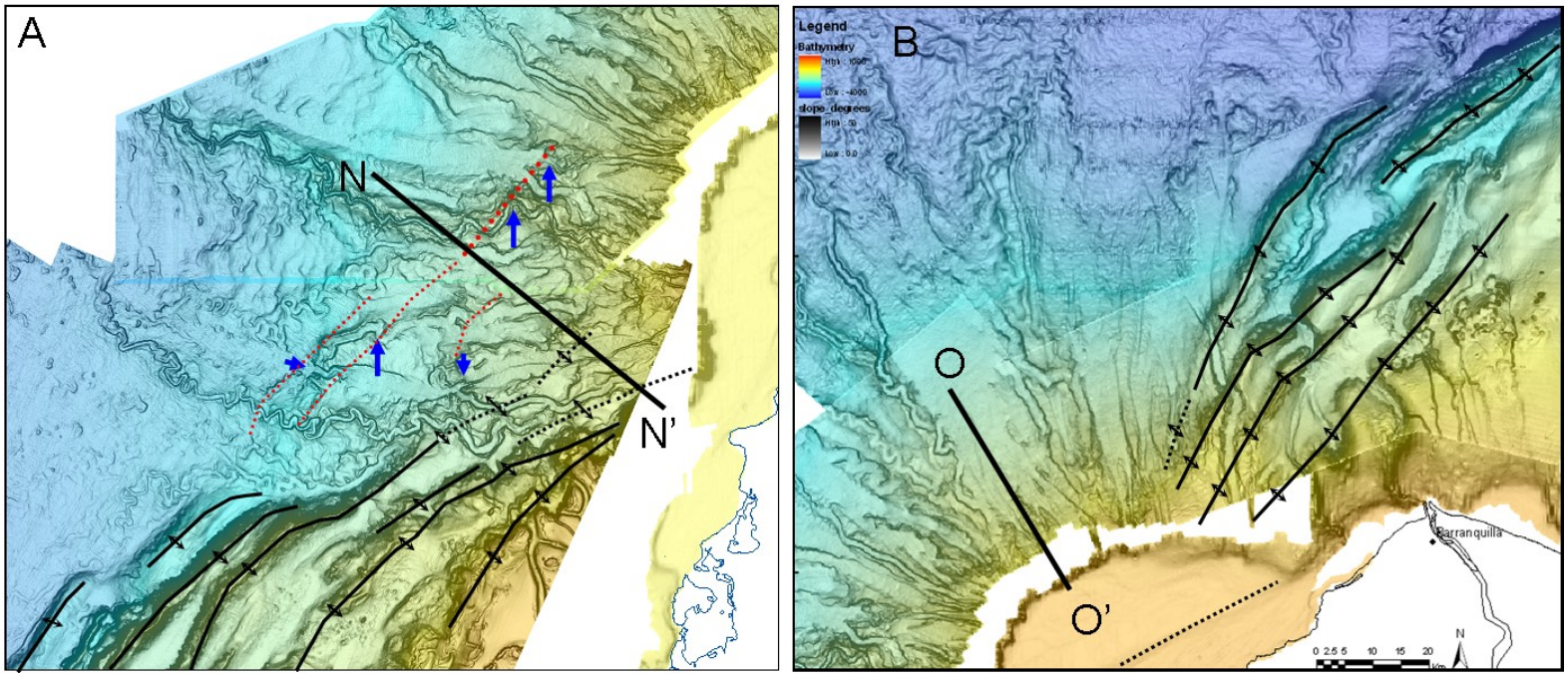


Figure 2.23. Major fold axis and alignment of knickpoints and channel bends on the southwestern fan. Continuous black lines are folds associated with thrust imbricates with seafloor expression. Dashed black lines are deeper fold geometries. Red dotted lines are possible faults. Knickpoint are highlighted with blue arrows.

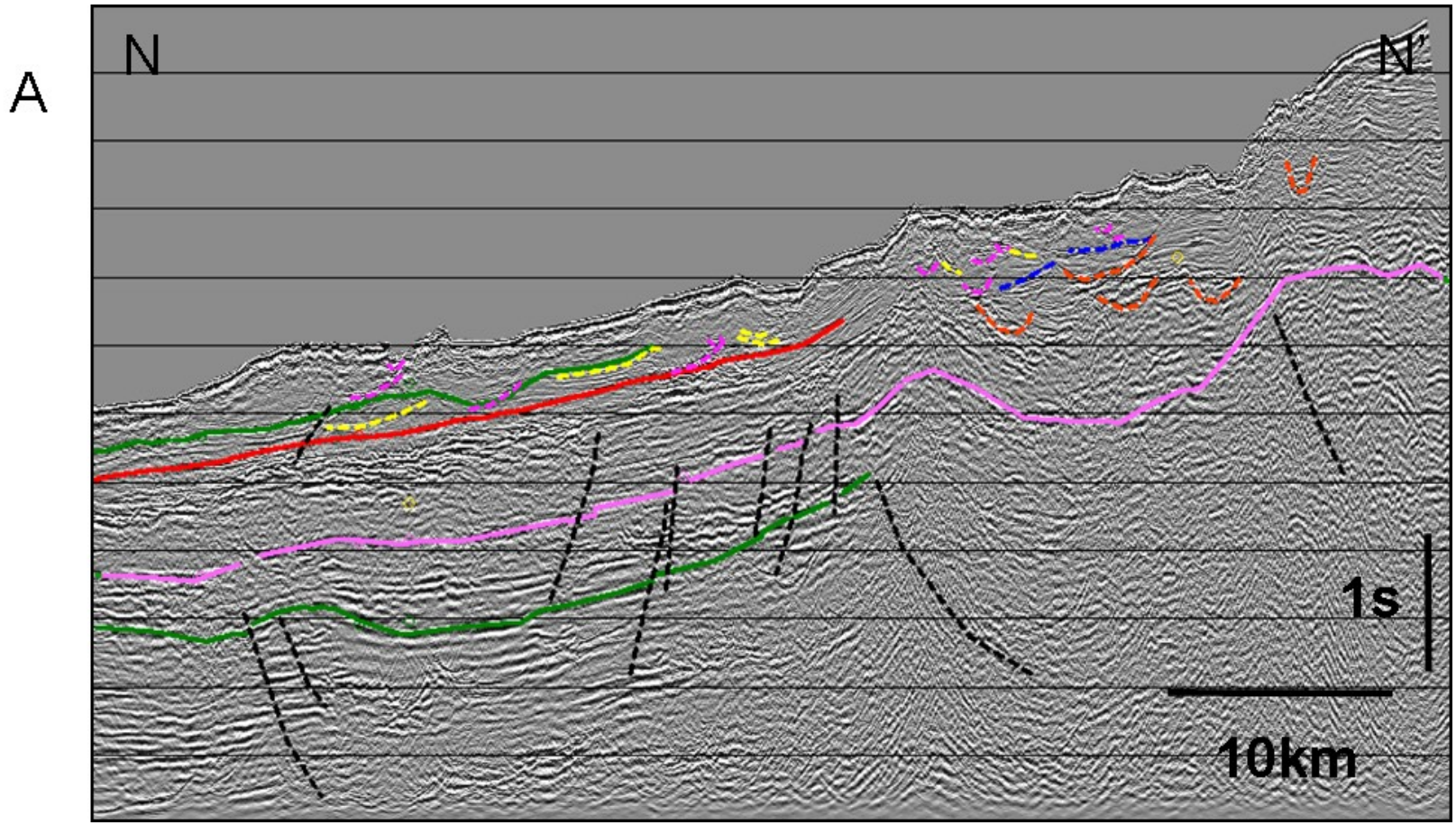


Figure 2.24. A. Western fan underlying deformation. Thrust faults, related fold and normal faults seem to be playing an important role in the development of high sinuosity channels.

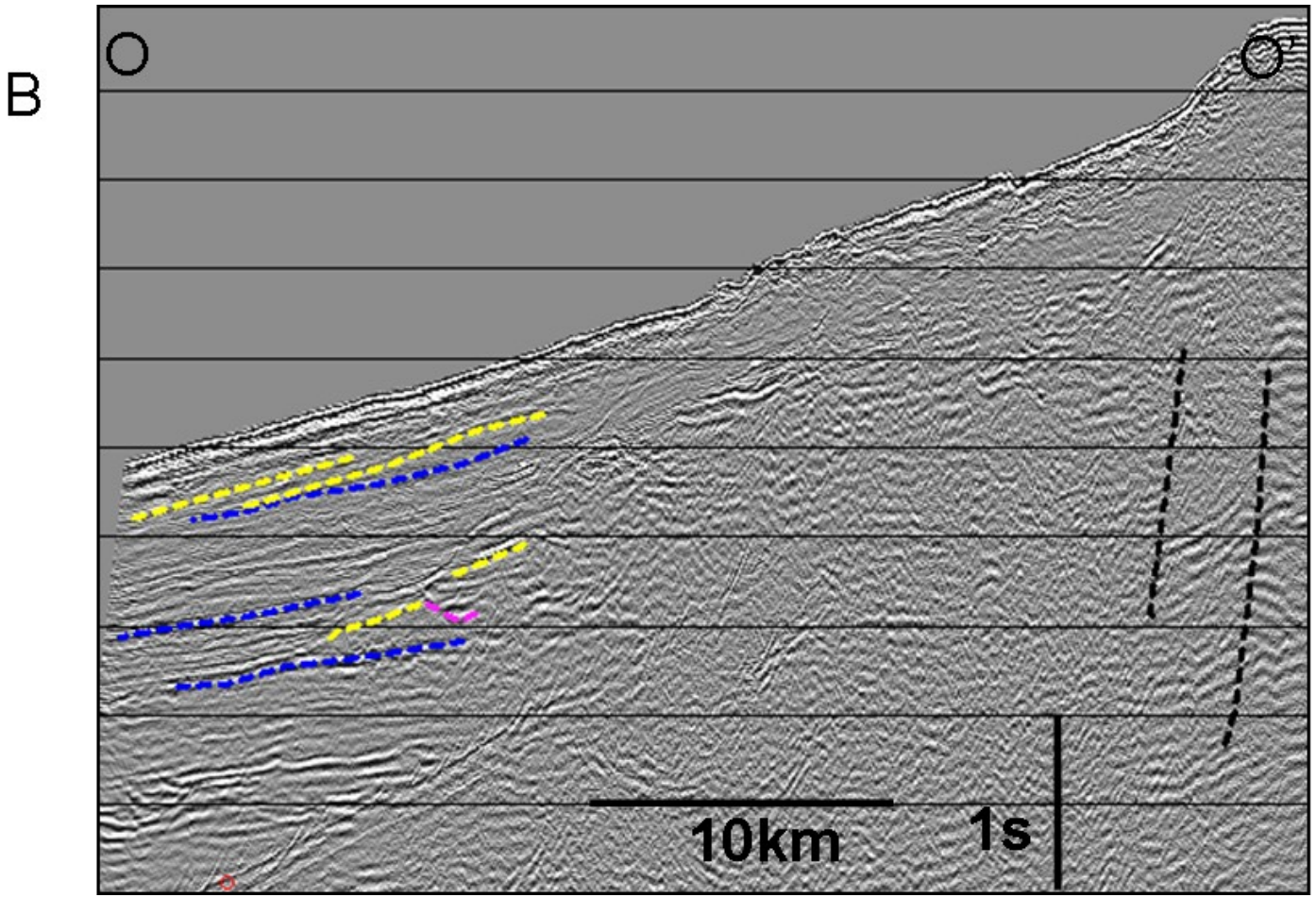


Figure 2.24. B. Central Fan, no major deformation is observed. Levees (Yellow), channels (pink), canyons (orange), channel-levee system base (blue).

growing, affecting the morphology of the sea floor by generating steeper slope sections (Figure 2.20, 2.22 and 2.24a). Forced migrations of the complete CLC IIc to the east as the deformation front was advancing are evidences of active deformation in the southwestern area during the Pleistocene (Figure 2.12a). The channel complex modified its course by increased sinuosity, becoming erosional or abandoning the course at avulsion points. Abandonment of CLS IIc2 seems to be related with the growth of the fold at the toe of the thrust front. CLS IIc3 is controlled by the thrust front, becoming erosional and straight in some segments. In addition, CLS IIc 2 and IIc3 present convex up thalweg sections, which may indicate post-abandonment deformation (90 km, Figure 2.13). The IIc4 thalweg does not present convex up morphology for the corresponding section on the slope; conversely it exhibits several cutoff loops (Figure 2.16). This suggests that deformation must have occurred concurrently or immediately following channel systems IIc1-3, and must have slowed or ceased once channel IIc4 began to form. Nonetheless, IIc4 thalweg is a convex up section at 50km indicating post-abandonment deformation, as it can also be observed on Figure 14 c, e, where CLS IIc3 and IIc4 are part of the folded sequence.

Besides CLC IIc, other complexes in the fan show convex up thalwegs (CLC IIb, CLC I), which may be caused by :1) channel abandonment before reaching the equilibrium profile or 2) deformation of the channel after abandonment (Figure 2.7). Based on the observations and high sinuosity of

the systems, it is more likely that the channels have evolved over time and have reached some level of equilibrium with the pre-existing valley, which suggest the geometry of the thalwegs (convex up) are related with post-abandoment deformation.

The fan channel thalweg profiles in the northeast upper slope (upper 100 km). are considerably deeper (~200 m) than those in the upper slope on the southwestern side of the fan (Figure 2.7). Sinuosity values are considerably lower for the upper slope in the northeastern area. In addition, CLC III and IV channel thalwegs exhibit sections with convex up profiles, indicating disequilibrium channels or post-abandonment deformation. This change in the basin depth could be due to: 1) lower sediment discharges at the time of earlier delta-fan building, 2) rapid migration of the river mouth toward the west (which occurred in the latest Pleistocene/Holocene), or 3) higher deformation in the western fan, uplifting the continental slope.

There are no age constrains for each system to properly support variations in the sedimentation rates during the evolution of the submarine fan, besides the relative ages provided by the correlations with the migration of the river on land. However, the lobate geometry of the whole fan and dimensions of the channel systems (depth and width) are similar throughout the fan, which may indicate that sediment flows were steady through time and generated systems with similar dimensions. The rapid westward migration of the river after establishment of the Magdalena drainage system in the basin, and

relative abundance of recent channel systems in the west may explain the change in depths and sediment accumulation on the western and eastern sides of the fan.

Nonetheless, it is important to take into account the active deformation of the upper slope in the southwestern deformed belt that was taking place during deposition of the western fan. Increments of sinuosity, forced migration of the channel systems and convex up thalweg profiles all indicate that deformation in the west was active and extended on the western fan upper slope. Conversely, the upper slope at the eastern fan (CLC III and IV) has lower sinuosity channels than counterparts on the western side. Deformation of the northeastern thrust belt seems not to have affected CLC IV and CLC III at the time of deposition (Figure 2.23b, 2.24b). There is no expression of faulting or deformation at the seafloor or at deeper levels. The northeastern deformation front was active before the generation of CLC IV. This is clearly evidenced by the presence of a channel system (probably older than CLC IV) that could not keep up with deformation leaving a beheaded hanging channel, and creating a new course orthogonal to the deformation front (Figure 2.22a). The deformation continued as is evidenced by the tilted position of the beheaded channel, while the old channel course continues to focus sediments down slope generating a new pathway. The continuation of deformation of the northeastern thrust belt restricted to few kilometers downslope of the shelf break, associated with the extension of

the older thrust imbricates towards the shelf. Multiple erosional features at the upper slope in this area (Figure 2.23b), uplift of the shelf and very steep angles for the upper slope thalweg on CLC III and IV indicate uplift and active deformation of this area.

In addition to the compressional tectonics it is important to mention that normal faulting seems to also have played an important role in the generation of steep angles on the slope. Slope overburden by the high sedimentation rates may cause normal faults generating steep slopes (Figures 2.24a and b), Normal faulting is common in the progradational sequences of the deltas, and have been mentioned as mechanisms to equilibrate the slope in the area (Flinch et al., 2003). Also, normal faulting associated with the growth of the thrust faults (Figure 2.24a)

2.7.2.2 Sinuosity and Slope Angle

Despite complex sea floor morphology, many submarine channels form concave-up profiles, constantly adjusting their profiles towards equilibrium (Pirmez et al., 2000). This is achieved by erosional and depositional processes of turbidity currents, including changes in channel sinuosity, channel incision/aggradation and development of distributary channels and aggradational sheets (Pirmez et al., 2000; Kneller,2003; Adeogba et al., 2005). A good example of this adjustment is shown in Figure 2.14, where

the sinuous channel thalweg exhibits a smooth profile, while the adjacent slope has steeper angles. The thalweg profiles provide information about the state of equilibrium during the formation of the channel, assuming the channels are free to erode/deposit without impediment (such as by abnormally lithified layers underneath), but once abandoned, deformation and erosional processes can modify the profile. Mayall et al. (2006) discuss at least four processes that influence the sinuosity of turbidite channels: initial erosive base, lateral stacking, lateral accretion and influence of pre-existing sea-floor topography. Even though lateral stacking and lateral accretion are present in the Magdalena Fan complexes, there is a direct indication of the relationship between sea-floor topography and sinuosity.

The variation of angle with distance shows in general a decreasing trend down slope, with local increases/decreases in angle that mark departures from the general trend (Figure 2.25a). The systems better fitting a concave curve are IIIc and IIIc1. The younger systems I and IIc4, exhibit a more variable profile with some extreme high values. It is important to note that angle values plotted represent today's slope, and are affected by post deposition modifications of the channel systems. This may represent an excess in slope angle for some of the values. The down slope distribution of sinuosity (Figure 2.25b) does not show a distinct trend, the middle slope (60-

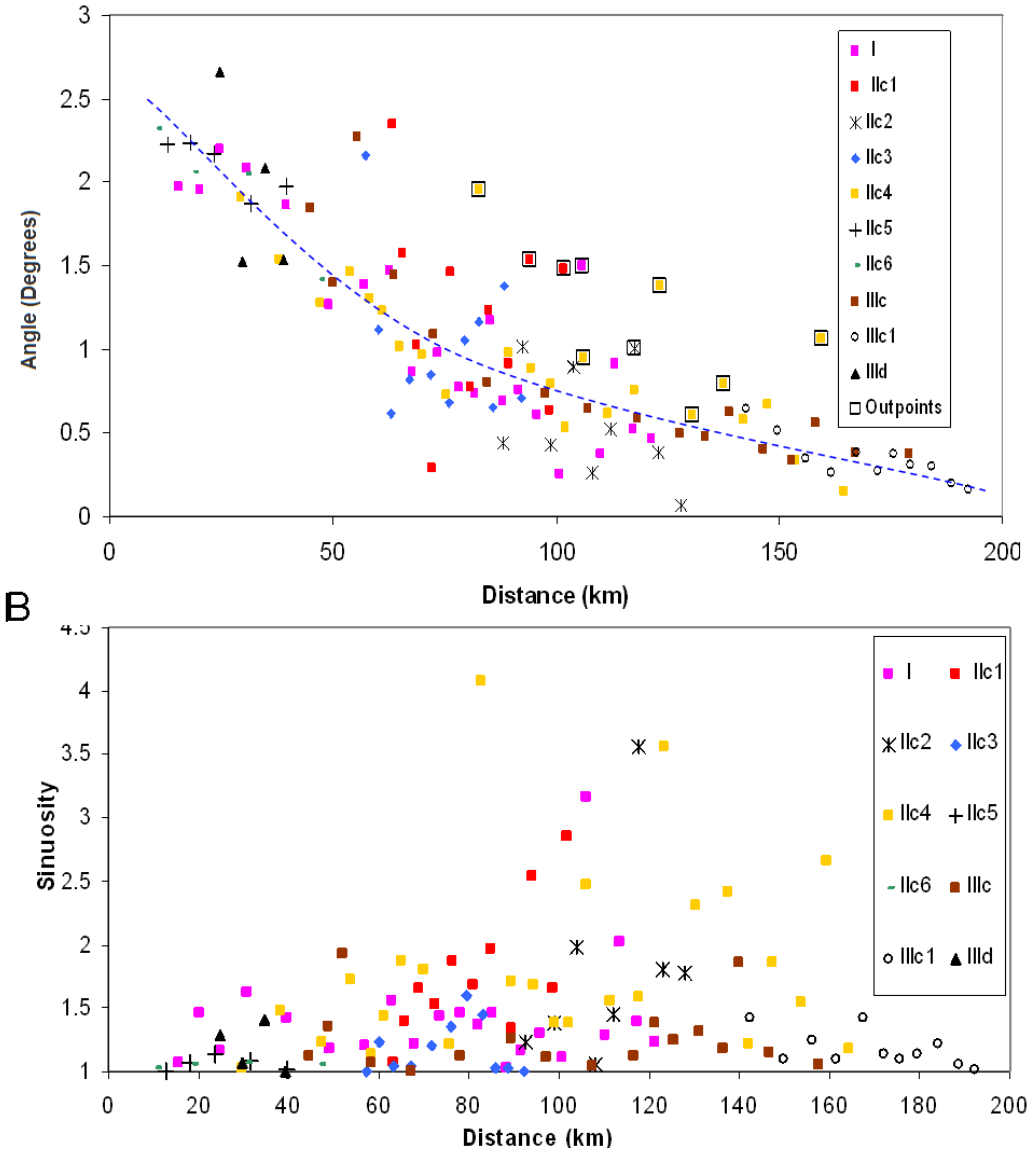


Figure 2.25. A. Slope angle changes through the slope measured for each channel system. All distances are referenced to the shelf break. The dashed line indicates a decreasing the gradient with distance (basinward), but there are many points that are showing higher vales from the tendency line. The out of trend points (squared data) are referenced in Figure 2.26. B. Sinuosity changes through the slope. There is a big variability of sinuosity through the slope.

120 km) exhibits larger variations. A comparison graph between slope angle and sinuosity for the entire fan is shown in Figure 2.26. Sinuosity on the Magdalena Fan (Figure 2.25b and 2.26) reaches high values up to 4, which is higher than previously reported for the Magdalena and other fans (Table 2.3). In addition, IIc4's high sinuosity segment (Figure 2.16) exhibits several cutoff bends, which as mentioned previously corresponds to a steep region of the slope. For the steeper angles (> ~2 degrees) the sinuosity is generally very low, sinuosity reaches a maximum value where valley angles reduce to about ~1 degree. For angles <1 degree, sinuosity generally decreases with slope angle (Figure 2.25, cf. Clark et al., 1992). Anomalous values are identified with very high sinuosity for any slope angle. Those values were identified in Figure 2.26a, as points corresponding to areas with slope angles outside of the general trend. These values correspond mainly to the IIc4 channel system, indicating that high sinuosity values correspond to stepper sectors in the slope, which are outside of the general profile for the fan.

In the western Magdalena Fan, two processes can be identified to accommodate the increase in slope angle by the continuous deformation in the area: 1) sinuosity increase in the channels and 2) generation of knickpoints on the slope.

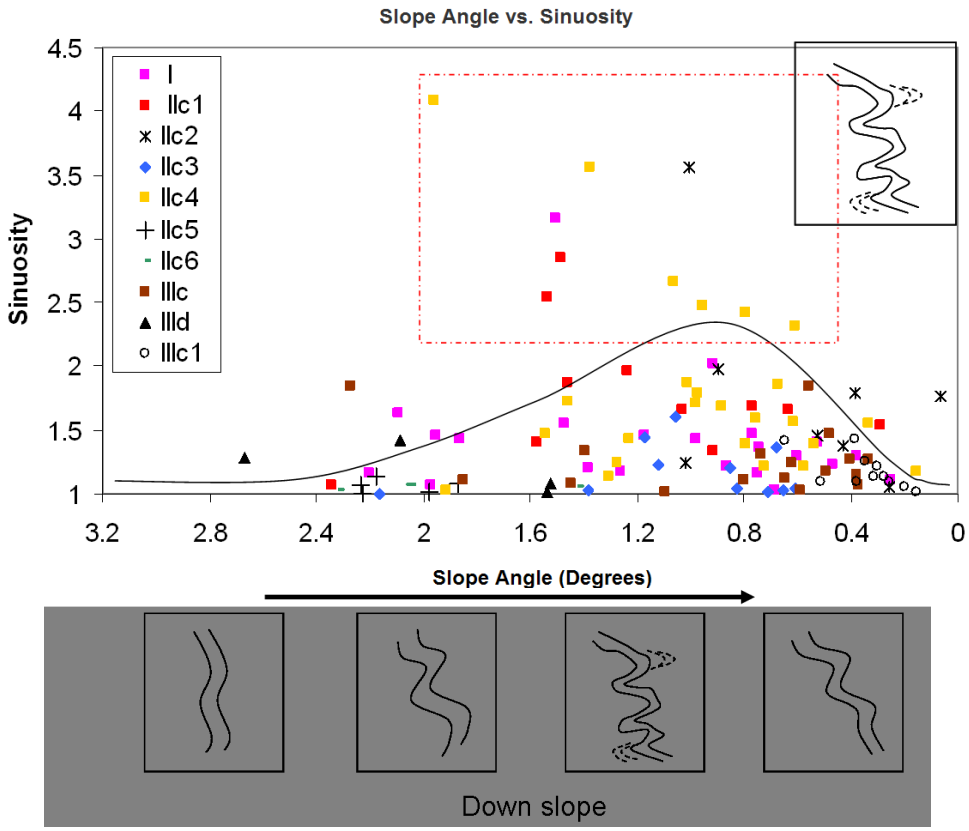


Figure 2.26. Slope angle vs sinuosity plot. For high slopes the sinuosity is low, as the gradient decreases the sinuosity increases generating highly sinuous channels, reached that point the sinuosity start decreasing down slope. The red box highlights points that exhibit high sinuosity values than the normal distribution. These points correspond to areas where the gradient is higher (Squared data in Figure 2.24) indicating irregularities on the slope.

System	Sinuosity	Reference
Offshore Angola	3.3	Kolla et al., 2001
Almeria Channel (Spain)	3.8	Cronin, 1995
Amazon Fan	3	Pirmez et al, 1997
Offshore Trinidad and Tobago	2.4	Wood and Mize,2008
Zaire	1.7 (10 km)	Babonneau et al., 2002
Magdalena	4	This work

Table 2.3. High sinuosity values on the literature.

2.7.2.3 Knickpoints

Another mechanism to reach the equilibrium profile is the formation of knickpoints, a well known process in fluvial channels which has been gaining influence in deepwater systems architecture in regions with evolving topography (Pirmez et al.2000; Mitchell, 2006; Heiniö and Davies, 2007). In fluvial systems knickpoints are defined as a steep slope section between lower angle sections along the river course, resulting from changes in base level, sediment flux, bedrock resistance and/or tectonic deformation (Howard et al,1994). Knickpoints may migrate upstream, leaving cut terraces or they may be smoothed out by slope replacement (Gardner, 1983; Howard et al, 1994).

Increases in incision and flow velocity occur as a result of increase of slope angle (Pirmez et al., 2000; Kneller, 2003). Channel width decreases toward the knickpoint lip, defined as the break in slope where the channel is oversteepened (Gardner, 1983). In areas of low slope angles (base of the knickpoint), velocity reduction, flow spreading and deposition occur (Pirmez et al, 2000; Prather, 2003).

A knickpoint begins as a small scour that grows at the inflection point of the slope (edge of the step). Erosion is enhanced at the knickpoint lip by an increase of the slope and at the knickpoint toe by increase in turbulence in the steeper part of the slope, (hydraulic jumps; Komar,1971). Heiniö and Davies (2007) proposed that “knickpoints grow into larger features by

positive feedback, in which steeper slope enhances erosion and this newly formed erosional scour promotes further erosion". Once the knickpoint is established, it may migrate upstream, creating incised conduits in the low slope areas (Figure 2.20). As the turbidity flows continue through the newly formed conduit, they tend toward an equilibrium profile by increasing erosion and even generating some bends in the conduit. It has been proposed that enhanced deposition will occur downdip of the knickpoint where slope decreases (e.g. Pirmez et al., 2000), perhaps even locally forming unconfined lobes (such as the perched slope fills of Beaubouef and Friedmann, 2000) at the lower angle steps of the slope by slope adjusted deceleration of the flows (Heiniö and Davies, 2007). Preservation of these deposits depends upon the growth geometry of the folds and the accommodation space created on the slope.

West of CLC IIc, four main steps in the slope are connected by fairly narrow and well developed knickpoints (section 2.5, Figure 2.20). They are connecting areas of unconfined deposits (lobes) (Figure 2.27a and b), truncating CLC IIc5 and filling low angle sections of the slope (Figure 2.12a, 2.20, 2.27a and b). KP1 is located down slope of the thrust fold (Figure 2.20 and 2.23a). KP2 is located at the slope step where CLS IIc4 increases its sinuosity, suggesting KP2 was established after deposition of IIc (Figure 2.16). KP3 is very incipient but is aligned with a strait segment of CLS IIc4, followed by a change in direction of the channel (Figure 20, 23A). The

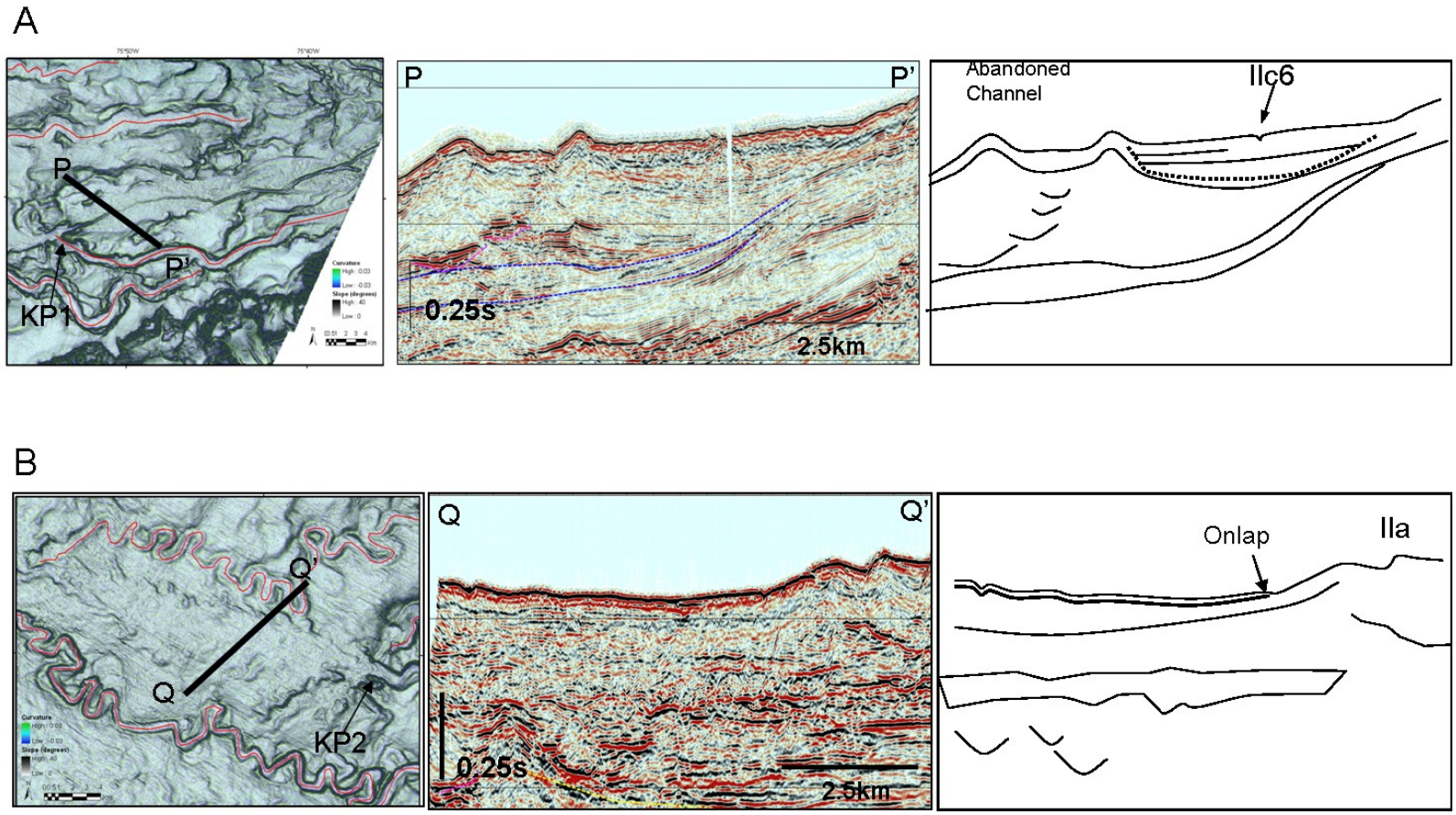


Figure 2.27. Low gradient sections of the slope allow the deposition of unconfined flows that heal the slope. A. Deposits upslope of KP1, the flows are filling an interchannel low. B. Lobate features down slope of KP2. Even though frequency of the seismic is low, it is possible to observe the onlap of the lobe against the channel overbank.

knickpoints are interpreted to have formed as a result of uplift caused by continuous deformation of the thrust belt (growth of folds). The location of the knickpoints down slope of the thrust and fold axes, associated with steeper angles of the nearby slope, suggests a structural control of their formation. The down slope knickpoint profile for IIc6 depicts clearly the slope changes (Figure 2.18A).

Alternatively, the knickpoint system could have been initiated by IIc5 (youngest conduit of CLC IIc) and later abandoned and fed by down slope flows traveling through IIc6. However, both interpretations agree on the formation of knickpoints as connectors that allow the sediment distribution throughout the slope.

2.7.3 Initiation of Channel Levee Systems

Major deepwater fans are characterized by the presence of a master canyon(s) feeding the continental slope, such as the Amazon fan, Mississippi fan, Zaire fan, and Indus fan (Damuth and Kumar, 1975; Kastens and Shor, 1985; McHargue and Webb, 1986; Droz et al, 1996; Normark and Carlson, 2003). In the presence of a constant source of sediments, what defines the initiation of a channel levee system in the Magdalena Fan without the presence of a confined canyon?.

The initiation of a deepwater channel system has been linked to gullies, which by progressive down slope enlargement by erosional processes evolve into channels. Examples of the Fuji and Einstein systems in the eastern Gulf of Mexico have been reported by Faultkenberry et al. (2005) and Sylvester et al. (submitted). Megaflutes in the Ross Formation have been described as examples of possible features to initiate channel levee systems, recording sediment bypass on an intraslope basin (Elliot, 2000). Several experimental efforts have been completed to understand the processes involved in the generation of channel levee systems (e.g. Métivier et al., 2005; Yu et al., 2006) but still there are no dynamic models to explain the processes involved.

A potential answer to the initiation of channels in this tectonically active setting may be related to continuous deformation on the slope. The flows start to erode the slope at the knickpoints, which migrate and link to other knickpoints, thus creating the initial course of a channel (Figure 2.28a). From the sequence of knickpoints described previously, it is important to notice that the formation of the knickpoints is possible on low slopes (~0.08) as is observed in KP3 (Figure 2.18A and 2.20). In addition, some of the CLS bases are characterized by flat continuous reflections and basal channel scours not deeply incised when observed on seismic profiles. A more complete data set that allows us to fully understand the spatial and temporal relationships will be needed to validate this hypothesis. However, the

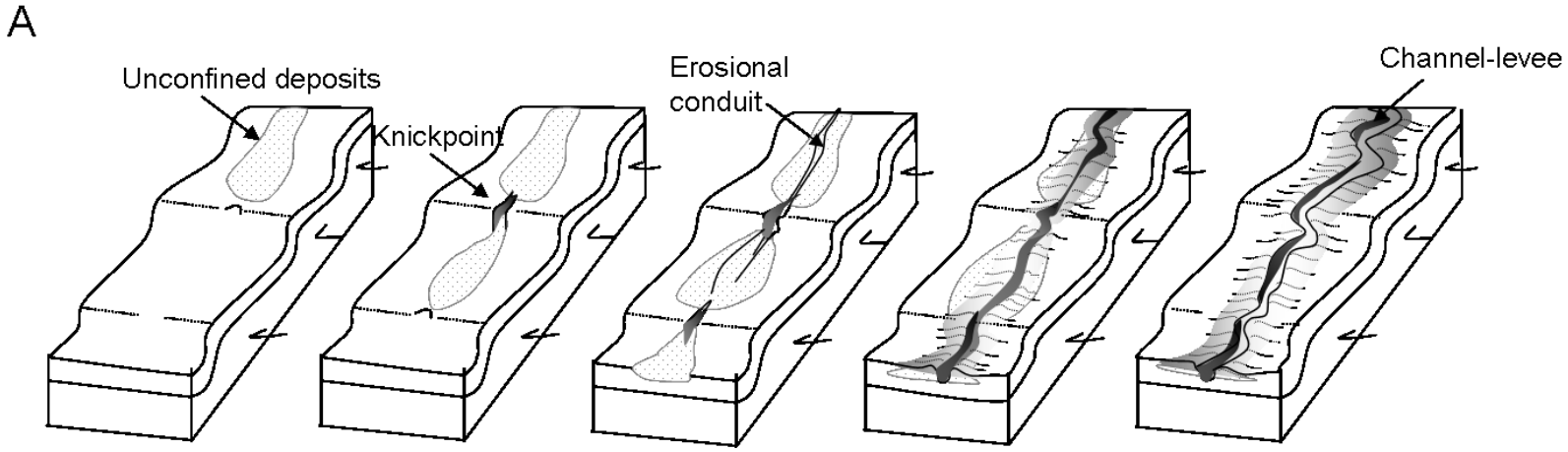


Figure 2.28.A Knickpoint evolution. Fault related folds may create areas in the slope where erosional processes generate knickpoints that migrate upslope and generating unconfined deposits down slope. Later these knickpoints are connected by an erosional conduit, which may explain the initiation of a channel levee system.

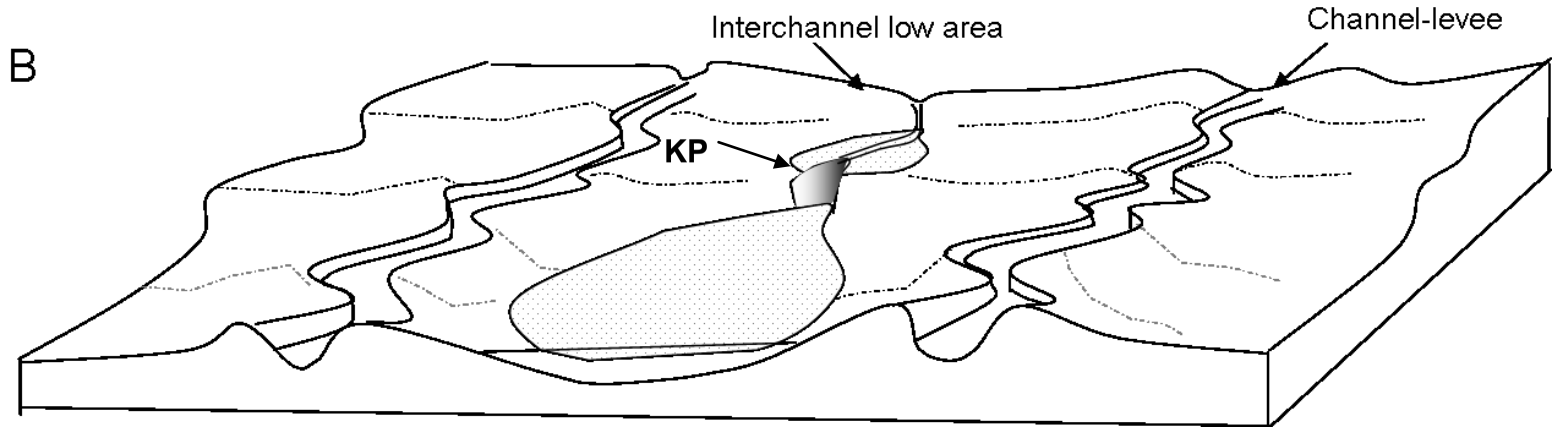


Figure 2.28. B The diagram depicts the same process of knickpoint migration constrained within the interchannel lows.

erosive nature and migration of knickpoints make it difficult to preserve them in the geologic record (Heiniö and Davies, 2007). To evaluate the influence of knickpoints on the formation of channels, one may need to study features associated with the presence of “arrested” knickpoints in the geologic record, such as erosional notches on slope deposits at the base of and adjacent to channel systems.

Continuous modification of the slope by active deformation will keep the slope above grade (Prather, 2003) and the channel systems out of the equilibrium profile, inducing mechanisms such as migration, avulsion, knickpoint formation or abandonment of the system, among others. Migration of knickpoints and subsequent establishment of channel systems have been used to explain the interaction between the growth of mobile shale ridges and turbidite deposition in stepped slope profiles, where at early stages, the low angle section of the slope is healed by unconfined deposits (lobes) (Figure 2.27a and b) with subsequent migration of knickpoints bypassing the previously healed section of the slope (e.g., O’Byrne et al., 2008). The Early Miocene shale sequence may play an important role on the deformation of the slope on the Magdalena Fan. This sequence is the décollement surface for the thrust imbricates and the source for the mud diapirism onshore and offshore (Duque-Caro, 1984; Vernette et al., 1992) and seems to extend across the fan area. Even though the deformation seems to be masked by the active sedimentation, the presence

of highly sinuous bends and knickpoint alignment on the slope and highly disrupted reflections may indicate continuous deformation on the Magdalena Fan area. The interaction between deformation and sedimentation (e.g. IIc4) (Figure 2.24) is in part obscured and suppressed by the late Pleistocene dump of sediment shown at the eastern fan (CLC III and IV).

Interchannel lows also may play an important role in the establishment of new CLS (Figure 2.28b). Commonly, unconfined flows and mass transport deposits fill the interchannel lows (Figure 2.4, 2.9, 2.10, 2.11 and 2.27a). Older levees serve as barriers to younger flows, increase the sediment accumulation in these areas, and facilitate the entrenchment and later connection of knickpoints (by healing the slope) (Figure 2.27a). In areas where changes in slope angles are the product of deformation, the initiation of channel-levee systems could be explain by the knickpoint formation model and subsequent development of channels, based on the tendency of slope systems to obtain a graded slope (Prather, 2003).

2.8 SIGNIFICANCE FOR HYDROCARBON EXPLORATION

Deepwater deposits are an important play for the oil and gas industry (Weimer and Slatt, 2007). This study contains important findings that can impact hydrocarbon exploration in this and other tectonically active basins. Facies distribution and preservation of deposits along the slope will depend

upon the interaction of slope deformation and deepwater sedimentation. Changes in slope control not only the CLC morphology but also the distribution of coarser sediments. Preservation of deposits such as the upstream lobes at low angle steps on the slope could be of importance (Adeogba et al., 2005; Heiniö and Davis, 2007; O'Byrne et al., 2008), as it is in the western Niger delta. Morphological parameters of the channels could be used as an analog for reservoir characterization for similar basins.

2.9 CONCLUSIONS

-The sea-floor morphology of the Magdalena deepwater fan is characterized by the presence of seven major channel levee complexes separated by interchannel-lows where mass transport deposits and unconfined flows are deposited. The older CLCs are labeled IV followed by III , II, IIa, IIb, IIc and I.

- Evolution of the fan is closely related to the Magdalena delta migration and the tectonic processes that occurred in northern Colombia during the Miocene to Present. The Plio-Pleistocene history of the Magdalena River is represented by at least eight different phases, beginning at the north (west of the present river location) (CLC IV- Early Pleistocene). Then, the river started migrating towards the south (CLCs III and II). The southernmost location reaches the Canal del Dique (Phase D) during the middle Pleistocene. Later, the river shifted north of Cartagena (Phase C), forming

CLC IIa, IIb, IIc and I (youngest CLC of the entire fan). A major northern shift of the river due to the Atlantico-Turbaco uplift generated phase B which focused sediments towards the Cienaga de Santa Marta. The establishment of the present day delta fan is very recent, switching positions between Boca Vieja and Sabanilla Canyon before stabilizing at its present position. The fan is active today with deposition of turbidite flows and mass transport deposits in piggyback basins formed as a result of deformation of the accretionary wedge. The shifts are corroborated by a decrease in carbonate content of the Colombia basin (6000 B.P.), growth of coralline limestone at the coastal margin (Barranquilla) and remnants of old river courses.

-In the older complexes, thalweg and levee morphology have been affected by degradational processes after the abandonment of each system. They increase channel width and the levees walls are modified by erosional processes, and are ultimately buried. Degradation of the channel should be considered when evaluating the dimensions of ancient deposits in order to obtain a better estimation of the size of the expected deposits. Degradation processes associated with mass-transport deposits also could be important elements of sealing and stratigraphic trapping of potential reservoirs in the underlying channel-levee deposits.

-Several CLS in the fan show convex up thalwegs, indicating: 1) the channel was abandoned before reaching its equilibrium profile or 2) deformation of the channel occurred after abandonment.

- The CLS's in the Magdalena Fan are highly sinuous. Higher values of sinuosity (up to 4) correspond of areas of the slope with high angles (out of the regional slope trend), which suggest that sinuosity is controlled by changes in the slope.

-There is evidence of multiple phases of deformation on the Magdalena Fan created by the deformation of the larger accretionary wedge. Decrease in bathymetric depths on the thalweg profiles for the western side seems to support the hypothesis of higher deformation (compression) and uplift in this area. Alignment of knickpoints, channel bends, and step profiles in the western side are a clear indication of the deformation that is active during and post formation of the channel facies. The presence of overpressured shales seems to play an important role in deformation of the fan.

- A sequence of knickpoints seems to connect deposition of sediments from the shelf break downslope through a series of steps, culminating in lobate unconfined deposits. Upstream knickpoint migration in slope steps as a response to deformation may represent a key process to explain the initiation of deepwater channel systems in the Magdalena Fan, but further research needs to be done to establish its importance. In addition, the interchannel lows could facilitate the rapid confinement of the slope to initiate the knickpoint migration.

- The distribution of sediments in the Magdalena deepwater fan is highly controlled by the actively deforming slope, which will serve as an analog for

basins where slope deformation was active during deposition of deepwater sediments.

2.10 ACKNOWLEDGEMENTS

This research forms part of a Ph.D. dissertation by the senior author. We especially thank Ecopetrol for providing the seismic and Bahia – Sinú bathymetry data, the Institut de Ciències del Mar-CSIC for allowing the use of the proprietary bathymetry; to the Centro de Investigaciones Oceanográficas e Hidrográficas de Colombia *(*CIOH), for providing complementary bathymetry. The Conoco Phillips School of Geology and Geophysics provided the financial support and computer facilities. Seismic Micro Technology and ESRI provided the educational software licenses. US-NSF grant OCE8901848 and OCE9712079 financed acquisition and processing of the seismic lines acquired during cruise CD40a onboard the HMS Charles Darwin. The crew and scientists aboard the RRS Charles Darwin and RRS Discovery during those cruises are thanked for their efforts.

CHAPTER 3

ACTIVE SEDIMENTATION AND SUBMARINE CABLE BREAKS ON THE MAGDALENA DEEPWATER FAN, COLOMBIA: LINKAGES WITH SHALLOW WATER PROCESSES AS STARTING POINT FOR SEDIMENT GRAVITY FLOWS.

ABSTRACT

The active Magdalena submarine fan is located north of the Magdalena River mouth, offshore Colombia, Caribbean Sea. Several cable breaks recorded the timing of sediment gravity flows between 1930 and 1956. Accompanying some of these events were reported ruptures of jetties at the river mouth. Multibeam bathymetry surveys provide the link between cable breaks and upper slope submarine canyons confined gravity flows.

The active fan occurs at the northeastern deformed thrust belt, which is part of the accretionary wedge generated by the subduction of the Caribbean plate under the South American plate. Four piggyback basins between the fault ridges accommodate sediments, generating an above grade slope. Three canyons (Sabanilla, Magdalena and Unnamed) and gullies east of the river mouth are the main pathways for the gravity flows. The piggyback basins are connected by channels, which allowed the transport of sediments to the abyssal plain. In addition, the Aguja Canyon, northeast of the active

fan, also experienced sediment gravity flows, which have caused submarine cable ruptures.

Integration of high resolution bathymetry, 2D seismic lines, GLORIA side scan images and piston cores allowed for the identification of sedimentation pathways and characterization of individual flow events from source to sink.

Three main sediment transport pathways were defined: 1) Western-directed flows through the Sabanilla, Unnamed and Magdalena canyons 2) Eastern-directed flows through the Magdalena Canyon and eastern gullies and 3) Aguja Canyon. High acoustic-reflectivity lobes at the toe of the PBB and at the abyssal plain detected in the GLORIA imagery, and turbidite deposits at the top of three piston cores corroborate the recent activity of the pathways. Several processes may have triggered the gravity flows: 1) High flood stages of the river, 2) coastal erosion, 3) longshore drift, 4) hyperpycnal flows and 5) river mouth instability. Mass transport deposits seem to play an important role in the distribution of the flows into the piggyback basins. The findings of the study provide unprecedented detail in the characterization of active turbidity current activity on an active continental margin, with hydrocarbon exploration and production implications for deepwater depositional models in structurally confined basins and connected tortuous corridors.

3.1 INTRODUCTION

The modern seafloor morphology of offshore northwestern Colombia is controlled by a series of channel-levee systems and mass transport complexes, formed by frequent transport and deposition of sediments by the Magdalena River, the main drainage system in Colombia (Figure 3.3.1). Like the modern Zaire Fan (Babonneau et al., 2002), offshore Angola and some California fans, the Magdalena deepwater fan is one of the few presently active fan systems, where there is documented activity of frequent sediment gravity flows in the last century.

Previous studies (Kolla and Buffler, 1984; Ercilla et al., 2002; Estrada et al., 2005a, this work (Chapter 2) have described some of the characteristics of the channel levee complexes and large mass transport complexes found within the Magdalena submarine fan. The acquisition of new bathymetry data sets provides a link among previous observations of active sediment transport on the fan, submarine cable breaks (Heezen, 1956), and core descriptions (Muñoz, 1966).

Numerous submarine cable breaks in the Magdalena Fan area were reported in the 1950's (Figure 3.2). Heezen (1955) wrote "Destruction and

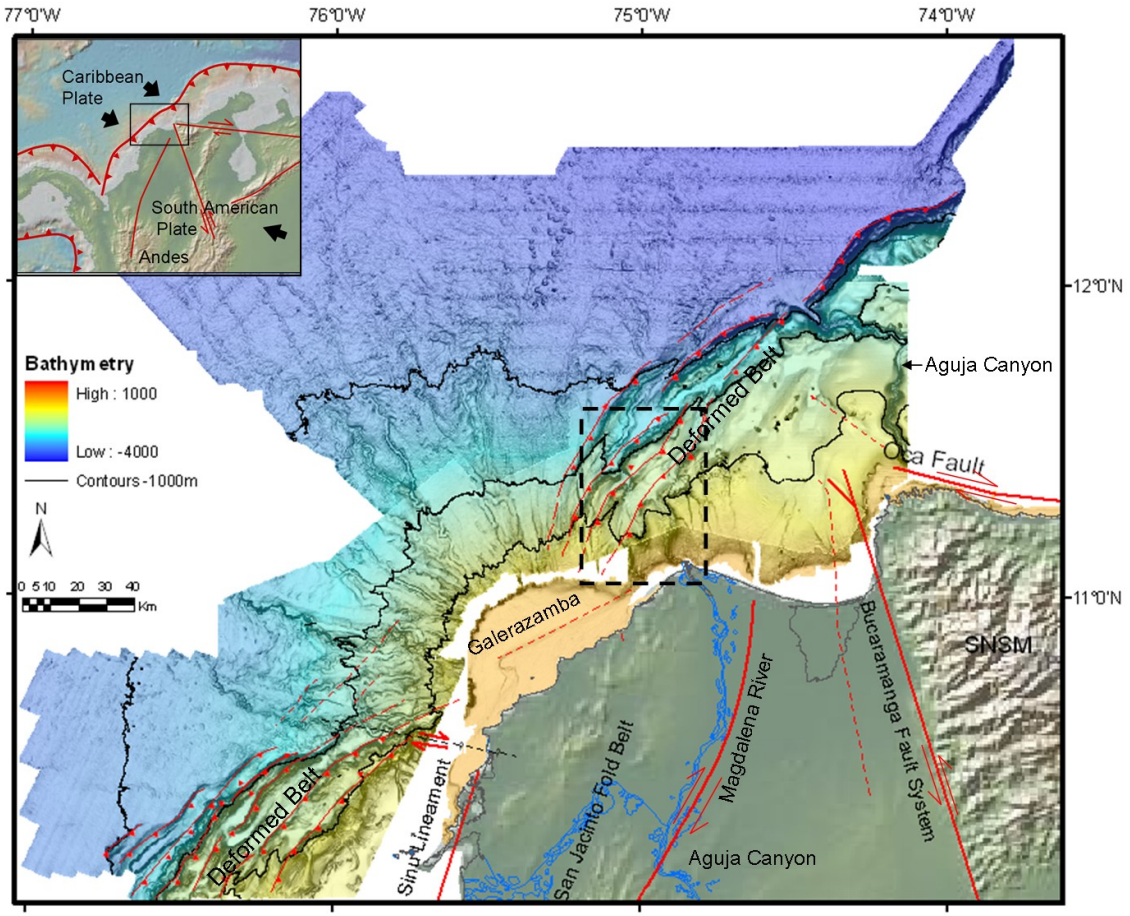


Figure 3.1.Bathymetry map of the Magdalena fan, southern Caribbean sea. Location of the active fan and regional structure. Contour interval is 1000 m .

sudden lowering of the Magdalena River mouth bar was followed by the breakage of a submarine cable which crosses the Magdalena submarine canyon in about 700 fathoms (1280 m), about 15 miles seaward of the river mouth. In 25 years this cable broke 14 times in the vicinity of canyon". The location of the cable breaks plotted over the new multibeam bathymetry map (Figure 3.2) shows that they correspond to areas where active canyons and mass transport complexes (MTCs) are found.

In this paper we present a detailed description of the active turbidite flow pathways that are capable of transporting sediments to the abyssal plain, based on multibeam bathymetry, GLORIA side scan images and core descriptions. Our observations are then discussed in the context of the processes that may be involved as trigger of the different sediment flows. Understanding of the sediment distribution and the processes involved in the generation of turbidite flows in active submarine fans will add to the knowledge of deepwater depositional systems. In addition, it will provide a more complete scenario in terms of the shallow hazard assessments and instability areas for submarine infrastructure in the area.

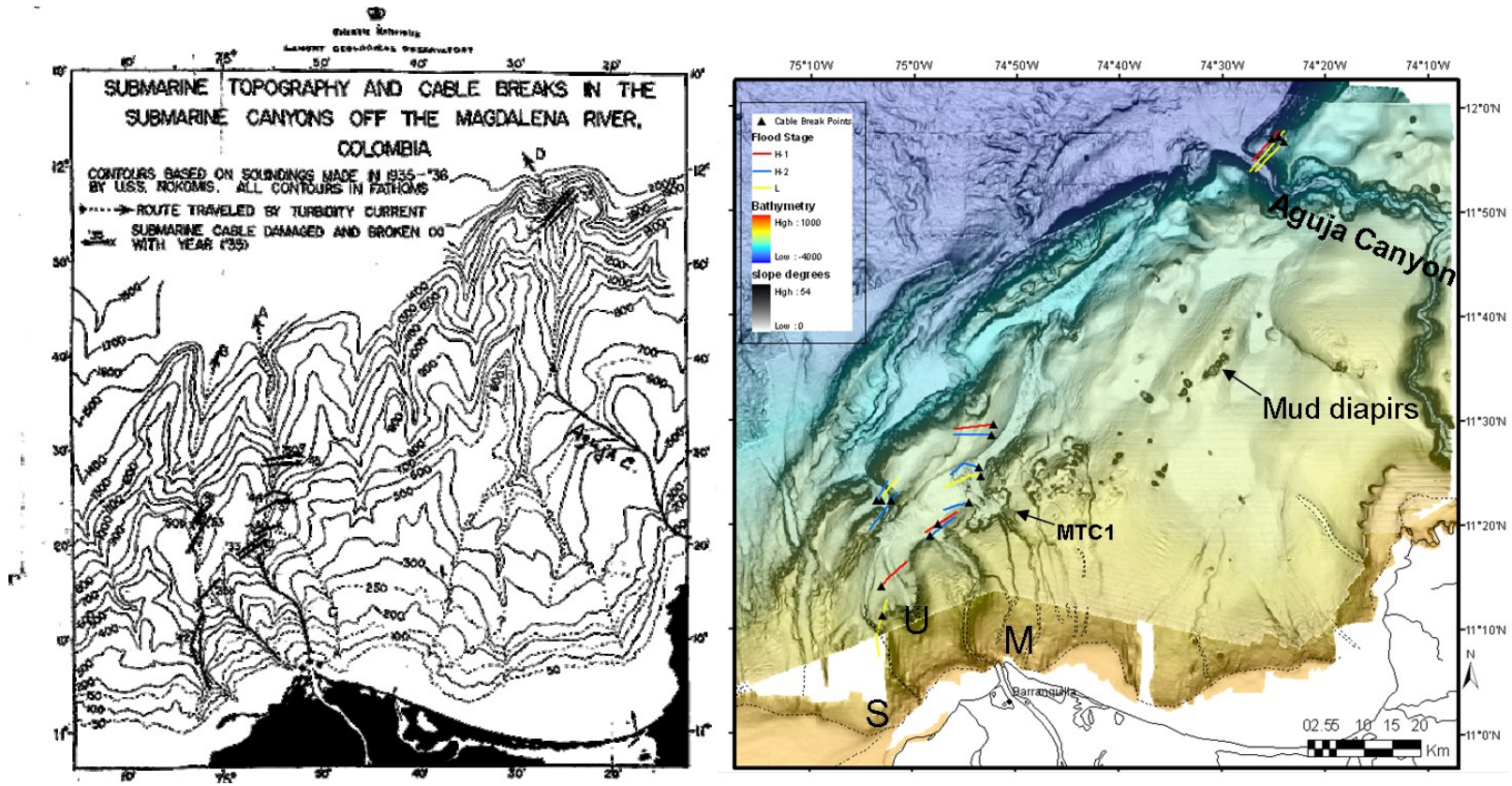


Figure 3.2. Historic bathymetry map from Heezen 1956, indicating his interpretation of the Cable break and possible flow pathways B. High resolution multibeam bathymetry. Main differences are the presence of the northeast trending thrust ridges that are not identified in the old bathymetry and the flow paths of the canyons. However, Heezen's work illustrates the presence of several canyons at the upper slope near the river mouth. Cable breaks are represented by triangles and the lines correspond to the replaced cable. The cable breaks are distinguished depending on the river flood stage at the time of their occurrence. H1 (Red) correspond to high flood stages during July and August. H2 high flood stages presented during November to December and low flood (L) occurring during the rest of the year.

3.1.1 Regional Setting

The Magdalena submarine fan, located in the Caribbean Sea, offshore Colombia (Figures 3.1 and 3.3), is an extensive bathymetric feature, part of the accretionary wedge complex formed by the collision of the Caribbean – South American plates (Duque-Caro, 1979; Kolla and Buffler, 1984; Breen, 1989). It covers an area of about 68,000 km^2, a volume of 180,000 km^3 and it extends to over 4,000m of water depth (Wetzel, 1993; Reading and Richards, 1994). The deepwater fan is fed by the Magdalena River, a major fluvial system that drains most of the Colombian Andes. The river is classified within the top 10 rivers in the world in terms of sediment load (150 MT/yr) (Restrepo and Syvitski, 2006). It discharges the sediment load into the Caribbean Sea, creating a 1,690 km^2 wave-dominated delta (Coleman, 1981; Restrepo and Lopez, 2007). Sediments are deposited offshore through submarine canyons with steep slopes (~3^o). The continental slope is characterized by the presence of compressional tectonic ridges, gas hydrates, mud diapirs and slumps (Shepard, 1973; Shipley, 1979; Kolla and Buffler, 1984; Vernette et al., 1992). In this paper we present new bathymetric data that illustrate that the submarine canyons near the mouth of the river are the site of active sediment gravity flows that were responsible for multiple submarine cable breaks in the last century (Heezen, 1956) (Figure 3.2).

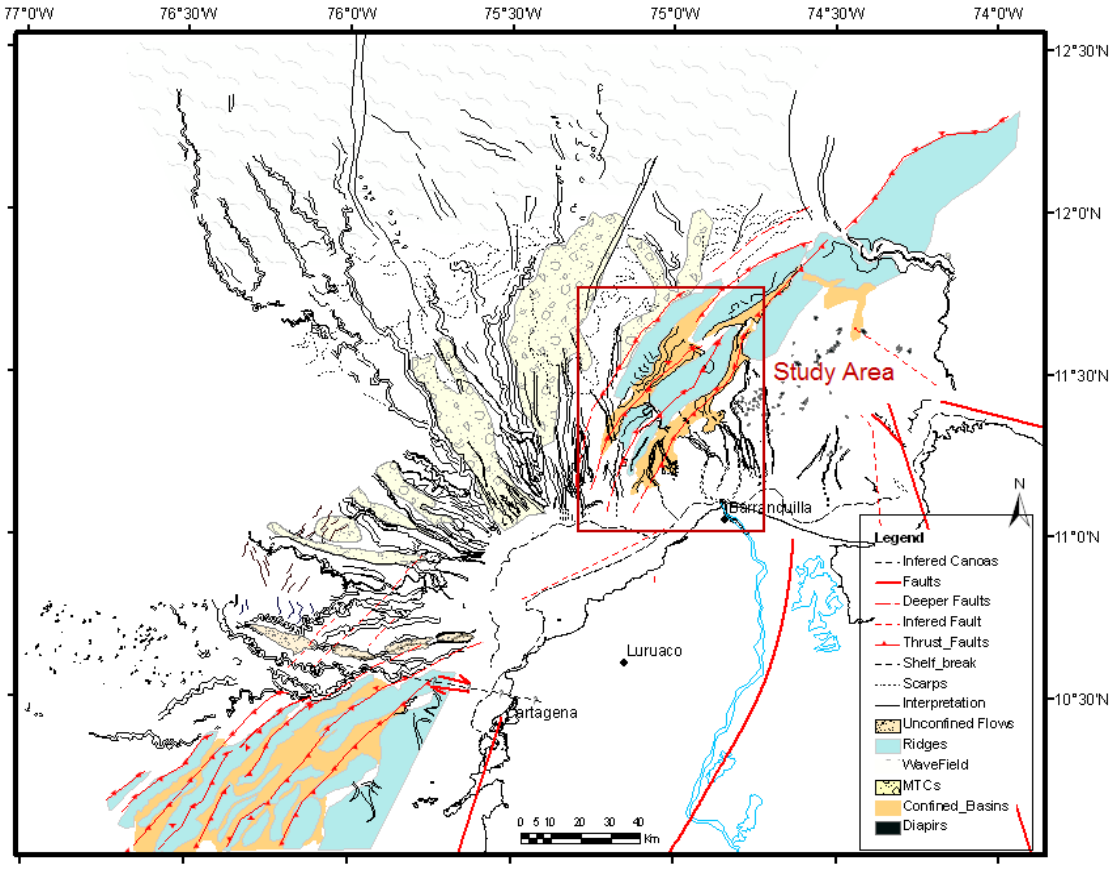


Figure 3.3. Architectural elements of the Magdalena fan. (Modified from Ercilla et al., 2002). Northeastern and southwestern deformation belts are the boundaries of the CLC studied. Note the presence of MTC's located at the interchannel system lows.

Magdalena Fan sedimentation was initiated during the middle Miocene, which was a time of low deformation rates on the margin (Kolla and Butter, 1984). The fan has been subdivided into upper, middle and lower parts, based on sub-bottom profiles and piston core examination (Kolla and Butter, 1984). Complex sea floor topography reveals several periods of incision and channel activity (Figure 3.3), reflecting uplift in the sediment source region, changes in sea level, and temporal and spatial shifts of deltas that began with the middle Pliocene Andean orogeny (Kolla and Butter, 1984; this work, Chapter 2).

The Magdalena Fan depocenter has shifted through time due to changes in location of the main Magdalena fluvial channel, so that several coalescing submarine fans were deposited (Hoover and Bebout, 1985; Pirmez et al., 1990; this work, Chapter 2). The eastern portion of the fan contains the oldest channel-levee systems (CLS) on the sea floor; it has been the focal point of several studies (Kolla and Buttler, 1984; Ercilla et al., 2002; Estrada et al., 2005a). The western fan contains younger CLS, which were influenced by deformation on the slope, (this work, Chapter 2). During the late Pleistocene, the Magdalena River shifted eastward, discharging sediments in what is now the Cienaga de Santa Marta area, as a result of the Atlantico-Turbaco uplift (Hoover and Bebout, 1985). The fan in this area migrated towards the west to its present day position (Heezen, 1956; Bordine, 1974; Pirmez et al., 1990; this work, Chapter 2).

The continental slope is characterized by two arcuate deformed belts, separated by a central area dominated by submarine fan deposition. The northeast and southwest thrust belts are expressed on the sea floor as ridges (Figure 3.1 and 3.3). Piggyback basins became sediment traps as the deformation front advanced. On the northeastern active fan, sediments were transported down slope through canyons and gullies, and emplaced as gravity flow deposits filling the piggyback basins. In this area, multiple collapse structures and normal faults are common, in addition to the presence of mud diapirs and gas hydrates (Vernette et al., 1992; Flinch et al., 2003).

3.1.2 Data and Methodology

Data available for the study include high resolution bathymetry images of the northwest Caribbean offshore Colombia. The bathymetry covers a major part of the Magdalena submarine fan, approximately 54,000 km^2 of the seafloor (Figure 3.1). Four different surveys cover the area of study. In 1997, the Spanish vessel BIO Hesperides acquired approximately 32,500 km^2 of bathymetry data (Ercilla et al., 2002) with the multibeam echosounder SimRad EM-12 S120. Two bathymetry surveys were acquired in 2002 on behalf of Ecopetrol (14,700 km^2) and Total E&P (11,400 km^2). Data were collected using a hull—mounted, multibeam echosounder Reson SeaBat 8169 (50 KHz; for water depths between 100 and 800 m) and Simrad EM

12D (13 kHz; for water depths between 800 and 3500 m). Additional bathymetry surveys that cover the shelf area and river mouth were provided by the CIOH (Centro de Investigaciones Oceanográficas e Hidrográficas, Colombia) (6,000 km^2). Data were tide-corrected and processed by the contractor, and were provided in final format compatible with geographic information systems. Proximity to the Magdalena River outflow area resulted in sounding errors due to fresh water input which altered sound velocity ranges. Bathymetry interpretations and quantification of the MTC dimensions were made using ArcGIS (ESRI, Environmental Systems Research Institute, Inc.). Calculation of attributes such as slope, azimuth and curvature were used to enhance and facilitate the identification and interpretation of deep water architectural elements.

GLORIA (Geological LOng Range Inclined Asdic) side-scan sonar image was available for the study (Figure 3.4), originally presented by Pirmez et al. (1990) and now integrated with the data in the area in the GIS database built in this study. The GLORIA data was acquired primarily during cruise CD40a and also includes an older swath acquired during cruise DIS109. The latter was originally presented by Vitali et al. (1985).

Lithologic description of sediment cores acquired by the Lamont Doherty Geological Observatory on the abyssal plain of the Colombian basin were published by Muñoz (1966) and used in this study (Figure 3.4). Revision of

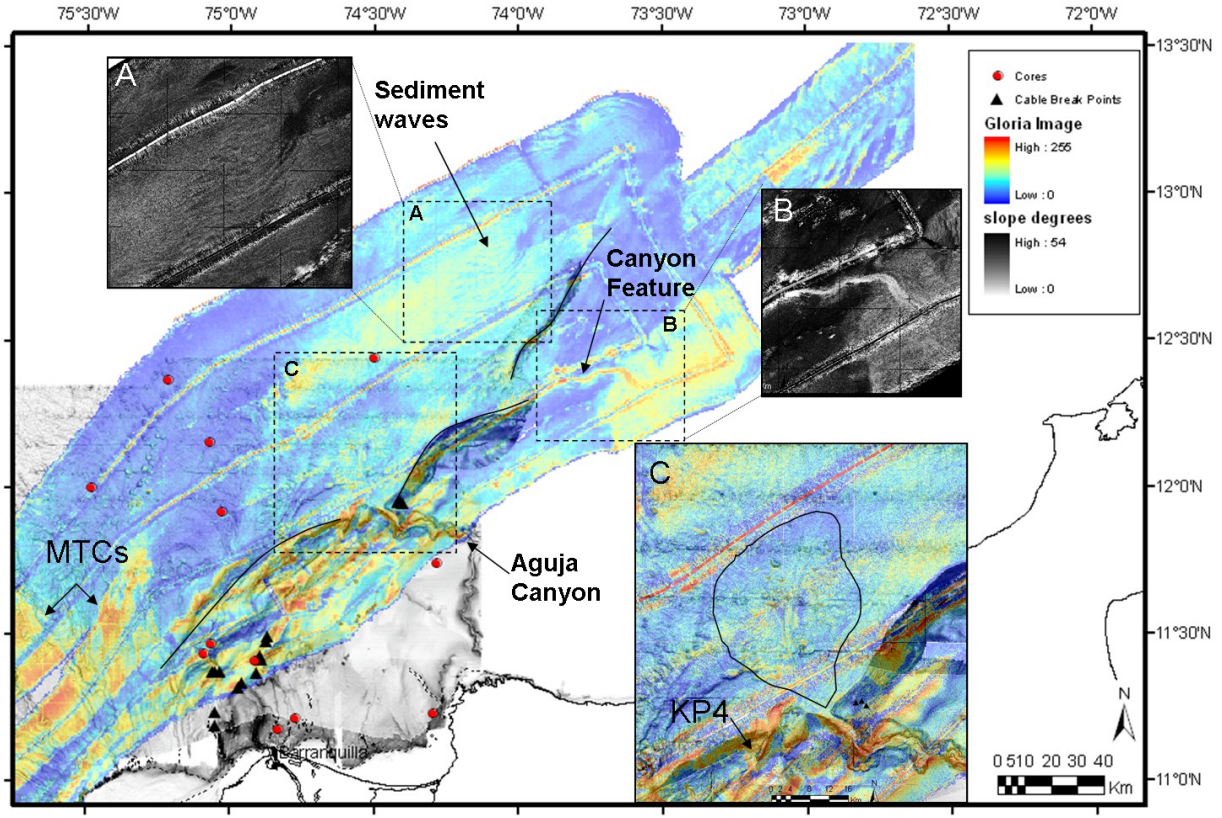


Figure 3.4. GLORIA image for the study area. High reflectivity is common in areas of active sedimentation or coarser material. A. Sediment waves at the abyssal plain. B. Northeastern canyon that communicate the upper slope with the abyssal plain. C. Distributary lobe feature at the toe of the thrust deformation front at the Aguja Canyon. Black triangles correspond to the cable break location and the red dots to piston cores.

the grain size descriptions and photographs were made, since new interpretations could not be performed due to the deterioration with time.

The 2D seismic lines shown in this paper illustrate the seismic expression of the recent sedimentation in the piggyback basins. They are part of a wider grid of seismic reflection data provided by Ecopetrol. Acquisition parameters are industry standard, near zero phase with SEG normal polarity. Frequencies range from 20 to 60 Hz at horizons of interest. Seismic interpretation was performed in Kingdom Suite 8.1.

3.2 MORPHOLOGY OF THE ACTIVE FAN AREA

3.2.1 Canyons

The active Magdalena Fan is located in a highly deformed area. Northeast-trending thrust fault ridges (Figures 3.1, 3.2, and 3.5) occur as a series of sea bottom slope steps creating confined basins (piggyback basins), where sediments transported down slope becomes trapped in the lower slope areas. Three main canyons and gullies have been carved on the slope which served as conduits for sediment flows to low relief areas of the slope through the ridges and abyssal plain (Romero et al., this volume). The Magdalena Canyon is a prominent feature on the slope (maximum incision of 260m and 2.5 km wide) directly connected with the current Magdalena River. It runs down slope about 30 km before it reaches a step in the slope

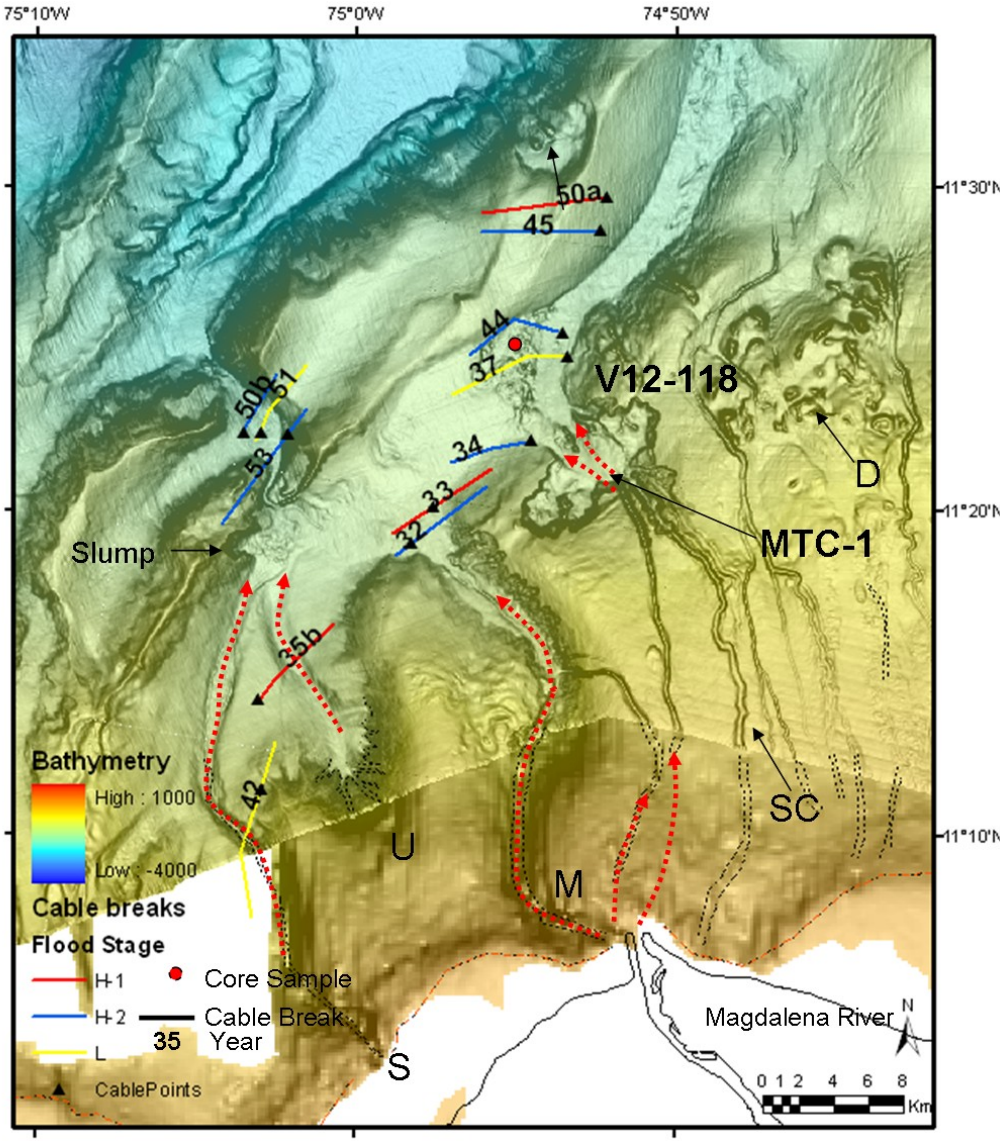


Figure 3.5. Active canyons of the Magdalena slope: S) Sabanilla, U) Unnamed, M) Magdalena. East of the Magdalena Canyon are found SC) Slope channels of gullies, MTC's, and D) Diapirs. Cable breaks are represented by triangles and the extension of the line corresponds to the replaced cable. The cable breaks are distinguished depending on the flood stage of the river at the time they were presented. H1 (Red) high flood stage during July and August. H2 high flood stage during November to December and low flood (L) during the rest of the year.

where it converges with the U and Sabanilla canyons to continue down slope. The U Canyon (incision of 80 m and 1.2 km wide) is located 10 km from the shelf break and is not connected to any present drainage. It is a tributary network of small gullies, which developed a channel-like feature beyond the slope break (Figure 3.5). Sabanilla Canyon is the westernmost canyon, being a narrow feature 1.4 to 0.6 km wide and with 120m of maximum incision. The Sabanilla Canyon is related with previous locations of the Magdalena River mouth during the Holocene (this work, Chapter 2).

East of the river mouth there are a series of slope channels (or gullies) (Figure 3.5) oriented down slope and connecting to a slump feature to the east. In addition, evidences of mass transport deposits and shale diapirs can be identified on the slope.

North of the Sierra Nevada de Santa Marta is the Aguja Canyon controlled by major faults that are present in the area (Figure 3.1 and 3.2b). This entrenched feature begins parallel to the Oca fault, then abruptly turns to the north for 40 km with a height of 430m and width of 2.1 km. The next segment, oriented east- west, is about 40 km long until reaching the deformation front debouching onto the abyssal plain. It is almost orthogonal to the upslope canyon segment, with 600 m of height and 5.2 km width. The canyon is characterized by a sinuous thalweg and at the lower slope section by the presence of terraces and slump scarps at the canyon walls. There is no major drainage associated with the canyon that provides sediment.

The Sierra Nevada de Santa Marta drainages are small and deposit their load on the coast and continental shelf.

3.2.2 Piggyback basins

A series of northeast trending piggyback basins (PBBs) were developed as a result of the thrust fault and fold growth (Figure 3.6). Three of them are actively receiving sediment flows coming from the delta front through canyons towards the abyssal plain. Fault growth, collapse structures (crestal collapse) and normal faulting generate MTCs which contribute to the fill of the basins floor (Romero et al., in press). PBB 1 is found at the toe of the active canyons (1300 m water depth, 55.2 km long and 5.9 km wide). It is connected to lower basins through knickpoints (KP1and KP2) and canyons. PBB2 (1490 m water depth, 23.5 km long and 3.7 km wide) is a hanging basin with its floor elevated with respect to the adjacent basins, and seems to not be receiving sediments today, since fault growth leaves it as a relatively high topographic area. It is dissected by an orthogonal canyon which feeds sediments to PBB4. PBB3 and PBB4 were connected in an early stage of deformation, and isolated by continued uplift of the thrust fault that confines PBB3, and which separated the piggyback basins by a 200m

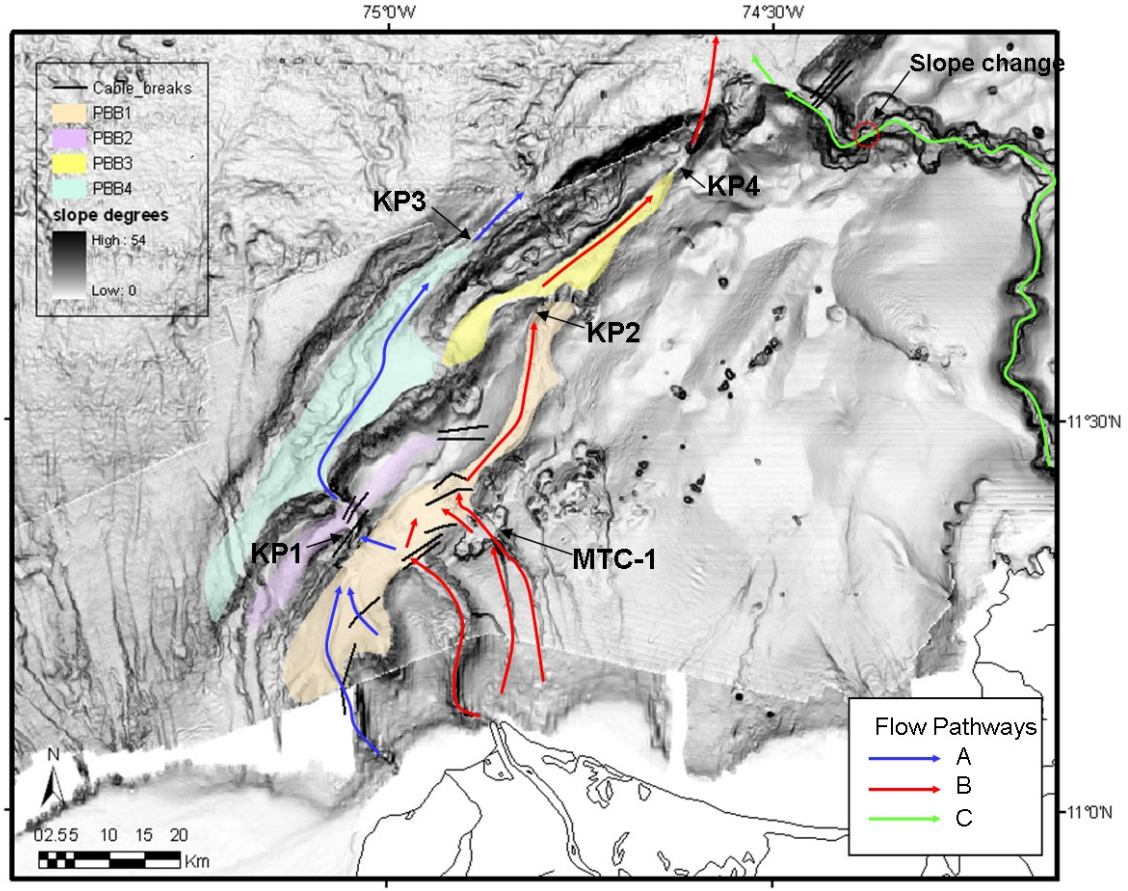


Figure 3.6. Piggyback basins and main flow path directions. (Blue) represent the gravity flows transported through the Sabanilla, U and Magdalena canyons that converge towards KP1 and continue down slope through PBB4 to the abyssal plain. (Red) represents the gravity flows that are diverged towards the east, transported through PBB1 and PBB3 to reach the abyssal plain. (Green) corresponds to the gravity flows transported by the Aguja Canyon.

high scarp, thus preventing sediments from the main canyons reaches PBB4 from the south. PBB3 (2290 m water depth, 38.4 km long and 4.2 km wide) is fed by flows traveling through PBB1 (KP2) and ultimately reaching the abyssal plain by KP4. PPB4 (2100 m water depth, 48 km long x 9.25 km wide) exhibits a hanging channel that at some time prior to deformation was connected to the shelf break. Due to deformation it was abandoned and replaced by a conduit orthogonal to the fault system (this work, Chapter 2). Continuous deformation is indicated by the onlap of sediments against the channel walls (Figure 3.6). Erosional conduits and knickpoints reveal the flow pathway towards the abyssal plain through KP3 (Figure 3.6). Figure 3.7 shows the slope profiles through the piggyback basins and the pathways that follow the sediments to reach the abyssal plain. The profiles are highly variable within the piggyback basins as can be observed in the slope section corresponding to PBB4 between KP1 to KP3 (Figure 3.7).

The slope map in Figure 3.6 outlines other nearly flat areas that form small basins. However, there is no record of recent sedimentation activity in these basins, as they are not in the path of sediment flows that ruptured the submarine cables. The flat nature of their floor however suggests that some relatively recent sediment gravity flows occurred there.

Another large intra-slope basin, the Rancheria Basin, is observed to the northeast of the area (Figure 3.4B). This basin is contained by the folded ridges of the accretionary belt to the north and west. The high acoustic

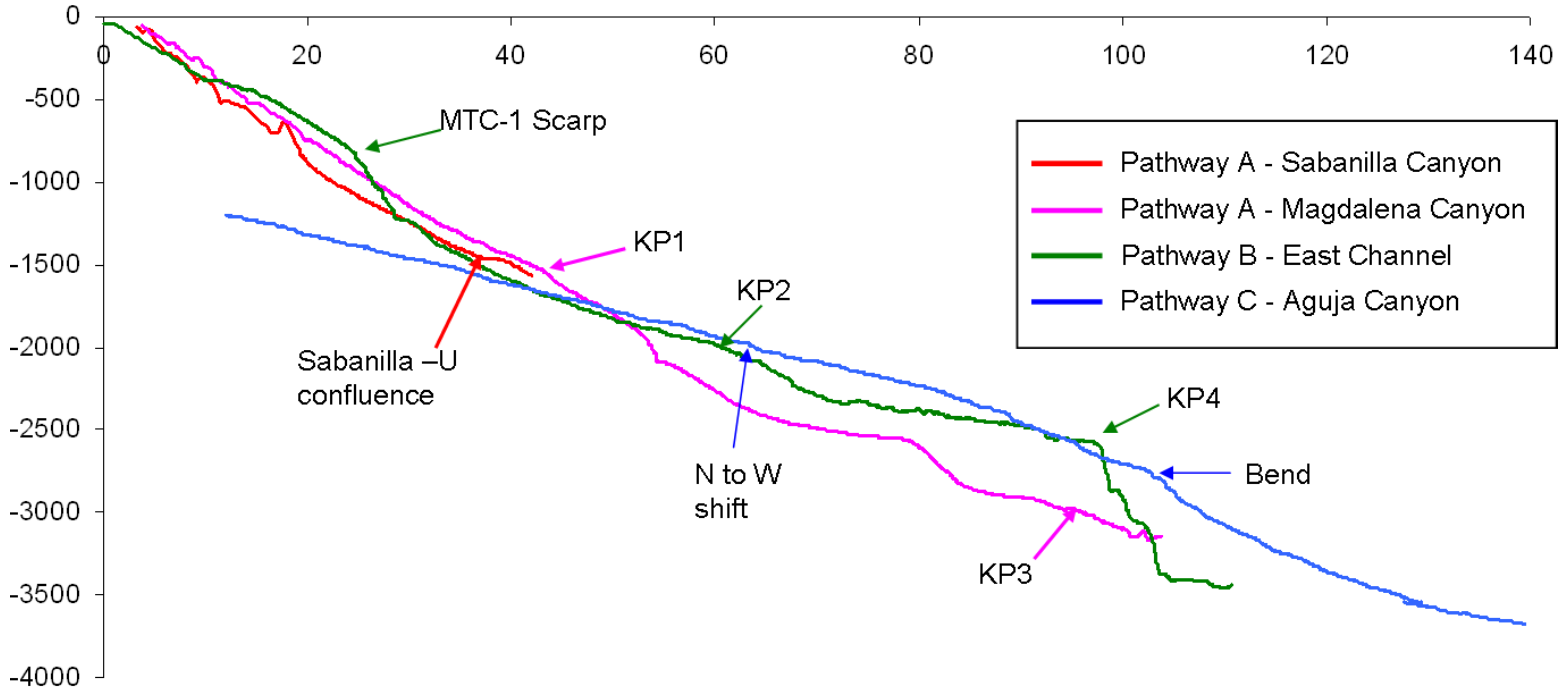


Figure 3.7. Pathway profiles (Figure 3.6). Pathway A is composed of the Magdalena (Pink), Sabanilla (Red) and U canyons. The confluence of the Sabanilla and U canyons is depicted by a convex-up change in the profile. The knickpoints KP1 and KP3 show breaks in the slope, additional breaks in the slope (convex up sections) are found in this pathway. Pathway B profile is characterized by marked breaks in the slope that correspond to the MTC-1 scarp and knickpoints 2 and 4. Pathway C- Aguja Canyon shows a smooth convex-up profile. The major break corresponds to the area were the canyon exhibits terraces, slumps and a conspicuous sinuous bend.

amplitude on the GLORIA image suggests that the basin has been receiving sandy sediment flows. These flows converge toward the exit canyon to the northwest and travel through a well-defined canyon that debouches onto the abyssal plain where it forms a sediment apron.

3.2.3 Mass transport complexes

Large MTC deposits associated with shelf processes have been described on the Magdalena Fan as filling the interchannel low areas (Ercilla et al., 2002; Estrada et al., 2005b; this work, Chapter 4) (Figure 3.4). In the deformation belt, numerous scarps and slumps are associated with the growth of imbricate faults and normal faults on the front limbs. An important MTC is located west of the Magdalena canyon, MTC-1 is 27 km from the river mouth (1,080 m water depth) (Figure 3.5). The slope angles around the MTCs head scarp ranges between 2-3 ^{o}, increasing down slope to a high angle ramp of 5-9 ^{o}. The MTC-1 is emplaced in PBB1 (0.5 -2 ^{o} slope). The head scarp is circular ("cookie bite type", Moscardelli and Wood, 2008) with an area of 32 km^2. The estimated column of sediment that has been evacuated corresponds to a volume of 6.4 km^3. Minor scarp features and slide blocks are observed at the northeastern and southwestern walls of the MTC-1 scarp. Three channel conduits trend down slope towards the MTC-1 escarpment and converge at the escarpment head. A channel-like feature occurs at the base of the escarpment that continues down slope towards

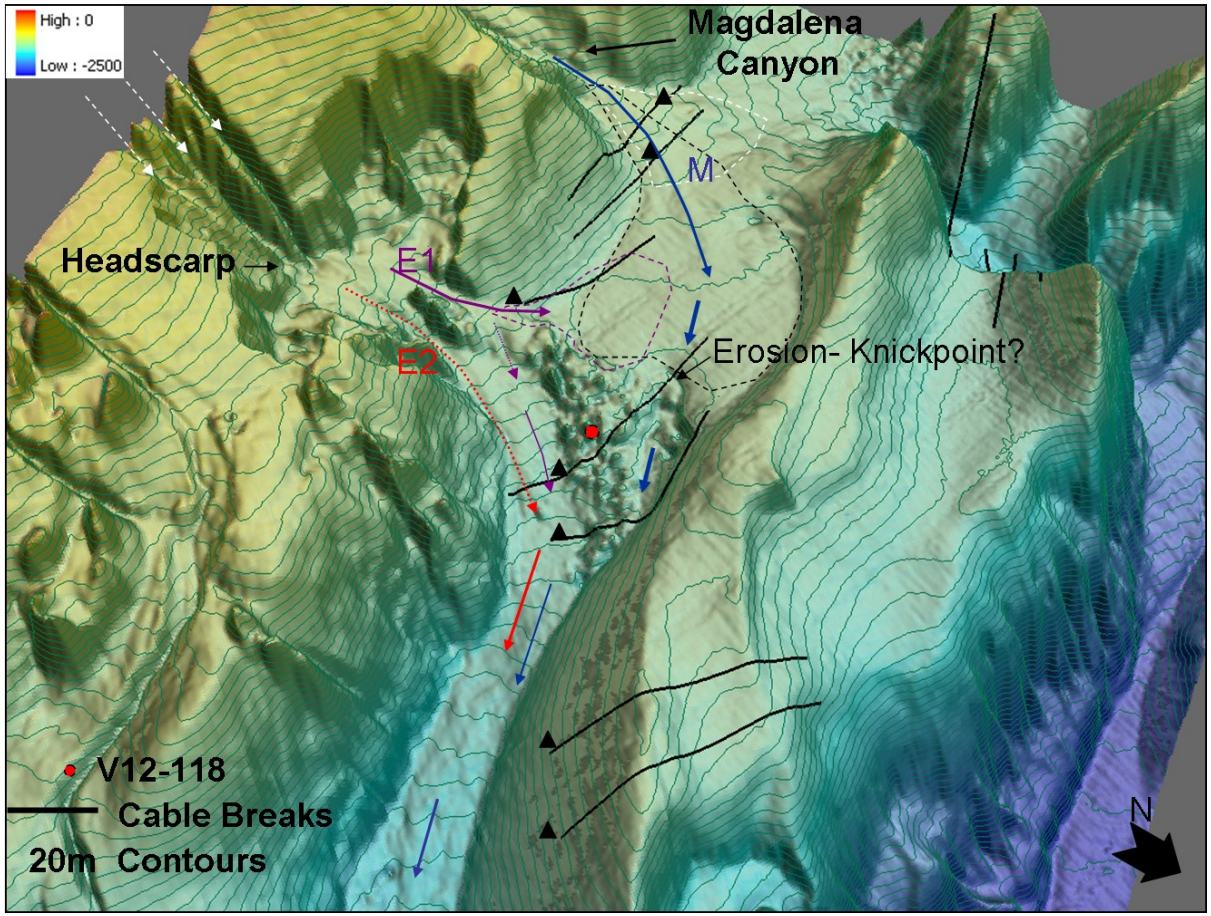


Figure 3.8. Turbiditic flows pathways. Main Magdalena Canyon flows (M), Eastern flows (E1) and (E2). 3D display of the MTC-1. Note the Knickpoint created at the toe of the thrust ridge back limb.

PBB1 between ridges where sediment gravity flows probably are deposited (Figure 3.8). This channel indicates active down slope transport of sediments occurred after the slope failure event responsible for the main scarp. Part of the sediments remobilized from the scarp occurs down slope of the scarp (Figure 3.8). The minimum estimated volume for the deposits is 0.27 km^3 with a possible mean height of approximately 17m. The runoff distance is approximately 9km from the escarpment toe to the deepest portion of the deposits. The MTC-1 can be classified as a frontally emergent submarine landslide using the classification of Frey-Martinez (2006) and as a detached MTC using the classification of Moscardelli and Wood (2008).

3.3 CABLE BREAKS

Heezen (1956) reported fifteen submarine cable breaks in the upper slope of the Caribbean coast of Colombia during the period 1930 to 1956 (Figures 2, 5, 8 and Table 1). In 1930 the submarine communication cable was installed. During the same time period jetties at the Magdalena River mouth were constructed. Two cable breaks were recorded which coincide with loss of the jetty structures. On August 29^{th,} 1935, 480m of the eastern jetty sank and the river sand bar disappeared overnight. On, November 20th, 1945, 200 m of the eastern jetty disappeared. Figure 3.9 depicts the location of the cable breaks. Note that broken cables were replaced further down slope to

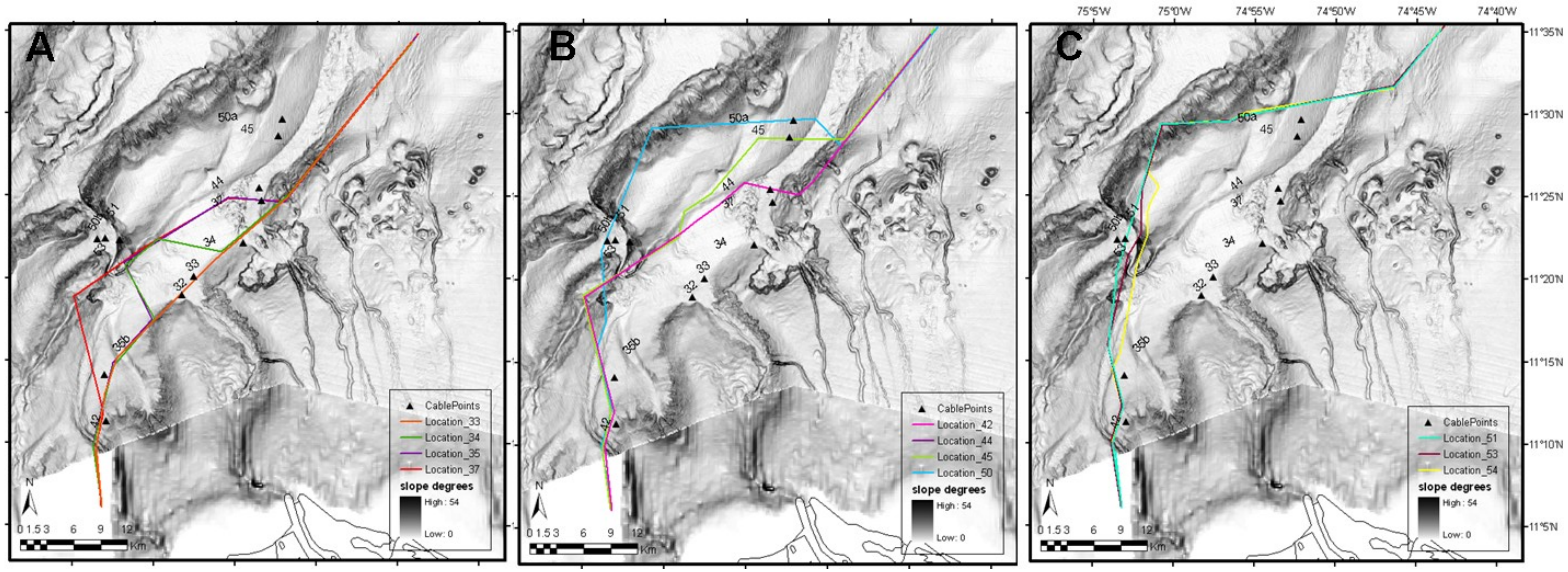


Figure 3.9. Location of the cable from 1930 to 1954. As a result of the rupture of the submarine cable the location was moved to deeper areas. A. Location of the cable line from 1930 to 1937. B. Location of the cable line from 1937 to 1950. C. Location of the cable line from 1950 to 1954.

Year	Date	Location	Flow Pathway*	River Flood stage**	River history
1927	-			-	Start Jetty construction
1928	-			-	-
				-	Interruption of Jetty
1929	-				construction
1930	-			-	Installation of MO-BN Cable
1931	-			-	Restart Jetty construction
1932	5-Nov	Magdalena	A	H-2	-
1933	30-Jul	Magdalena	A	H-1	-
1934	2-Dec	MTC-1 west	B	H-2	-
1935a*	20-Jul	Aguja	C	H-1	Rupture in the Aguja Canyon
		U	A	H-1	480m of Eastern Jetty sank.
1935b	29-Aug				River sand bar disappear
1936	-			-	-
1937	24-Feb	MTC-1 east	B	L	-
1938	-			-	-
1939	-			-	-
1940	-			-	-
1941	-			-	-
1942	18-Apr	Sabanilla	A	L	-
1943	?			-	-
1944	7-Dec	MTC-1 east	B	H-2	-
1945	20-Nov	MTC-1 east	B	H-2	200m of Eastern Jetty sank
1946	-			-	-
1947	-			-	-
1948	-			-	-
1949	-			-	-
1950a	8-Aug	MTC-1 east	B	H-1	-
		KP1	A	H-2	
1950b	11-Dec				Sand bars in the river mouth interrupted the cargo ships traffic
1951	31-May	KP1	A	L	-
1952	?			-	Restart Jetty construction
1953	21-Dec	KP1	A	H-2	-
1954*	?	Aguja	C	L	Rupture in the Aguja Canyon
					Jetty reconstruction was
		Aguja	C	L	almost ready on January 1955
1955*	9-Feb				Rupture in the Aguja Canyon.
1956	4-Jun			-	-

Table 3.1. Cable Breaks Events (Modified from Heezen, 1956a).

deeper waters in an attempt to avoid new ruptures. Three ruptures (Table 1) were also reported from the Aguja canyon, though these are not directly linked with the Magdalena River.

3.4 GLORIA IMAGE

The Gloria sidescan sonar record the reflected sound waves (backscatter) from the seafloor, which are a function of the slope , surface roughness and the textural characteristics of the sediments (Somers et al., 1978). The GLORIA imagery depicts areas of high reflectivity related to areas of active sediment transport and deposition (Figure 3.10). Channel and lobate like features can be recognized on the image, but with further integration of the bathymetry (figure 10 B), the relation of these features with the canyons and the toe of the canyon areas was identified (Figure 3.10 C). Degradation of the slope is a common process with scarps and MTCs being identified by higher reflections (this work, Chapter 4). It is important to note that due to the abrupt morphologies of some ridges, high reflectivity areas may be associated with changes in the slope of the sea floor (Figure 3.10B).

The abyssal plain northeast of the active fan is characterized by high reflectivity north of KP3, KP4 and Aguja Canyon, and extends towards the abyssal plain of the Guajira-Rancheria area (Figure 3.4). The Aguja Canyon is characterized by high reflectivity in the thalweg areas, forming a sediment apron at the toe of the deformation front (Figure 3.4C). North of the Aguja

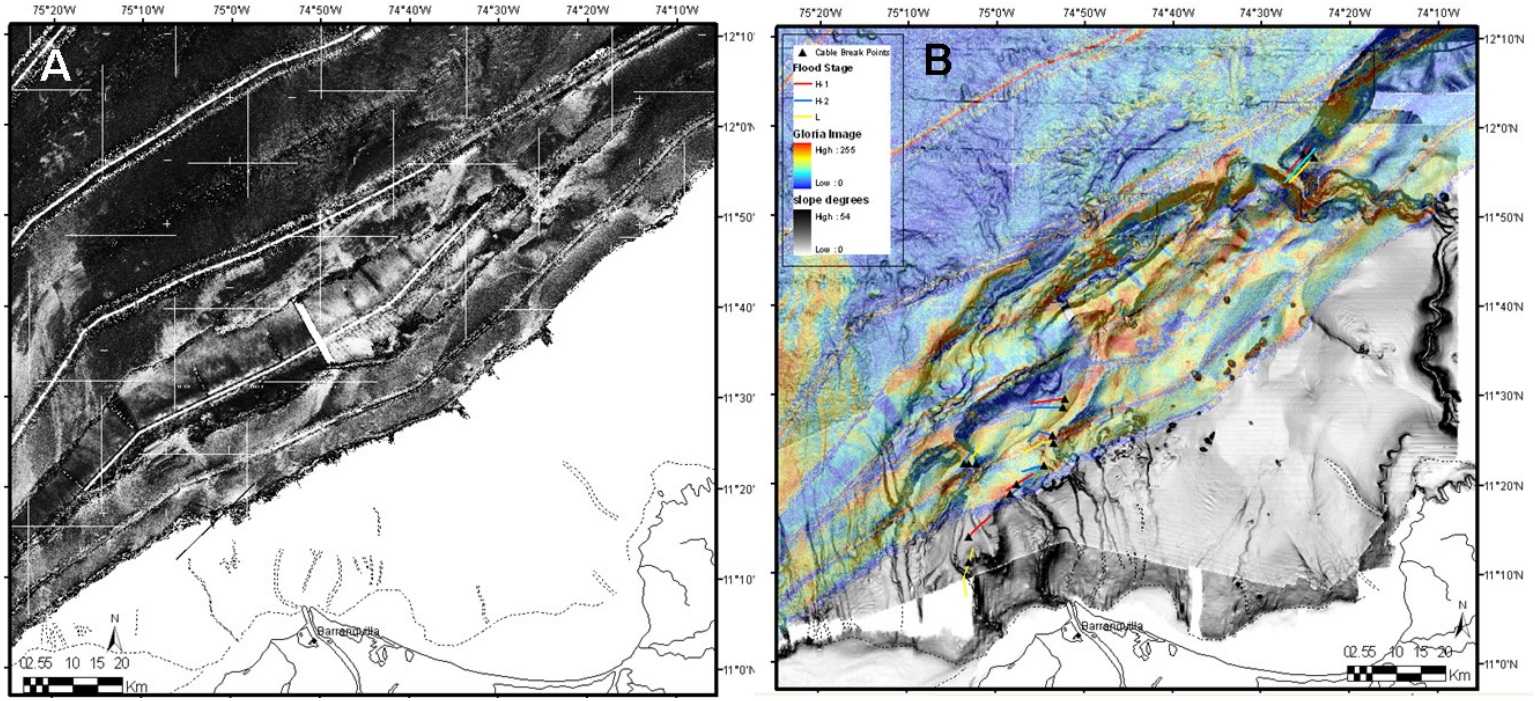


Figure 3.10. A. GLORIA image in a gray scale. High reflectivity areas correspond to the whiter colors. B. GLORIA image in a color scale integrated with the bathymetry map.

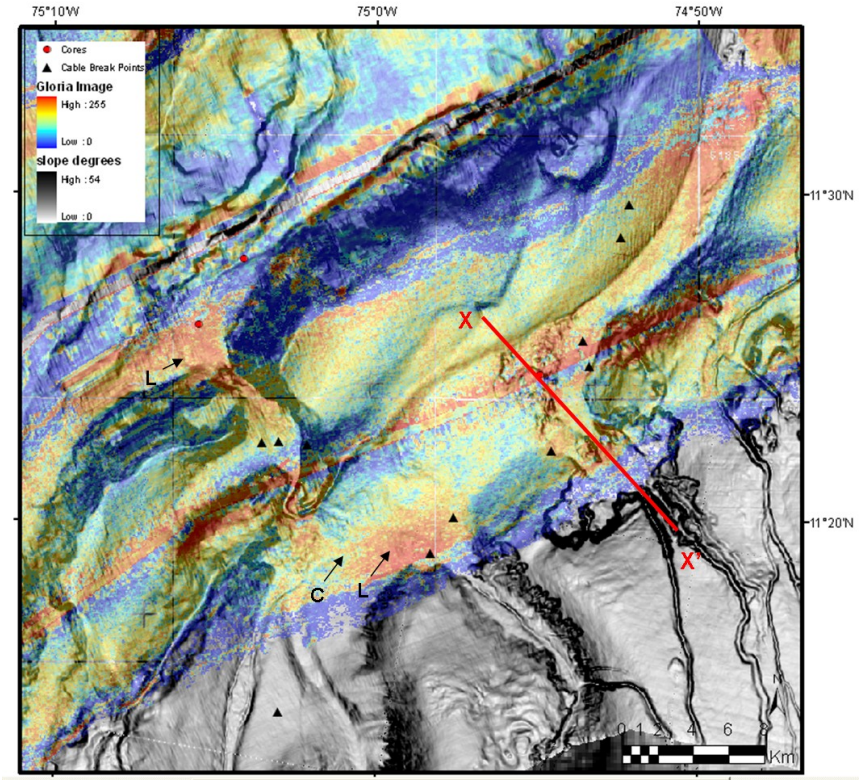


Figure 3.10. C. Detail of the GLORIA image in PBB1 (L) Lobate features. (C) Conduit of sediments feature. X-X' seismic profile through the PBB1 (Figure 3.11)

Canyon, a highly defined canyon can be recognized, which dissects the continuation of the northeastern deformation front (Figure 3.4B). Upslope of this canyon is a highly reflective area, the Rancheria Basin, which is confined by the fold ridges (Figure 3.4B). The abyssal plain is characterized by reflective sediments, fed by the active fan and Aguja Canyon (southwest) and the Guajira area (east) (Figure 3.4A). The imagery reveals features that are probably associated with bedforms caused by the sediment gravity flows both in the sediment aprons (Fig 4C) and on the abyssal plain (Fig 4A).

3.5 FLOW PATHWAYS AND DISTRIBUTION OF CABLE BREAKS

Sediment gravity flows in the active Magdalena Fan are distributed through the different canyons travelling down slope, leaving deposits at the lower slope areas (PBB) until reaching the abyssal plain. The active flow pathways can be grouped into three corridors (Figure 3.6): A) Flows from the Magdalena , Sabanilla and U canyons in direction to PBB 3 through KP1 and reaching the abyssal plain through KP3; B) Flows starting at the Magdalena Canyon or at the eastern gullies diverging towards the east in PBB1, traveling downslope through KP2, continuing in PBB3 and reaching the abyssal plain through KP4; C) Flows initiated at the shelf margin, traveling downslope through the Aguja Canyon until they reach the abyssal plain. Table 1 characterizes the cable breaks with their associated sediment flow pathways. Figure 3.7 shows the pathway topographic profiles from the river/shelf to the abyssal plain. The slope profiles show high variability, with

several convex-up sections beside the breaks were the knickpoints are located, indicating areas of erosion and deposition within the piggyback basins.

3.5.1 Active Magdalena Canyon

The first cable breaks occurred in 1932 and 1933 at the toe of the Magdalena Canyon. Flows traveling through the canyon deposited sediments at the break in slope as indicated by the presence of a lobate feature and high reflectivity in the GLORIA image (Figure 3.5, 10 C). The flows were deflected towards the east (Flow pathway B) and were deposited on the piggyback basin floor obstructed by the MTC-1. Some flows may have overridden the MTC-1, while others eroded the MTC to open a pathway through it (Figure 3.8). This is corroborated by the flat parallel seismic reflections that onlap the MTC (Figure 3.11). Also, there are indications of erosion and flows diverging towards the west (Flow pathway A) (Figure 3.8). GLORIA image shows a linear channel pattern of high reflectivity which could indicate recent sediment flows through this area (Figure 3.10 C), converging with the western canyons flows, and traveling down slope through KP1and entrenched on the canyon that is cutting PBB2 until reaching PBB3 (Figure 3.6). The GLORIA image exhibits a lobate shape with high reflectivity at the toe of the canyon, indicating sediment deposition in this area (Figure 3.10 C). In addition, three cable breaks are

located in this canyon (1950b, 51, 53, in Figure 3.5), indicating periodic active sediment transport.

3.5.2 Delta west

Cable breaks were reported west of the Magdalena Canyon during 1935b and 1942 (Figure 3.5). The 1935 break coincided with the eastern jetty disappearing at the river mouth (Table 1). The rupture of the cable is associated with the U Canyon that, interestingly, is not directly connected with the river mouth. The 1942 cable break occurred in the Sabanilla Canyon. The U and Sabanilla canyons exhibit incision on the slope and converge towards KP1. The Sabanilla Canyon contains incised thalwegs that cut the U Canyon, indicating greater or more recent erosive processes in the Sabanilla Canyon. In addition, a slump deposit was emplaced by instability of the confining ridge, deflecting the flows coming from the Sabanilla Canyon (Figure 3.5). The flows traveling through these conduits should have been deposited partly on PPB 1 or down slope in PPB 4 through KP1 (Flow pathway A) (Figure 3.6). Part of the flows through the Magdalena Canyon converged towards the KP1 following the same pathway as the Sabanilla and U flows ((Flow pathway A). with the river mouth. The 1942 cable break occurred in the Sabanilla Canyon. The U and Sabanilla canyons are exhibit incision on the slope and converge towards KP1. The Sabanilla canyon contains incised thalwegs that cut the U Canyon,

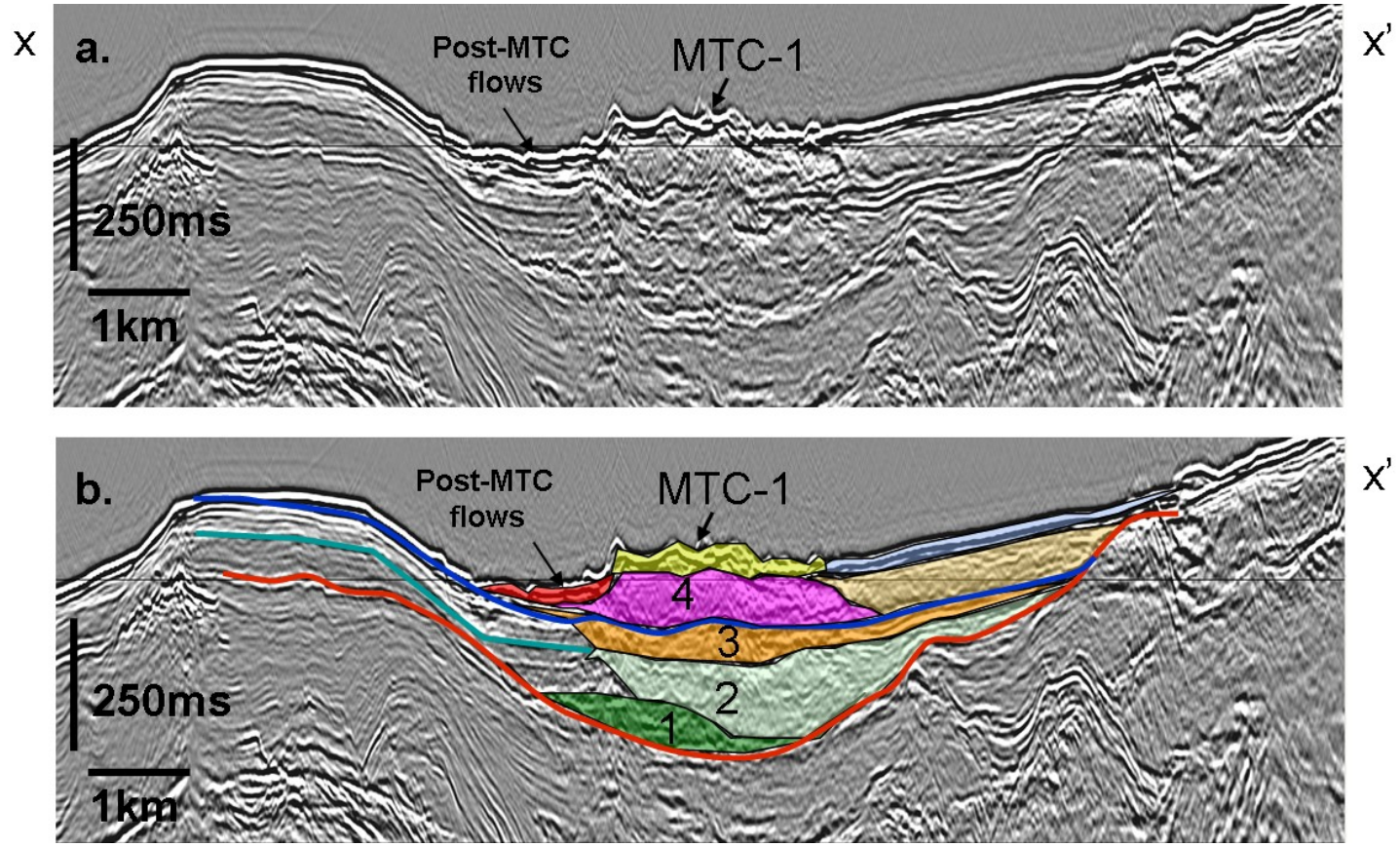


Figure 3.11. MTC-1 seismic interpretation. Corresponds to line X-X' in figure 9c. A. Uninterpreted seismic profile. B. Interpreted profile showing the multiple stacking of chaotic packages in the piggyback basin.

indicating greater or more recent erosive processes in the Sabanilla canyon. In addition, a slump deposit was emplaced by instability of the confining ridge, deflecting the flows coming from the Sabanilla canyon (Figure 3.5). The flows traveling through these conduits should have been deposited partly on PPB 1 or down slope in PPB 4 through KP1 (Flow pathway A) (Figure 3.6). Part of the flows through the Magdalena Canyon converged towards the KP1 following the same pathway as the Sabanilla and U flows ((Flow pathway A).

3.5.3 Delta East

Five rupture events have been reported east of the Magdalena Canyon. Breaks that occurred in the years 1934, 1937 and 1944 are located in the MTC-1 area (Figure 3.5). The eastern part of pathway B seems to have had recent activity as is illustrated by the erosion at the scarp floor (Figure 3.8). All eastern (including Magdalena Canyon) pathways contribute to the transport of flows toward the abyssal plain as well as infilling the PBB1. The 1934 break at the western conduit is located at the toe of the MTC-1 scarp, and possibly allowed transport of sediment towards both the west and northeast (basinward) (Figure 3.5). Two main flow pathways are identified: 1) flows from the headscarp conduits that are deflected towards the west of the MTC-1 (E1) and 2) flows deflected eastward of the MTC-1 (E2) (Figures 3.5 and 3.7).

The 1937 and 1944 cable breaks are located east of the MTC-1, at the main sediment flow corridor into the piggyback basin. Flows traveling through the west pathway (E1 - 1934 cable break) (Figure 3.8) may have contributed to fill the back side of MTC-1, ultimately deflecting Magdalena Canyon flows toward the west. Also, evidence of western flows (E1) deflecting towards the east through the MTC remnants is the change in morphology (smoothing) at the head of the MTC deposit, leaving remnant blocks separated from the main deposit.

Two breaks occurred during 1945 and 1950a (Table 1, Figure 3.5). The location of these breaks is not associated directly with the canyons or PPB1, but at the back limb of the ridge (Figure 3.8). It is important to consider the errors on the location of these events. Due to 1950's geo-positioning methods, errors of 1 km or more may change the location of the cable breaks. In addition, not reliably pinpointing stretching and rupture of the cable may have modified the location. In particular, flows traveling northeast on the adjacent canyon could have stretched the cable, pushing the apparent break location to the north. We interpret that these rupture events were related to down slope flows going through PBB1. Flows transported through E2 continued down slope through PPB1, which in combination with the Magdalena flows reached the abyssal plain passing through KP2, PBB3 and KP4 (Figure 3.6).

3.5.4 Aguja Canyon

The Aguja Canyon is not directly related to the Magdalena River sediment transport, but also presently receives sediment flows which are transported to the abyssal plain (Figure 3.2). Cable breaks in 1935a (July), 1954 and 1955 (February) were reported in this area. Heezen (1956) linked the Aguja Canyon with the Magdalena River, apparently by associating the cable breaks there with flows originating from the Magdalena River. This interpretation was allowed due to sparse bathymetry data available at that time (Figure 3.2B). With higher resolution bathymetry it is now evident that there is a separate system which seems to be fed from the continental shelf to the east of the Sierra Nevada de Santa Marta where there are no large rivers.

3.6 SEDIMENT DISTRIBUTION – PISTON CORES.

Part of the research performed in the Magdalena area by Heezen in the 1950's and 60's included a series of piston cores taken on the active fan area and the abyssal fan based on the interpretation of the flow paths (Figure 3.2A). Muñoz (1966) published detailed descriptions and grain size analyses of cores acquired close to areas where submarine cable breaks were reported in the Magdalena turbidite fan. Fourteen core descriptions were revised and only three of them exhibit recent turbidites (Figure 3.4 and 3.12). Two of these cores are located in the piggyback basins: V12-112 and

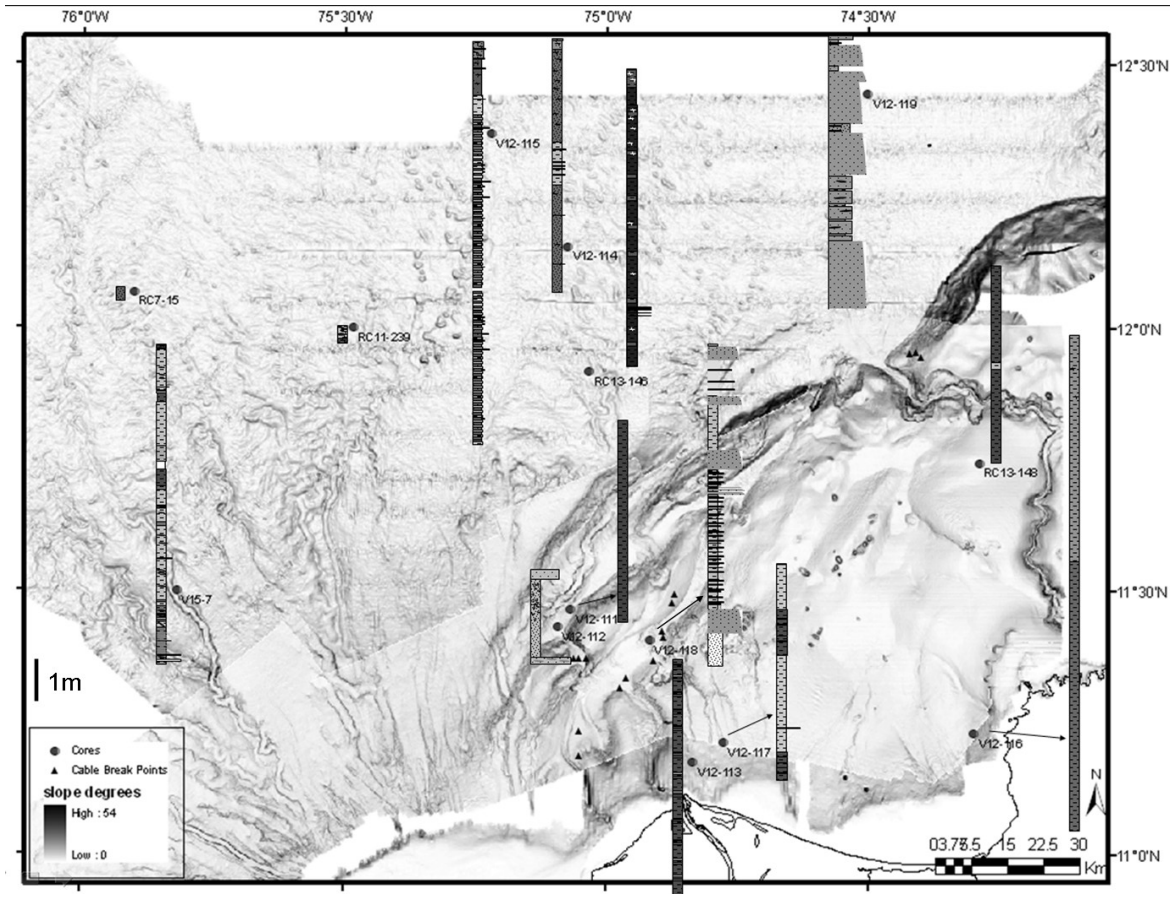


Figure 3.12. Lithologic description of piston cores in the Magdalena. Vema acquisition. Data obtained from the Lamont Doherty Laboratory repository. Note the only cores that have evidences of turbidites flows are V12-112 in PBB4, V12-118 in PBB1 and V12-119 at the abyssal plain. The rest of the cores are composed of fine-grained sediments, mainly mud and silty claystone . (See complete description Appendix 1)

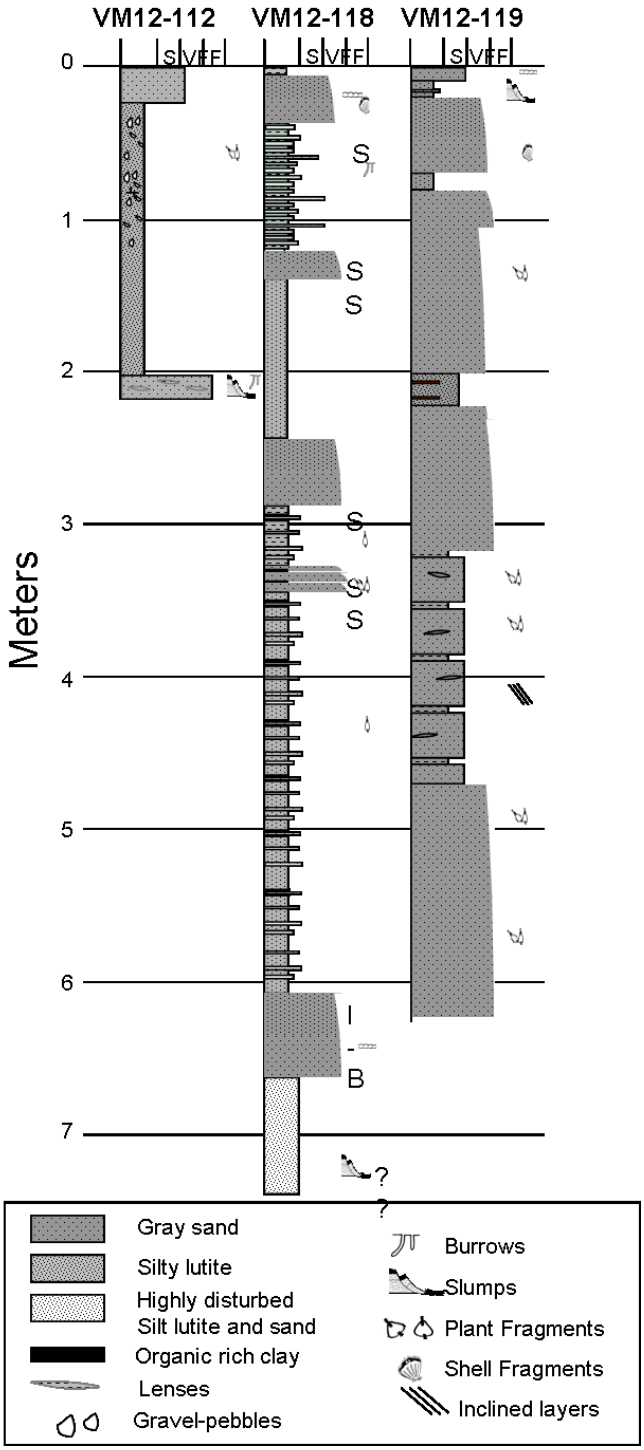


Figure 3.13. Lithologic description for piston cores VM12-112, VM12-118 and VM12-119. Note the abundance of turbidites for the three cores. Location at Figure 3.12.

V12-118, and the third is located on the abyssal plain, V12-119 (Figures 3.12 and 3.13).

V12-112 contains two main lithologies (Figure 3.13). The top bed (23cm) represents a turbidite composed of very fine sand to silt, angular quartz grains, with abundant plant fragments. The basal bed has similar characteristics to the upper layers but with some disturbance at the bottom. The middle lithology suggests slump deposits composed of silty mud, with abundant granules, pebbles, foraminifera and shells fragments. It has been suggested that this interval corresponds to slump deposits (Muñoz, 1996). The muddy lithology and poor sorting suggests massive deposition, likely from a debris flow.

The V12-118 core (Figures 12 and 13) is located within the MTC-1 deposit area. Muñoz' (1966) description (Figure 3.14) highlights the abundance of turbidites as approximately 10 per meter in the cored section, with individual bed thicknesses reaching 57 cm. The core is mainly composed of alternations of turbidites (very fine sand to coarse silt), clay and silty clay. The sand grains are mainly angular to subangular quartz grains, mica flakes and other mineral fragments. There is a notable similarity between the sediments in the core and the sediments at the river mouth (both bed load and suspension). Some turbidites exhibit sharp basal contacts (Figure 3.14).

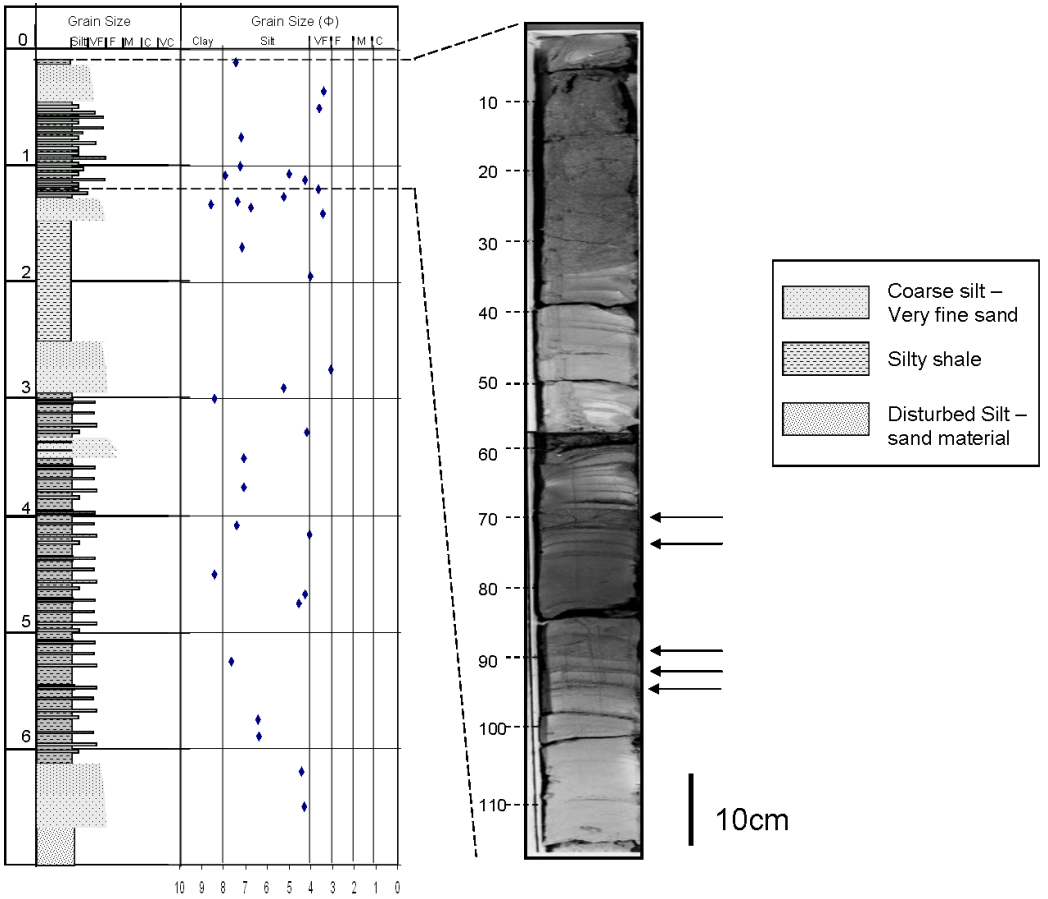


Figure 3.14. V12-118 core description and grain size analysis from Muñoz (1966). Note the absence of pelagic drape at the top of the core. Arrows indicate possible hyperpycnal flow deposits. Core photograph LDEO Deep-sea sample repository http://www.ldeo.columbia.edu/res/fac/CORE_REPOSITORY/RHP1.html)

A

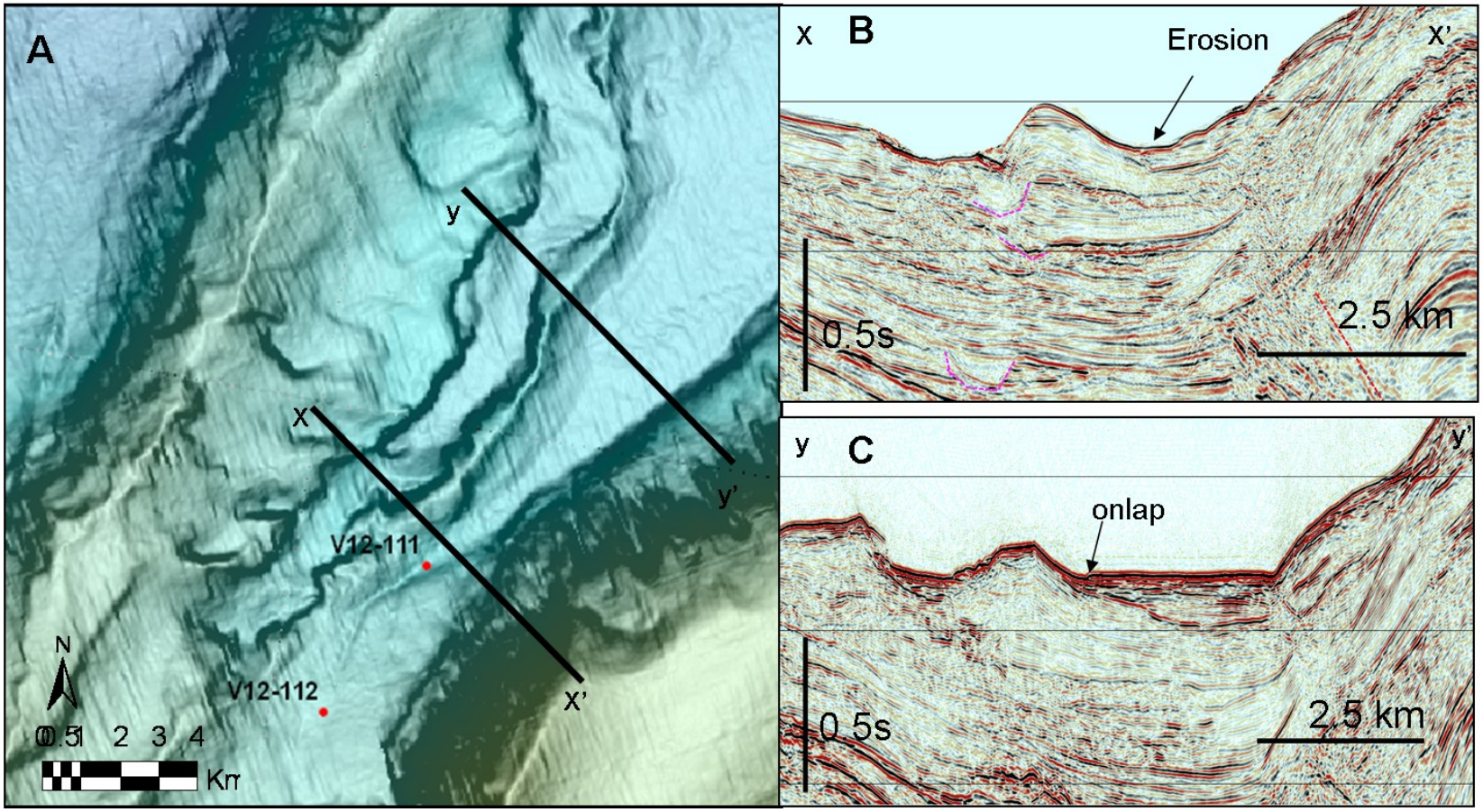


Figure 3.15. A. The core VM12-111 do not exhibit turbidites since is located in a bypass area. B (x-x') depicts the erosive nature of the area close to the V12-111. C (y-y') exhibits horizontal and continuous reflectors that are missing on the proximal line and may correspond to turbidite flows deposited in PBB4.

high content of plant debris occurs throughout the core, sometimes concentrated in laminae 1 mm thick and associated with very fine sand. Neither terrigenous mud nor pelagic material occurs above the turbidites, thus indicating their recent deposition. Some beds are graded. Frequently the graded sequence is not complete, and massive, 5-60cm thick homogeneous sand beds are present. The sand beds are well sorted and similar to the sands in the up-current river channel bedload. This similarity suggests little sorting between the river mouth and the site of deposition about 30 km away. It is important to note that the typical facies expected for MTC deposits (debrites, slumps) are not present in the core, which could indicate that the MTC is composed mainly of undeformed slide blocks (Moscardelli and Wood,2008) or, as is more likely, that the shallow core sampled turbidite deposits that are younger than the slumped deposits (Figure 3.14).

V12-119 is located on the abyssal plain near the Aguja Canyon. It is mainly composed of gray, very fine to fine grained, moderately to poorly sorted turbidite beds (Figure 3.12 and 3.13). Abundant plant material is found throughout the section. Finer grained intervals correspond to silty lutites with the presence of lenses and reworked sediments (“inclined layers”; Munoz, 1966).

It is important to note that none of these three cores has a pelagic mud drape, which confirms the active sediment transport through this area. The

sediments of the rest of the cores are mainly constituted by silty mudstones and mudstones (Figure 3.12). Content of foraminifera is generally low, and plant and shell fragment are not very common. (2.12, 2.16, 2.35 m) depict negative asymmetry, which could be related to slumped material (Figure 3.12).

3.7 PISTON CORES INTERPRETATION

Only four of the piston cores are located on the possible recent pathway of active turbidity currents. Three of these (VM12-112, V12-118 and VM12-119) depict recent turbidity current activity by the presence of a turbidite layer at the top of the core (Figure 3.12) as was discussed above. The fourth core, V12-111, is located on PBB4 (Figure 3.15 A), in the middle of an entrenched area (incipient knickpoint) between an abandoned channel and the front limb of a ridge. If the location of the core is correct, the absence of turbidite deposits similar to the ones found in the upslope VM12-112 core suggests this area to be a bypass zone. The turbidite flows are eroding this part of the slope (Figure 3.15A) and continuing down slope to be deposited on PBB-4 or the abyssal plain, as is evidenced by the morphology of the PPB-4 down slope of this core. Seismic profiles down slope of V12-111 (Figure 3.15 B and C) show the different style of sedimentation at the proximal and more distal area on the PBB4. Figure 3.15B shows thinner

deposits against the abandoned levee and truncated by the sea-bottom reflector. In contrast, Figure 3.15C exhibits horizontal, continuous reflectors that onlap against the levee; and those are clearly missing on the proximal line and may correspond to turbidite flows deposited in this part of PBB4.

Grain size distribution and sorting of the V12-118, V12-112 and V12-119 sediments are plotted in Figure 3.16. For turbidite intervals containing more that 40% sand, the grain size is mainly very fine to fine sand (Figure 3.16A). Sorting is more variable (Figure 3.16B). The sample with nearly 80% sand corresponds to the upper turbidite in V12-112. The three extremely poorly sorted fine sand samples correspond to the lower turbidite interval.

There is no clear evidence of changes in the grain size with an increase in the source distance; the V12-118 and V-12 119 cores show similar values of sorting and grain size (Figure 3.16A). Core V12-119, located in the abyssal plain, does not show a major change in grain size or sorting that may indicate changes in the sediment source (Figure 3.16). The seafloor imagery (Figures 4C and 6) suggests that flows from both the Aguja and Magdalena River areas could have reached the site in recent times. Detailed mineralogy studies could possibly be used to distinguish turbidites sourced from the two areas.

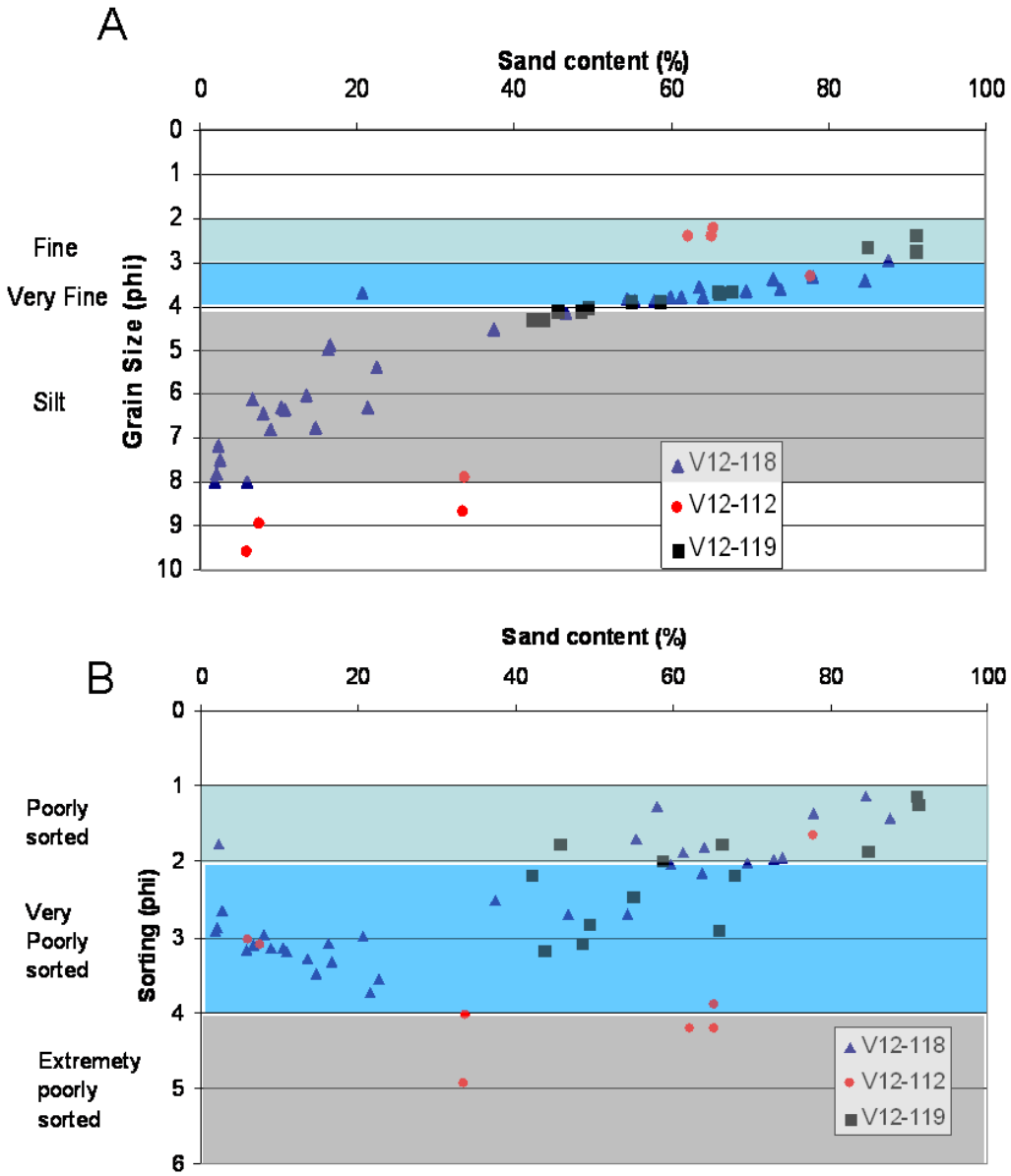


Figure 3.16. Grain size, sand content and sorting of the V12-118, V12-112 and V12-118. A) Sand content (%) vs grain size (phi), note the samples for the V12-112 core are out of the main trend. B) Sand content (%) vs sorting (phi), the sand rich sediment are very to poorly sorted with the exception of the V12-112 samples that are extremely poor sorted.

3.8 DISCUSSION

The importance of recognizing the mechanisms for turbidite flow initiation lies in the characteristics of the deposits that are generated from the different flows (see Weimer and Slatt, 2007 for a comprehensive review). Characteristics such as flow velocity, viscosity, size, and erosional capability will differ depending upon the origin of the flow (Kneller and Buckee, 2000). In the same way, the deposits will differ in textural characteristics, sedimentary structures and areal distribution of the flows.

On the active Magdalena Fan more than one flow initiation mechanism may be present. River mouth failure, longshore drift, coastal erosion, high river flood stages, and hyperpycnal flows are considered in this paper as possible mechanisms responsible for the turbidite flows causing the cable breaks. In addition, the active compressional deformation, uplift of the shelf and upper slope area, and seismicity (this work, Chapter 4), may have destabilized the sediments at the proximities of the river mouth.

3.8.1 River sediment discharge and flood stages -cable breaks

Cable breaks associated with maximum river bed-load transport during floods have been recognized in the Zaire Fan, at a frequency of 60 events per century (Droz et al., 1996). A similar frequency (about 48 events/century) has been determined for the cable breaks in the Magdalena

River area (excluding the breaks in the Aguja Canyon). The Magdalena River annual sediment load of 143.9 $x10^6$ t yr^{-1} (130.5 metric ton per year) is a very large amount and accounts for 9% of the sediment transported in the east coast of South America, and is of same order of magnitude as the Amazon, Orinoco and Parana rivers which have larger drainage basins (Restrepo and Kjerfve, 2000). Sediment load and discharge during the last 25 years exhibit maximum values during November and December, and a secondary peak during June and July (Figure 3.17). These increments coincide with the months with higher occurrence of cable breaks or during periods just prior to the cable breaks. This correlation indicates the likely influence of the river-borne sediment load and the generation of submarine flows. The presence of terrigenous plant material in the cores is also confirming river derived sediment flow processes.

The annual discharge of the river from 1940 to 1960 (Winkley et al., 1994) also showed high volumes during several periods. This corresponds to a period of time when seven cable-breaks occurred (Figure 3.18). During years of higher discharge, cable breaks occurred mainly during the second high discharge season (Nov- Dec). The river discharge record for the period from 1930 to 1940 is not available; during this timeframe five cable breaks were recorded.

The sediment load data indicate three possible correlations with sediment flows: 1) due to the large amount of sediments transported by the river, 1)

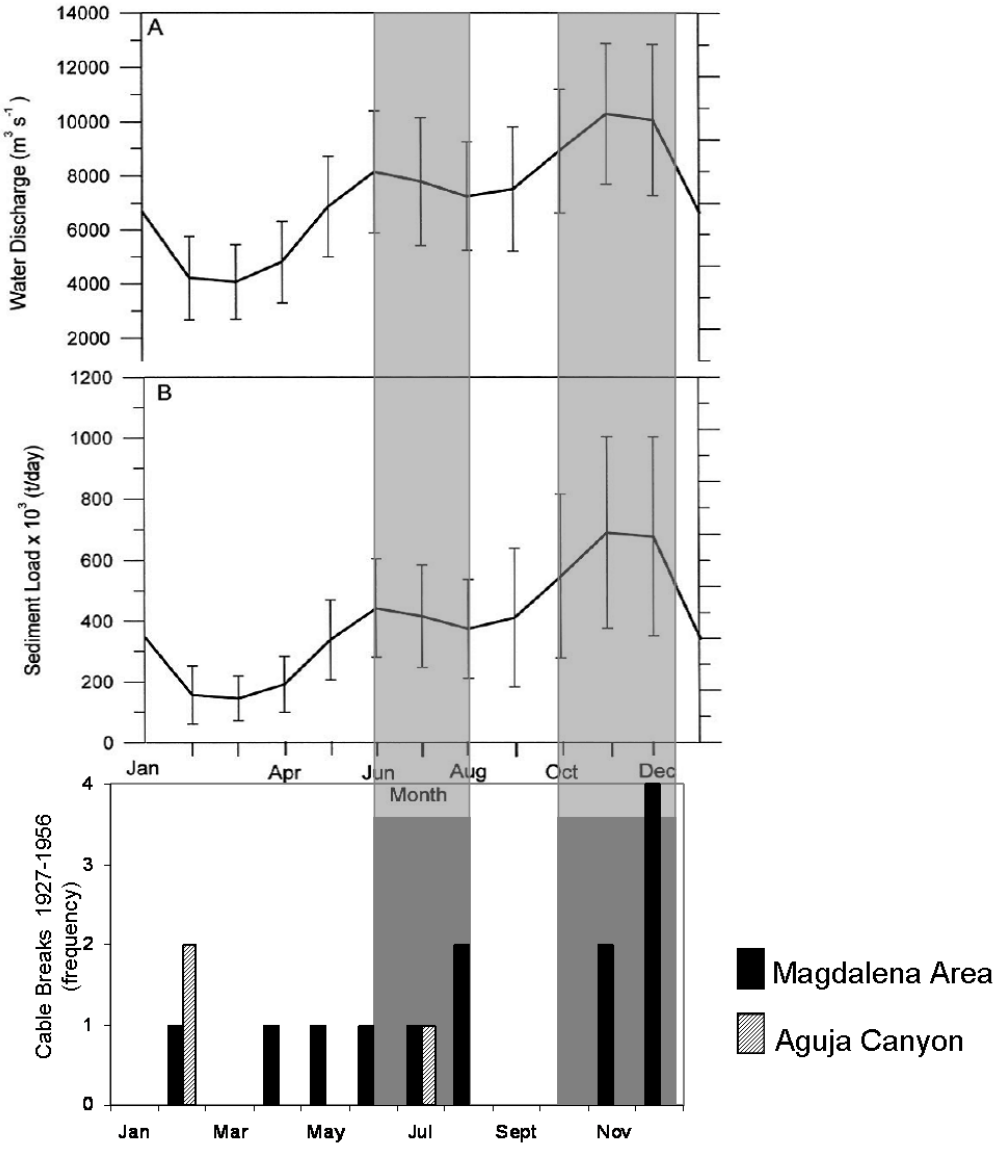


Figure 3.17. (A) Monthly mean and standard deviation of water discharge; and (B) sediment load, in the Magdalena River at Calamar, 1975–1995. (From Restrepo and Kjerfve,2000). (C) Cable breaks monthly distribution: 1927-1956. The seasonal distribution of sediment load indicates high values of 690 $x10^3$ t day^{-1} and 678 $x10^3$ t day^{-1}during November and December. Secondary high sediment loads occur during June–July with loads reaching 443 $x10^3$ t day^{-1}. These periods coincide with some of the cable breaks.

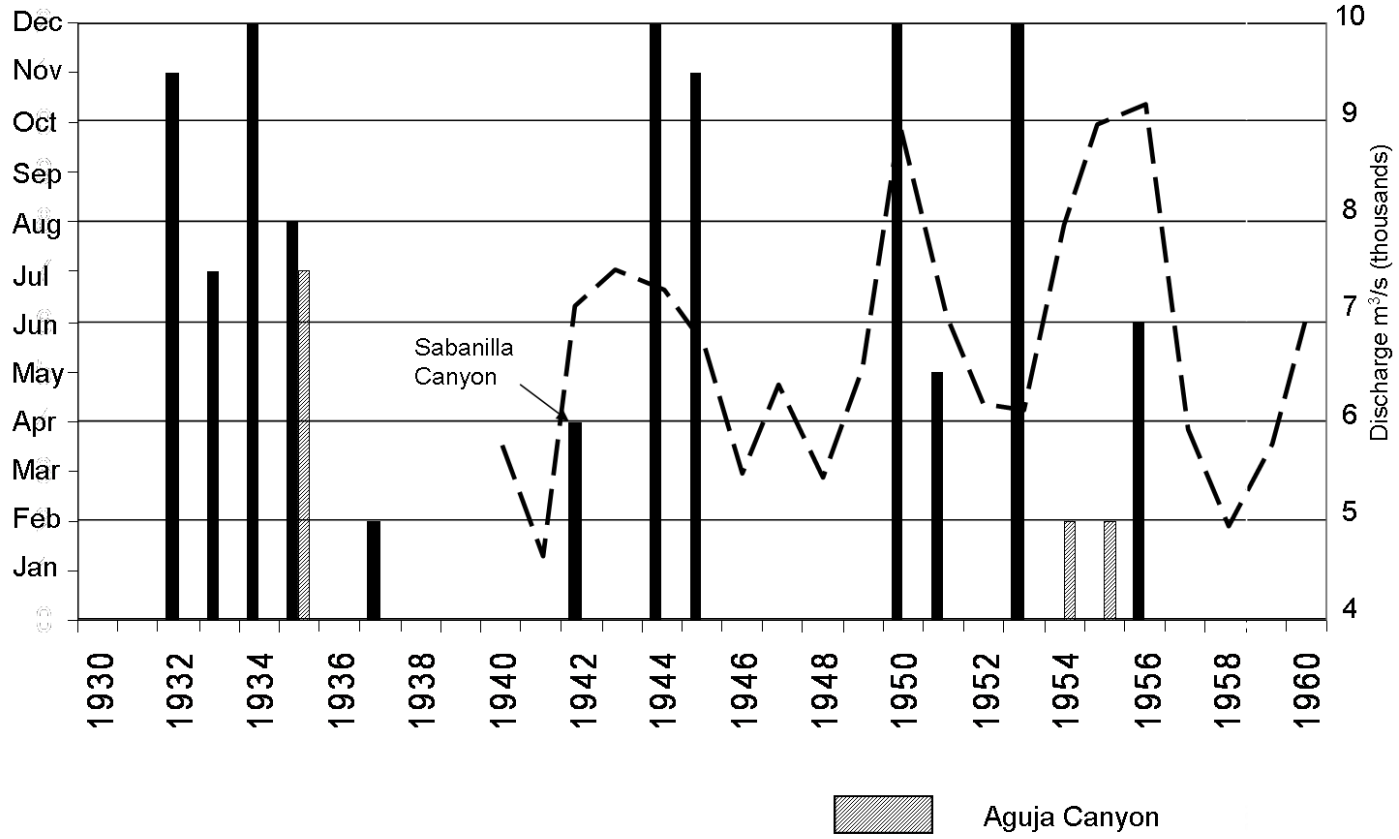


Figure 3.18. Cable breaks (1927-1956) and Mean Annual Discharge, Calamar Gage 1941 to 1970 (Modified from Winkley et al., 1994). The cable breaks are separated from the Magdalena River area breaks. Note the correlation between high discharge years and the rupture of the cables.

turbidity flows or 2) hyperpycnal flows are generated by water masses of higher sediment concentration during flood stages, or 3) increased sediment accumulation at the delta front, which creates instability and generates slope sediment transport.

3.8.2 Hyperpycnites in the Magdalena Fan?

Hyperpycnal flows are defined as sustained flows formed during high sediment discharge periods that are transported down slope along the sea floor due to differences in the density of the flow and that of overlying sea water (Mulder et al., 2003). Heezen and Muñoz (1965) calculated a sedimentation rate of approximately 100 km^3 per 100,000 years (25 m per million years) for the Magdalena Fan, which when compared with the present discharge of the Magdalena River of about 426.6 km^3 per 100,000 years, indicates the river as the major sediment source to the fan. Hyperpycnal flows are non-ignitive processes (flows fed by sediment transported into the slope from rivers, not by slope erosion) common in major rivers in the world (84%) with frequencies of more than 1 event every 100 years, excluding turbidity currents generated by slumps or foreset failures (Mulder et al., 2003).

The critical concentration needed to produce hyperpycnal flows in marine water depends on the properties of the coastal zone. For equatorial zones,

concentrations of sediments should exceed 36.25 kg m^{-3} (Kennish, 1989) in order to overcome the density difference between fresh and salt water. However, several factors may reduce the critical concentration to as low as 5 kg m^{-3} to generate hyperpycnal flows. Mulder et al. (2003) presented a summary of these factors, including: convective instability of hyperpycnal flows, geological setting (easily eroded drainage basins), extreme geologic events (jökulhaups, lahars, dam breaking), dilution of sea-water by fresh water during long flood stages, and erosion on mouth bars. In addition, discovery of hyperpycnal flow-related sediments in the Zaire deep-sea fan (Migeon, 2000), which was earlier classified as a "clean river" [river that cannot produce hyperpycnal flows (Mulder and Syvitski, 1995)], suggest that hyperpycnal flows are not yet fully understood and could be generated in rivers with low concentration of sediments.

Due to a narrow shelf (~2km) the Magdalena River mouth connects directly to a slope canyon (Figure 3.5). This condition differentiates the Magdalena River from other larger rivers where sediment is first deposited on the continental shelf. The Magdalena River was classified by Mulder and Syvitski (1995) as a river which rarely (>10,000 Yrs) will produce hyperpycnal plumes. Certainly, following the methodology of Mulder and Syvitski (1995), if we calculate the sediment concentration at flood conditions with the maximum average data published for the Magdalena River (Figure 3.17) and the maximum values for years with cable breaks

(during 1956) (Figure 3.18), the concentrations obtained do not exceed the 36.25 kg m^{-3} required for initiation of a hyperpycnal flow (Table 2), but will be higher than 5 kg m^{-3} when convective instability is considered. This indicates that hyperpycnal flows in the Magdalena Fan are feasible. It is important to note that average values are being used and do not properly reflect the relationship of water discharge and sediment load at individual flood conditions.

Taking this into account, it is possible that periodic hyperpycnal flows rather than only sea-water turbiditic flows are responsible for some submarine cable breaks, as first stated by Heezen and Muñoz (1965). Some of the thinly laminated intervals described by Muñoz (1966) in the core at 70 and 90 cm (Figure 3.14) are similar to hyperpycnal deposits (i.e. “hyperpycnites”) described by Bhattacharya and MacEachern (2008). Even though the grain size distribution for this interval shows the presence of very fine sand and silt, further analyses are required to establish if the sediments reveal inverse grading, that is one of the main characteristics to identify hyperpycnal deposits (Soyinka and Slatt, 2008).

Data Source		Area (km^2)	Q (m^3s^{-1})	Qs (kgs^{-1})	Css ($kg\ m^{-3}$)	Qflood (m^3s^{-1})	Cflood ($kg\ m^{-3}$)
Mulder & Syvitski, 1995		240000	7530	6970.0	0.9	51500.0	43.3
Restrepo et a.l 2000	1975-1995 mean values	257438	7200	4148.1	0.6	51874.7	29.9
	Maximum value (November)	257438	10287	7139.9	0.7	51874.7	17.6
	1950 _Cable break	257438	9000	5774.9	0.6	51874.7	21.3
Restrepo et al. 2006	Mean values (Calamar gauge)	266540	7100	4148.1	0.6	52066.9	31.4

Table 3. 2. Magdalena River flood concentrations, calculated for different periods of high water discharge. (Q) water discharge, (Qs) sediment load, Css average suspended particle concentration values. (Qflood) maximum flood discharge. (Cflood) maximum flood concentration in suspended particles. Cflood is always below the concentration threshold Cc =36.25 kg m^{-3} (Mulder &Syvitski, 1995). But if other conditions are considered where Cc could be as low as 5 kg m^{-3} , then the Magdalena fan is likely to produce hyperpycnal flows. (see Appendix 2) .

3.8.3 Shallow Processes

In addition to high river flood derived turbidite and hyperpycnal flows,, shallow processes may play an important role in the distribution of sediments to the continental slope. Coastal erosion, longshore drift and river mouth instability are considered to be fundamental processes that provide sediments to the turbidite flows.

3.8.3.1 Coastal erosion

The Magdalena is a wave dominated delta, with nearshore wave power of 35 x10^6 s^{-1}m and deep wave power (9m depth contours) of 45x 10^6 $ergs^{-1}$m, making it the most significant power in Colombia and along the Atlantic coast of South America (Restrepo and Lopez, 2007). This condition causes extensive reworking of the shoreline. The discharge of the river peaks in November, while the wave power reaches its maximum in December. This slight out of phase condition has allowed the delta to grow in the vicinity of the river mouth. However, the wave dominance redistributes sediments along the delta plain as beach ridges and dunes (Restrepo and Lopez, 2007).

Jetties construction has created an open channel into the Caribbean Sea, directing fluvial sediments towards the Magdalena Canyon and resulting in bypass of sediments along the delta shoreline and deposition offshore

(Alvarado, 2005). This decrease in sediment delivery to the delta is a significant factor in the modification of the downstream coastal bodies and land loss on the western part of the delta (Martinez et al., 1990; Restrepo and Lopez, 2007). Historic maps show an asymmetric delta front with the main distributary channel oriented to the west-southwest (Martinez et al., 1990). Figure 3.19 depicts coastal retreat at the western jetty between the 1930's and the present day. Rapid retreat of the western delta front occurred immediately after construction of the jetties, with an average of 65m /yr (range 21-150 m/yr) loss from 1939 to 1987 (Martinez et al.1990). Analysis of satellite images for the period 1989–2000, indicates an average coastal retreat of 55 m yr^{-1} in the western part of the delta. The net estimate of beach erosion on the western part of the delta for the period 1936–2002 is ~1500 m (Alvarado, 2005; Restrepo and Lopez, 2007). In addition, the Magdalena delta has the lowest wave attenuation ratio of any Colombian delta. The steep offshore profile does not attenuate the incoming deep-water waves, resulting in extremely high energy waves along the shoreline which increases coastal erosion processes (Restrepo and Lopez, 2007).

The fate of the material eroded from the coast is unclear. A significant amount must be directed to deepwater, as the sediment is fed into the canyons and gullies that are observed in the upper slope, adjacent to the narrow shelf.

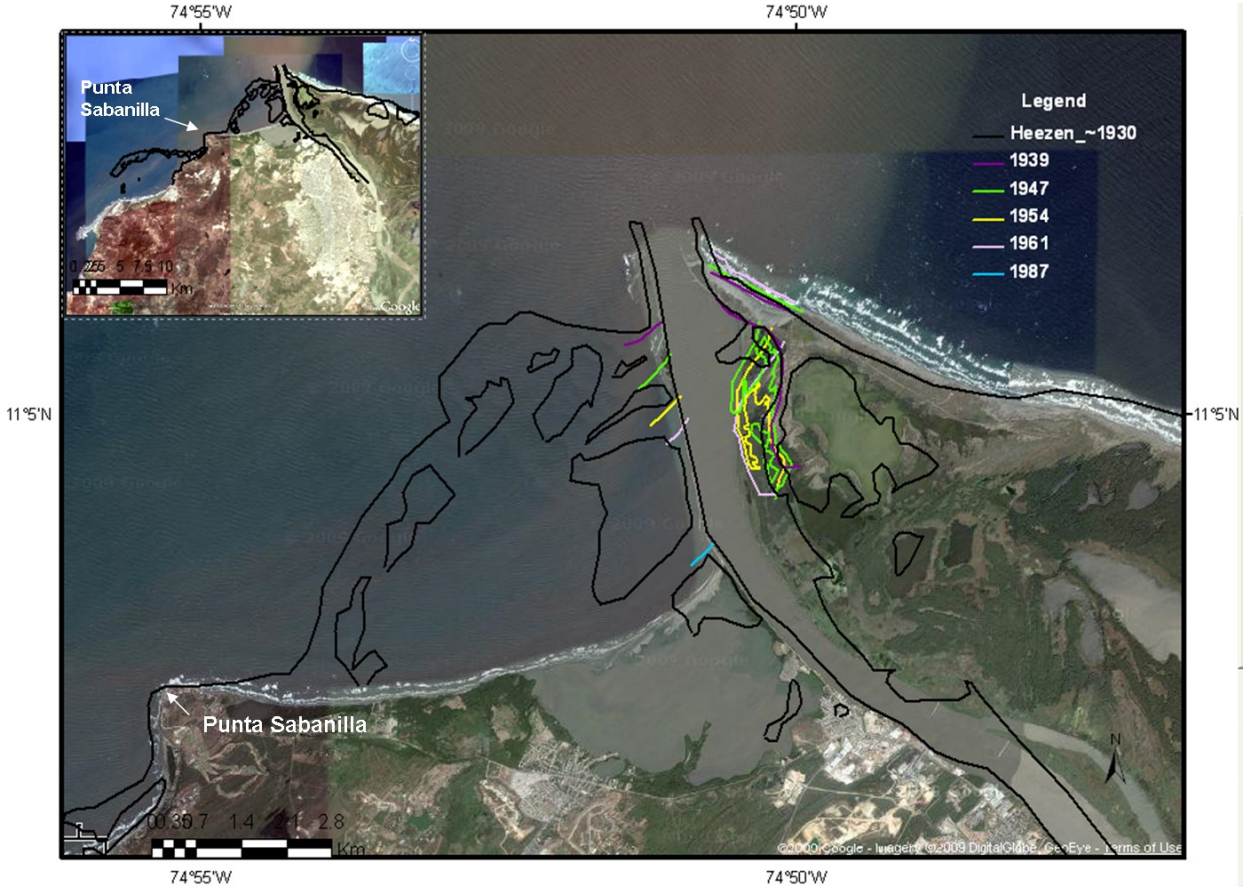


Figure 3.19. Retreat of the coast line by erosional processes. Construction of jetties increases the erosion of the western arm of the Magdalena delta and builds up downstream sand bodies. Shore line retreats between 21-150 m/yr during 1939-1987 period. Black morphology lines correspond to the coastline published by Heezen and should correspond to a map from the 1930's. Lines of coastal retreat (color lines) are taken from Martinez et al. (1985).

3.8.3.2 Longshore drift

Strong northeasterly winds throughout the year cause a persistent northeast –southwest longshore drift; which controls the sediments coming from the Sierra Nevada drainage deflecting the sediment plume parallel to the shore. Figure 3.20 shows the modification of the shelf floor by the longshore drift; forming linear features oriented northeast-southwest. The remobilization of sand from the continental shelf may have been enhanced after the jetty-induced delta retreat, which modified the wave pattern (Figure 3.19). Sand lost from the delta front probably has been added to longshore transport, developing large temporary spits which grow at an angle to the coast (Martinez et al.,1990).

During the wet season (May to November), the Magdalena turbid plume is diverted five nautical miles from the coast towards the east due to the Panama countercurrent. During the dry season (December to April) the sediment plume is diverted back towards the west due to the presence of the longshore drift and the absence of the countercurrent (Figure 3.21) which remains restricted to the Darien Gulf during this time of the year (Pujos et al., 1991).

The cable breaks recorded at the Sabanilla Canyon (April, 1942) and the Aguja Canyon (February,1955) occurred during a period of low fluvial discharge (Figure 3.18). At this time of the year (Dry season) the longshore drift and wave power were at their maximum (Figure 3.22). Due to the lack

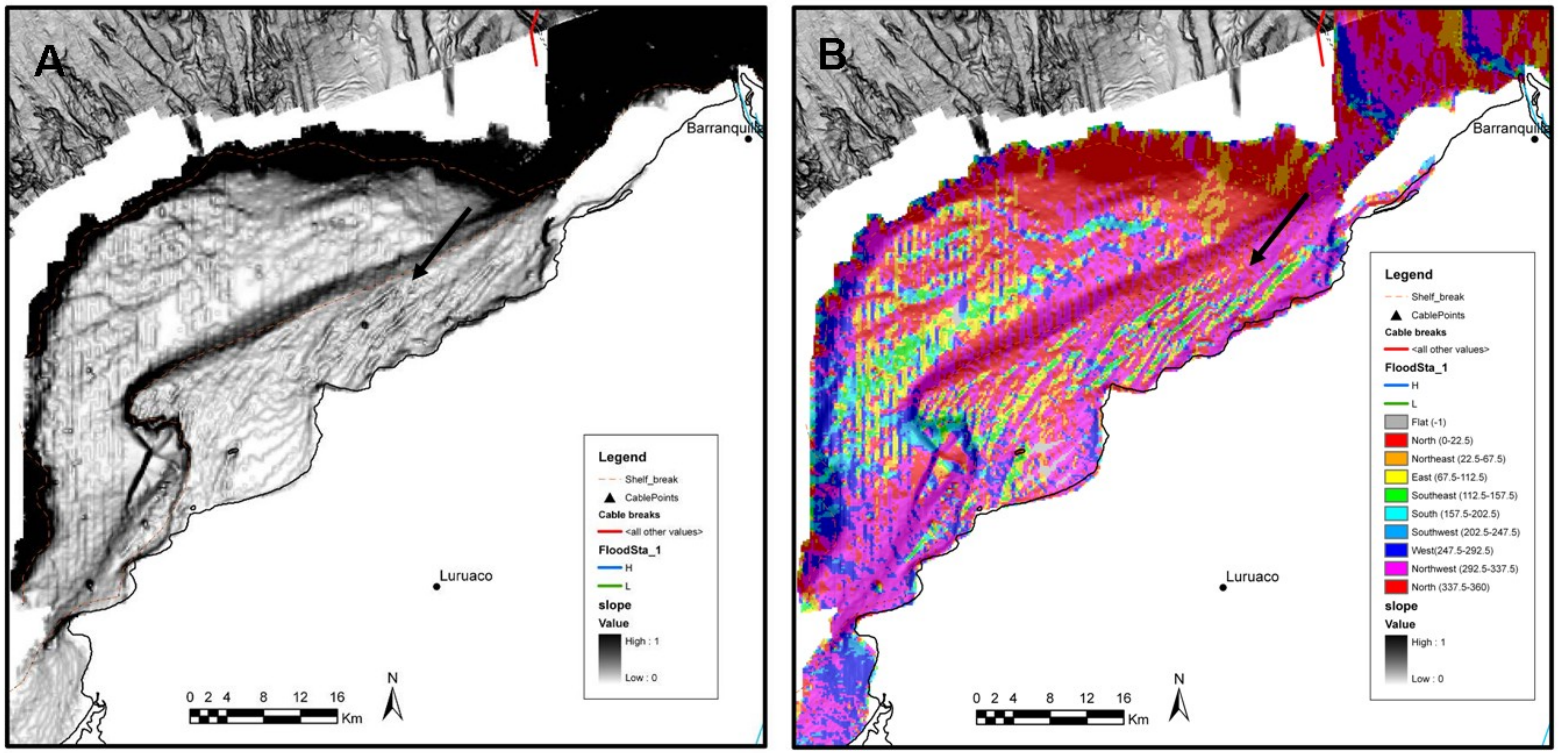


Figure 3.20. Northeasterly winds throughout the year causing persistent NE to SW longshore drift. Construction of jetties increased the erosional processes of the western arm of the Magdalena delta and build up downstream sand bodies. The shelf floor depicts reworking of sediments forming linear features parallel to the wind direction. A) Slope of bathymetry and B) Azimuth of the bathymetry.

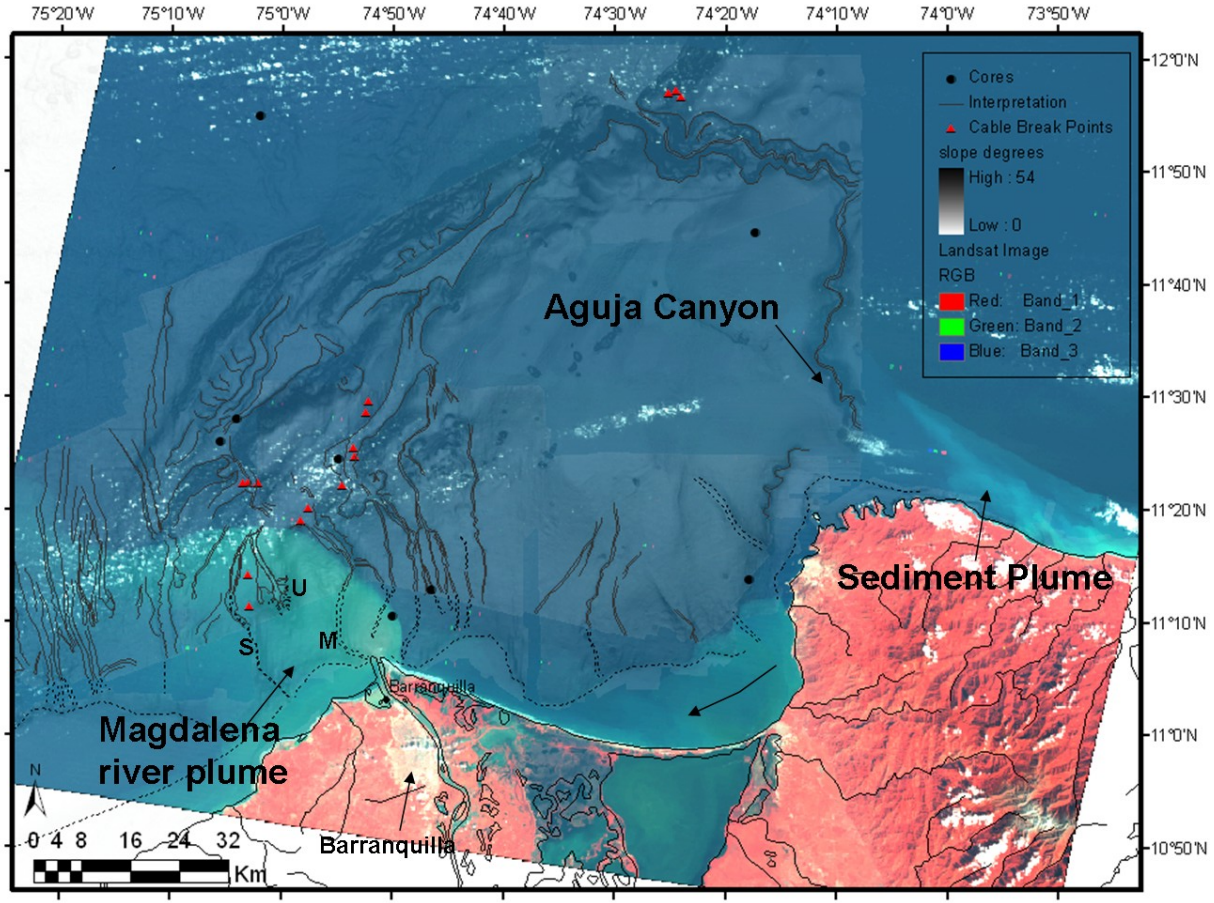


Figure 3.21. Landsat Orthorectified image in false color from January 11, 1989. Magdalena River plume is deflected towards the west at the dry season. In addition, a sediment plume is observed directed towards the Aguja Canyon. TM (1989/1/11 ID: ET009R52_4T19890111) USGS Tri-decadal global Landsat Orthorectified http://eros.usgs.gov/products/satellite/landsat_ortho.php

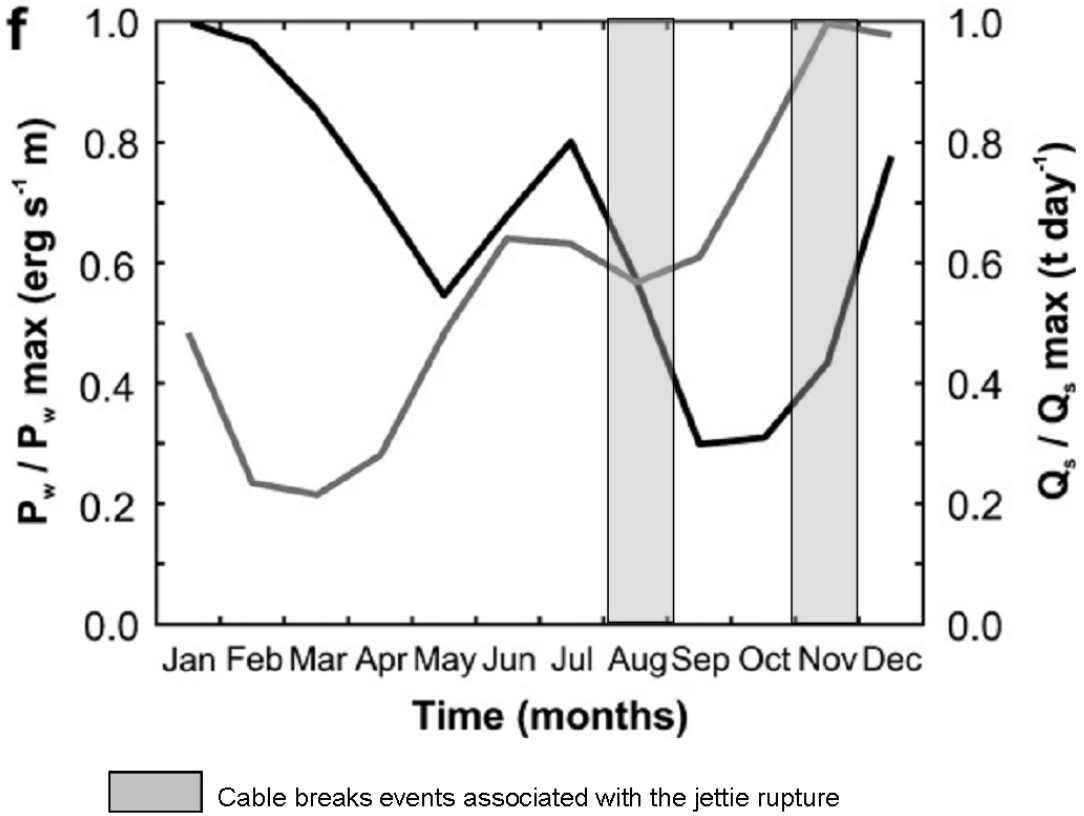


Figure 3.22. Sediment load (gray line)/nearshore wave power (bold line). The system is out of phase which allowed the formation of a delta shape at the river mouth. The cable breaks associated with the rupture of the jetty occurred during the months after a peak and at the rising of the wave power. (Modified from Restrepo et al. 2008)

of a near sediment source for these two locations, it is possible that longshore drift transported sands are the sediment source for the Sabanilla and Aguja Canyon turbidites. Landsat images of the northeastern coast (Figure 3.21) depict a sediment plume traveling towards the Aguja Canyon. Erosion and migration of the coastal sand bodies caused by these processes may be an important source of sediments.

3.8.3.3 River mouth instability

Processes associated with river mouth instability in the area are directly verified by the collapse of the western jetty on two occasions (August 1935 and November 1945, Table 1). Even though the ruptures did not occur during the peak months of higher wave power (Figure 3.22), the events could have been caused by the intense erosion to which the western jetty is exposed during these periods. In addition, the sediment load for August and November corresponds to the periods of highest sediment load over the year (Figure 3.22) which may have contributed to destabilizing the jetty structure at the river mouth.

In summary, the analysis presented above indicates that active sediment flows caused the cable breaks. These sediments are periodically being transported through the canyons and piggyback basins on the continental slope are generated by different processes that may act in conjunction or be

separated. For example, coastal erosion may affect the stability of the jetties and associated deposits, which may be responsible for some flows. Longshore drift is clearly present in the Aguja Canyon and possibly in the Sabanilla Canyon, and sediment instability, related to the rapid accumulation of sediment at the river mouth has demonstrably occurred in two of the thirteen cable break events off the Magdalena River mouth,

Some cable breaks in the past, such as at the Grand Banks (Heezen et al., 1952, 1964; Piper et al., 1988) and Algeria (Babonneau et al., 2007), have been associated with earthquake activity. Even though the area of this study is part of an actively deforming accretionary wedge no earthquake activity has been associated directly with sediment gravity flows. Earthquakes in this area have been recorded at depth between 30 -100 km and with magnitudes not greater than 4 (this work, Chapter 4). But there is no evidence of catastrophic collapses of the slope which could provide a connection to earthquake-generated events (Moscardelli and Wood, 2008).

3.8.4 MTC-1 and Interaction of turbidity flows

Even though it was established that emplacement of the MTC-1 in the PBB1 is not related with the generation of the documented cable breaks, the presence of this MTC depicts their importance in the distribution of the sediment gravity flows. The flows may override the obstacles found on the

sea floor, be deflected around the MTC, be confined by them or cause a local reversal in flow direction (Kneller and Buckee, 2000). When the sediment flows from the Magdalena Canyon reach the low slope angle seafloor (PPB1) and decelerate, the coarser sediment probably was deposited and confined by the MTC-1 (Figure 3.8). Part of the sediment load deposited in PBB1 is truncated by the MTC, but the presence of cable breaks is evidence of down slope sediment flow, as is the sediments found in V12-118 (Figure 3.14), development of knickpoints and erosive morphologies on the piggyback basins floors.

3.8.5 Origin of the 1935b Cable break

Most of the cable breaks can be associated with flows traveling from the shelf break through conduits and reaching deeper parts of the slope. The 1935b cable break is the exception, even though the rupture is directly related in time to the collapse of the delta mouth (400m of jetty sank overnight, and the cable broke soon after). The location of the cable break is associated with U Canyon. There are no evident conduits on the bathymetry map that may link the river mouth with the U Canyon (Figure 3.5). Various hypotheses may explain the linkage between the rupture site and the documented failure of the jetty at the river mouth: 1) The flow did not travel through the Magdalena Canyon, but instead overrode the slope to reach the U Canyon; 2) The flow was entrenched in the Magdalena Canyon, and once

it reached the PBB, the cable stretched and ruptured 12 km west of the canyon; and 3) the cable break could be associated with a flow produced from the Sabanilla Canyon. The last hypothesis seems to be the most unlikely, since there is evidence of a flow produced at the river mouth. The remaining hypotheses are plausible, but weak points, including: a) the flows have to override the western channel wall that is approximately 100 m in height, and b) the cable break occurred 12 km from Magdalena Canyon, the locations of all the cable breaks in the area are suspect. One possible alternative is that there were two flow events that initiated at about the same time at two different locations. The exact time of cable break versus the failure of the river mouth is not known, so this hypothesis is quite plausible as well.

3.8.6 Recurrence of sediment gravity flows

Observations in other systems indicate high occurrence of sediment gravity flow events. In the Congo (Zaire) submarine canyon between 1887 and 1937, 30 submarine cable breaks occurred which have been related with high bedload discharge from the Congo River (Heezen et al., 1952, 1964). On the Amazon Fan, 1 flow event every 2 years on a 20ka year interval have been calculated (Pirmez et al., 2000).

Various points are important to discuss in terms of the periodicity of the flows generated at the Magdalena submarine fan. 1) Recurrence of the events is high. During a 25 year period 12 turbidite flows have been identified, indicating a high frequency occurrence like on the Amazon Fan (once every 2 years). Some events correspond to years with high river water discharge conditions and cable breaks. It is important to point out that even though cable breaks can be related to strongest flows, less energetic flows may have occurred during this time interval which did not rupture the cable. 2) Change of the cable location also influences the flow record. Early cables were more susceptible to ruptures since they were located at the toe of the canyons (Figure 3.9). As these cables were repaired, they were relocated farther down slope, thus flows that travels farther were required to rupture a cable. 3) Distribution of the breaks seems to be related to the accommodation space on the slope (PBB). The first years after cable installation, cable breaks occurred at the toe of the canyons in PBB1, i.e. five breaks during a six year period. The second group of breaks corresponds to the cables along the western pathway in PBB1, with three events during a four year period. The last group corresponds to the cable breaks at the canyon which dissects PPB2, with three breaks in a five year period. The distribution of the cable breaks suggests that sediment gravity flows produced at the river mouth and associated with the Magdalena Canyon were being transported towards the northeast through the PBB1.

Once, the accommodation space was occupied by sediments at the PBB1 east of the canyon, flows became more frequent towards the west, where they were transported through KP1 and directed towards PBB2.

3.8.7 Similar depositional settings

The active Magdalena Fan is a modern example of deepwater deposition in structurally confined basins, connected by tortuous corridors for sediment transport. The fan is a good analog for some areas offshore Brazil, Brunei, and Angola (Smith, 2004). This type of deposition differs from the older Magdalena submarine fan that was characterized by leveed channel systems. On the Brunei slope, prospective reservoir occurs as lobes deposited in subtle depressions or at breaks in the slope (Demyttenaere et al., 2000). Dimensions of the lobes and structures are similar to the Magdalena Fan.

This depositional model has also been recognized at the outcrop scale in the upper Miocene Gorgoglione Flysch sequence in southern Italy (Boiano, 1997). The present day slope of northwest Borneo (Brunei) (Ingram et al. 2004) and late Pleistocene deposits offshore eastern Corsica (Gervais et al., 2006) constitute additional modern analogs. Mainly coarse sediments that are fed by the Golo River into the shelf area, sediments are transported

downslope through canyons and deposited as lobe complexes in the Corsican trough which confines deposition. The Corsica example includes sinuous channels within the canyons, which could produce similar morphology as in the Agua Canyon.

3.8.8 Slope deposition

The Magdalena slope is an above-grade slope (Prather, 2003). The lack of the 3D control of the basal sequences to establish the connectivity within the different PBB prevents the designation of ponded accommodation (Prather, 2003). Seismic profiles (Figure 3.11) depict the stacking of MTCs, gravity flows and pelagic deposition, but 3D connectivity of them cannot be determined.

The gravity flows travel at least 100 km to reach the abyssal plain through any of the flow pathways, a distance in which the characteristics of the flow properties change. In relatively small flow volumes comparative to the scale of the receiving basin, changes in properties from axial to lateral and proximal to distal are expected, including changes such as sand content, amalgamation percentage and bed thickness (Smith, 2004). Properties changes in the PBB are expected at two scales: intrabasinal changes and the complete connected flow pathway scale. However, the lack in age control and availability of sample analysis from the cores that contain

turbidites, do not allow establishing variations in the composition and textural changes for the different flows in this study (Figure 3.16).

The relationship between flow character and equilibrium profile can also be studied. The gravity flows that encounter slopes steeper than the equilibrium profile tend to be more erosive (Pirmez et al, 2000), as observed in the V12-111 area and at the knickpoints that are connecting the different PBB (Figure 3.15).

Conversely, on lower slope areas, the equilibrium profile will generate decelerating flows (Pirmez et al., 2000). At the connected pathways scale, changes in slope angle will occur in segments of substrate erosion alternating with segments of enhanced deposition (Smith, 2004). The PBB with lower slopes depict recent sedimentation (horizontal reflectors) and onlap geometries against the obstacles of the basin (walls or MTCs) (Figure 3.8). All these characteristics may change through time since the slope is actively modified by the continuous compressional tectonic forces. Therefore, variation of geometries and distribution of sediments should be considered when evaluating this depositional setting.

3.8.9 Importance

This study contributes to understanding the interaction between topographic obstacles and gravity flows and understanding the effect of slope on the flow

distribution. These flows can be considered analogs for different areas of the world where hydrocarbon exploration is taking place in a similar tectonically active setting. The authors would like to emphasize the importance of this area as a natural laboratory to study sediment distribution through tortuous pathways, evolution of gravity flows through the slope and differences within gravity flows from different initiation processes.

3.9 SUMMARY AND CONCLUSIONS

-The active Magdalena deepwater fan provides sediment gravity flows that generate submarine cable breaks. Twelve such breaks were recorded in a 25 year period. The sediments are transported down slope mainly through the Magdalena Canyon, but now abandoned canyons and gullies also served as conduits for sediment flows. The Sabanilla and U canyons to the west and some gullies to the east of the Magdalena Canyon constitute a network of active conduits. The Aguja Canyon, northeast of the river delta, also has had three cable ruptures.

-The upper slope is characterized by the presence of piggyback basins that are communicated through knickpoints that allow the transport of sediments

down to the abyssal plain. These basins partially retain the sediment by decelerating the flows, leaving some deposits on the lower slope areas.

-Three main flow pathways were identified: 1) flows from the Magdalena, Sabanilla and U canyons transported through PBB1 and PBB4, 2) flows from the Magdalena Canyon and western gullies that are transported through PBB1 and PBB3, and 3) flows transported by the Aguja Canyon.

-The sediment flow events seem to be related to different processes on the continental shelf: 1) High flood stages of the river, 2) coastal erosion, 3) long shore drift, 4) hyperpycnal flows and 5) river mouth instability. The sedimentological characteristics of the different deposits should differ as the flow properties are different.

- Flows related to the active Magdalena Canyon and western gullies may be related to high flood stages of the river. Direct evidence from failures linked to flow events suggests river mouth instability or hyperpycnal flows as starting points for turbidite flows. Flows related to the Sabanilla and Aguja canyons are probably related with sediments directed into canyons from long-shore drift

-MTC deposits play an important role in the distribution of sediment flows in confined basins, serving as obstacles to the flow and changing the distribution of sediments in the basin.

- Important applications in hydrocarbon exploration and reservoir distributions can be obtained from this study when used as an analog of deepwater deposition in structurally confined basins or connected by tortuous corridors. In addition, this study characterizes the continental slope in terms of stability and shallow hazards for submarine infrastructure.

3.10 ACKNOWLEDGEMENTS

This research forms part of a Ph.D. dissertation by the senior author. We especially thank Ecopetrol for providing the seismic and Bahia – Sinú for bathymetry data, the Institut de Ciències del Mar-CSIC for allowing the use of the proprietary bathymetry; to the Centro de Investigaciones Oceanográficas e Hidrográficas de Colombia (CIOH) for providing complementary bathymetry. The Conoco-Phillips School of Geology and Geophysics provided the financial support and computer facilities. Seismic Micro Technology and ESRI provided educational software licenses. GLORIA data were acquired during cruises CD40a and DIS109. The crew and scientists aboard the RRS Charles Darwin and RRS Discovery during those cruises are thanked for their efforts. Funding for GLORIA data

acquisition and processing were provided by the US-NSF under grants OCE8901848 and OCE9712079.

CHAPTER 4

DETACHED AND SHELF–ATTACHED MASS TRANSPORT COMPLEXES ON THE MAGDALENA DEEPWATER FAN

ABSTRACT

The Magdalena submarine fan, fed mainly by the Magdalena River, is part of a Miocene-Recent accretionary prism off the Caribbean coast of Colombia, S.A. Periodic shifts of the Magdalena River controlled the evolution of the fan. The integration of multibeam bathymetry, GLORIA image, and 2D seismic profiles reveal a series of deep-water channel systems and mass transport complexes (MTCs) on the seafloor. The MTCs have been subdivided into detached and shelf-attached types. Relative timing of the detached MTC processes cannot be determined due to their local character. Four major shelf attached slope MTCs are described from interchannel areas. We hypothesize that these attached MTCs began to be generated during a low stand of sea level (140-120 ka) which prompted hydrostatic pressure changes and/or gas hydrate dissolution on the slope, leading to collapse. Later processes of slope deformation and slope instability continued feeding MTCs to the interchannel lows. A southerly shift of the Magdalena River depocenter (middle Pleistocene) and abandonment

of the Galerazamba region channel-levee systems coincided with the lowstand.

4.1 INTRODUCTION

The combination of active margin tectonics with one of the larger fluvial sediment sources to the ocean makes the Magdalena Fan an important area to understand the development of MTCs. Integration of multibeam bathymetry, GLORIA image and seismic profiles were used to characterize the MTCs on the continental slope of northern offshore Colombia. This paper documents the different submarine mass movement deposits recorded on the submarine fan, by describing the morphologies of the scarps and their related deposits. The mass transport classification of Moscardelli and Wood (2008) is used because it is based on seismic observations that emphasize the relationship between mass failures and the geomorphology of their source areas (Table 1). This classification is based on three main aspects: 1) sourcing regions of MTCs, 2) geomorphological expression of MTCs on their updip part (e.g. scarp) and 3) dimensions and geometries of MTCs.

4.1.1Regional Setting

The Magdalena submarine fan, located in the Caribbean Sea, offshore Colombia (Figure 1), is a bathymetric feature that is part of the accretionary wedge complex formed by the collision of the Caribbean and South American plates (Duque-Caro, 1979; Breen, 1989). It covers an area of about 68,000 km2, contains a volume of 180,000 km3 and extends into areas > 4,000m of water depth (Reading and Richards, 1994). The deepwater fan is fed by the Magdalena River, a major fluvial system that drains most of the Colombian Andes. The submarine fan sedimentation was initiated during the middle Miocene, a time of low deformation rates (Kolla and Butter, 1984b).

Ercilla et al. (2002a) first reported the existence of large MTCs with a radial distribution throughout the continental slope. Tongue-shaped mass flow deposits smooth the slope between channel systems and perpendicular to thrust ridges. They are characterized by erosive (concave) and depositional (convex) sections of the slope. The uplifting of the continental shelf, steep slopes and the high availability of uncompacted sediments in the abandoned Galerazamba area seem to have played an important role in the development of large-scale mass flows. In addition, interchannel lows formed barriers to confine the sediment flows (Estrada et al., 2005b).

The fan is subdivided into: 1) deformed compressional belts and 2) main fan area. The deformed area includes the arcuate northeast and

		Causal mechanisms	Source Area
Attached MTCs Area =100s to 1000s km2 Width and length =10s Km	Slope-attached MTCs	Tectonism (earthquakes) Volcanism Gas hydrate dissociation Longshore currents Storms and hurricanes	Upper-slope collapses (mega cookie bites)
	Shelf-attached MTC	Relative sea-level fluctia-tions. High sedimentation rates	Paleoshelf edge deltas
Detached MTCs Area =10s km2 Width and length=Few km		Gravitational instabilities on the flanks of mud-volcano ridges/salt masses and levee-channel complexes. Tectonic pulses Oversteepening Mud-volcano activ-ity/methane release	Flanks mud-volcano ridge/salt diapirs/levees Flanks of collapsing mid-oceanic ridges

Table 4.1. Classification, causal mechanisms, and source areas of MTC's (Moscardelli and Wood, 2008)

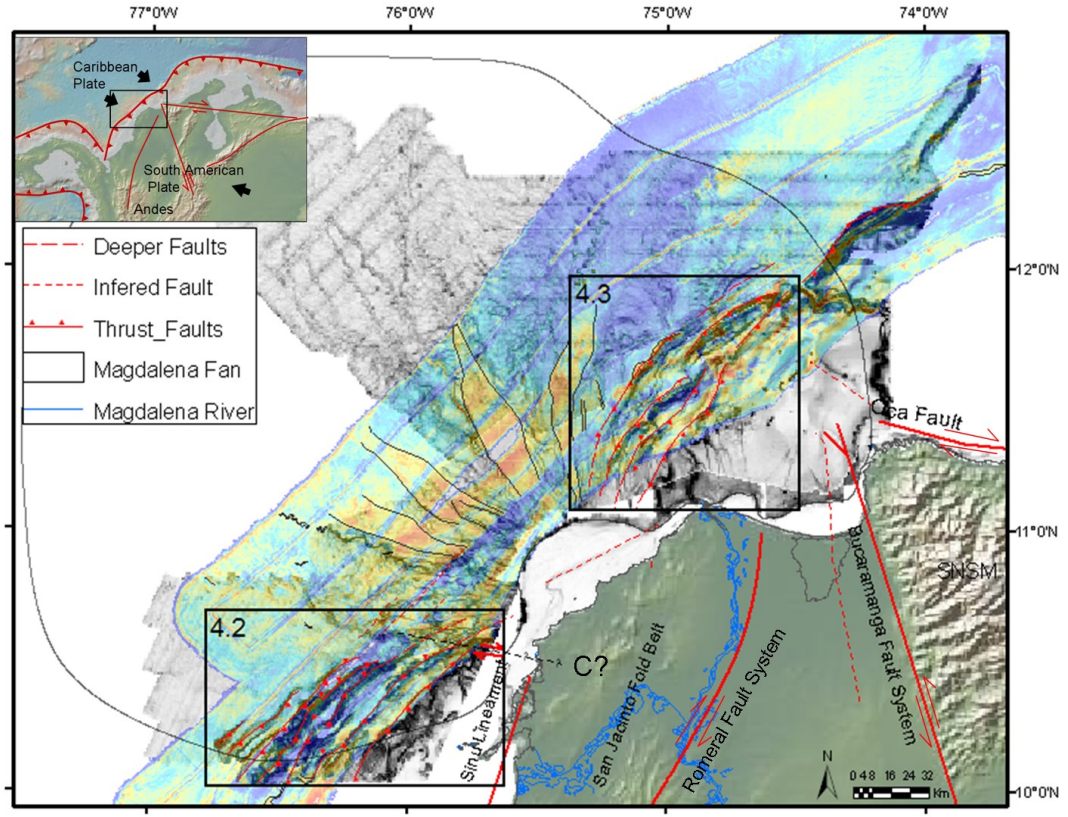


Figure 4.1. . Location and general structure of the area of study located offshore Colombia, Northern South America. Slope of bathymetry and GLORIA image. Major structural features include SNSM Sierra Nevada de Santa Marta., Romeral and Bucaramanga Fault systems. (C?) Canoas Fault. Rectangles are indicating the location of Figures 4.2 and 4.3.

southwest thrust belts, expressed on the sea floor as ridges (Figure 4.1, 4.2 and 4.3). The main fan area is characterized by leveed channel complexes, large-scale MTCs, and scars of slumps (Figure 4.1). The eastern part of the main fan contains the oldest channel-levee systems (CLS) at the seafloor (Kolla and Buffler, 1984b; Ercilla et al., 2002a; Estrada et al., 2005a). The western part of the main fan contains younger CLS and greater influence of deformation on the slope, which clearly affected the evolution of the channels (this work, Chapter 2). The CLS are partially destroyed and cannibalized by mass-flow deposits. Although, deformation is not regionally extensive, it is present in the fan areas, particularly near the thrust belts. The most recent active fan is located in the northeastern deformed belt, where sediments are transported downslope through canyons with steep slopes (~2.5^{o}) and gullies, emplaced as gravity deposits filling the piggyback basins which are formed as a result of deformation. New bathymetric data (this work, Chapter 2) reveal a series of recently active canyons, based on the occurrence of multiple submarine cables breaks in the recent past (Heezen, 1956a). Gas hydrates (Figure 4.4), mud diapirs (Figure 4.3) and slumps have been documented in the basin (Shepard, 1973, Shipley, 1979; Kolla and Buffler, 1984a,b; Vernette et al., 1992).

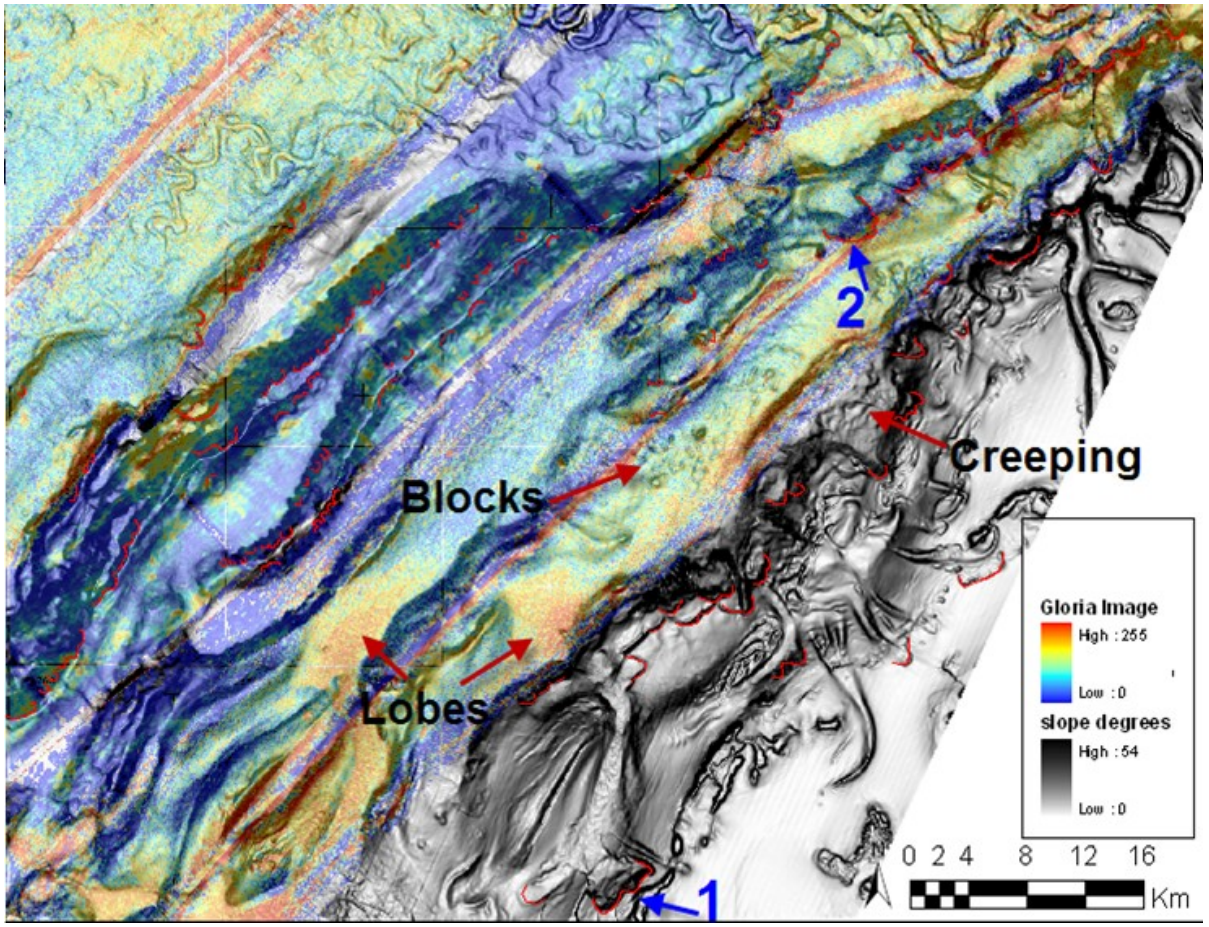


Figure 4.2. Southwestern deformed belt. Arcuate scarps in red. GLORIA color image over slope of the bathymetry .Numbers are scarps in Table 4.2.

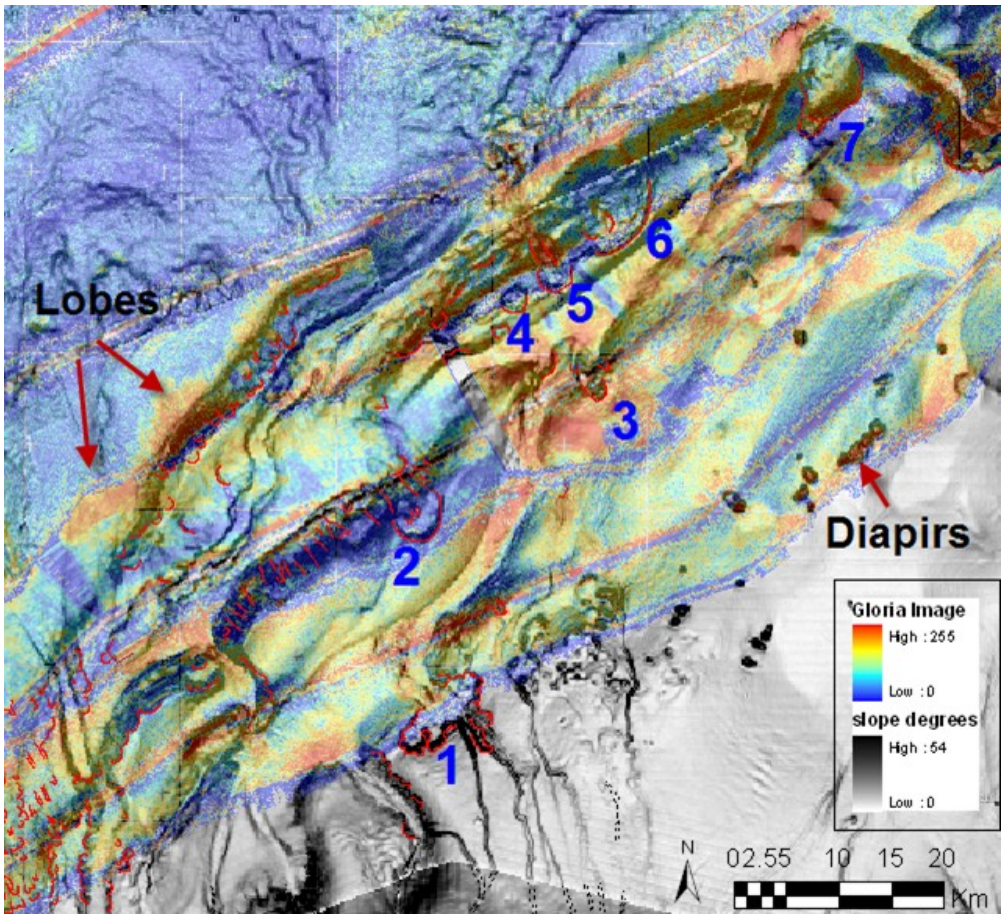


Figure 4.3. Northeastern deformation belt. Major scarps are labeled with numbers characterized on table 4.2. Arcuate scarps in red. GLORIA color image over slope of the bathymetry. Numbers are scarps in Table 4.2.

4.1.2 Data and Methods

Data available for the study include high resolution bathymetry images of the northwest Caribbean offshore Colombia. The bathymetry covers a major part of the Magdalena deepwater fan, approximately 54,000km^2 of the seafloor (Figure 4.1). Four different surveys cover the area of study. In 1997 the Spanish vessel Bio-Hesperides acquired approximately 15,000 km^2 of bathymetry data (Ercilla et al, 2002a) with the multibeam echosounder SimRad EM-12 S120. Two surveys were acquired in 2002 on behalf of Ecopetrol and Total E&P., using a hull-mounted, multibeam echosounder Reson SeaBat 8169 (50KHz; for water depths between 100 and 800 m) and Simrad EM 12D (13 kHz; for water depths between 800 and 3500 m). Additional bathymetry surveys that cover the shelf area and river mouth were provided by the CIOH. Bathymetry interpretations and quantification of the MTC dimensions were made using Arc map (ESRI). These observations are complemented by a GLORIA side-scan sonar mosaic acquired during CD40a and RMS Discovery expedition DIS109 (Pirmez et al., 1990). Figures 4.1, 4.2 and 4.3 are a combination of slope in degrees calculated to enhance the morphological changes and a transparent display of the GLORIA image in a color scale. The 2D seismic lines (Figure 4.4) grid was provided by Ecopetrol. Acquisition and processing parameters are industry standard, near zero phase with SEG normal polarity. Frequencies range

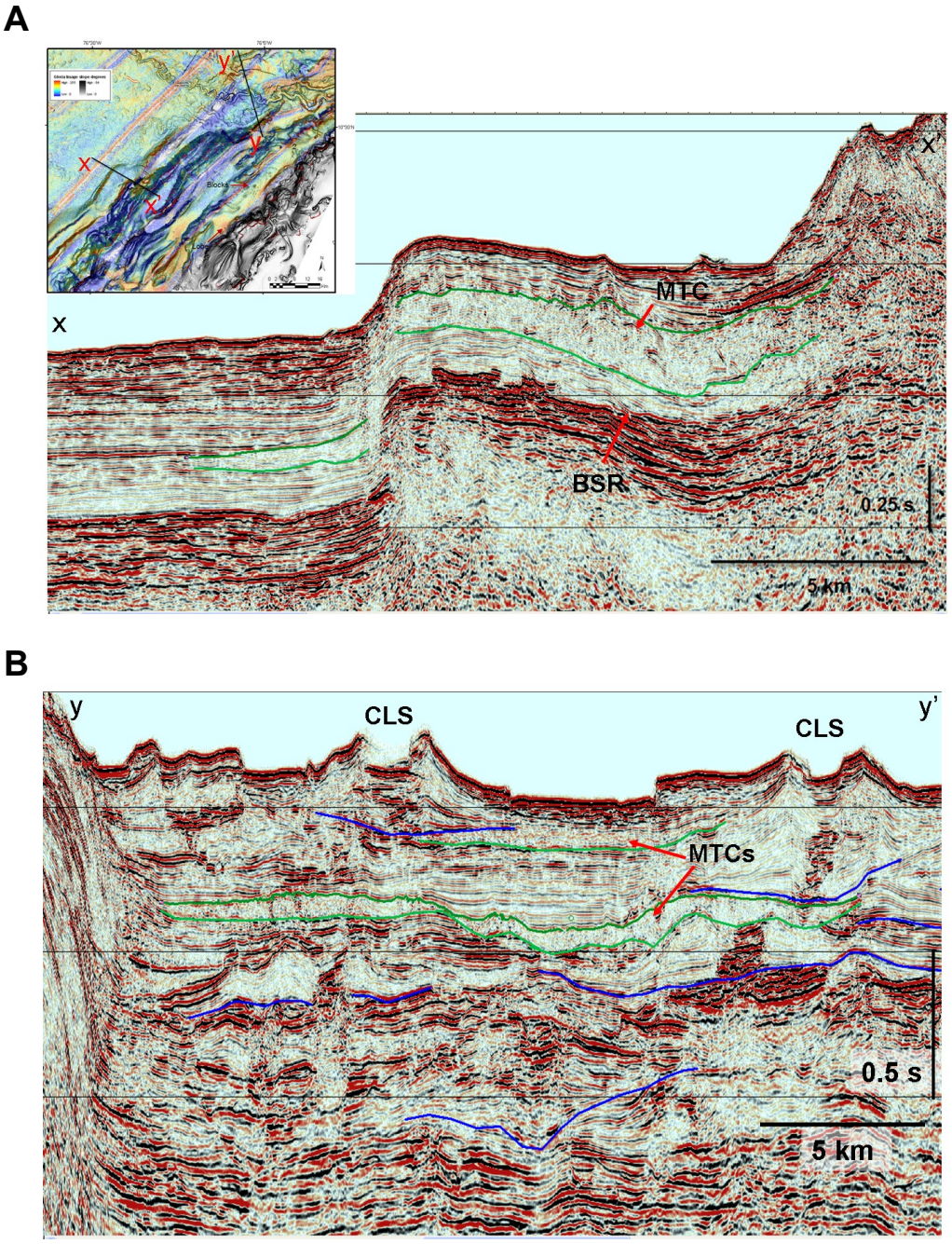


Figure 4.4. A. x-x' seismic profile of the southwestern deformed belt. MTC (green) are part of the deformed sequences generated as a result of the thrust imbricate advancement. Notice the presence of gas hydrates in the area (BSR). B. y-y' seismic profile of the southwestern Magdalena Fan. MTC (green lines) were deposited at the deformed belt toe as a result of thrust imbricate advancement. Notice the abundance of channel levee systems (blue lines represent the base of the CLS).

from 20 to 60 Hz around the level of interest. Seismic interpretation was performed in SMT Kingdom Suite 8.1.

4.2 LOCATION AND CHARACTERISTICS OF MTCS

The different MTCs in the area were subdivided into three groups by association with the causal mechanism based on Moscardelli and Wood (2008) classification (Table 4.1). Detached MTCs are associated with: 1. Thrust deformed belts and 2. Channel-levee systems. Shelf attached MTCs are 3. Inter channel lows – shelf break MTCs.

4.2.1 Thrust deformed belts MTCs

Thrust belts are an important bathymetric feature in the continental slope offshore Colombia. Several buried MTCs related to thrust imbricate growth were recognized at the toe of the thrusted sheets on seismic profiles, but they are not expressed on the seafloor morphology.

At the southwestern deformation belt seafloor morphologies are associated with slump deposits, slide blocks and collapse scours (Figures 4.2, 4.4 and 4.5). The collapse scours are common at the front limb and back limb of the thrust imbricates (Figure 4.2). Erosional features are represented by arcuate headscarps and grooves or “linear features” that commonly modify the front

limbs of slope ridges (Figures 4.2 and 4.5). Elongate scarps seem to be the sum of several small collapses at the edge of the thrust ridges (Table 4.2). Lobate deposits occur at the toe of the slump scarps or fill the piggyback

Deformed Belt	Scarp	Water depth mbsl	Width km	Length km	Height m	Area Km^2	Volume Km^3
SW	1	202	2	4.6	80	7.7	0.61
	2	1140	2.3	3.2	60	7.04	0.42
NE	1	1090	3.3	10	200	32	6.4
	2	1500	3.1	4.8	150	10.2	1.53
	3	1780	1.6	1.8	50	3.08	0.15
	4	2042	1.7	2.7	60	3.2	0.19
	5	2126	2.5	3.2	95	6.4	0.6
	6	2130	4.6	16	300	27	8.1
	7	2460	4.7	6.5	220	28.7	6.31

Table 4.2. Morphometry of main scarps on the deformation fronts. Location is shown in figures 4.2 and 4.3.

basins as result of sediment remobilization from the front limb of the structures (Figure 4.2). High reflectivity on the GLORIA images characterizes these areas of MTC deposition as well as slide blocks and evidence of sediment creep.

Evidence of MTC processes in the northwestern thrust belt are more pronounced. Arcuate headscarps are present on the ridges with lengths of 1 to 3.2 km. Larger collapse structures are developed on the thrust ridge flanks (Table 4.2) and can be traced to their associated MTCs (Figure 4.3). High reflectivity on the GLORIA image is identified at the toe of some scarps

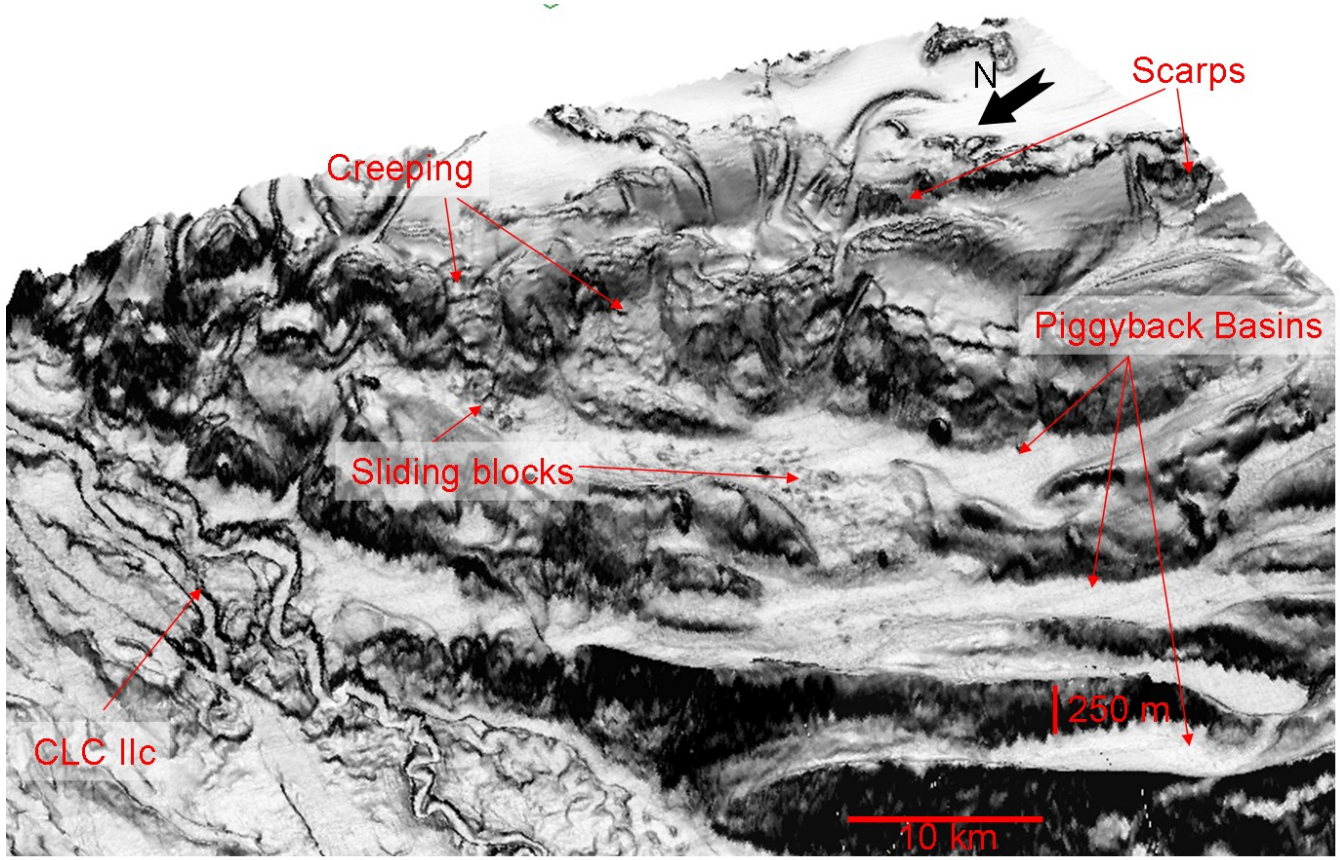


Figure 4.5. Slope of bathymetry 3D view of the northwestern section. Highlighting the thrust ridges degradation and the presence of MTCs : sliding blocks, scarps and creeping of sediments . Vertical exaggeration 10x.

and low slope areas within the piggyback basins. Lobate geometries (Figure 4.3) are associated with scarps on the front limbs.

4.2.1.1 MTC-1

The most striking northeastern scarp feature is a narrow morphological slope collapse structure, recognizable at 1,080 m water depth and 27 km to the northeast of the river mouth (Table 4.2, Figures 4.3, 4.6). From here, sediments were transported downslope to depths of 1590m below sea level. The head scarp is semi-circular (cookie bite type, Moscardelli and Wood, 2008) with an area of 32 km^2. The estimated column of sediment that has been evacuated from the escarpment reaches 300 m in height, corresponding to an evacuated volume of 6.4 km^3. Minor scar features and slide blocks occur at the northeastern and southwestern walls of the scarp (Figure 4.7). Three channel conduits trend downslope from the shelf towards the MTC-1 escarpment and converge at the escarpment head. A channel-like feature occurs at the base of the escarpment that continues downslope towards confined, elongated basins between ridges, where sediment gravity flows probably were deposited (Figures 4.7).

The MTC-1 deposits are represented by slump blocks (Figure 4.7) covering an area of approximately 15 km2. The deposits are truncated downslope by a southwest-northeast trending ridge and are deflected towards the

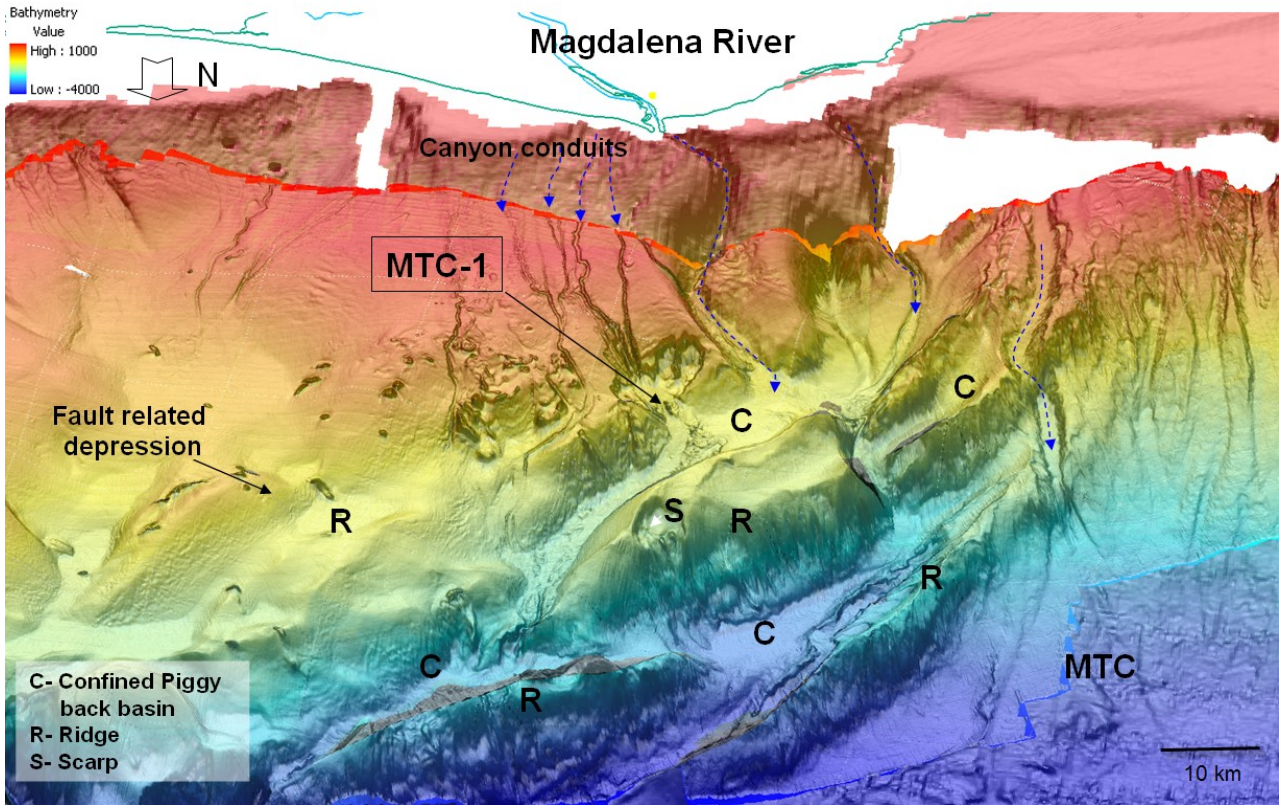


Figure 4.6. Bathymetry 3D view of the northeastern section. Highlighting the location of MTC-1 and thrust ridges. Sediments from the Magdalena River flow downward through the canyons conduits, and are deposited in Ridges (R) or confined piggyback basins (C). The MTC-1 deposits are deflected eastward due to the presence of the structural ridge. A morphologic depression is observed with the same fault trend related with the MTC-1 scarp. Vertical exaggeration 10x.

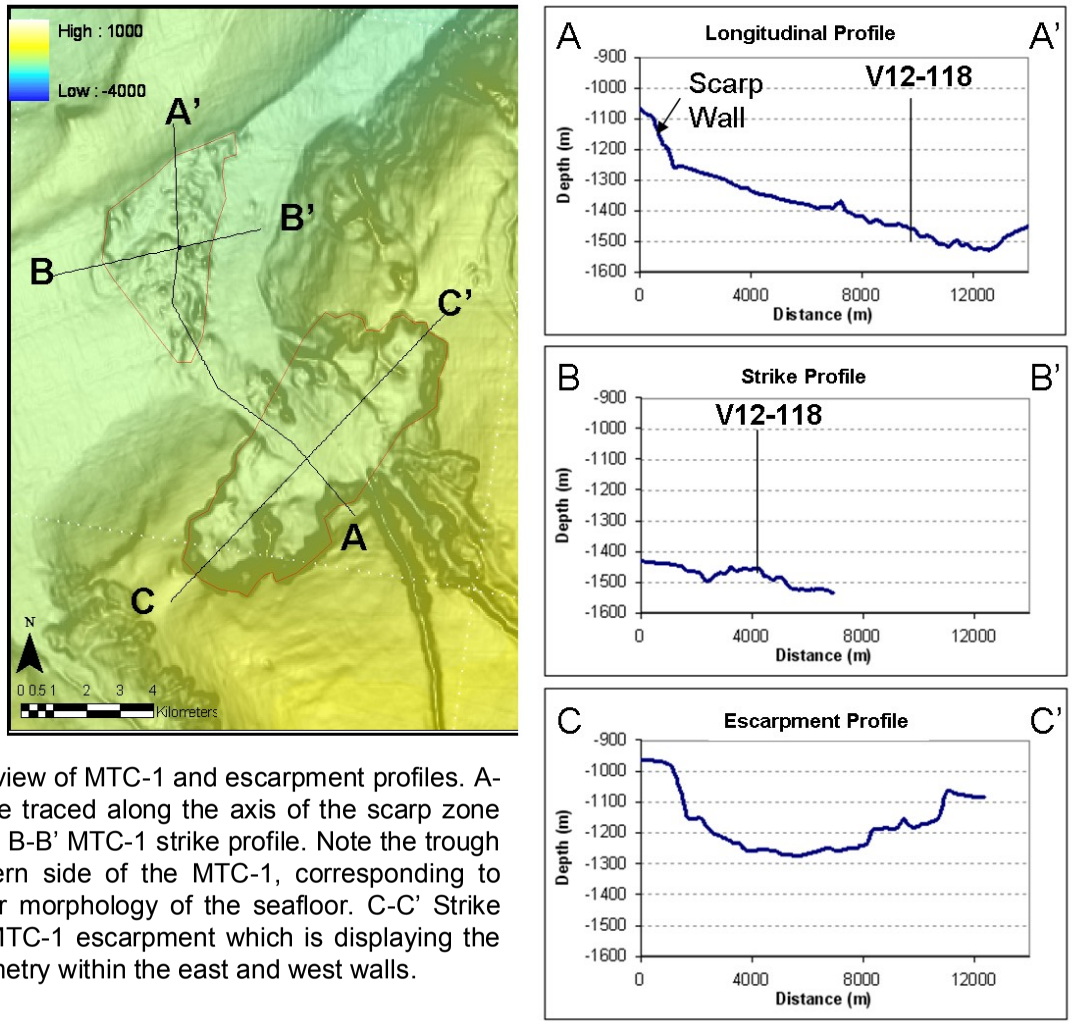


Figure 4.7. Detailed view of MTC-1 and escarpment profiles. A-A' Longitudinal profile traced along the axis of the scarp zone and MTC-1 deposits. B-B' MTC-1 strike profile. Note the trough formed at the western side of the MTC-1, corresponding to local slides or earlier morphology of the seafloor. C-C' Strike profile through the MTC-1 escarpment which is displaying the differences of bathymetry within the east and west walls.

northeast. The minimum estimated volume for the deposit is 0.27 km3 with a possible mean height of approximately 17m. This suggests that several events were needed to generate this geometry. The runoff distance is approximately 9km from the escarpment to the deepest part of the deposits.

4.2.2 Channel walls and levees MTCs

All of the CLS present in the seafloor on the Magdalena Fan were abandoned after the shifts of the Magdalena River during the Pleistocene. Features such as inner levee and overbank collapses are found in some areas of the fan (Figures 4.8, 4.9 and 4.10) Levee breaks are caused by major MTCs that flowed through the abandoned conduits, modifying the morphology of the channels (Figure 4.9). It can be observed on the GLORIA image that some of the channels were cannibalized by eroding flows, leaving deposits with high reflectivity (opportunistic MTC, Figure 4.11A). Arcuate scarps are found in the inner levees as a result of the deformation of some channels.

4.2.3 Interchannel lows MTCs

Shifting of CLS's through time produced interchannel low areas, with radial distribution on the slope. The interchannel lows are characterized by the presence of several large MTCs connected to the Galerazamba area, and

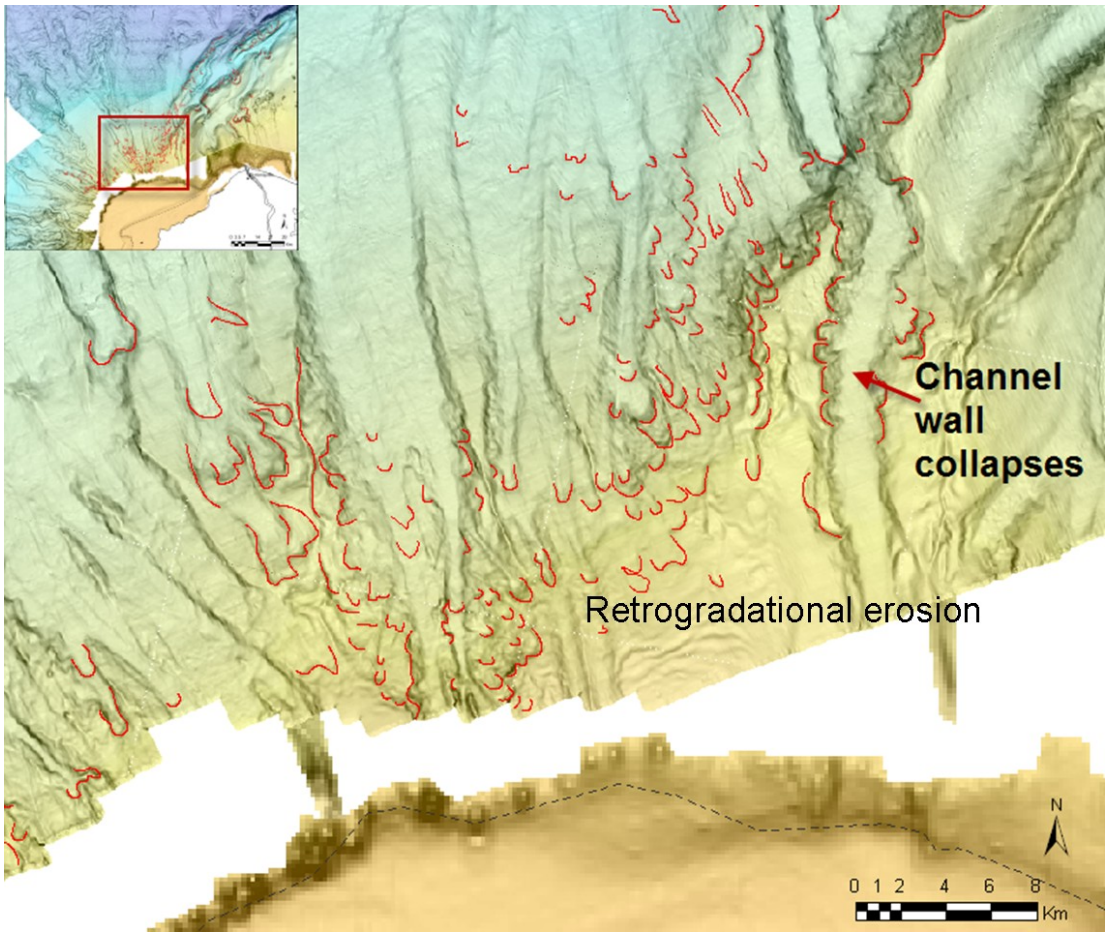


Figure 4.8. Upper slope multiple arcuate scarps and canyons due to retrogradational erosion. Also note the channel inner wall collapses at the eastern channel (Detached MTCs)

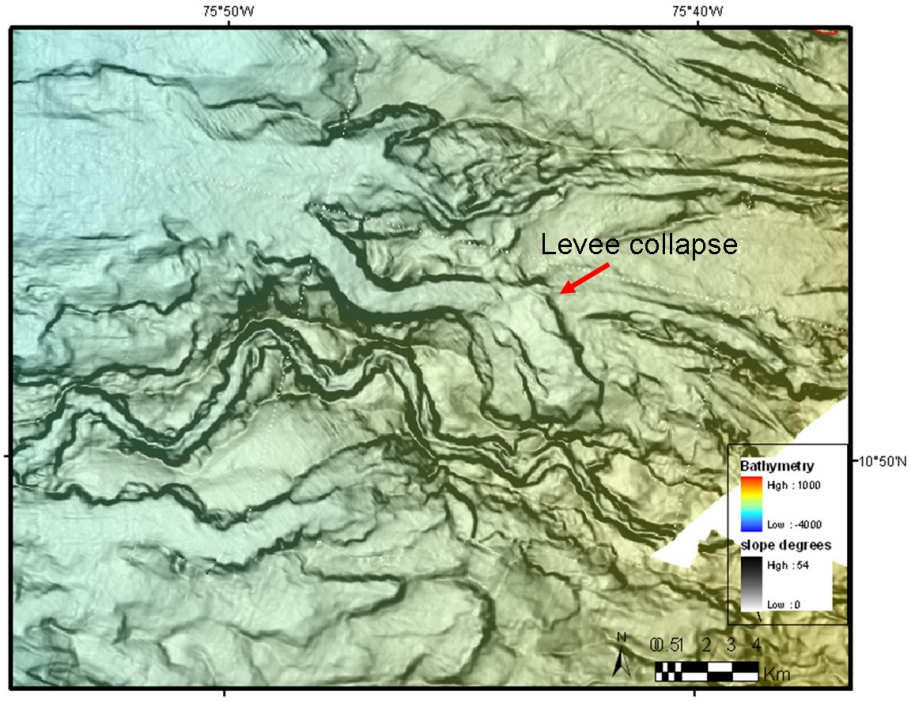


Figure 4.9. Channel levee collapse scarps (Detached MTC). The scarp is linked with an abandoned channel which served as a conduit to transport the deposits downslope.

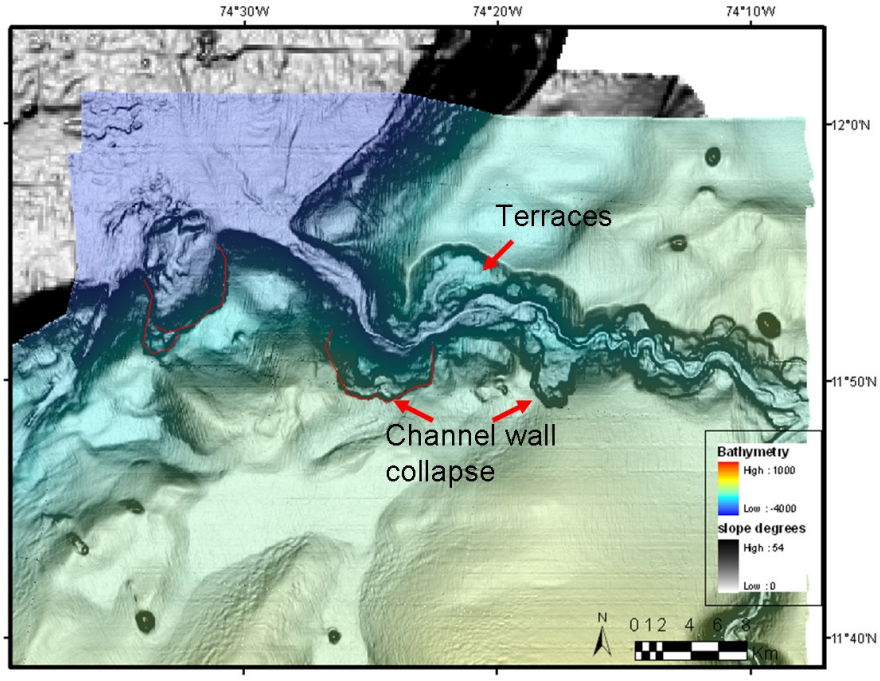


Figure 4.10. Channel levee collapse scarps in the Aguja Canyon (Detached MTC). Also observe the different levels of terraces on the canyon.

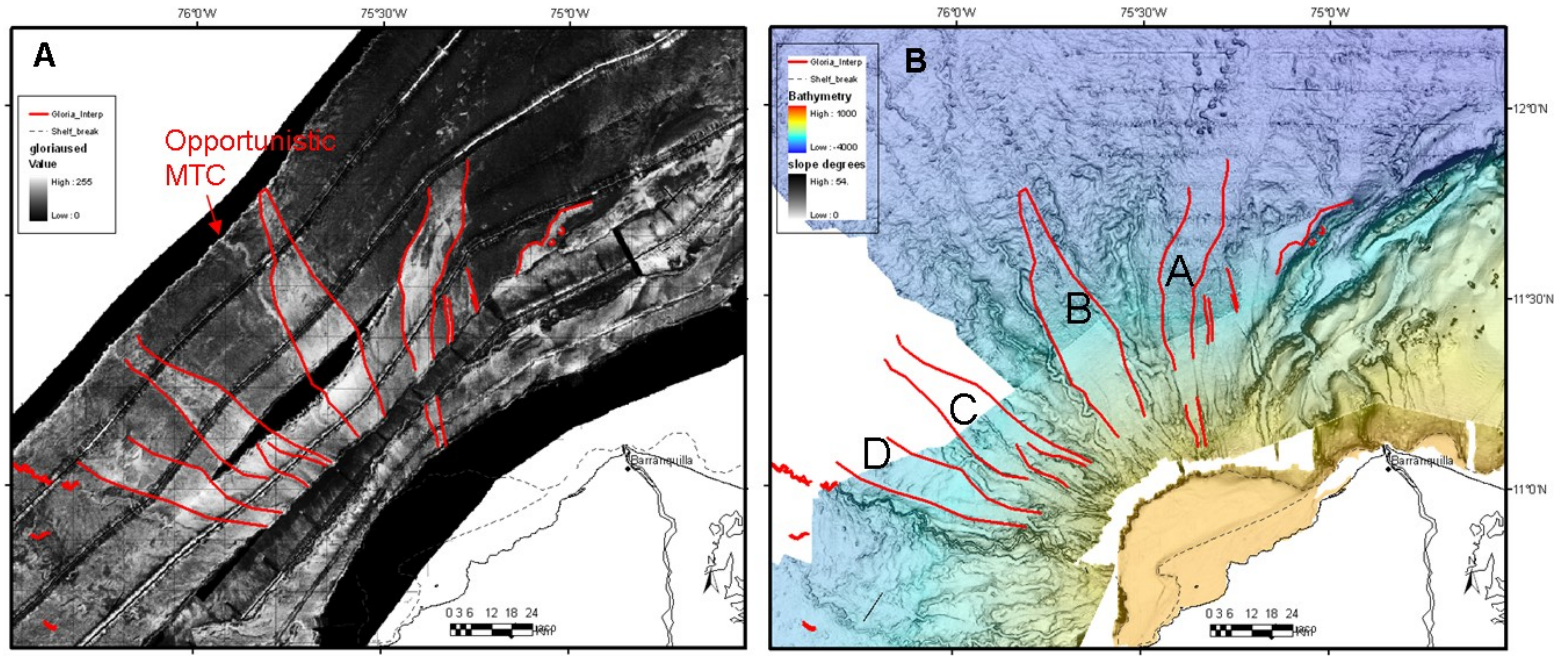


Figure 4.11. GLORIA image (A) and bathymetry (B) for the main fan. Four MTCs filling the interchannel lows can be recognized. Also lobate forms (north of thrust ridges) are highlighted on both images.

infilling low areas adjacent to channels. The GLORIA image is characterized by four high reflectivity zones in the central fan (Figure 4.11A) that correspond to interchannel lows and can be followed from near the shelf break down to the lower fan. Linear features within the MTC on GLORIA images correspond to canyons and conduits on the bathymetry image. Dimensions of the MTCs are presented in Table 4.3. The MTCs in the eastern area could extend farther downslope than the indicated by the high reflectivity on the GLORIA image, as indicated by the morphology of the seafloor (Figure 4.11B). These MTCs may be composed of several depositional events, with the younger being characterized by higher reflectivity (Figure 4.11B).

The upper slope is characterized by arcuate scarps and canyons which focus flows downslope through the interchannel lows (Figure 4.8). Some of the canyons may be following the deeper abandoned channels. Downslope the floors of these lows appear to be very smooth except where cut by younger channels. Slope angle in the interchannel lows varies from 2.5° downslope to 0.5° in the continental rise. Several arcuate scours (scarps) are located in the first 30 km downslope from the shelf break. The eastern part of the main fan exhibits higher slope angles (3.5-4°) and appears aligned with the extension of the deformation front (Figure 4.8).

4.3 TYPES OF MTCS

4.3.1 Detached MTCs

MTC-1 (Table 4.3) is a detached MTC (Figure 4.12) confined by thrust fault-ridges barriers setting (Mayall and Stewart, 2000). The triggering mechanisms of detached MTCs are related to local gravitational instabilities on localized bathymetric highs. Unstable flanks collapse and generate debris flows or slumps (Moscardelli and Wood, 2008) such as MTC-1. Younger deposits filled the trough and reduced the slope angle as they stacked vertically. The modern bathymetry shows that the deposits can reach longer run-off distances down dip, possibly reaching the basin floor for the larger events. The volumetric calculations and seismic interpretation indicate that the MTC-1 scarp is the result of several mass transport events.

MTC Classification*	MTC	Area (km^2)	Length (km)	Width (km)	Thickness (m)	Volume (km^3)	L/W	Max. water depth (m)
Shelf? Attached	A	705	85	12	NA	NA	7.1	3300
	B	1085	90	18	NA	NA	5	3180
	C	966	80	15	NA	NA	5.3	~3000
	D	716	69	12			5.7	~2600
Detached	MTC -1	15	5.7	3.4	~20	0.27	1.7	1590

Table 4.3 Magdalena Fan MTCs classification (base on Moscardelli and Wood, 2008).

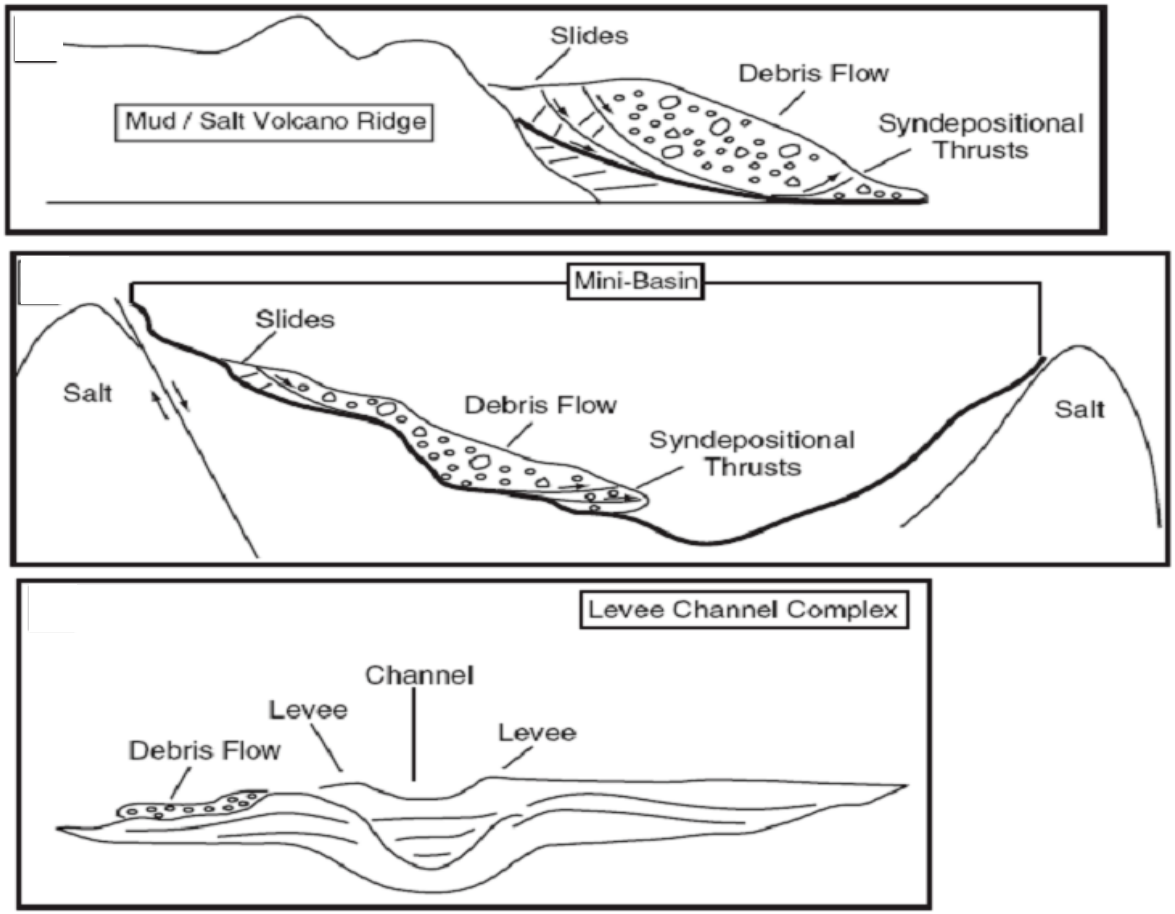


Figure 4.12. Types of detached MTCs (Moscardelli and Wood, 2008).

The scarp is associated with a trend of normal faults that have morphologic expression on the sea-bottom. It is likely that instability of the slope is due to regional deformation and local stresses, possibly amplified by local seismicity (Figure 4.13). Channels at the head and toe of the escarpment indicate that continental slope instability is not the only trigger for the sediment flows traveling basinward through this area (Figure 4.7). Flows associated with formation of the channels may have triggered mass wasting events.

In addition to MTC-1, all thrust belt-related slumps can be classified as detached MTCs. Even though the major MTCs are buried in the piggyback basins or at toes of the deformation belt, continuous growth of imbricate ridges allows these mechanisms to recur in the area (Figures 4.4 A and B).

Also, degradation of the thrust ridges is an important process in the thrust belt areas. The northeastern deformational belt is more active than the southwestern deformational belt, with a number of detached MTCs and lobate deposits at the toe of the ridges (high reflectivity features) (Figure 4.3).

Even though the deposits generated by the levee collapse are feeding the interchannel low areas, hence modifying the geometries of the large MTCs, these MTCs are classified as detached MTCs. Increase of the slope angle at abandoned channels generates inner levee collapses that modify the geometry of the channels margins.

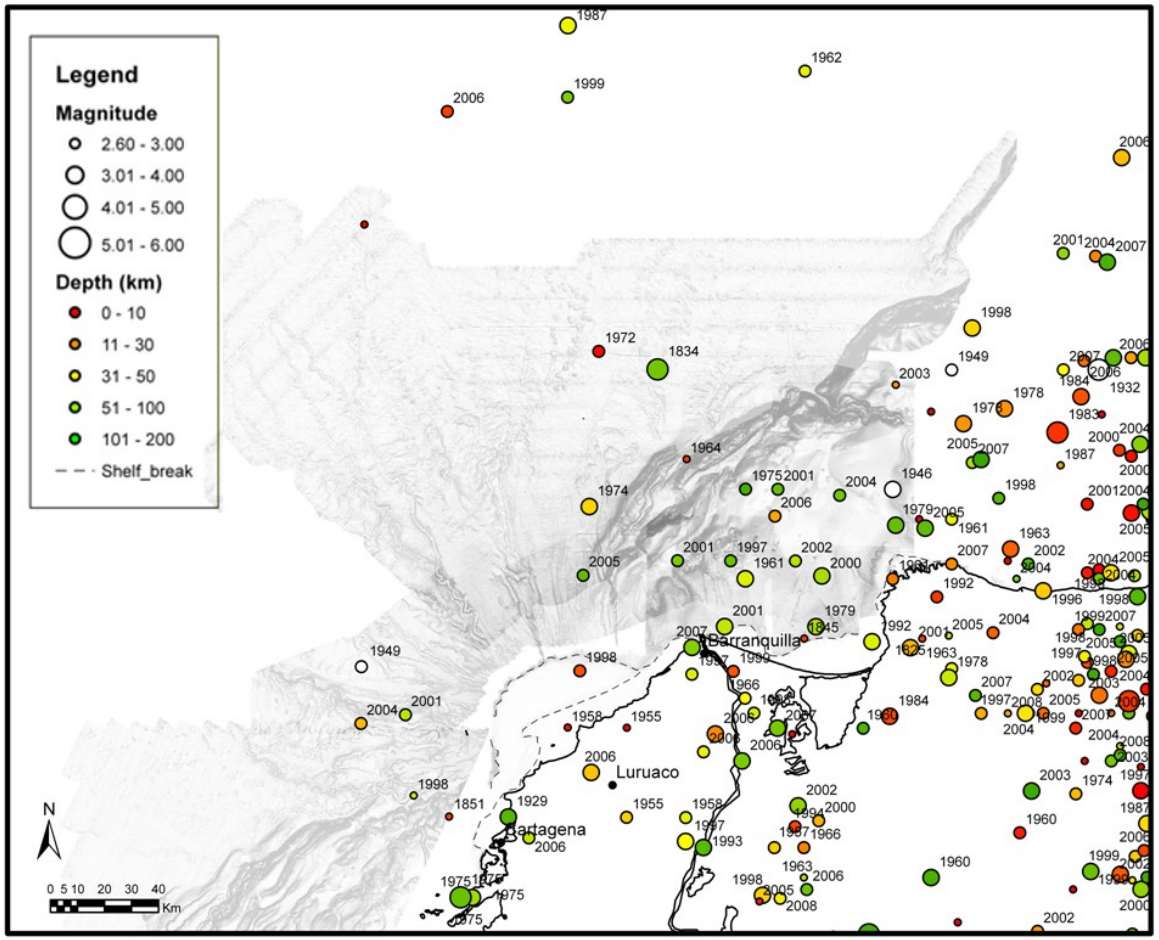


Figure 4.13. Earthquake activity of the margin.

4.3.2 Shelf Attached MTC

The large MTCs A, B, C and D, are attached MTCs (Table 4.3, Figure 4.14). Whether or not the MTCs are slope-attached or shelf-attached is ambiguous with the available information. These large deposits seem to have been more likely generated after migration of the submarine fan southward, since the deposits are confined between abandoned channel levee systems, eroding and smoothing the slope with similar reflectivity on the GLORIA image. Therefore, these deposits cannot be classified as typical shelf edge delta MTCs since they are not fed directly by unstable active deltas, nor did they respond to changes in the sedimentation rates (Moscardelli and Wood, 2008). However, the abandonment of the delta front may have caused instability of the shelf margin and was the source for the MTCs. Abandonment could have been initiated after the late Pleistocene shift of the fan towards the south (Dique canal) (Bordine,1974; Pirmez et al., 1990; this work, Chapter 2).

Conversely, the driving mechanism for slope-attached MTCs may be associated with catastrophic and extensive collapses of the upper continental slope due to earthquakes, long-shore currents, hydrate dissociation or strong storms and/or hurricanes (Moscardelli and Wood, 2008). However, in this area no large upper slope collapses have been recognized with the available data. Instead, a series of canyons and gullies that followed older channels, eroded the upper slope and channelized

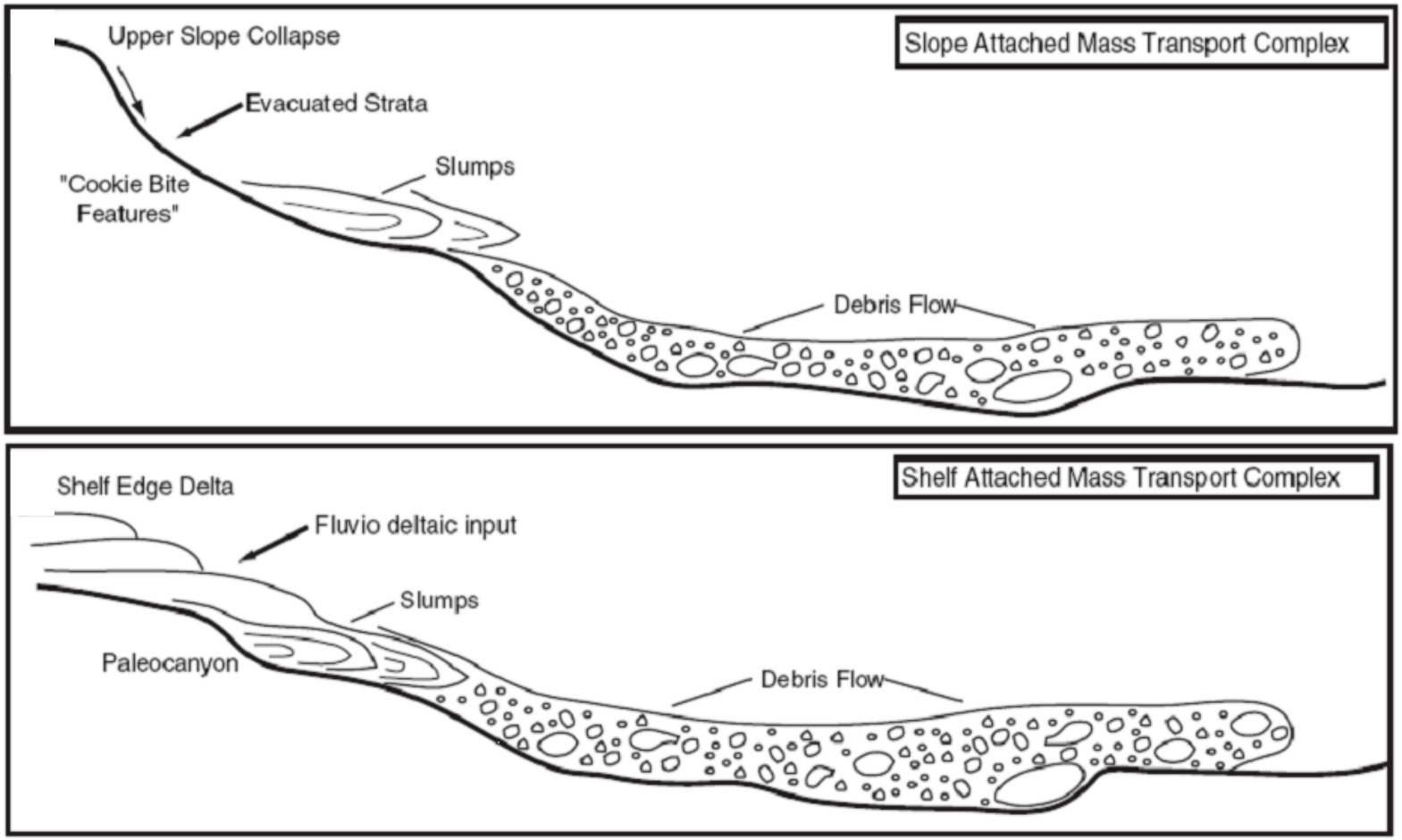


Figure 4.14. Types of attached MTCs (Moscardelli and Wood, 2008)

sediment flows through them. The abundance of these linear features on the GLORIA image and the presence of these MTCs filling all the interchannel lows indicate that this process was common for the entire fan and may not be the product of isolated catastrophic events.

4.3.3 Other Causal Mechanisms

Additional causal mechanisms may have been present in the Magdalena Fan in order to generate the MTCs found on the slope. Besides the abandonment of the delta front as the possible main trigger, changes in the hydrostatic pressure due to sea level changes could have been involved in the generation of attached MTCs. Hydrostatic pressure changes may have induced mass collapse of the abandoned delta (Maslin, 2004).

Global sea level changes and climatic conditions during the Pleistocene seem to be related with many of the MTCs studied throughout the world (Maslin 2004) (Figure 4.15). The Colombian basin δ18O records (ODP Core 999) (Martinez et al., 2007) indicate several major drops of sea level (similar to global changes) which may have influenced the stability of the shelf (Figure 4.16).

The active deformation of the area also may have constituted a major trigger for MTCs. Uplift of the shelf area may have caused remobilization of sediments contributing to the development of MTCs. There are multiple

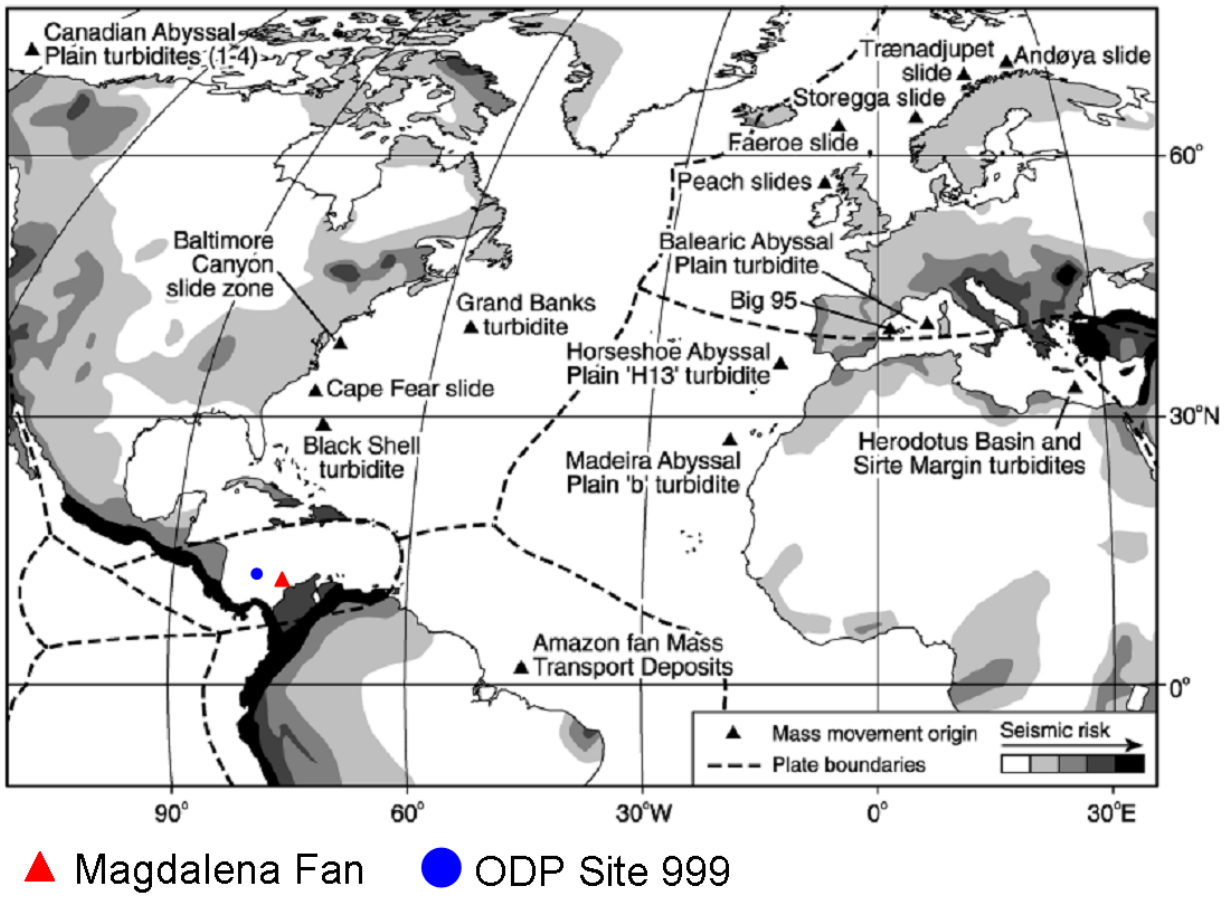


Figure 4.15. Global distribution of MTCs compared with modern-day seismic risk and plate boundaries. The Magdalena Fan in red triangle and ODP Site 999 location is highlighted with the blue circle. (Modified from Maslin et al., 2004)

evidences for active deformation in the area. The Magdalena River shift toward the east (Cienaga de Santa Marta area) was a result of active tectonics (Hoover et al., 1985). Pleistocene units such as the La Popa Formation (coralline limestone) exhibit stress tensors (115°/24°) that respond to the tectonic models of northern South America, in addition to uplifted terraces in coastal areas (Reyes et al., 2001). Evidences of continental slope uplift are associated to high slope angles along the eastern channel thalwegs (this work, Chapter 2), abundant scarps and retrogradational erosion.

Historic seismicity of the area (Figure 4.13) shows strong activity in the northeastern sector. At least 25 earthquakes have occurred on the slope during the last 25 years (Ingeominas, 2008). Their magnitude ranges from 3 to 4.5. They are distributed from a few kilometers up to 90km of depth. However, the earthquakes cannot be directly correlated with the MTCs. Their distribution indicates that they possibly responded to stress-induced accretionary wedge deformation, with pressure release through existing faults. These events may have triggered some MTCs at unstable sectors of the slope, which were then deposited in the piggyback basins.

4.3.4 Possible Timing of Events

Relative timing of the detached MTCs cannot be determined due to their local character. Causal mechanisms are controlled by the growth of arcuate deformation fronts (east and west of the fan) and instability of active and abandoned CLS.

During the middle Pleistocene, a southerly shift of the Magdalena River depocenter resulted in abandonment of the Galerazamba region channel levee systems. This shift coincided with a low stand of sea level (140-120 ka). We hypothesize that the MTCs in the interchannel lows could have been initiated during this sea level drop due to changes in hydrostatic pressure and/or gas hydrate dissolution on the slope, in addition to the abandonment of the Galerazamba area. Similar processes are postulated to have occurred 40-45ka on the Amazon fan, where large MTCs are found (Maslin et al. 2005). Based on δ18O records of ODP Core 999, Martinez et al. (2007) interpreted temperature changes during 120-140 ka are similar to the 40-45ka time interval in the Amazon area (Figure 4.16 and 4.17). In contrast, the large MTCs in the Magdalena Fan could not be related to increases in sedimentation rates due to the Andes latest deglaciation (Younger Amazon MTCs, 10-13 ka), since the delta depocenter was east of the Galerazamba shelf-edge during that time.

The multiple mass flow products of the retrogradation of the slope by continuous uplift seems to be the most recent process, retrogradation

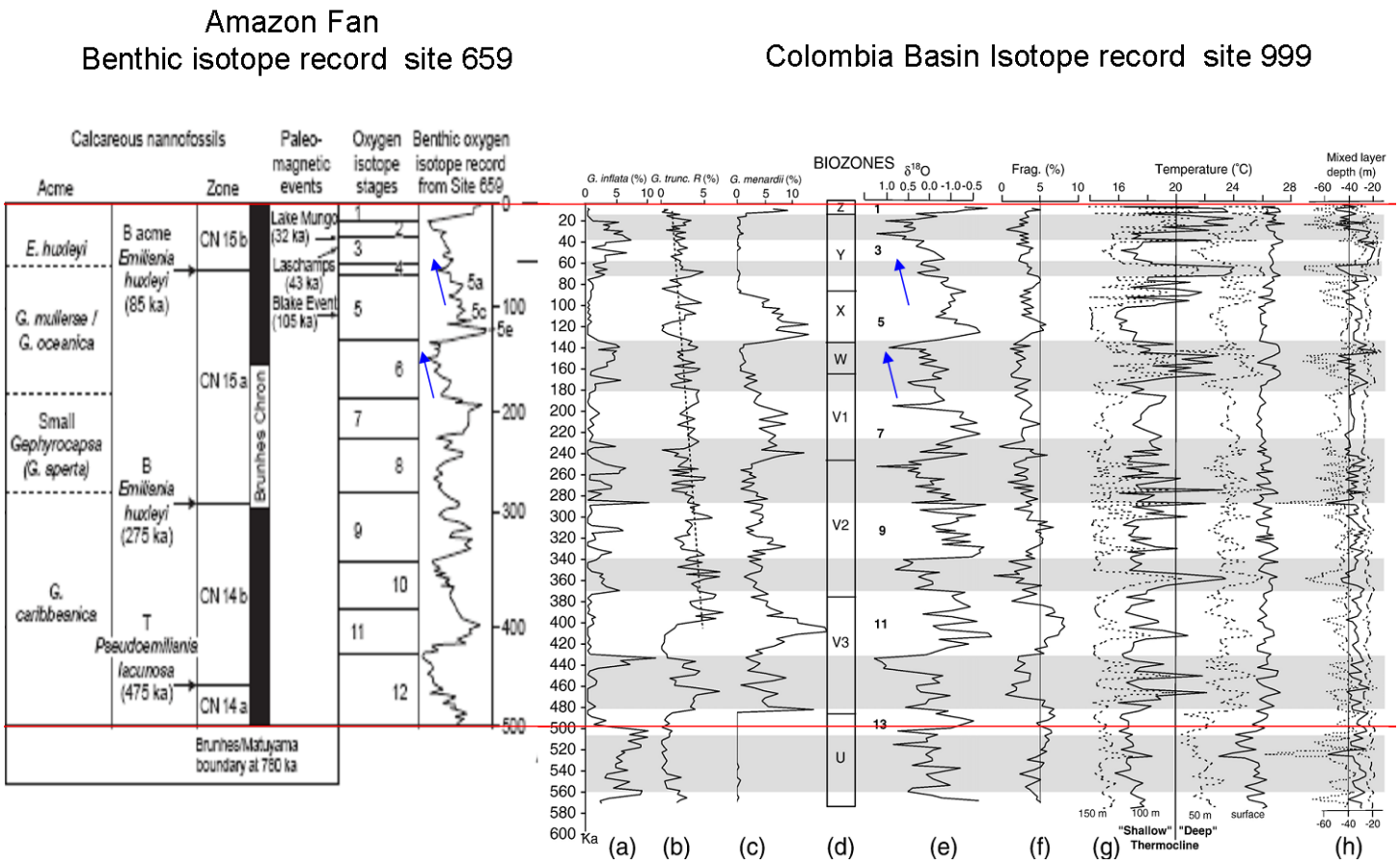


Figure 4.16.Comparision of the Isotope record in the Amazon fan and the ODP site 999 in the Colombian basin. Note the similarity of the record on both sites, which indicate that the Colombian basin present similar sea level changes to the Amazon Fan for the last 500 Ky. (Compiled from Maslin (2005) and Martinez et al. (2007).

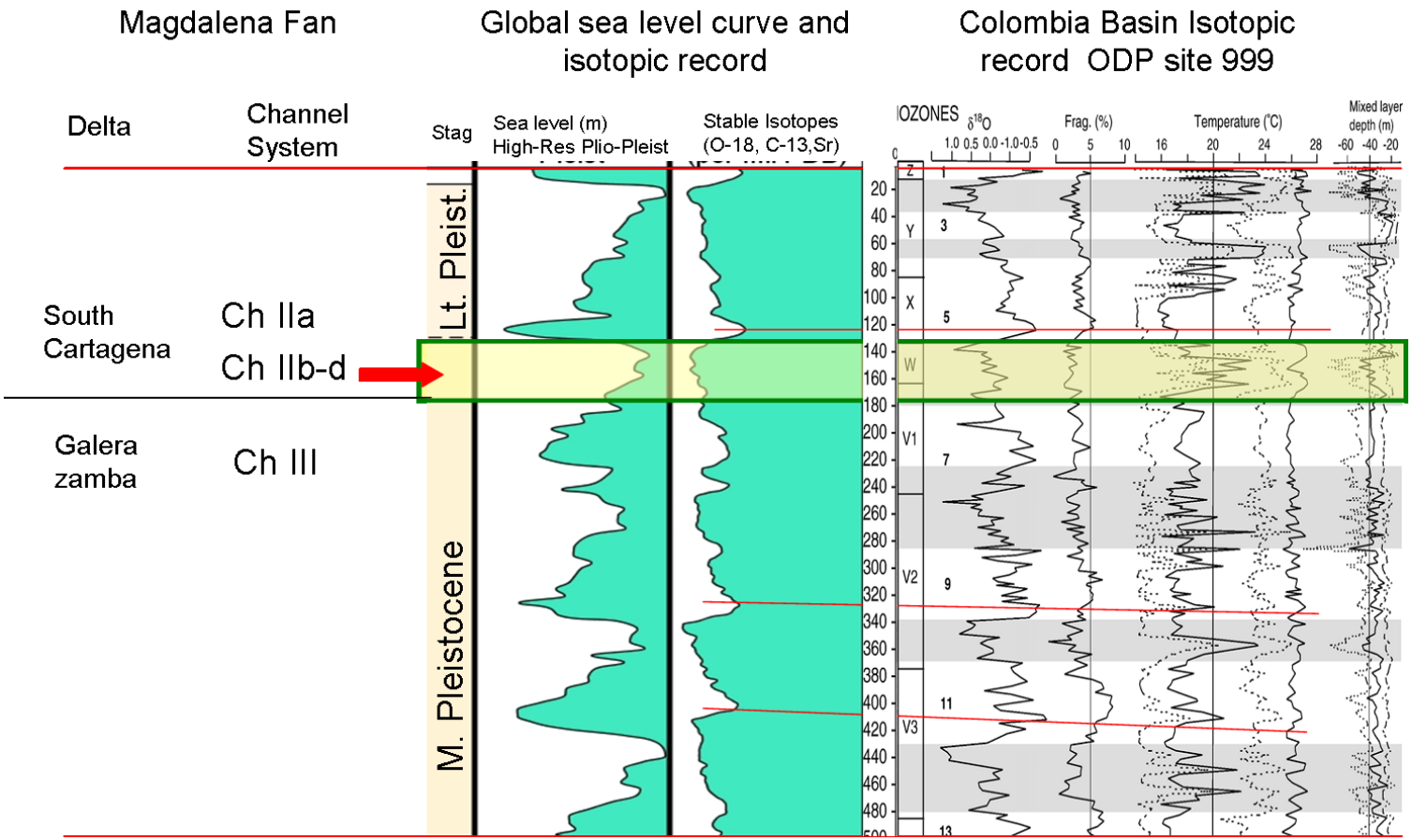


Figure 4.17. Global sea level changes and Isotopic record from the OPD site 999 compared with the Magdalena delta and submarine fan shifts.

promoted erosion and modification of the upper slope, creating instability and feeding the interchannel low areas (Shelf attached MTCs). The westernmost section of the fan does not exhibit the scours or the similar reflectivity response. This may indicate fundamental differences in the deformation of the slope.

4.4 CONCLUSIONS

The combination of bathymetry, GLORIA, and seismic profiles allowed identification of multiple MTCs on the Magdalena Fan. These can be grouped into detached and shelf attached MTCs based on the causal mechanisms: 1) growth of thrust structures (detached), 2) instability of slope canyon and channel walls (detached), 3) major delta front- upper slope failures (shelf-attached).

Four major shelf-attached MTCs occur in the interchannel lows on the fan. This classification is ambiguous since there are no changes in the adjacent delta load, and there is no evidence of major slope collapse. Furthermore the regional extent of the MTCs indicates a more regional process. Causal mechanisms that could have triggered these MTCs are instability after abandonment of the delta front, sea level changes, seismic activity in the area and active deformation of the upper slope.

Possible initiation of the shelf attached MTCs may be related to the southern shift of the delta/fan and relative lowstand of sea level during the middle Pleistocene. The shelf edge may have become unstable, but further investigation is necessary to test this hypothesis. Observations of the upper slope morphologies and downslope deposits suggest that these MTCs are the result of multiple events enhanced by the retrogadational erosion of the upper slope.

4.5 ACKNOWLEDGMENTS

We especially thank Ecopetrol for providing the seismic and Bahia - Sinú bathymetry data, the Institut de Ciències del Mar-CSIC for allowing the use of the proprietary bathymetry; to the Centro de Investigaciones Oceanográficas e Hidrográficas de Colombia (CIOH), for providing complementary bathymetry. The Conoco-Phillips School of Geology and Geophysics provided the financial support and computer facilities. Seismic Micro Technology and ESRI provided the educational software licenses. GLORIA data were acquired during cruises CD40a and DIS109. The crew and scientists aboard the RRS Charles Darwin and RRS Discovery during those cruises are thanked for their efforts. Funding for GLORIA data acquisition and processing were provided by the US-NSF under grant OCE8901848 and OCE9712079.

CHAPTER 5

INTEGRATION OF RESULTS

This chapter integrates the most important findings of the three papers previously presented. It covers final thoughts on fan deformation, deepwater sedimentation and depositional styles that characterize the Magdalena Fan area. It also presents limitations of the study and future work that would complement the results shown in this dissertation.

5.1 FAN DEFORMATION

Variations in the morphology of the channel levee systems comprising the Magdalena Fan are closely related to modification of the slope as a result of deformation created by the compressional stresses in the basin.

One of the main results of this dissertation was establishing the presence of deformed areas within the Magdalena Fan. However, deformation is not recognized throughout the fan, but is restricted to the area's contiguous deformation belts.

Deformation of the northeastern fan occurred before deposition of the main fan, affecting the older sea floor morphologies (channel levee complexes). The presence of hanging, beheaded channels (previous to CLC IV) parallel

to thrust ridges indicates that the channel system was active during the deformation events and had time to adjust to deformation, generating a confined channel system parallel to the axis of thrust ridges. Deformation continued and finally the channel was abandoned and replaced by a course perpendicular to the deformation front.

Deformation on the upper slope (uplift) generated steep slope angles for the central fan (CLC III and IV). Retrogressive erosion and mass transport events on the northeastern upper slope is interpreted to indicate a response to tectonic oversteepening. However, the northeast deformation belt terminates in the direction of the central fan (Galerazamba area), suggesting that slope modification is more related to continuation of the thrust deformation front than to displacement of stress inland. The uplift and overteepening of the central channel thalwegs may indicate migration of the accretionary deformation inland as a result of lowering the fan slope or upper-plate taper.

The buried extension of the southwestern deformation front modified the slope, creating a stepped slope on the western fan, generating high sinuosity channels, forced avulsions and knickpoint formation. The CLC IIc geometries are clearly modified by deformation changes on the slope, which forced the system to abandon areas near the deformation front, and creating avulsion points. In addition, an increase in sinuosity and associated meander cutoff bends are a result of an increase in slope angle in this case

caused by oversteepening of the seafloor topography by deeper folds and faults.

The migration of the sediment source and depocenters could have an effect in the internal deformation of the sedimentary wedge. The sediments began to be deposited at the northeastern part of the fan. Therefore the southwestern area could have been at angles greater than the critical taper wedge; hence thrust growth was taking place on that area (deeper structures). The fan migration southward lowered the critical taper for that area of the slope inhibiting temporally grow of thrust faults. However at the stages of deposition of CLC II, the slope was still being modified by the thrust faults indicating that the critical taper was not inhibited yet.

The eastern fan could have being subject of internal deformation earlier by lowering the critical taper. Thalweg profiles for the eastern fan exhibit some weak convex up profiles that could be related with that deformation.

Consequently the effect of lowering the critical taper wedge (internal deformation) is evident in the central and western fan areas since the sediment pile was deposited earlier than the western fan. Conversely, the deformation of the southwestern area is more pronounced by the later establishment of the fan depocenters.

5.2 DEEPWATER SEDIMENTATION:

The variations in slope topography and location of the sediment source are key controlling factors for sediment distribution on the Magdalena Fan. The Magdalena system is classified as a mud-rich, point-sourced fan system by Reading and Richards (1994). Other modern fan systems in this class include the Amazon, Bengal, Indus, and Mississippi fans.

The Magdalena Fan has previously been described as similar to passive margin fans based on the morphologies of the different architectural elements (Kolla and Buffler, 1984b; Ercilla et al., 2002a). However this present research revealed some important differences between the classic passive margin systems and the Magdalena Fan.

One main characteristic of the Magdalena Fan is the narrow nature of the adjacent shelf. The shelf is on average only ~2km wide, whereas the Amazon and Mississippi fan systems have continental shelves which extend for more than 100 km. This narrow shelf allowed sediment input to the continental slope during all stages of sea level fluctuation.

Because the narrow shelf allowed regular input of sediments to the slope–basin, variations in sedimentation rates and distribution are mainly controlled by river discharge and the inland processes that modified the type, size and composition of the sediments. In general it can be stated that this submarine

fan is controlled mainly by processes associated with fluvial discharge, with a secondary response to sea level changes.

Due to the constant input of sediments to the slope, pelagic sedimentation and condensed sections are restricted to inactive areas of the fan. Some of the cores exhibit high percentages of foraminifera at the top layers (RC13-146, RC11-239, V12-114 and V12-115, Figure 3-12 and Appendix 1). Where as the eastern fan has turbidity current activity today, with flows reaching hundreds of km into the abyssal plain. Regional extension of condensed sections is discontinuous throughout the area due to the erosional processes of channel systems that cannibalized the underlying sequences during early stages of development.

No major canyon system was identified for the different stages of growth of the Magdalena Fan associated with the channel-levee systems. This is an important difference between this system and other passive margin systems. The lack of a single, well defined canyon promoted lateral migration of the fan and the establishment of channel levee systems. In addition the channel levee systems in the Magdalena Fan exhibit a pattern commonly seen in other large submarine fans, where each channel levee systems overlaps each other, suggesting only one channel system active a time. In contrast, the active eastern area there is no individual canyon established, but multiple pathways are active over the period of time confirmed by the cable breaks distribution over the slope.

The active fan canyons are a result of the higher angles of the upper slope. Entrenchment of the Magdalena canyon could also be enhanced by the anthropogenic modification of the river mouth after construction of jetties.

5.3 MAGDALENA FAN DEPOSITIONAL STYLES

On the Magdalena Fan, morphologies seem to be more related to the sediment source and slope morphology than to the tectonic setting. Different depositional styles have been recognized that were the result of interaction between sediment input and deformation of the slope.

The main fan area exhibits three main types of deposits (Figure 5.1 A): channel-levee systems, mass transport complexes and sand waves. In addition to these architectural elements, unconfined flow deposits were also identified (lobate morphologies), that could have been deposited in the interchannel lows, low angle sections of the slope, or at the toe of slope at the mouth of the canyons systems on the eastern side of the fan. These deposits are associated with knickpoint formation and establishment of the channel levee systems (Figure 5.1 B). Commonly the lobe deposits are found at the base of the channel levee system and could be of economic importance. Later establishment of the channel course will define the preservation and fluid communication between these geobodies.

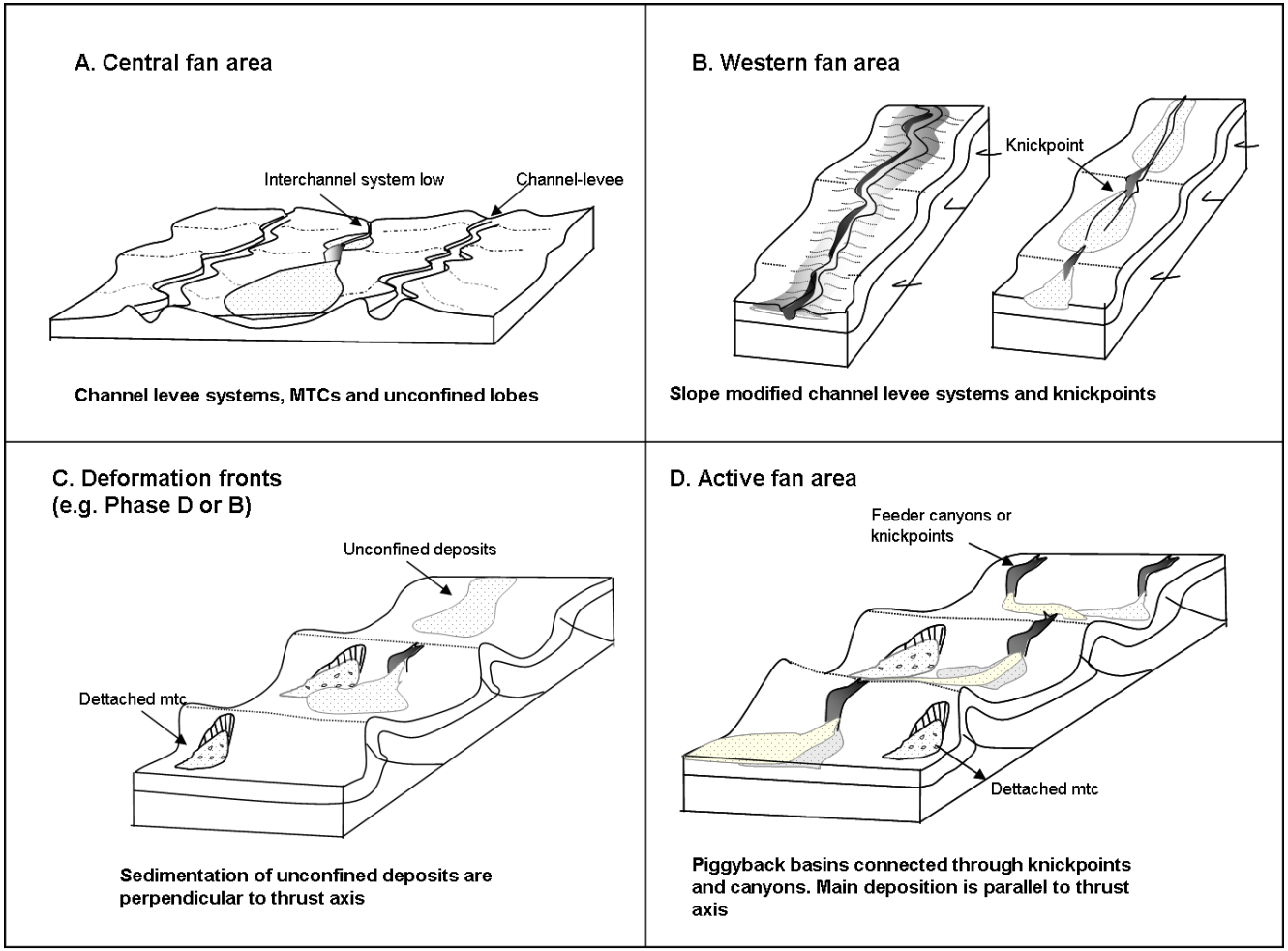


Figure 5.1. Depositional styles on the Magdalena fan.

Sand rich lobate deposits were identified at the toe of the thrust ridges, and on different low angle positions on the slope. These deposits are distributed along the piggyback basins and the abyssal plain. Bypass areas such as canyons and knickpoints within and communicating between the piggyback basins are common and should be significant to recognize in the subsurface when estimating reservoir location and properties, because they represent zones of erosion and therefore may impact reservoir continuity.

The depositional systems at the thrust deformed belts differ from the rest of the fan ((Figure 5.1 C): Even though the river mouth was located at the southwestern (Phase D) and northeastern (Phase B) deformed belts during the late Pleistocene and Holocene, respectively, there is no evidence of channel levee system development. The depositional axis in both cases is perpendicular to the deformation. This sedimentation style should correspond to above-grade accommodation (Prather, 2003) with sediment accumulation on the toe of the thrust ridges (piggyback basins). Unconfined turbidite flows should dominate the slope deposition processes.

Later development of slope canyons at the present location of the river mouth resulted in variation of the distribution of sediments. The turbidity flows traveled along and were deposited parallel to the thrust ridges axis ((Figure 5.1 D): As discussed earlier variation of properties of the deposit away from the point source will be a key to consider when estimating the reservoir properties of this type of deposit. The presence of beheaded –

hanging channels is an indicator of the interaction between deformation and sedimentation; this is important when evaluating depositional styles.

Figure 5.1 depicts a progression on the amount of deformation from A to D and consequently the irregularity of the seafloor morphologies appear to increase from the central fan toward the deformed thrust belts.

In addition to the spatial progression, also it is important to note the time progression of the deformation. The older sections of the fan seem to present lower rates of slope modification (higher internal deformation?) and the younger sections of the fan were deposited in areas where the slope have experienced strong modifications by the thrust deformation.

A close interaction between the sediment influx and deformation rates are observed on the fan. The areas with very irregular topography may reflect higher deformation than sediment accumulation. Over time, the continuation of sediment accumulation may overcome the deformation resulting in a smoother topography. This observation will directly support the changes in deformation style in presence of high rates of sedimentation that is the basis of the critical taper wedge model.

Sediment deposition in the Aguja Canyon may have been different since it is not linked to the Magdalena River system. Characteristics are more related to a sand-rich system (Reading and Richards, 1994) that is mainly fed by longshore drift through a main canyon. However, composition of the

sediment and abundance of plant fragments on the abyssal plain near the Aguja canyon indicates mixing of sediments transported by the two systems.

5.4 LIMITATIONS

Interpretations of the data utilized in this study were highly limited by the low vertical resolution of the seismic profiles and poor imaging of some data available. Furthermore the seismic signal was obscured by the presence of gas, mud diapirs, and gas hydrates, which in conjunction with the complexity of the structures, made the identification and interpretation of the many elements identified on the bathymetry data difficult.

A second constraint was the lack of age control for the different elements. The highly erosional nature of the upper slope and lack of age control of the sedimentary sections in the basin limit regional correlation. Even though correlation with the river migration inland and lateral overlapping relationships allowed determination of relative ages for the different elements, a better age control would allow timing of establishment of the channel systems, changes in sedimentation rate, etc. to be determined.

Poor preservation of the few surface sediment piston cores in the area also limited interpretations about the variation of sediments in the different areas, textural changes and even identification of processes that were associated

with each flow deposit. New or alternative techniques may be used to try to extract additional information from these cores.

5.5 FUTURE WORK

The Magdalena Fan system could provide opportunities to better understand deepwater depositional systems. The interaction of deformation, different styles of deposition and active turbidite sedimentation of this system make it fairly unique. Future work may include the following:

- Age dating for some of the major elements in order to establish timing of channel-levee system growth, variations in sedimentation rates, fan migration, and possibly recurrence of turbidite flows. Not only it is necessary to know the age of the turbidite fan, but also to better link the activity of the sediments from the coast line.

- Availability of new 2D and 3D seismic surveys as a result of the increasing exploration interest of the area will provide the basis to expand and corroborate the interpretation of some of the architectural elements. 3D imaging of the fan deposits will allow new understanding in the evolution of the channel-levee systems in time by definition of changes in sinuosity, lateral migration and slope modification. Corroboration of some of the ideas presented in this work, such as the

initiation of the channel levee systems, could be achieved with better seismic coverage.

- Revising the existing piston core descriptions and applying new concepts and alternative methodologies that allow extracting valuable information about the active turbidite flows.

- New acquisition of piston cores at different distances from flows would allow determining the evolution of such flows and their erosional and depositional capability.

- A detailed study of the Aguja Canyon sand rich system would be valuable to characterize longshore drift-fed turbidites and quantify the influence that this system had on abyssal plain sedimentation. Also characterization of northern (Guajira area) sand rich canyons could be of economic importance if those systems were common before the establishment of the northern drainage system (Magdalena system) in the basin.

- The cable break record is limited to the 1950's, but it is likely that information about ruptures on submarine infrastructure exist, even though it is not in the public domain. A rupture of the internet cable that provided this service to Colombia and Venezuela was reported on June 20th, 2007 on the Arcos network (Columbus Networks). An attempt to identify the location of the rupture was not provided by the company on

security grounds. However institutions such as the CIOH in Colombia may be interested in continuing this type of work and finding records of additional ruptures in the area.

- There is considerable opportunity to establish the structural evolution of the thrust-deformed belts, in particular the piggyback basins.

- Quantification of mass transport deposits vs turbidite deposits as part of the above-grade deposition will provide important information as an analog to exploration and reservoir characterization in this type of setting.

- Biostratigraphy and age dating of the sequences in the deformed areas is needed to calculate sedimentation rates and timing of compressional phases of deformation.

CHAPTER 6

CONCLUSIONS

- The Magdalena submarine fan is a mud-rich system that extends 68,000 km^2 into the southern Caribbean Sea. It has been fed by the Magdalena River since establishment of the northern drainage system in Miocene time. It is part of the accretionary wedge generated by the interaction of the Caribbean and South American plates. Two arcuate thrust belts developed at the northeastern and southwestern extensions of the main fan deposition. Sedimentation is characterized by the presence of multiple channel levee complexes (CLC), mass transport deposits (MTCs) and fewer unconfined flows.

- Pleistocene to Holocene deposits on the seafloor were studied, using bathymetry and seismic profiles, in order to define the variations within the system. The fan evolution is closely linked to Magdalena delta migration and tectonic processes. The Plio-Pleistocene history of the Magdalena River is represented by at least eight different phases, beginning at the north (west of the present river location) (CLC IV- Early Pleistocene). Then, the river migrated towards the south (CLCs III and II, Phase E). The southern most location of the river reached the

Canal del Dique (Phase D) during the middle Pleistocene. Later, the river migrated north of Cartagena (Phase C), forming CLC IIa, IIb, IIc and I (youngest CLC of the entire fan). A major northern shift of the river due to the Atlantico-Turbaco uplift shifted sedimentation towards the Cienaga de Santa Marta (phase B). The present day delta fan switched positions between Boca Vieja and Sabanilla Canyon before stabilizing at its present position (Phase A). The fan is active today with deposition of turbidite flows and mass transport deposits in piggyback basins formed as a result of deformation of the accretionary wedge. Sedimentation shifts are corroborated by a decrease in the carbonate content of the Colombia basin (6000 B.P.), growth of coralline limestone at the coastal margin (Barranquilla) and remnants of old river courses.

- Several CLS's in the fan show segments with convex up thalweg profiles indicating: 1) the channel was abandoned before reaching its equilibrium profile or 2) deformation of the channel occurred after abandonment. There is evidence of multiple phases of deformation on the Magdalena Fan due to the deformation of the larger accretionary wedge. Decrease in bathymetric depths on the thalweg profiles for the western fan seems to support the idea of higher deformation (compression) in this area. Alignment of knickpoints and channel bends, and step profiles in the western side are a clear indication of the

deformation that is active during and post-formation of the channel facies. The presence of overpressured shales seems to have played an important role in the deformation of the fan.

- A sequence of knickpoints connects deposition of sediments from the shelf break downslope through a series of steps, culminating in lobate unconfined deposits. Upstream knickpoint migration in slope steps as a response to deformation may represent a key process to explain the initiation of deepwater channel systems on the Magdalena Fan, but further research needs to be done to establish this. In addition, the interchannel lows could facilitate the rapid confinement of the slope to initiate the knickpoint migration.

- Modern sediment gravity flows generated submarine cable breaks occurred on the Magdalena Fan. Fifteen breaks were recorded in a 30 year period. The sediments are apparently transported downslope mainly through the Magdalena Canyon, but abandoned canyons and gullies also served as conduits for past sediment flows. Three main flow pathways were identified: 1) flows from the Magdalena, Sabanilla and U canyons transported through piggyback basins PBB1 and PBB4, 2) flows from the Magdalena Canyon and western gullies that are transported through piggy-back basins on the back of thrust- and fault-cored

anticlinal ridges (PBB1 and PBB3), and 3) flows transported by the Aguja Canyon.

- Individual flows seem to be related to different processes on the continental shelf: 1) High flood stages of the river, 2) coastal erosion, 3) longshore drift, 4) hyperpycnal flows and 5) river mouth instability. The sedimentological characteristics of the different deposits should differ as the flow properties are different. Flows related to the active Magdalena canyon and western gullies may be related to high flood stages of the river, hyperpycnal flows and instability of the delta front.

- Mass transport deposits (MTCs) in the Magdalena Fan are grouped by causal mechanisms: 1) growth of thrust structures (detached MTCs), 2) instability of slope canyon and channel walls (detached MTCs), and 3) major slope failures (shelf attached MTC). Degradation of thrust ridges and retrogradational erosion are also important modifiers on the continental slope.

- Four major shelf-attached, slope MTCs occur in the interchannel lows on the fan. Causal mechanisms that may have triggered these MTCs are instability after abandonment of the delta front, sea level changes, seismic activity in the area and active deformation of

the upper slope. Possible initiation of the MTCs may be related to the southern shift of the delta/fan and relative lowstand of sea level during the middle Pleistocene. The shelf edge may have become unstable, but further investigation is necessary to test this hypothesis. Observations of the upper slope morphologies and downslope deposits suggest that these MTCs are the result of multiple events enhanced by retrogradational erosion of the upper slope.

- Deformation on the Magdalena Fan occurs within occurs within the deformed belts on each side of the fan and along the edges in proximity of the deformation fronts. The northeast deformation is found on the upper slope and shelf areas where the northeastern deformation belt closes in the direction of the central fan (Galerazamba area). The southwest deformation is represented by the buried extension of the southwestern deformation front which modifies the slope, creating step-slopes, generating high sinuosity channels, forced avulsions and knickpoints.

- The fan deposition lower the critical taper wedge (internal deformation) in the central and western fan areas since the sediment pile was deposited earlier than the western fan. Conversely, the deformation

of the southwestern area is more pronounced by the later establishment of the fan depocenters.

- Depositional styles vary from the main fan to the thrust-deformed areas. Channel levee systems, unconfined flows and MTCs are typical of the main fan. Thrust deformed areas are characterized by unconfined deposits filling the piggyback basins with directions of flow perpendicular and parallel to the main axis of the thrust structures.

- The Aguja Canyon, is identified as a sand rich system because it has no significant river linked to the canyon head. Instead the canyon must be receiving sandy sediments transported by longshore drift along the eastern coast of Colombia. Submarine cable ruptures across the lower reaches of this canyon indicates that sediment gravity flows also are active in this area, away from the Magdalena River mouth.

- Important applications to hydrocarbon exploration and reservoir distributions have been obtained from this study when the fan is used as a modern analog, particularly in the Caribbean basins and similar basins in tectonically active parts of the world. In addition, it

characterizes the Colombian continental slope in terms of stability and shallow hazards for submarine infrastructure.

- Future studies were suggested to better understand the interaction of deformation and the deepwater architectural elements. Integration of information such as biostratigraphy, additional seismic surveys and sediment samples for the Magdalena fan area, will provide further advances on the generation of deepwater depositional models for tectonically active margins.

REFERENCES

Adeogba, A.A., McHargue, T.R., Graham, S.A., 2005, Transient fan architecture and depositional controls from near-surface 3-D seismic data, Niger Delta continental slope. AAPG Bulletin v. 89, no. 5, p. 627–643.

Alvarado, M., 2005, Cartagena y el plan de restauración ambiental del Canal del Dique, y Barranquilla y las obras de profundización del canal navegable de acceso a la zona portuaria: Visión general. In: Restrepo, J.D. (Ed.), Los Sedimentos del Río Magdalena: Reflejo de la Crisis Ambiental. EAFIT Univ. Press, Medellín, Colombia, p. 217– 254.

Babonneau, N., Savoye, B., Cremer, M., Klein, B., 2002, Morphology and architecture of the present canyon and channel system of the Zaire deep-sea fan. Marine and Petroleum Geology v.19, no.4, p. 445–467.

Babonneau N., Cattaneo A., Harster M., Deverchere J., Yelles, K., Savoye, B., Domzig, A., 2007, Morphology and Structure of the Algiers Deep-Sea Fan and Possible Sedimentary Record of the 2003 Boumerdès Earthquake (Maradja Project), American Geophysical Union, Fall Meeting 2007, abstract #H41F-0840.

Beaubouef, R.T., Friedman, S.J., 2000, High resolution seismic/sequence stratigraphic framework for the evolution of Pleistocene intra slope basins, western Gulf of Mexico: depositional models and reservoir analogs: GCSSEPM Foundation 20th Annual Research Conference, Deep-Water Reservoirs of the World, Dec. 3-6, p. 40-60.

Bhattacharya J.P., MacEachern J.A., 2008, Hyperpycnal rivers and prodeltaic shelves in the Cretaceous seaway of North America. Search & Discovery Art# 50069.

Boiano U., 1997, Anatomy of a siliciclastic turbidite basin: the Gorgoglione Flysch, Upper Miocene, southern Italy: physical stratigraphy, sedimentology and sequence-stratigraphic framework, Sedimentary Geology, v. 107, p. 231–262.

Bordine, B.W., 1974, Neogene biostratigraphy and paleoenvironments, lower Magdalena Basin, Colombia. PhD Thesis, Louisiana State University, 295 p.

Breen, N.A., 1989, Structural effect of Magdalena Fan deposition on the northern Colombia convergent margin. Geology, v. 17 January, p. 34-37.

Clark, J.D., Kenyon N.H., Pickering K.T., 1992, Quantitative analysis of the geometry of submarine channels: Implications for the classification of submarine fans, Geology v. 20, p. 633-636.

Coleman, J.M., 1981, Deltas: Processes of Deposition and Models for Exploration, second ed. Burgess Publishing Company, Minneapolis, 102 p.

Corredor, F., 2003, Seismic strain rates and distributed continental deformation in the northern Andes and three dimensional seismotectonics of northwestern South America, Tectonophysics, v. 372, p. 147–166.

Cronin, B.T., 1995, Structurally-controlled deep sea channel courses; examples from the Miocene of Southeast Spain and the Alboran Sea, Southwest Mediterranean. In: Hartley A.J. and Prosser J., Editors, Characterization of Deep Marine Clastic Systems, Geological Society Special Publications, London, p. 115–135.

Damuth, J.E., Kumar, N., 1975, Amazon Cone: morphology, sediments, age and growth pattern. Geological Society of America Bulletin v. 86, p. 873–878.

Davis, D., Suppe, J., Dahlen, F.A., 1983, Mechanics of fold and thrust belts and accretionary wedges, Journal of Geophysical Research , v. 88, p. 1153-1172.

Demyttenaere, R., Tromp J. P., Ibrahim A., Allman-Ward P., Meckel T., 2000, Brunei deep water exploration: From sea-floor images and shallow seismic analogues to depositional models in a slope turbidite setting, in: Weimer P., Slatt, R.M., Coleman, J.L., Rosen, N., Nelson, C.H., Bouma, A.H., Styzen, M.,Lawrence D.T., eds., Global deep-water reservoirs: Gulf Coast Section–

SEPM Foundation 20th Annual Bob F.Perkins Research Conference, p. 304–317.

Deptuck, M.E., Sylvester, Z., Pirmez, C., O'Byrne, C., 2007, Migration-aggradation history and 3D seismic geomorphology of submarine channels in the Pleistocene Benin-major Canyon, western Niger Delta Slope, Marine and Petroleum Geology, v. 24, p. 406–433.

Droz, L., Rigaut, F., Cochonat, P., Tofani, R., 1996, Morphology and recent evolution of the Zaire turbidite system (Gulf of Guinea), Bulletin of the Geological Society of America, v. 108, no. 3, p. 253-269.

Duque-Caro, H., 1979, Major structural elements and evolution of northwestern Colombia, in Geological and geophysical investigations of continental margins: AAPG Memoir, v. 29, p. 329-351.

Duque-Caro, H., 1984, Structural style, diapirism, end accretionary episodes of the Sinu-San Jacinto terrane, southwestern Caribbean borderland, in: W.E. Bonnini, R.B. Hargraves (eds), The Caribbean-South American Plate Boundary and Regional Tectonics. Geological Society of America, Memoir, v. 162, p. 303-316.

Elliott, T., 2000, Megaflute erosion surfaces and the initiation of turbidite channels. Geology, v. 28, p. 119–122.

Ercilla, G., Alonso, B., Estrada, F., Chiocci, F.L., Baraza, J., Farran, M., 2002a. The Magdalena turbidite system (Caribbean Sea): present-day morphology and architecture model. Marine Geology, v. 185, p. 303–318.

Ercilla, G., Wynn, R.B., Alonso, B., Baraza, J., 2002b, Initiation and evolution of tubidity current sediment waves in the Magdalena turbidite system. Marine Geology, v. 192, p. 153-169.

Estrada, F., Ercilla, G., Alonso B., 2005a, Quantitative study of a Magdalena submarine channel (Caribbean Sea): implications for sedimentary dynamics, Marine and Petroleum Geology, v.22, p. 623–635.

Estrada, F., Ercilla, G., Alonso, B., 2005b, Large-scale mass-flows in the Magdalena turbidite system. Geophysical Research Abstracts, v. 7, 03410, European Geosciences Union.

Faulkenberry L., Peakall J., Kneller B., 2005, Submarine Channel Initiation from Gullies on the Upper Slope: Fuji and Einstein Channels, Gulf of Mexico. 2005 AAPG Annual Convention (June 19-22, 2005) Technical Program.

Flinch, J. F., Amaral J., Doulcet, A., Mouly, B., Osorio, C. Pince, J. M., 2003, Onshore-Offshore Structure of the Northern Colombia Accretionary Complex, Memory AAPG International Conference Barcelona, Spain, September, 2003, p. 1 – 5.

Flood, R.D., Damuth, J.E., 1987, Quantitative characteristics of sinuous distributary channels on the Amazon deep-sea fan. GSA Bulletin. v.98, p. 728-738.

Flynn, J. J., Guerrero, J., and Swisher, C. C., 1997, Geochronology of the Honda Group, in Kay, R. F., Madden, R. H, Cifelli, R L, Flynn, John J., eds. Vertebrate paleontology in the neotropics; the Miocene fauna of La Venta, Colombia, Washington, D. C., Smithsonian Institution Press, p. 44-59.

Gardner, T.W., 1983, Experimental study of knickpoint and longitudinal profile evolution in cohesive, homogeneous material. Geological Society of America Bulletin, v. 94, no. 5, p. 664–672.

Gervais A., Savoye B., Mulder T., Gonthier E., 2006, Sandy modern turbidite lobes : Anew insight from high resolution seismic data. Marine and Petroleum Geology, v. 23, p. 485-502, doi:10.1016/j.marpetgeo.2005.10.006

Guerrero, J., 1993, Magnetostratigraphy of the upper part of the Honda Group and Neiva Formation. Miocene uplift of the Colombian Andes [Ph.D. thesis]: Durham, North Carolina, Duke University, 108 p.

Hay, W.W., Aloan, J.L., Wold, C.N., 1988, Mass/age distribution and composition of sediments on the ocean floor and the global rate of sediment subduction, 1988, Journal of Geophysical Research, v. 93, p. 14933-114940.

Heezen, B.C., Ewing M.H., 1952, Turbidity currents and submarine slumps, and the 1929 Grand Banks earthquake. American Journal of Science, v. 250, p. 849–873.

Heezen, B.C., 1955, Turbidity currents from the Magdalena River. Bull. Geol. Soc. Am. Vol 66 pp. 1572.

Heezen, B.C., 1956a, Corrientes de turbidez del Río Magdalena.
Bol. Soc. Geol. Colomb, v. 51-52, p. 135-143.

Heezen, B.C., 1956b, Turbidity currents from the Magdalena River. Bulletin of the Geological Society of America, v. 66 p. 1572.

Heezen, B.C., Menzies R.J., Schneider E.D., Ewing M.H., Grainelli, N.C., 1964, Congo submarine canyon, AAPG Bulletin, v. 48, p. 1126–1149.

Heezen, B.C., Muñoz, J., 1965, Magdalena turbidites in deep-sea sediments. Fourth Caribbean Geological Conference Proceedings, Trinidad, 342p.

Heiniö, P., Davies, R.J., 2007, Knickpoint migration in submarine channels in response to fold growth, western Niger Delta, Marine and Petroleum Geology, v. 24, p. 434–449.

Hoorn, C., Guerrero, J., Sarmiento, G., Lorente, M., 1995, Andean tectonics as a cause for changing drainage patterns in Miocene northern South America, Geology, v. 23, p. 237–240.

Hoover, R.A., Bebout, D.G., 1985, Submarine fan diversion by tectonic processes- Magdalena Fan and slope, Southern Caribbean. Gulf Coast Association of Geological Societies Transactions, v. 35, p. 395-395.

Howard, A.D., Dietrich, W.E., Seidl, M.A., 1994, Modeling fluvial erosion on regional to continental scales. Journal of Geophysical Research, B, Solid Earth and Planets, v. 99, no. 13, p. 971-986.

Huyghe, P., Foata, M., Deville, E., Mascle, G., Caramba Working Group, 2004, Channel profiles through the active thrust front of the southern Barbados prism. Geology, v. 32, no. 5, p. 429–432.

Imran, J., Parker, G., Pirmez, C., 1999, A nonlinear model of flow in meandering submarine and subaerial channels. Journal of Fluid Mechanics, v. 400, p. 295–331.

Ingeominas, 2008, Red Sismologica Nacional de Colombia. Catalogo de sismicidad instrumental (1993-Present).
http://seisan.ingeominas.gov.co/RSNC/Formulario.html

Ingram G.M., Chisholm T.J., Grant C.J., Hedlund C.A., Stuart-Smith P., Teasdale J., 2004, Deepwater north west Borneo: hydrocarbon accumulation in an active fold and thrust belt. Marine and Petroleum Geology, v. 21, p. 879-887. doi:10.1016/j.marpetgeo.2003.12.007

Kastens, K.A., Shor, A.N., 1985, Depositional processes of a meandering channel on Mississip.i Fan. AAPG Bulletin, v. 69, p. 190–202.

Kellog, J., Bonini, W.E., 1982, Subduction of the Caribbean Plate and basement uplifts in the overriding South America Plate, Tectonics, v. 1, p 251–276.

Kellog, J., Vega, V., 1995, Tectonic development of Panama, Costa Rica, and Colombian Andes: Constrain from Global positioning System geodetic studies and gravity, Mann Paul (editor), Geologic and Tectonic Development of the Caribbean Plate boundary in southern Central America, GSA Special Paper, v. 295, p. 75–90.

Kendall, C., Haughton, P., 2006, Deepwater Fans & Mass Transport Debris – Depositional Settings & Source Terrains. 14 May 2009. http://strata.geol.sc.edu/Deepwater/DeepwaterClasticSettings.html.

Kennish, M.J., 1989, Practical handbook of marine science. Boca Raton, FL: CRC Press, 710p.

Kneller B.C., Buckee C.M., 2000, The structure and fluid mechanics of suspension currents; a review of some recent studies and their geological implications. Sedimentology, v. 47, no. 1, 62-94.

Kneller, B., 2003, The influence of flow parameters on turbidite slope channel architecture. Marine and Petroleum Geology, v. 20, no. 6–8, p. 901–910.

Kolla, V., Buffler R.T., 1984a, Morphologic, Acoustic and sedimentologic characteristics of the Magdalena Fan, Geo-Marine Letters, v. 3, p. 85-91.

Kolla, V., Buffler, T., 1984b, Seismic stratigraphy and sedimentation of Magdalena Fan, Southern Colombia basin, Caribbean Sea. AAPG Bulletin, v. 68, p. 316– 332.

Kolla, V., Bourgues, P.H., Urruty, J.M., Safa, P., 2001, Evolution of deep-water Tertiary sinuous channels offshore Angola (West Africa) and implications for reservoir architecture. AAPG Bulletin, v. 85, no. 8, p. 1373-1405.

Komar, P.D., 1971, Hydraulic jumps in turbidity currents. Bulletin of the Geological Society of America, v. 82, no. 6, p. 1477–1487.

Link,T. A., 1927, Post-Tertiary strand-line oscillations in the Caribbean Coastal area of Colombia. S. Am. Journal of Geology, v. 35, no. 1, p. 58-72. Chicago.

Martinez J.O., Pilkey O.H., Neal W.J., 1990, Rapid formation of large coastal sand bodies after emplacement of the Magdalena River jetties, northern Colombia, Environmental Geological Water Science, v. 16, no. 3, p. 187-194.

Martinez, N.J., Robertson, K.D., 1997, Variaciones cuaternarias del nivel del mar y sus implicaciones en las amenazas litorales del caribe colombiano. IDEAM - 1er Seminario Nacional sobre manejo integrado de zonas costeras, Cartagena, 19-21 de Noviembre de 1997.

Martinez, J.I., Mora, G., Barrows, T.T., 2007, Paleoceanographic conditions in the western Caribbean Sea for the last 560 kyr as inferred from planktonic foraminifera. Marine Micropaleontology, v. 64, p. 177-188.

Maslin, M., Owen, M., Day, S., Long, D., 2004, Linking continental-slope failures and climate change: Testing the clathrate gun hypothesis. Geology, v. 32, p. 53–56. doi: 10.1130/G20114.1

Maslin, M., Vilela, C., Mikkelsen, N., Grootes, P., 2005, Causes of catastrophic sediment failures of the Amazon Fan. Quaternary Science Reviews v. 24, p. 2180-2193.

Migeon S., 2000, Dunes géantes et levées sédimentaires en domaine marin profond: approche morphologique, sismique et sédimentologique PhD Thesis, Univ. Bordeaux 1, 288 p.

Mayall, M., Stewart I., 2000, The architecture of turbidite slope channels. In: Weimer P, Slatt RM, Coleman JL, Rosen N, Nelson CH, Bouma AH, Styzen M, Lawrence DT (eds) Global Deep-Water Reservoirs: Gulf Coast Section-SEPM Bob F. Perkins 20th Annual Research Conference. p. 578-586.

Mayall, M., Jones, E., Casey, M., 2006, Turbidite channel reservoirs—key elements in facies prediction and effective development. Marine and Petroleum Geology, v. 23, p. 821–841.

McHargue, T.R., Webb, J.E., 1986, Internal geometry, seismic facies and petroleum potential of canyons and inner fan channels of the Indus Submarine Fan. AAPG Bulletin, v. 70, p. 161–180.

Métivier, F., Lajeunesse, E., Cacas, M., 2005, Submarine canyons in the bathtub: Journal of Sedimentary Research, v. 75, p. 6–11.

Mitchell, N.C., 2006, Morphologies of knickpoints in submarine canyons. Geological Society of America Bulletin, v. 118, no. 5–6, p. 589–605.

Moscardelli, L., Wood, L.J., 2008, New classification system for mass transport complexes in offshore Trinidad: Basin Research, v. 20, no. 1, p. 73-98, doi: 10.1111/j1365-2117.2007.00340x [26 p.].

Mulder, T., Syvitski, J.P.M.,1995, Turbidity currents generated at river mouths during exceptional discharges to the world oceans. Journal of Geology, v. 103, p. 285–299.

Mulder, T., Syvitski, J.P.M., Migeon, S., Faugeres J.C., Savoye B., 2003, Marine hyperpycnal flows: Initiation, behavior and related deposits: A review: Marine and Petroleum Geology, v. 20, p. 861–882.

Muñoz, J., 1966, Turbiditas en sedimentos profundos de la cuenca oceanica de Colombia e influencia del Río Magdalena. Geos, no. 15, p. 7-101.

Normark, W.R., Carlson, P.R., 2003, Giant submarine canyons: is size any clue to their importance in the rock record?. In: Chan M.A. and Archer A.W., eds, Extreme Depositional Environments: Mega End Members in Geologic Time: Boulder, Colorado, Geol. Soc. Am., Special Paper, v. 370, p. 170–190.

O'Byrne, C.J., Prather, B.E., Pirmez, C., Steffens, G.S., 2004, Reservoir Architectural Styles across Stepped Slope Profiles: Implications for Exploration, Appraisal and Development AAPG International Conference and Exhibition, Cancun, Mexico 2004.

Pelzhen, Z., Molnar P., Downs W., 2001, Increased sedimentation rates and grain sizes 2-4 Myr ago due to the influence of climatine on erosion rates. Nature, v. 410, p. 892-897.

Piper, D.J.W., Normark, W.R., 1983, Turbidite depositional patterns and flow characteristics, Navy submarine fan, California Borderland. Sedimentology, v. 30, p. 681–694.

Piper, D.J.W., Shor A.N., Hughes-Clarke J.E., 1988, The 1929 “Grand Banks” Earthquake, slump and turbidity current, in H. E. Clifton, ed., Sedimentologic consequences of convulsive geologic events: GSA Special Paper 229, p. 77-92.

Pirmez, C., Breen, N.A., Flood, R.D., O’Connell, S., Jacobi, R.D., Ladd, J.W., Westbrook, G., Franco, J.V., Garzon, M., Arias-Isaza, F.A., 1990, Gloria Mosaic of the Magdalena Deep-Sea Fan, Northern Colombian Convergent Margin. Meeting Abstract .AAPG Bulletin, v. 74, no. 5, p. 741–741.

Pirmez, C., Flood, R.D., 1995, Morphology and structure of Amazon Channel. In: Flood, R.D., Piper, D.J.W., Klaus, A., et al., Proc. ODP, Int Repts., v.155, Ocean Drilling Program, College Station, TX, p. 23-45.

Pirmez, C., Beaubouef R.T., Friedmann, S.J., 2000, Equilibrium profile and base level in submarine channels: Examples from Late Pleistocene systems and implications for the architecture of deepwater reservoirs, in Weimer P., Slatt R. M., Coleman J. L., Rosen N., Nelson C. H., Bouma A. H., Styzen M., and Lawrence D. T., eds., Global Deep-Water Reservoirs: Gulf Coast Section SEPM Foundation 20th Annual Bob F. Perkins Research Conference, p. 782-805.

Posamentier, H.W. Meizarwin, Wisman P.S., Plawman, T., 2000, Deep water depositional systems-ultra-deep Makassar Strait, Indonesia, in Weimer P., Slatt R. M., Coleman J. L., Rosen N., Nelson C. H., Bouma A. H., Styzen M., and Lawrence D. T., eds., Global deep-water reservoirs: Gulf Coast Section–SEPM Foundation 20th Annual Bob F. Perkins Research Conference, p. 806–816.

Posamentier, H. W., and Kolla, V., 2003, Seismic geomorphology and stratigraphy of depositional elements in deepwater settings: Journal of Sedimentary Research, v. 73, p. 367–388.

Prather, B.E., 2003, Controls on reservoir distribution, architecture and stratigraphic trapping in slope settings. Marine and Petroleum Geology, v. 20, no. 6–8, 529–545.

Prell, W.L., 1978, Upper Quaternary sediments of the Colombia Basin: Spatial and stratigraphic variation. Geological Society of America Bulletin, v. 89, p. 1241-1255.

Pujos, M., Pagliardini, J.L., Steer, R., Vernette, G., Weber, O., 1986, Influencia de la contra-corriente norte colombiana para la circulación de las aguas en la plataforma continental su acción sobre la dispersión de los efluentes en suspensión del río Magdalena. Boletin Cientifico CIOH, v. 6, p. 3-15.

Pujos, M., Javelaud, O., 1991, Depositional facies of a mud shelf between the Sinú River and the Darien Gulf (Caribbean coast of Colombia): environmental factors that control its sedimentation and origin of deposits, Continental Shelf Research, v. 11, no.7, p. 601–623.

Reading, H.G., Richards, M., 1994, Turbidite systems in deepwater basin margins classified by grain size and feeder system. AAPG Bulletin, v. 78, p. 792-822.

Restrepo J.D., Kjerfve, B., 2000, Magdalena River: interannual variability (1975–1995) and revised water discharge and sediment load estimates, Journal of Hydrology , v. 235, p. 137–149.

Restrepo JD, Syvitski J.P.M., 2006, Assessing the Effect of Natural Controls and Land Use Change on Sediment Yield in a Major Andean River: The Magdalena Drainage Basin, Colombia. AMBIO: A Journal of the Human Environment: v. 35, no. 2, p. 65–74.

Restrepo J.D., Lopez S.A., 2007, Morphodynamics of the Pacific and Caribbean deltas of Colombia, South America, Journal of South American Earth Sciences, v. 25, no. 1, p. 1-21.

Reyes, G. A., Guzmán, G., Barbosa, G., Zapata, G.,2001, Geología de las planchas 23 Cartagena y 29-30 Arjona. Memoria Explicativa. Ingeominas, Ministerio de Minas y Energía, Colombia.

Ruiz, C., Davis, N., Bentham, P., Price, A., Carvajal, D., 2000, Structure and Tectonic evolution of the South Caribbean Basin, southern offshore Colombia: A progressive accretionary system, Memorias VII Simposio Bolivariano, Exploración Petrolera en las Cuencas Subandinas, Sociedad Venezolana de Geólogos, Caracas, September 2000, p 334–355.

Shepard, F.P., 1973, Sea floor off the Magdalena Delta and Santa Marta Area, Colombia. Geological Society of America bulletin, v. 84, p. 1955–1972.

Shipley, T.H., Houston, M.H., Buffler, R.T., Shaub, F.J., McMillen K.J., Ladd J.W., Worzel J.L., 1979, Seismic Evidence for Widespread Possible Gas Hydrate Horizons on Continental Slopes and Rises. AAPG Bulletin, v. 63, no. 12, p. 2204-2213.

Smith R., 2004, Silled sub-basins to connected tortuous corridors: sediment distribution systems on topographically complex sub-aqueous slopes, in: Lomas, S.A., Joseph P. eds. Confined Turbidite Systems, Geological Society of London, Special Publications, v. 222, p. 23-43.

Somers, M.L., Carson, R.M., Revie, J.A., Edge, R.H., Barrows, B.J., Andrews, A.G., 1978, GLORIA II-an improved long range sidescan sonar, in Processings of the Institute of Electrical Engineering on Offshore Instrumentation and Communications, Oceanology International Technical Session J: London, BPS Publications Ltd., p.16-24.

Soyinka, O.A. Slatt R.M., 2008, Identification and micro-stratigraphy of hyperpycnites and turbidites in Cretaceous Lewis Shale, Wyoming. Sedimentology. doi: 10.1111/j.1365-3091.2007.00938.x

Sylvester, Z., Deptuck, M., Prather, B., Pirmez, C., O'Byrne, C., submitted, Seismic stratigraphy of a shelf-edge delta and linked submarine channels in the NE Gulf of Mexico, in: Application of Seismic Geomorphology Principles to Continental Slope and Base-of-slope Systems: Case Studies from Seafloor and Near-Seafloor Analogues, SEPM Special Publication.

Vernette, G., Mauffret, A., Bobier, C., Briceno, L., Gayet, J., 1992. Mud diapirism, fan sedimentation and strike-slip faulting, Caribbean Colombia Margin, Tectonophysics, v. 202, p. 335-349.

Trenkamp, R., J.N. Kellogg, J.T. Freymueller, and H.P. Mora, 2002, Wide plate margin deformation, southern Central America and northwestern South America, CASA GPS observations: Journal of South American Earth Sciences, v. 15, p. 157-171.

Weimer, P., and Slatt, R.M., 2007, Introduction to the Petroleum Geology of Deepwater Settings, AAPG Studies in Geology 57. AAPG Datapages Discovery Series 8, 816 p.

Wetzel, F.C., 1993. The transfer of river load to deep-sea fans: A quantitative approach. AAPG Bulletin, v. 77, p. 1679-1692.

Winkley, B.R., Ordonez, J.E. Saenz, Duque, R., 1994, The Magdalena River, Colombia. Chapter 7 in: The variability of large alluvial rivers. Ed. Schumm S.A. and Winkley B.R. American Society of Civil Engineers, p. 139-160

Wood L.J., Mize-Spansky K.L., 2009, Quantitative seismic geomorphology of a Quaternary leveed-channel system, offshore eastern Trinidad and Tobago, northeastern South America. AAPG Bulletin, v. 93, p.101-125

YU, B., Cantelli, A., Marr, J., Pirmez, C., O'byrne, C., Parker, G., 2006, Experiment on self-channelized subaqueous fans emplaced by turbidity currents and dilute mudflows. Journal of Sedimentary Research, 2006, v. 76, p. 889–902. Research Article DOI: 10.2110/jsr.2006.069.

APPEDIX 1

CORE DESCRIPTION

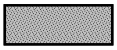
Core location

Core	Basal age	Core length	Date julian day	Latitude	Longitude	TW Length	Type	water depth m
RC11-239	Pleistocene	36	22-Oct-67	12N	75.483W	33	P	3301
RC7-15	Pleistocene	30	2-Oct-63	12.0666N	74.89999W	0	P	3612
RC13-146	Upper, Late Pleistocene	675	29-Jun-70	11.917N	75.03299W	40	P	3387
VM12-111	Pleistocene	457	21-Jul-57	11.467N	75.06702W	22	P	1853
VM12-112	Early, Lower Pleistocene	215	22-Jul-57	11.433N	75.10001W	0	P	2136
VM12-113	No age determined	650	22-Jul-57	11.183N	74.85001W	31	P	232
VM12-114	Pleistocene	575	23-Jul-57	12.15N	75.06702W	23	P	3601
VM12-115	Pleistocene	925	23-Jul-57	12.367N	75.21701W	34	P	3691
VM12-116	No age determined	1175	25-Jul-57	11.233N	74.29999W	18	P	357
VM12-117	No age determined	490	25-Jul-57	11.217N	74.767W	7	P	284
VM12-118	No age determined	735	26-Jul-57	11.4N	74.91699W	0	P	1430
VM12-119	No age determined	615	27-Jul-57	12.45N	74.5W	0	P	3862
RC13-148	Pleistocene	37	1-Jul-70	11.745N	74.2883W	32	P	1257

http://ingrid.ldgo.columbia.edu/SOURCES/.LDEO/.Deep_Sea_Core/

Core Legend


Gray sand


Silty lutite


Highly disturbed
Silt lutite and sand


Organic rich clay

Lenses


Gravel-pebbles


Foraminifera


Radiolaria


Pteropods


siliceous
spicules


Burrows


Slumps


Plant Fragments


Shell Fragments


Inclined layers

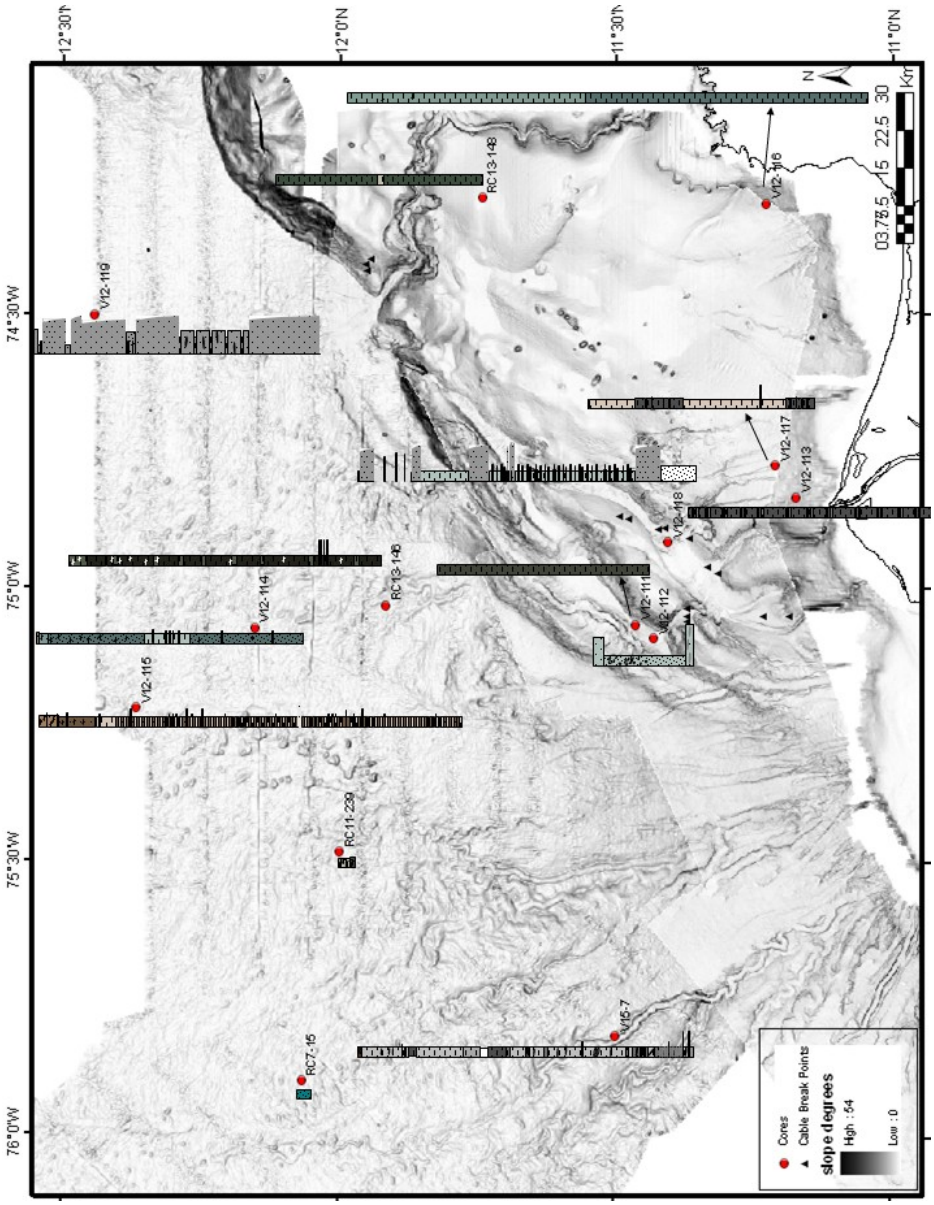

Contoured
laminae

G
Graded
Contact

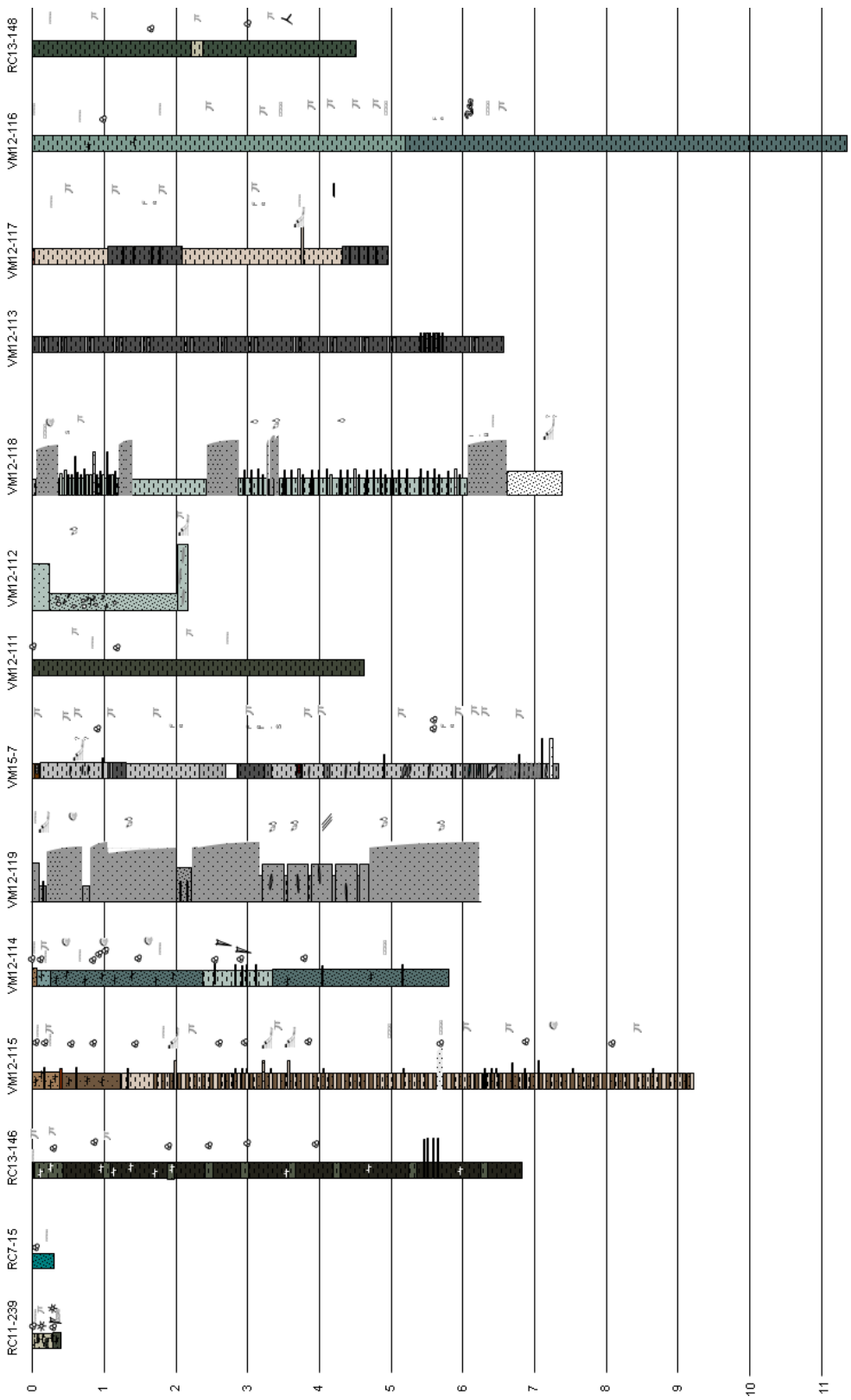

Manganese
micronodules

Fe
iron oxide

Colors: GSA Rock color chart

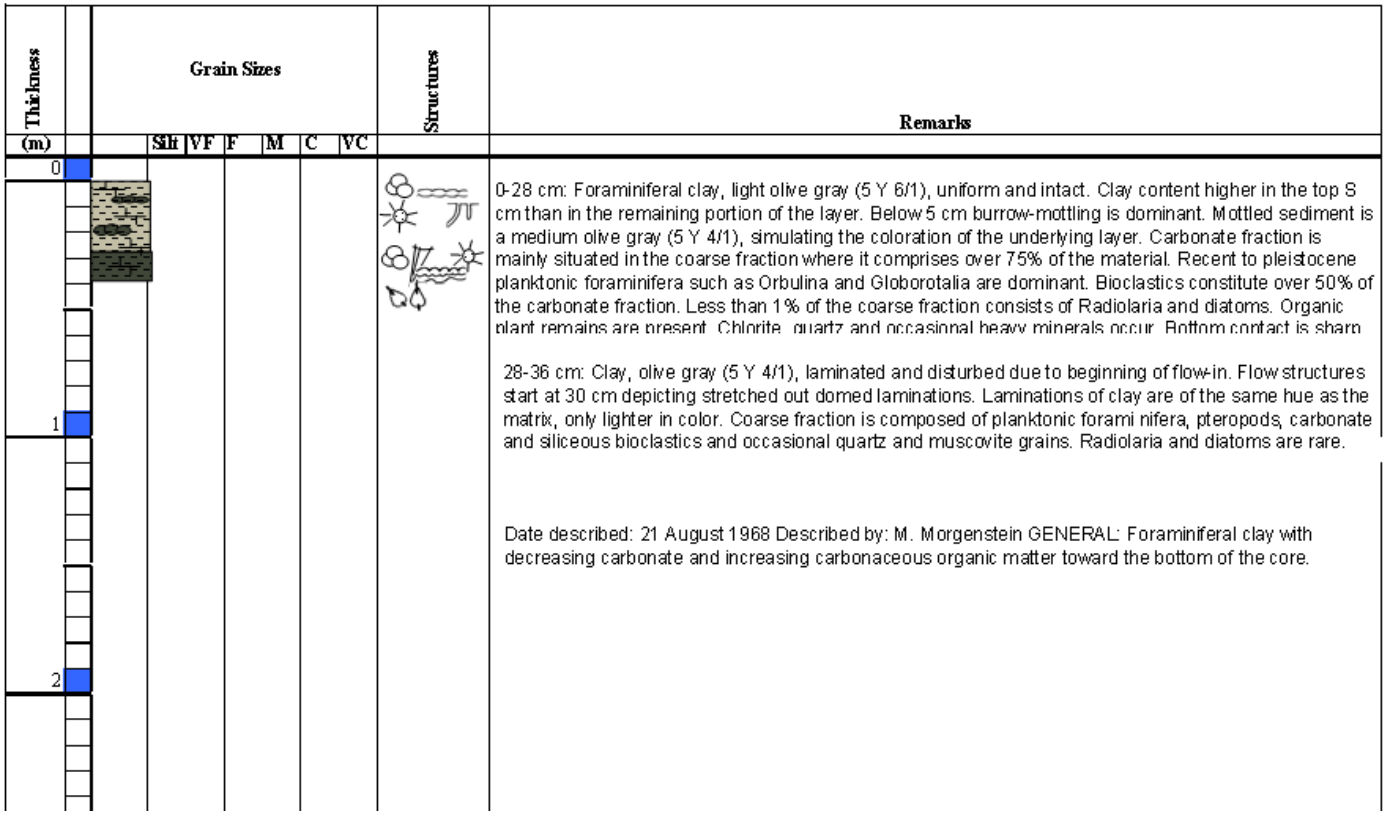


Location of Piston Cores in the Study area

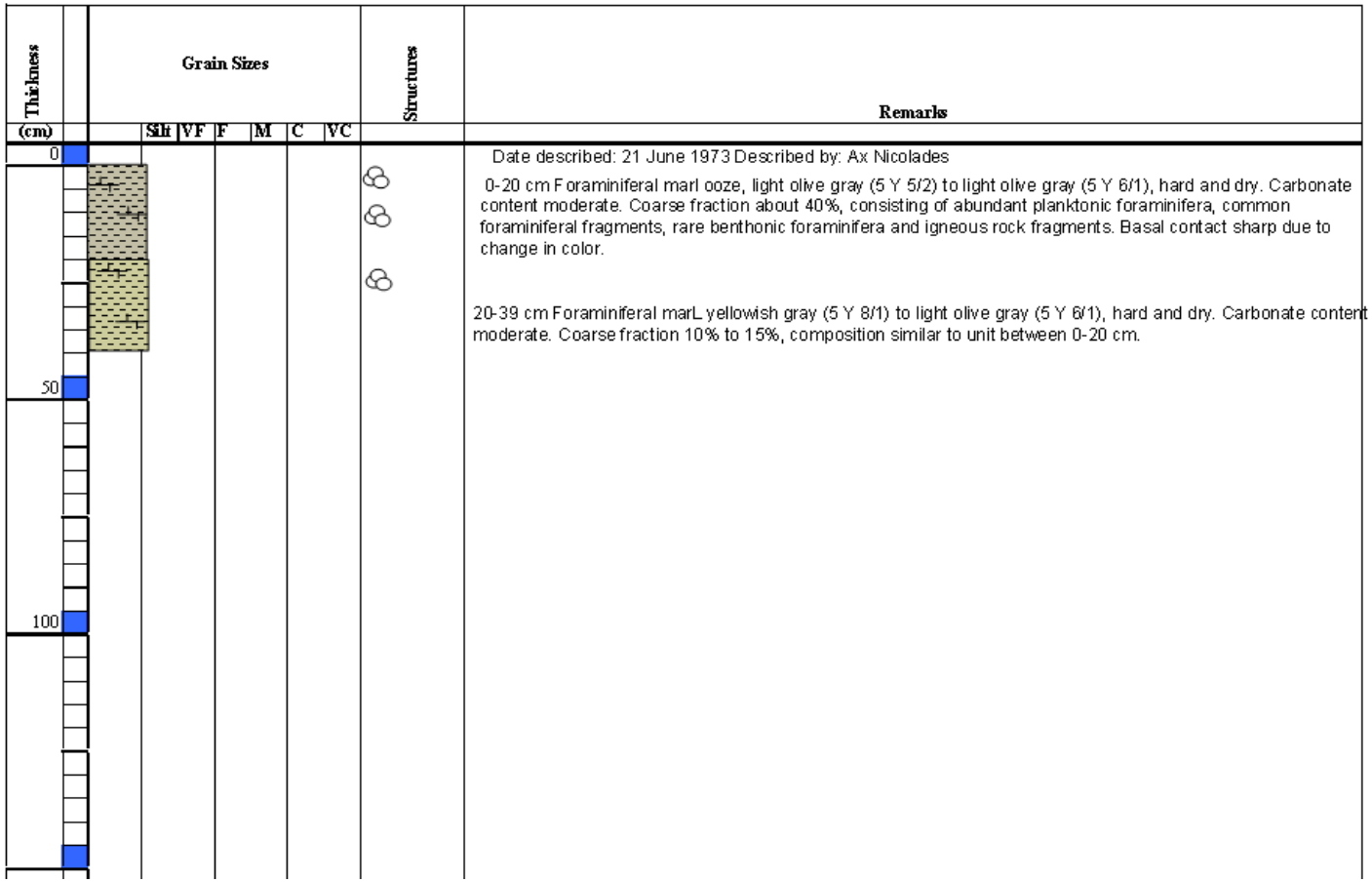


Cross Section of the Piston Cores in the Study area

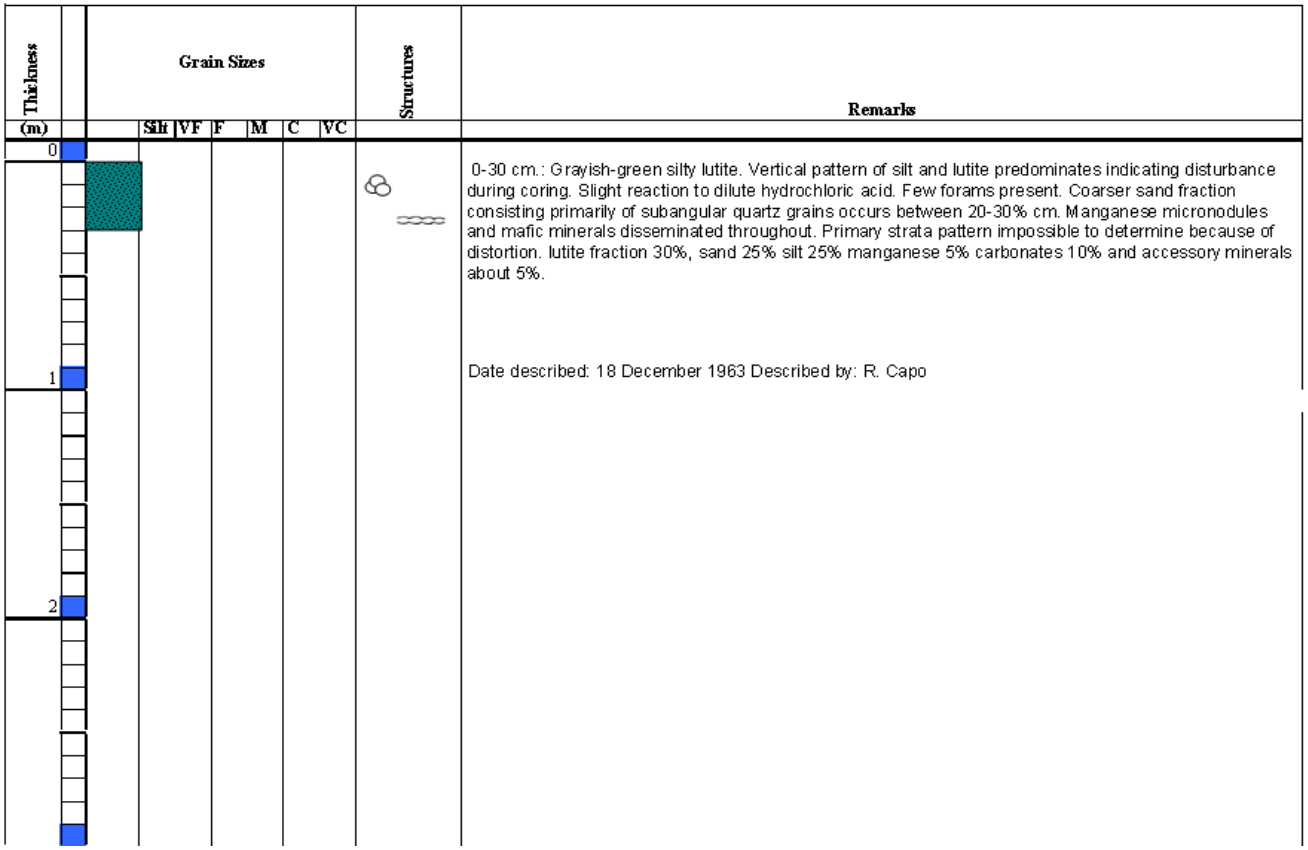
CORE RC11-239



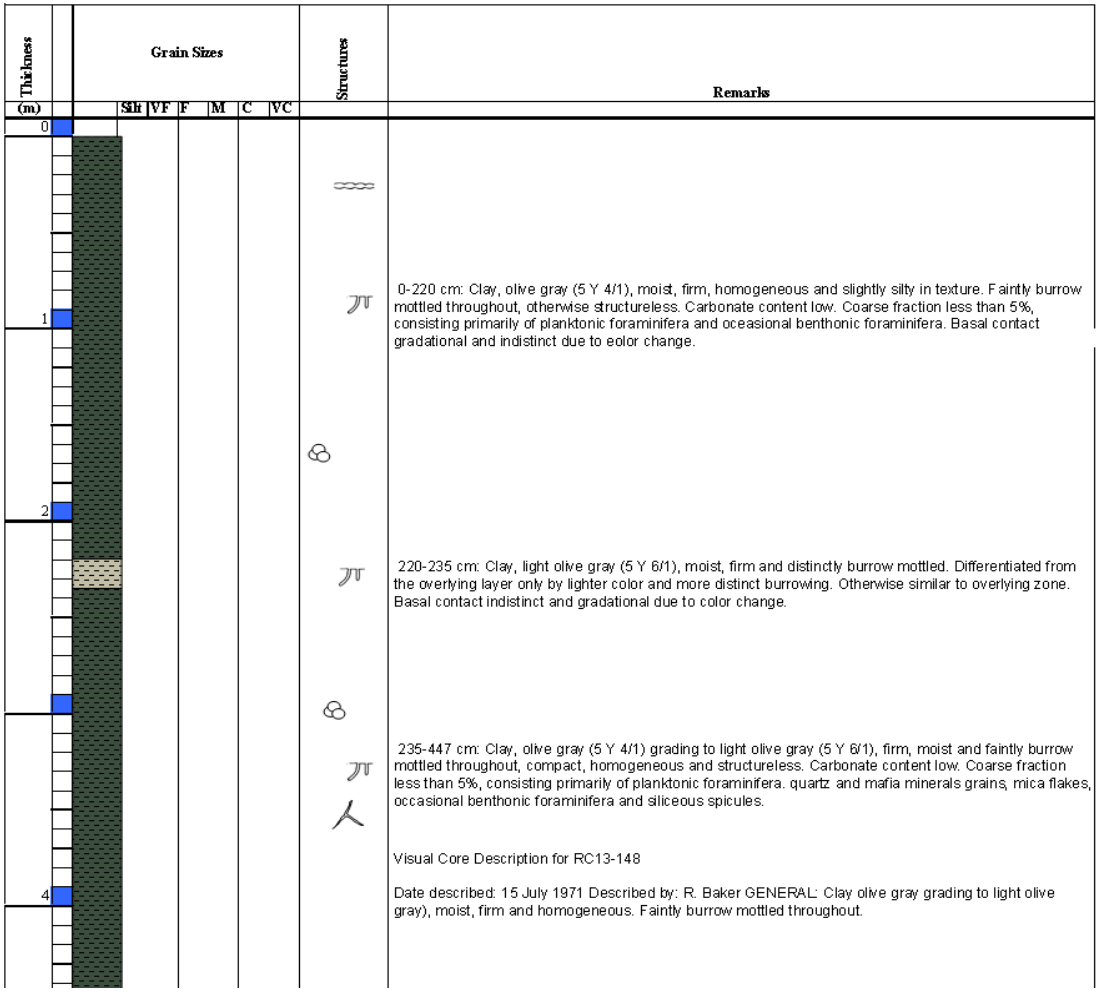
CORE RC11-239 TW (Trigger Weight)



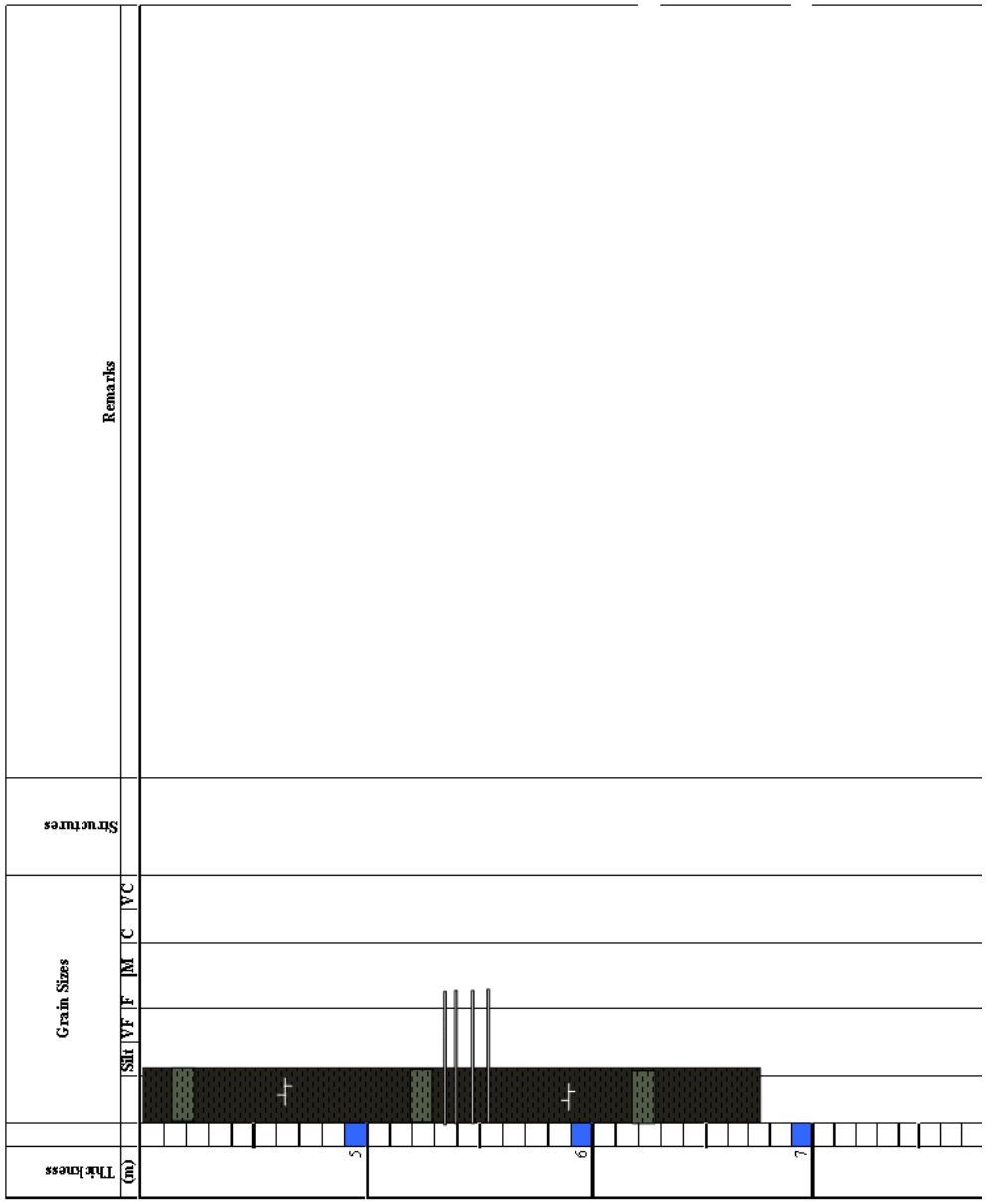
CORE RC7-15


Thickness
(m)
Grain Sizes
Silt
VF
F
M
C
VC
Structures
Remarks
0
1
2
0-30 cm.: Grayish-green silty lutite. Vertical pattern of silt and lutite predominates indicating disturbance during coring. Slight reaction to dilute hydrochloric acid. Few forams present. Coarser sand fraction consisting primarily of subangular quartz grains occurs between 20-30% cm. Manganese micronodules and mafic minerals disseminated throughout. Primary strata pattern impossible to determine because of distortion. lutite fraction 30%, sand 25% silt 25% manganese 5% carbonates 10% and accessory minerals about 5%.
Date described: 18 December 1963 Described by: R. Capo

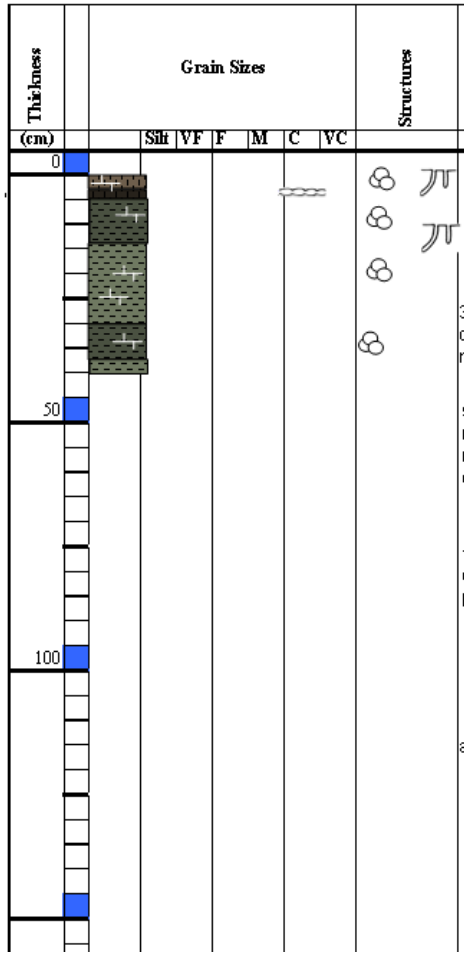
CORE RC13-146 (1)



CORE RC13-146 (2)

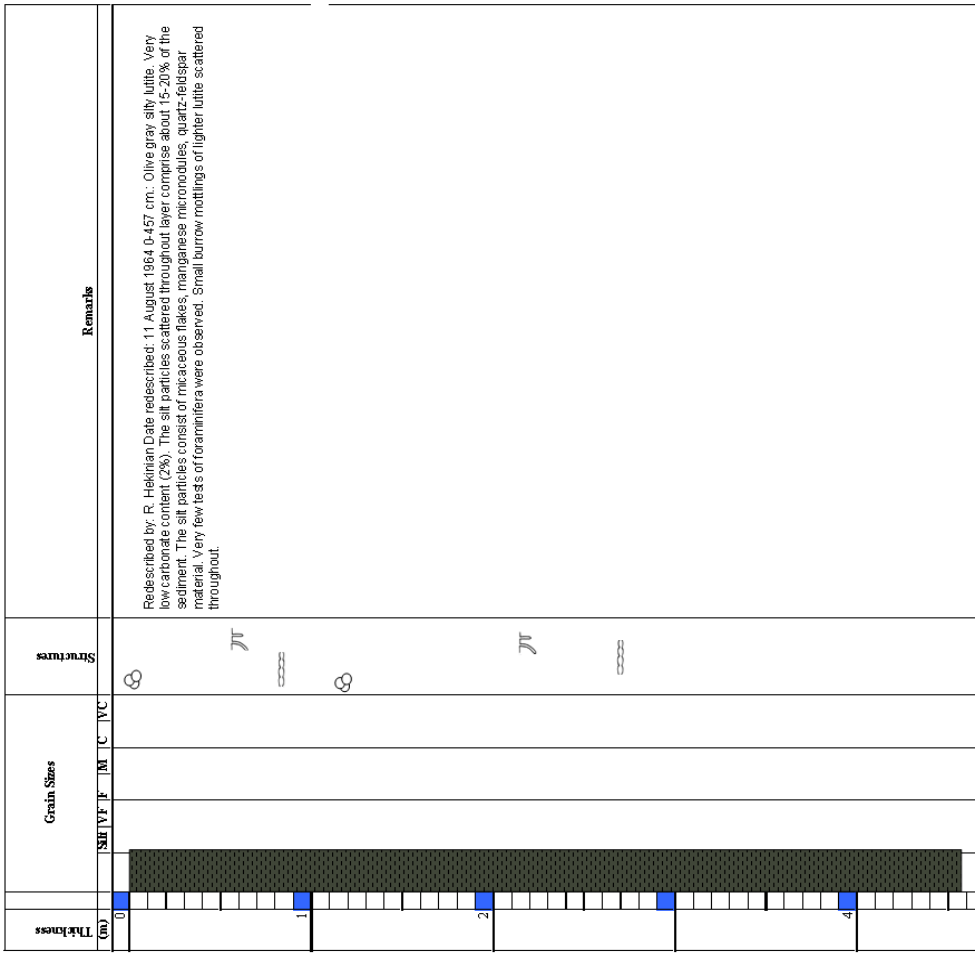


CORE RC13-146 TW

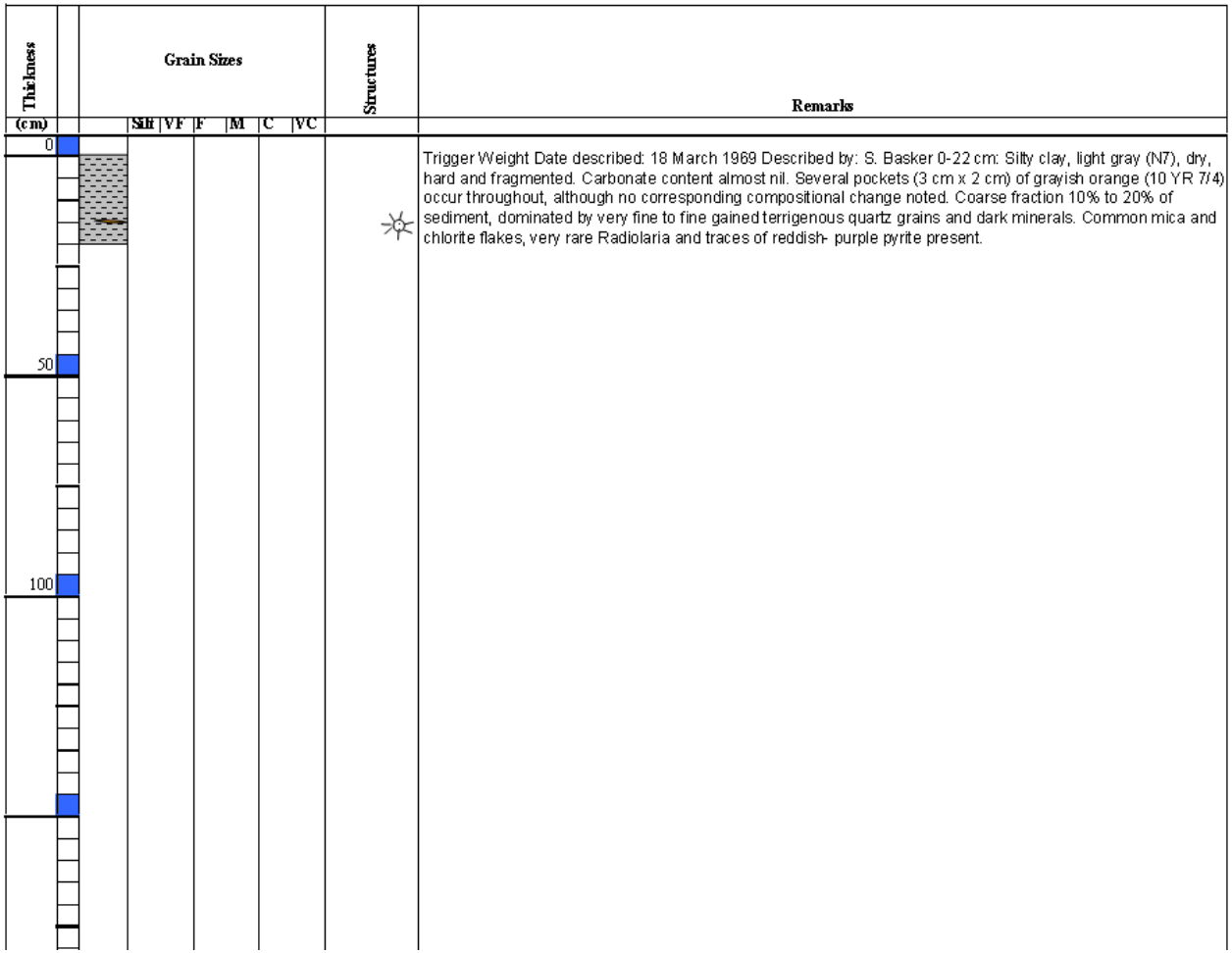


Remarks
CONRAD 13-146 TW Date described: 15 June 1971 Described by: R. Krauser 0-3 cm\Sandy foraminiferal marl, dark yellowish brown (10 YR 4/2) firm, moist and burrowed. Carbonate content moderate. Coarse fraction about 20% consisting of planktonic foraminifera fragments, quartz, chlorite, rare Radiolaria and rare dark minerals. Basal contact a sharp, burrowed eolor change.
3-5 cm Sandy foraminiferal marl, very dark yellowish brown (10 YR 3.5/2) firm, moist and burrowed. Carbonate content moderate. Coarse fraction about 10%, consisting of planktonic foraminifera, quartz, ehlorite and rare dark minerals. Basal contact a sharp color change.
5-14 cm Foraminiferal marl, moderate olive brown (5 Y 4.5/2), firm, moist and burrowed. Carbonate content moderate. Coarse fraction about 10%, Consisting of planktonie foraminifera and fragments (dominant), quartz, rare dark minerals and rare chlorite. A slightly ferruginous zone occurs at 12 cm. Basal contact a sharp, burrowed color change.
14-30 cm Foraminiferal marl, light olive gray (5 Y 5/2) firm, moist and burrowed. Carbonate content moderate. Coarse fraction about 20%ow consisting of planktonic foraminifera and fragments. Basal contact a sharp, burrowed color change.
30-37 cm Foraminiferal marl, moderate olive brown (5 Y 4.5/2) Similar to zone at 5-14 cm. Basal contact a sharp, burrowed color change.
37-40 cm Foraminiferal marl, light olive gray (5 Y 5/2) Similar to zone at 14- 30 cm. Note: Trigger core at 5-40 cm appears to correlate with top of piston core. Top 5 cm of piston core is missing.

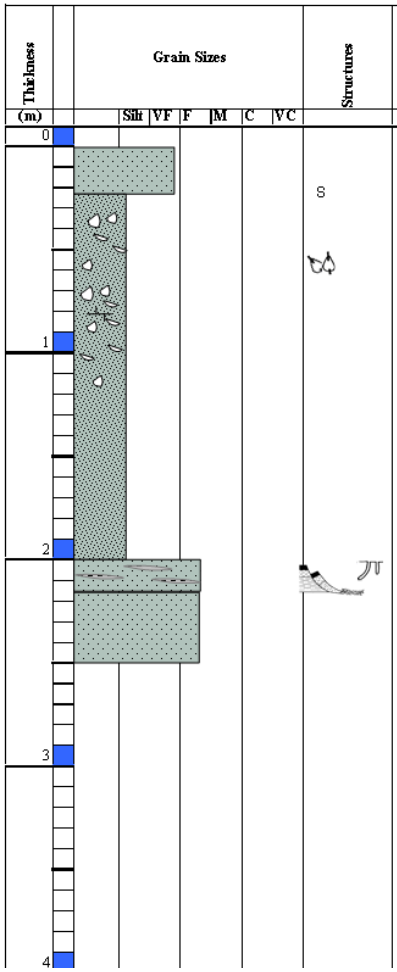
CORE VM12-111



CORE VM12-111 TW

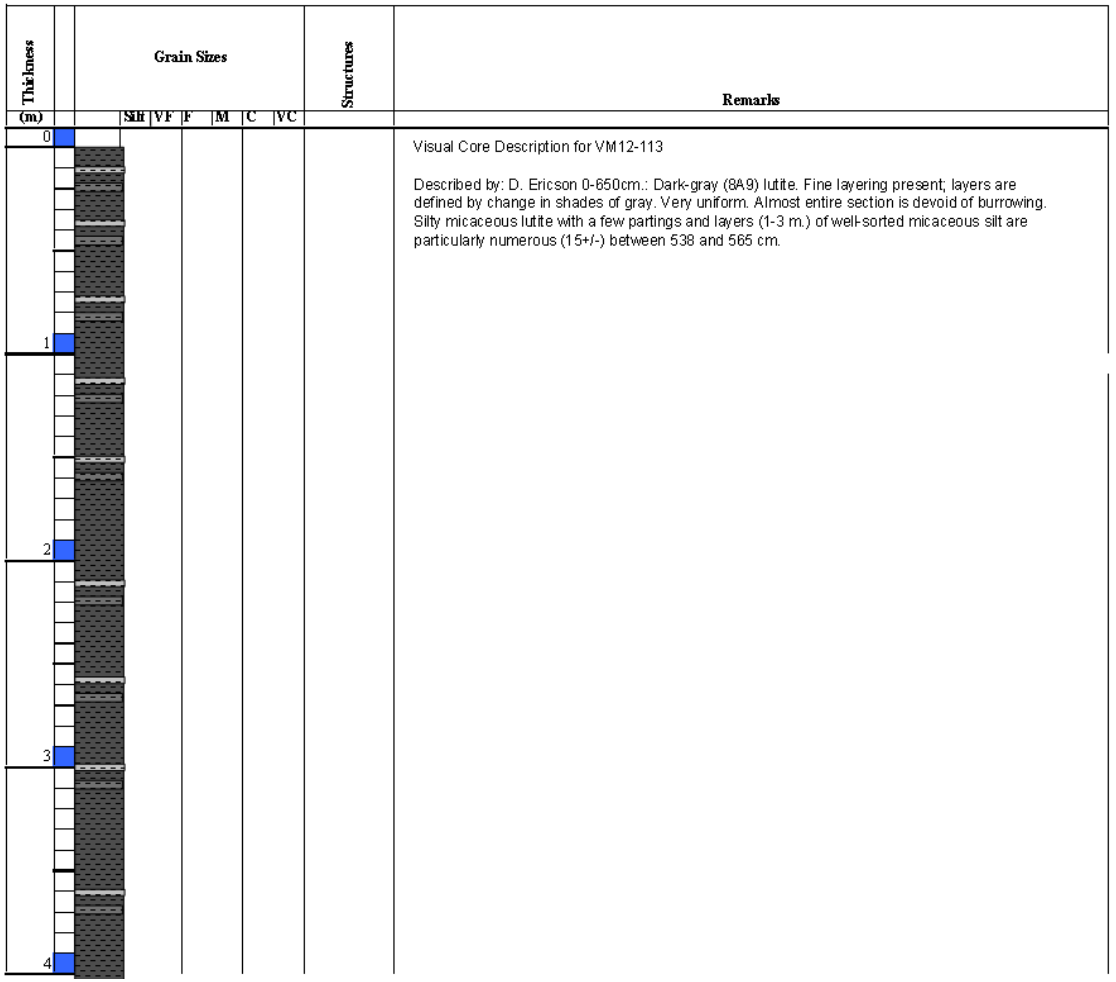


CORE VM12-112

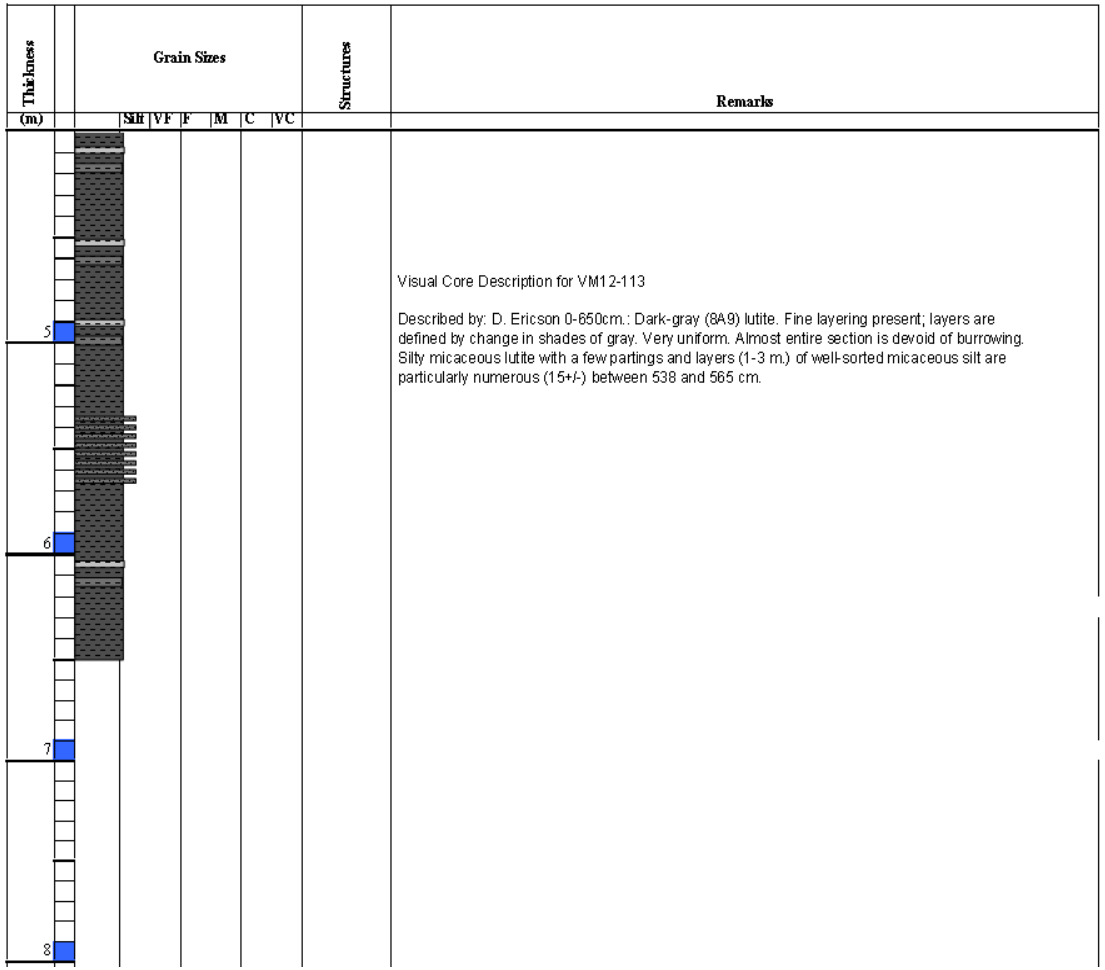


Remarks
0-23 cm.: Greenish-gray medium poorly sorted clastic sand mixed with ac cessory wood pieces and organic fragments. mineralogy of sand consists of abundant rounded quartz-feldspar grains, fairly common, glauconite and coarse flakes of mica. Pyroxene and dark fragments (may be rock) occur as accessory components. Sharp bottom contact due to textural change.
23-200 cm.: Greenish-gray unsorted silty lutite mixed with rounded gravel rock fragments, irregularly scattered throughout layer. These later decrease with depth. Silty lutite contains very low car bonate. No foraminifera were seen. Contact with the underlying layer is sharp due mainly to decrease to textural change
200-215 cm.: Very coarse sand with occasional light gray patches of lutite due probably to burrow mottlings and also slumpings. The sand consist of 70-80% rounded quartzofeldspathic grains and minor constituent of rounded rock fragments (igneous). This layer shows disturbance at bottom. Flow-in is from 215 to 245 cm.
Re-described by: R. Hekinian

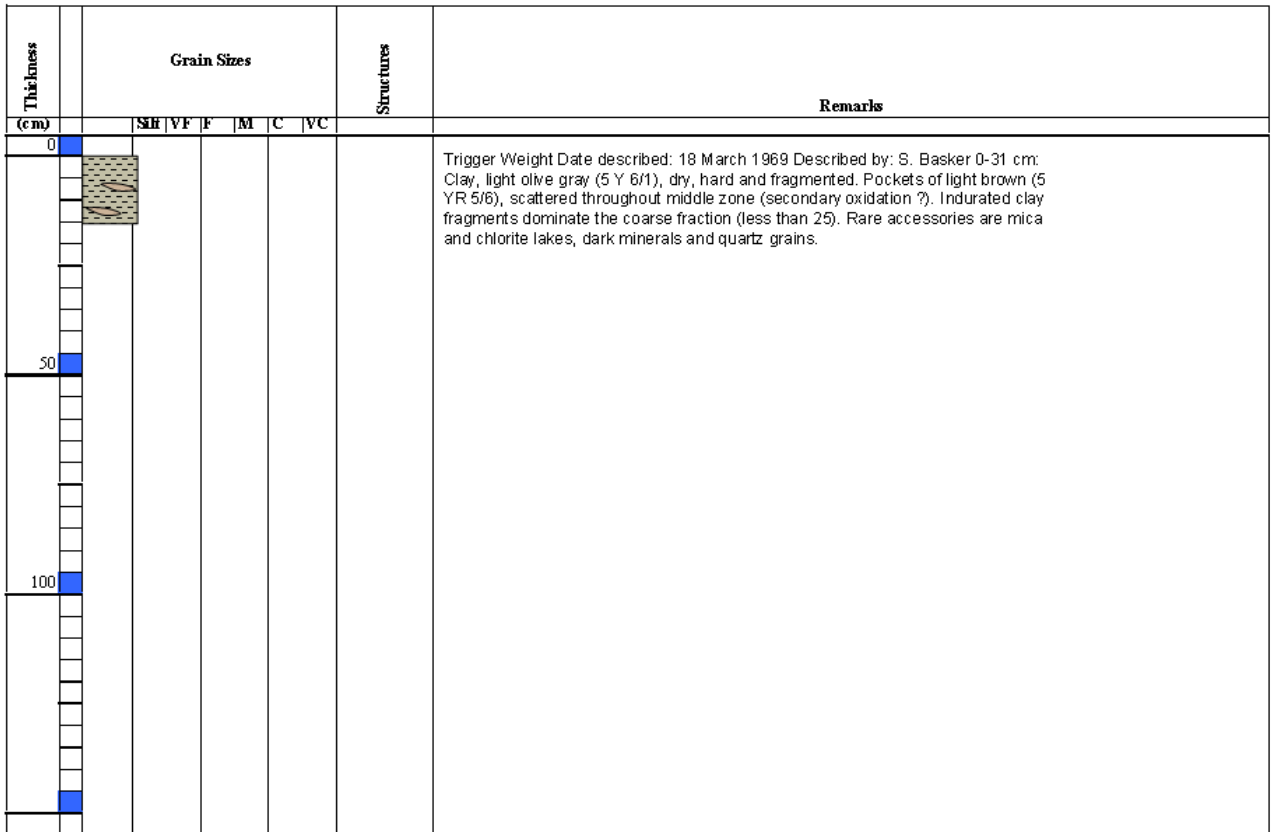
CORE VM12-113 (1)



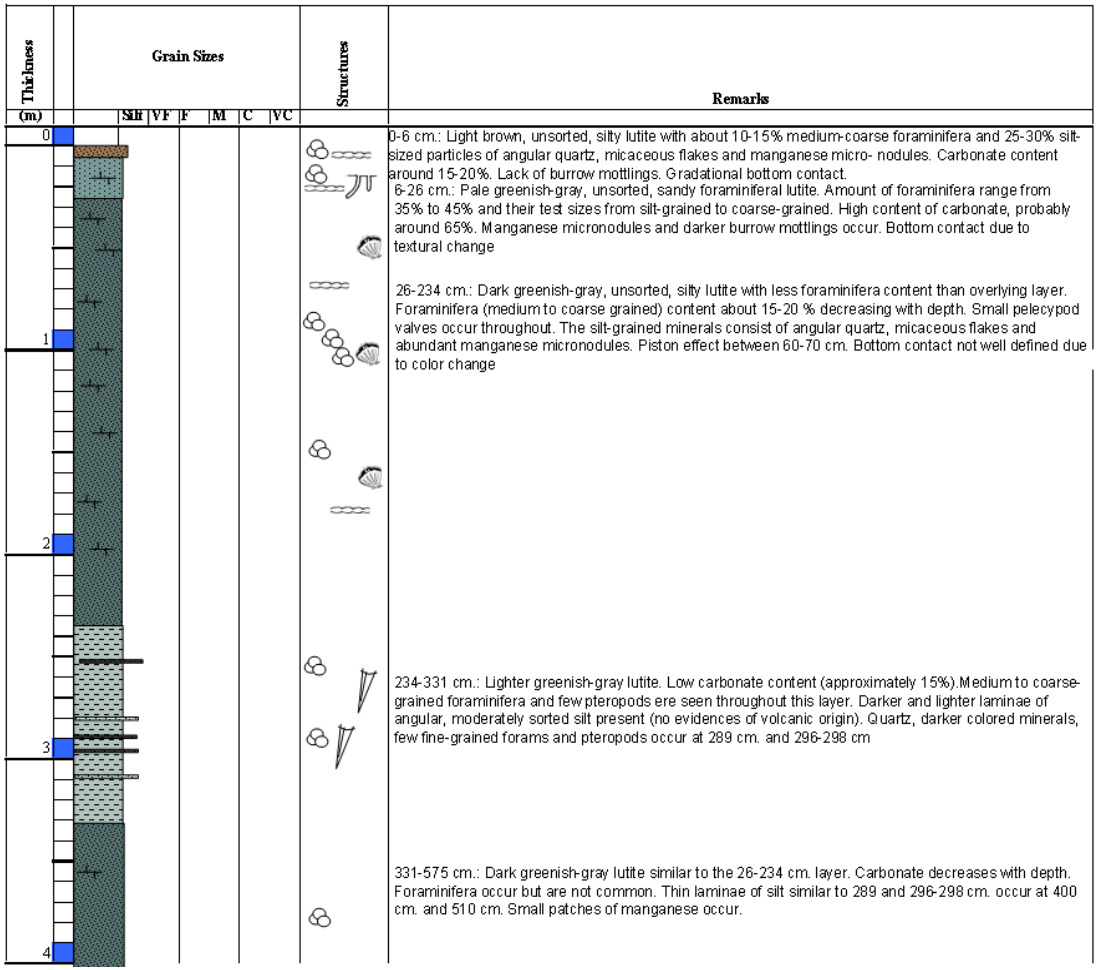
CORE VM12-113 (2)



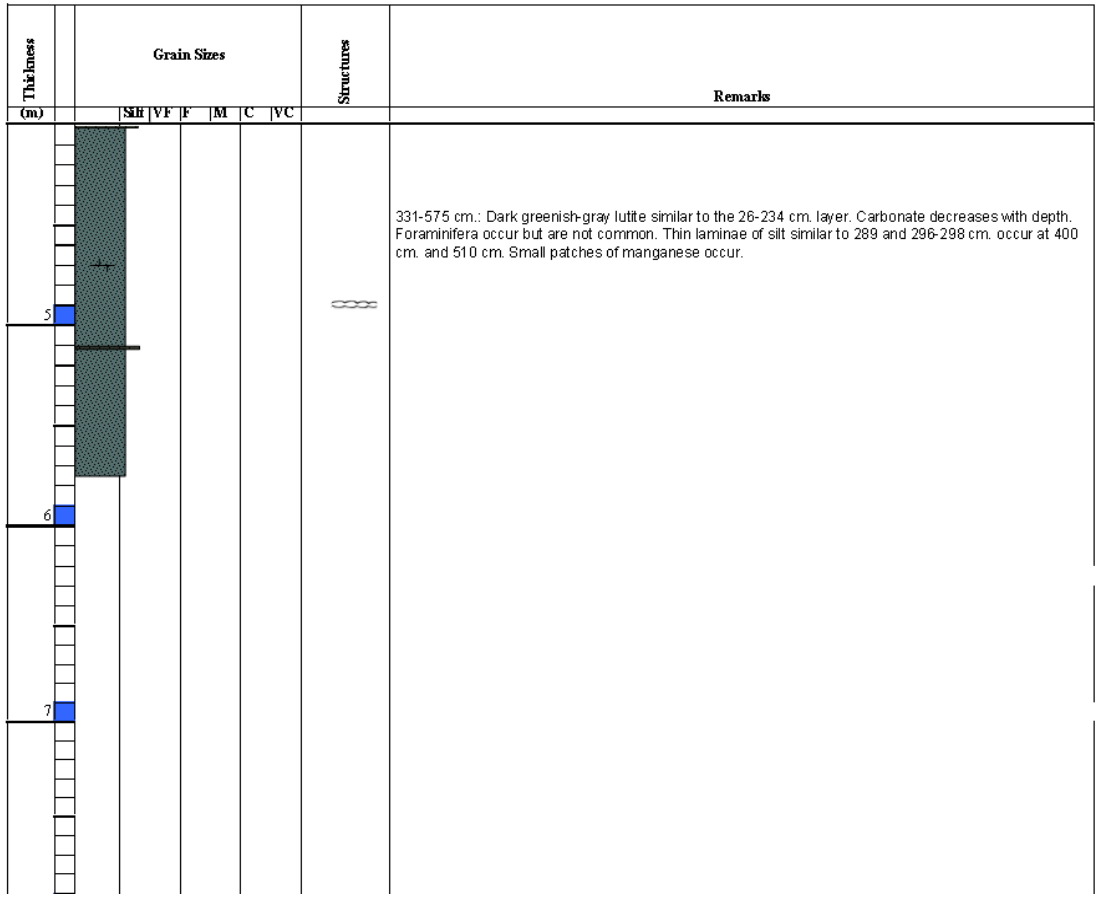
CORE VM12-113 TW



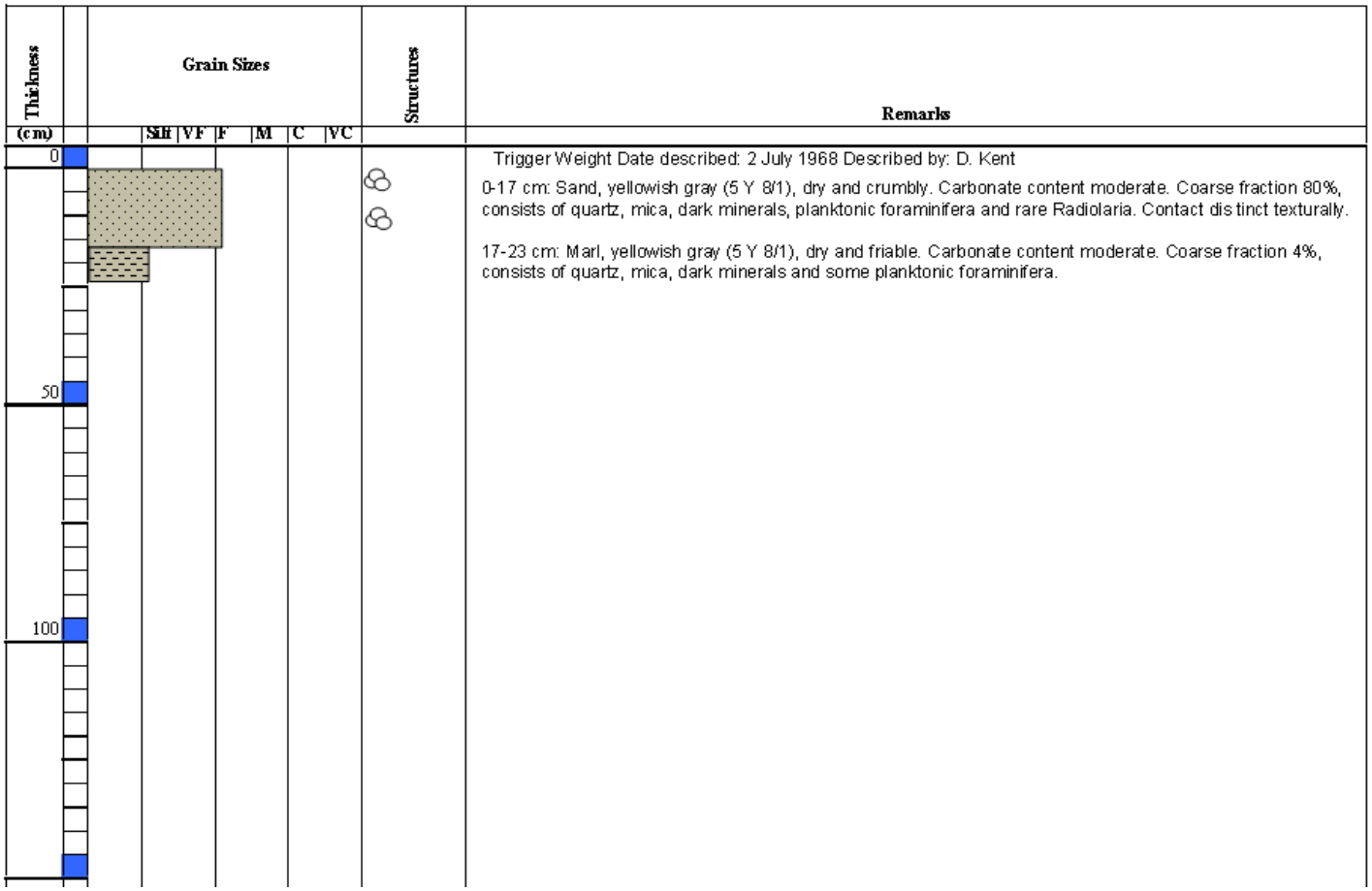
CORE VM12-114 (1)



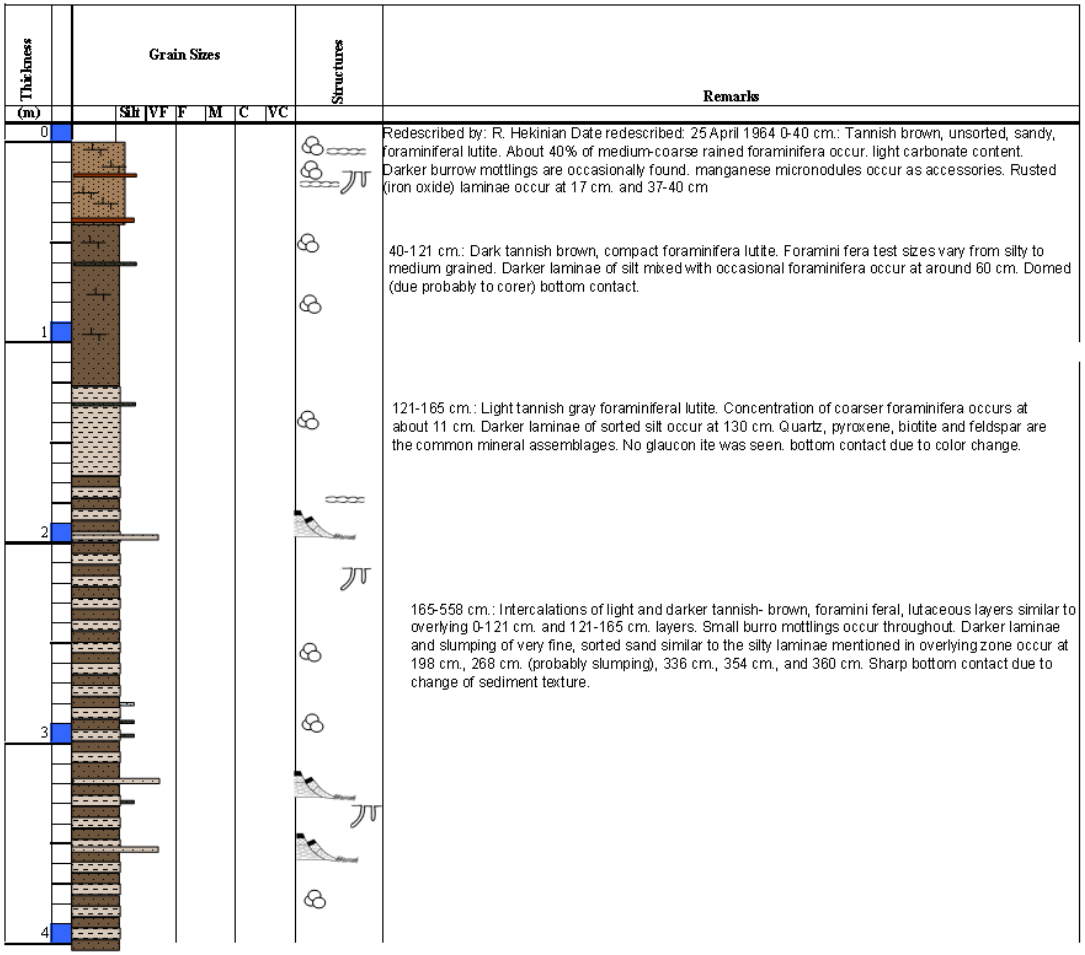
CORE VM12-114 (2)



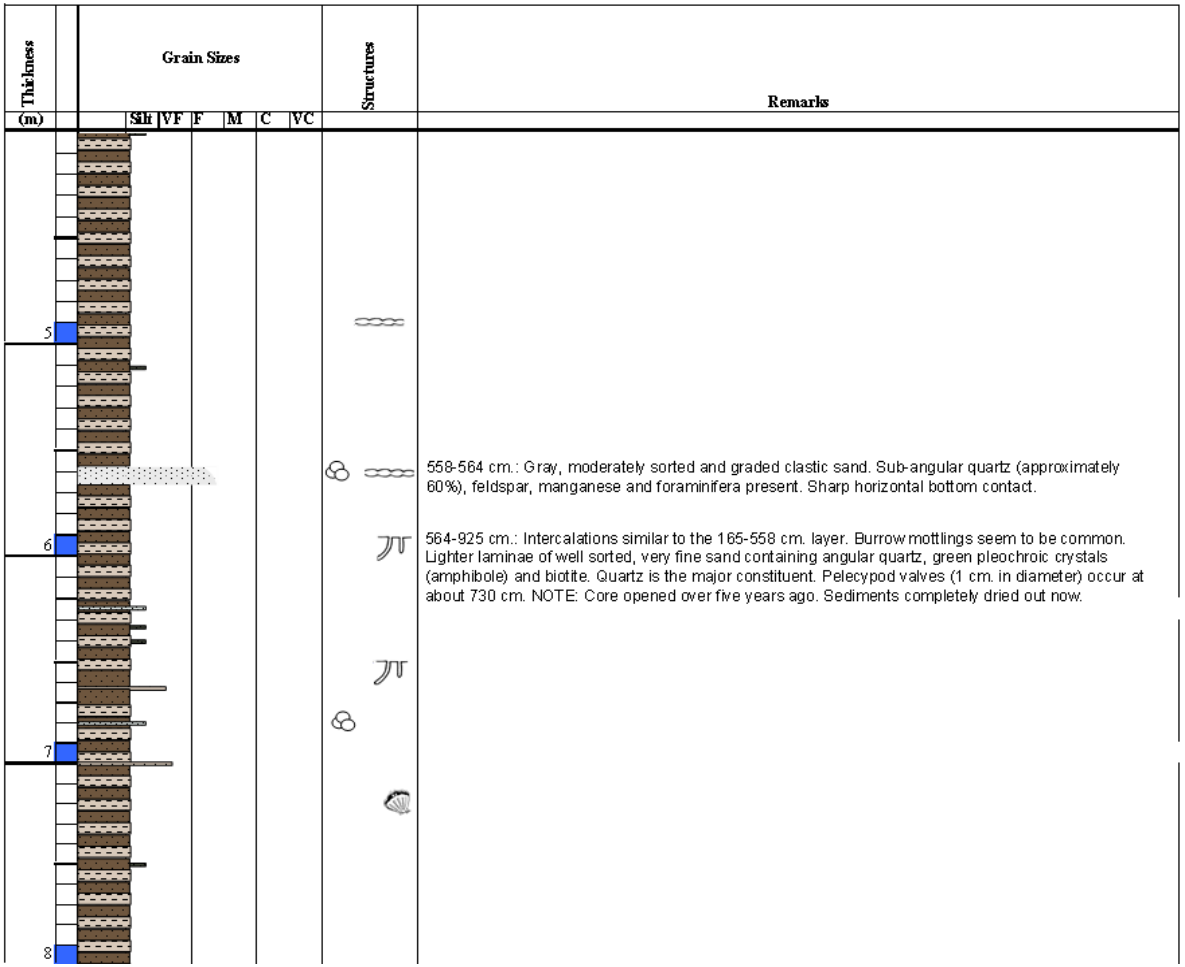
CORE VM12-114 TW



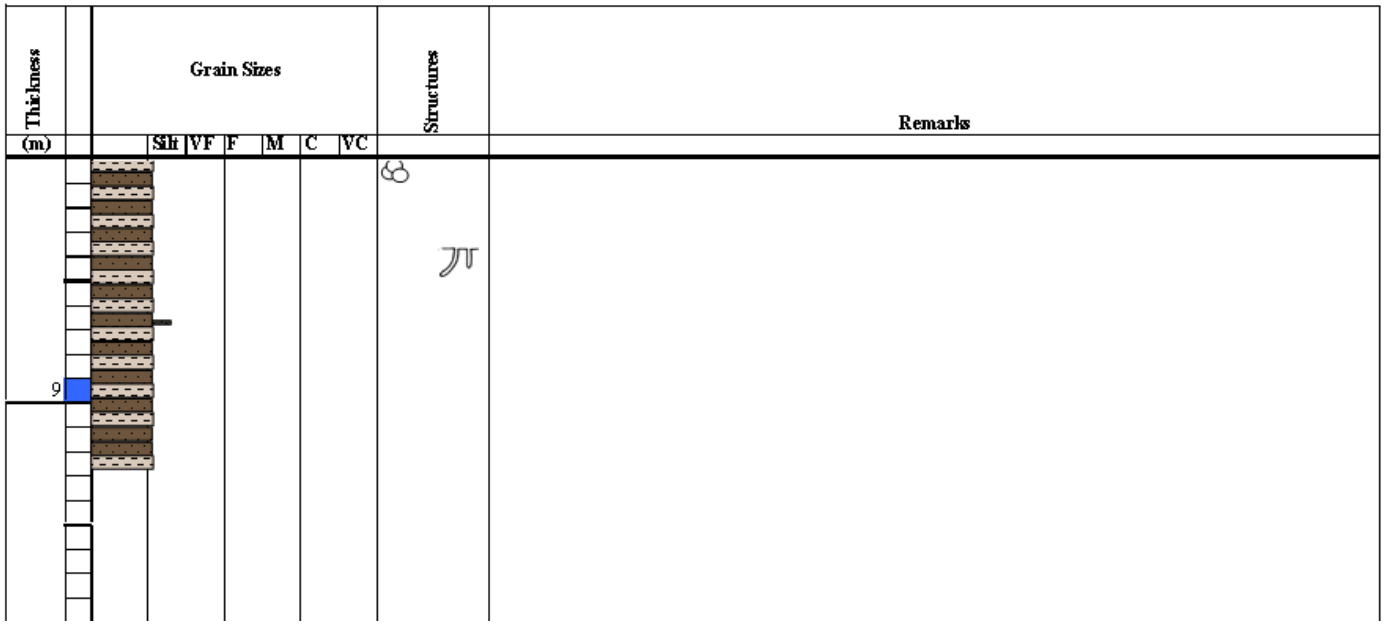
CORE VM12-115 (1)



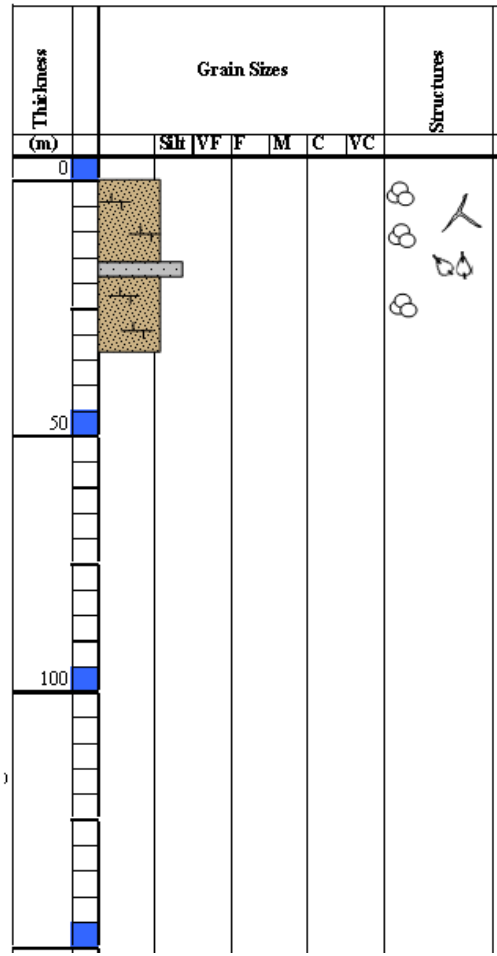
CORE VM12-115 (2)



CORE VM12-115 (3)



CORE VM12-115 TW



Remarks

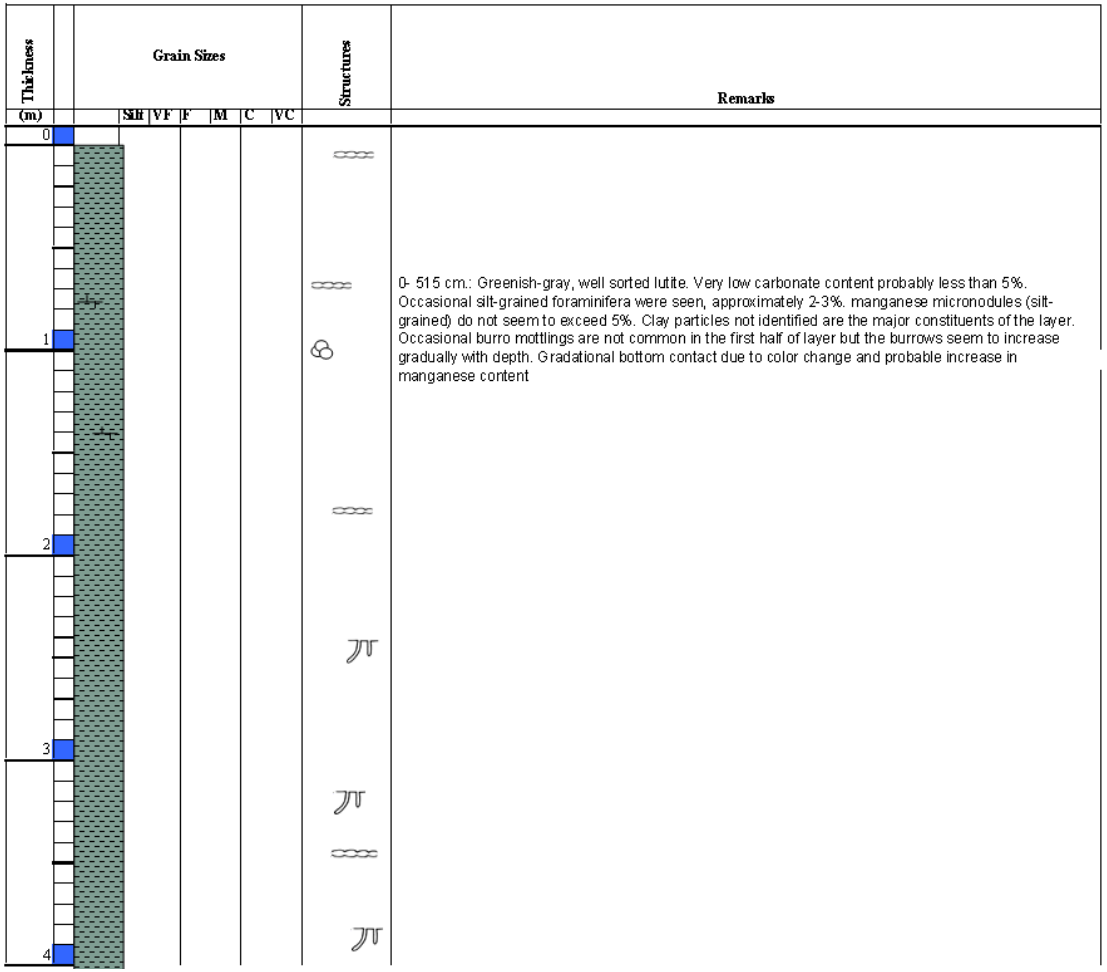
Trigger Weight Date described: 1 March 1969 Described by: S. Basker

0-16 cm: Foraminiferal marl, pale yellowish orange brown (10 YR 7/2), dry, firm, slightly friable and fragmented. Carbonate content high (70%). Coarse fraction contains planktonic foraminifera (dominant), benthonic foraminifera (common), rare to scarce dark minerals, rare basic igneous rock fragments, arenaceous foraminifera and traces of echinoid spines and sponge spicules. Basal contact gradational, based on color and lithological changes.

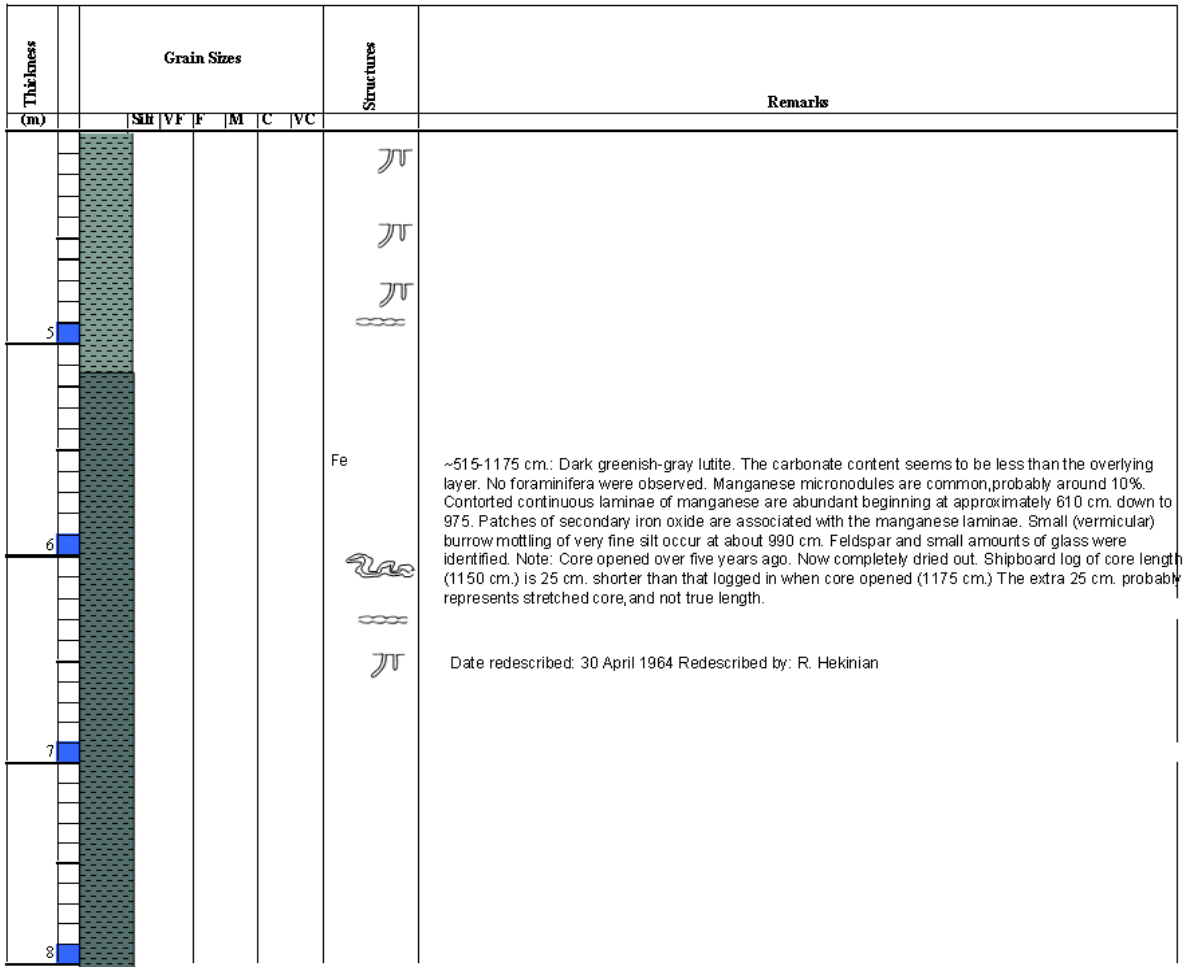
16-18 cmSilty clay, light gray (N7), dry, firm and fragmented. Carbonate content nil to very low. Coarse fraction less than 50%, con- sisting of plant debris, very common mica, chlorite, dark minerals and gypsum, rare quartz grains and traces of foraminifera. Basal contact sharp, defined by color and lithological changes.

18-34 cmForaminiferal marl, pale yellowish orange brown (10 YR 7/2), dry and very firm. Carbonate content high. Coarse fraction similar to 0-16 cm layer.

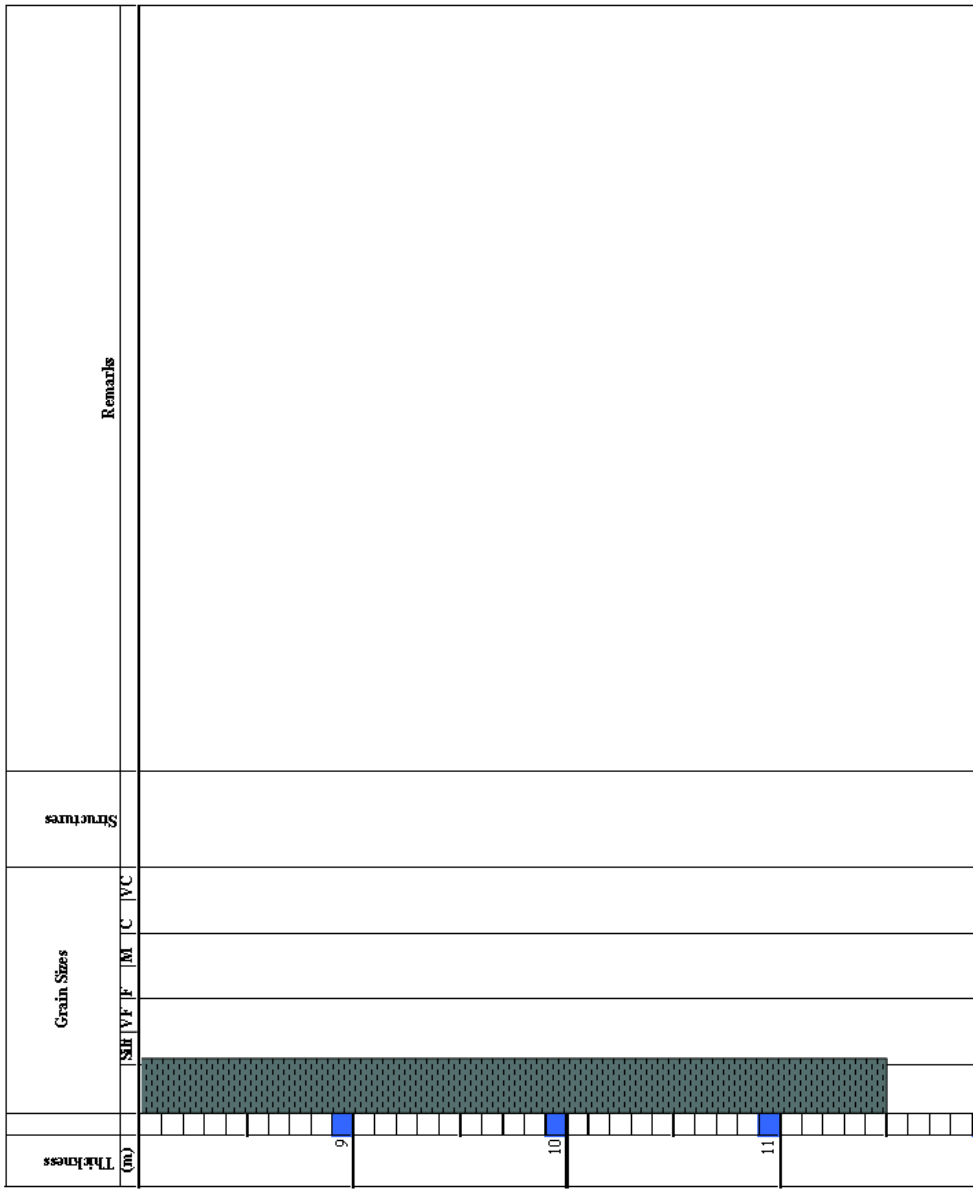
CORE VM12-116 (1)



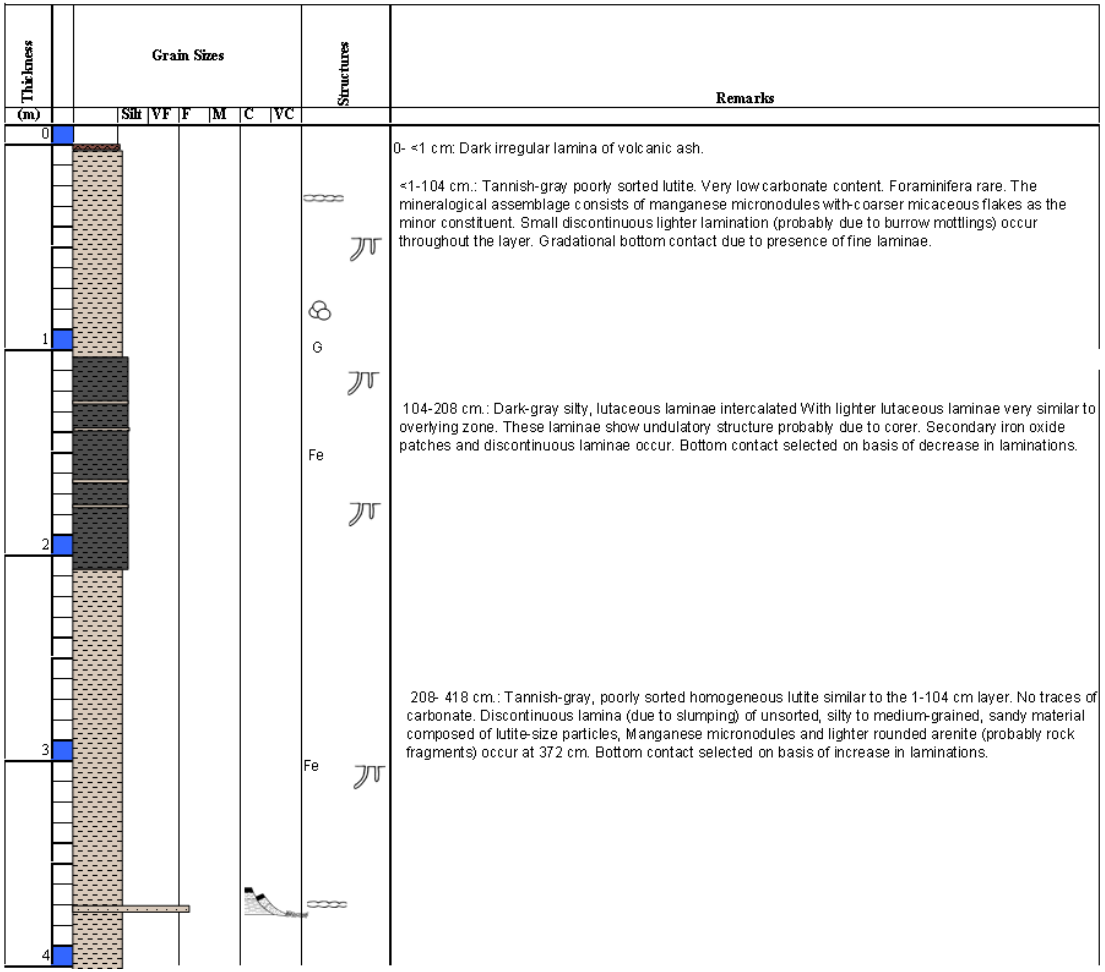
CORE VM12-116 (2)



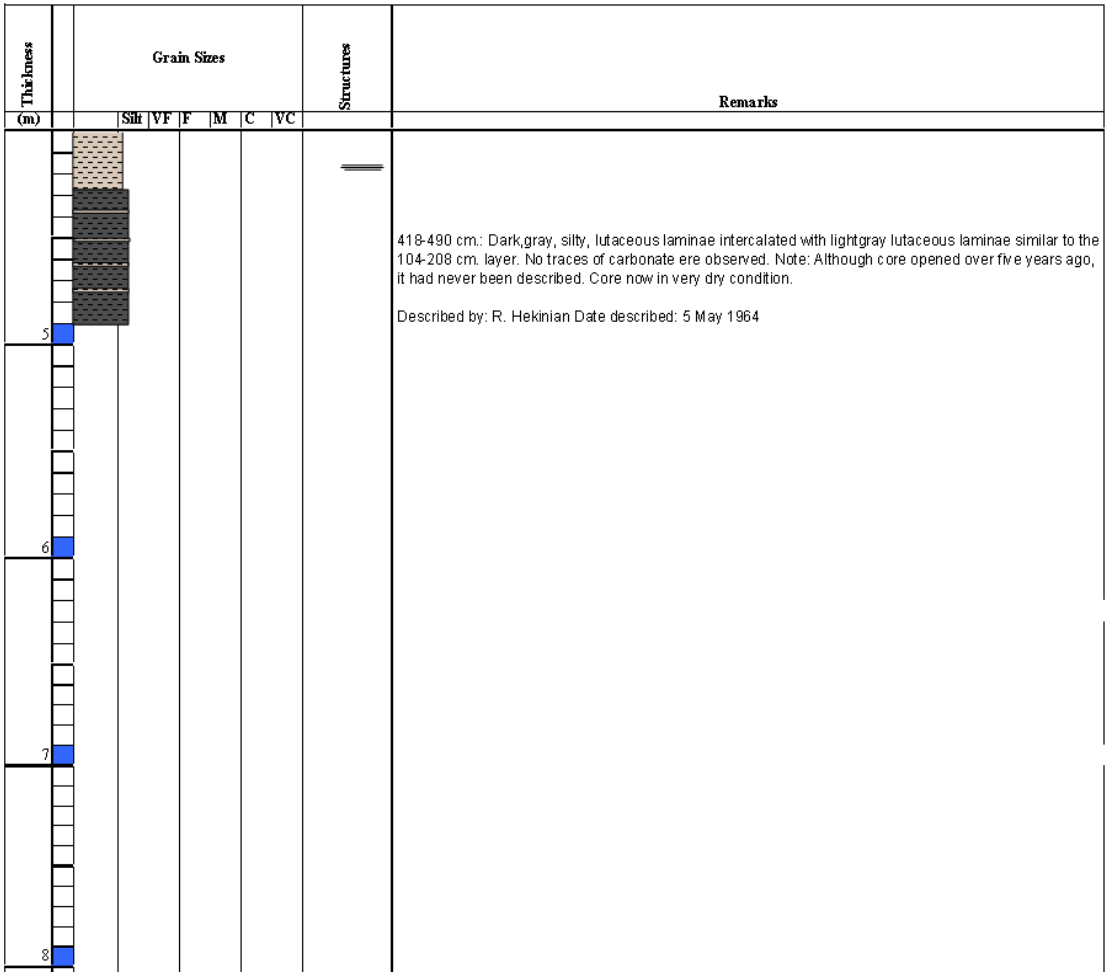
CORE VM12-116 (3)



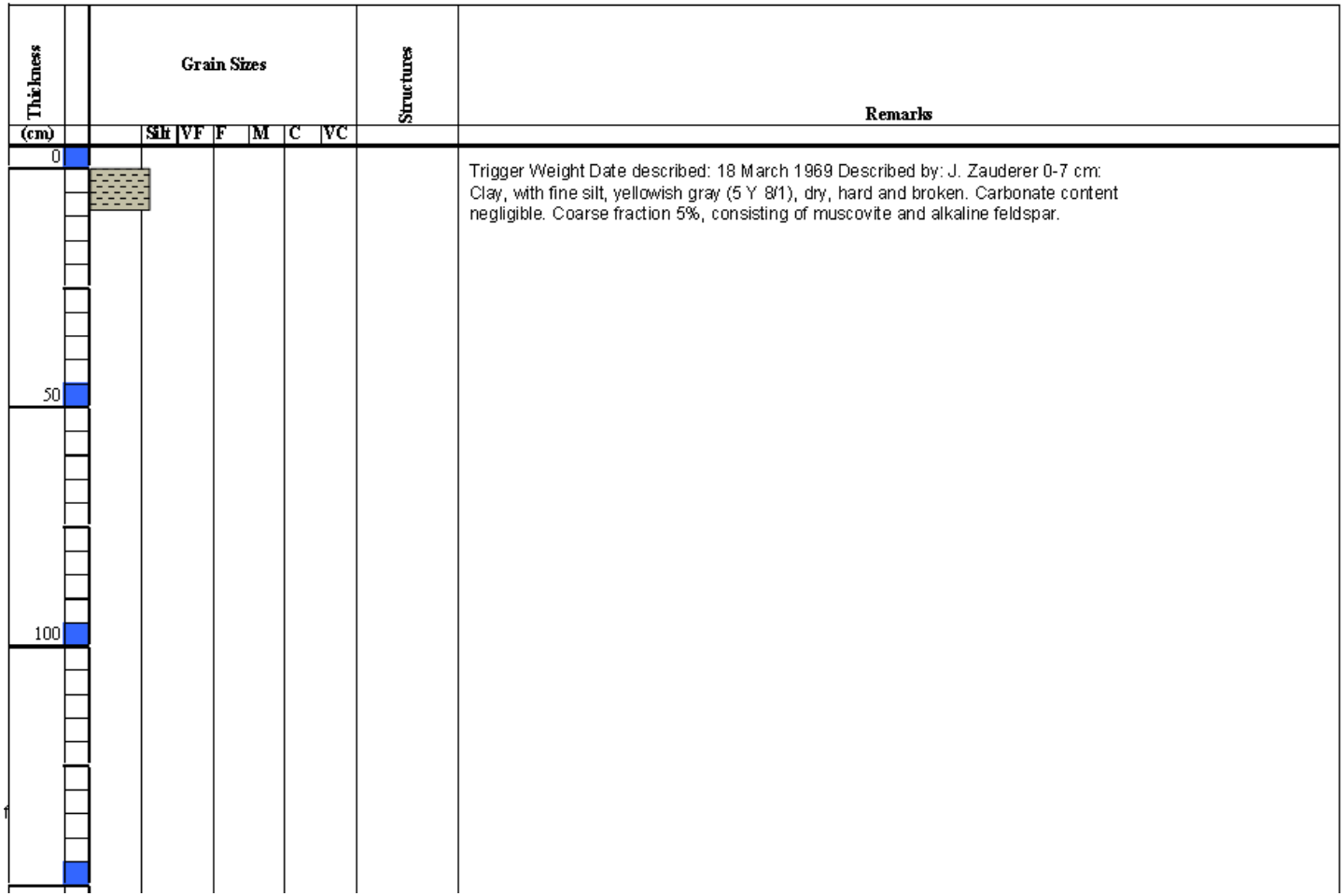
CORE VM12-117 (1)



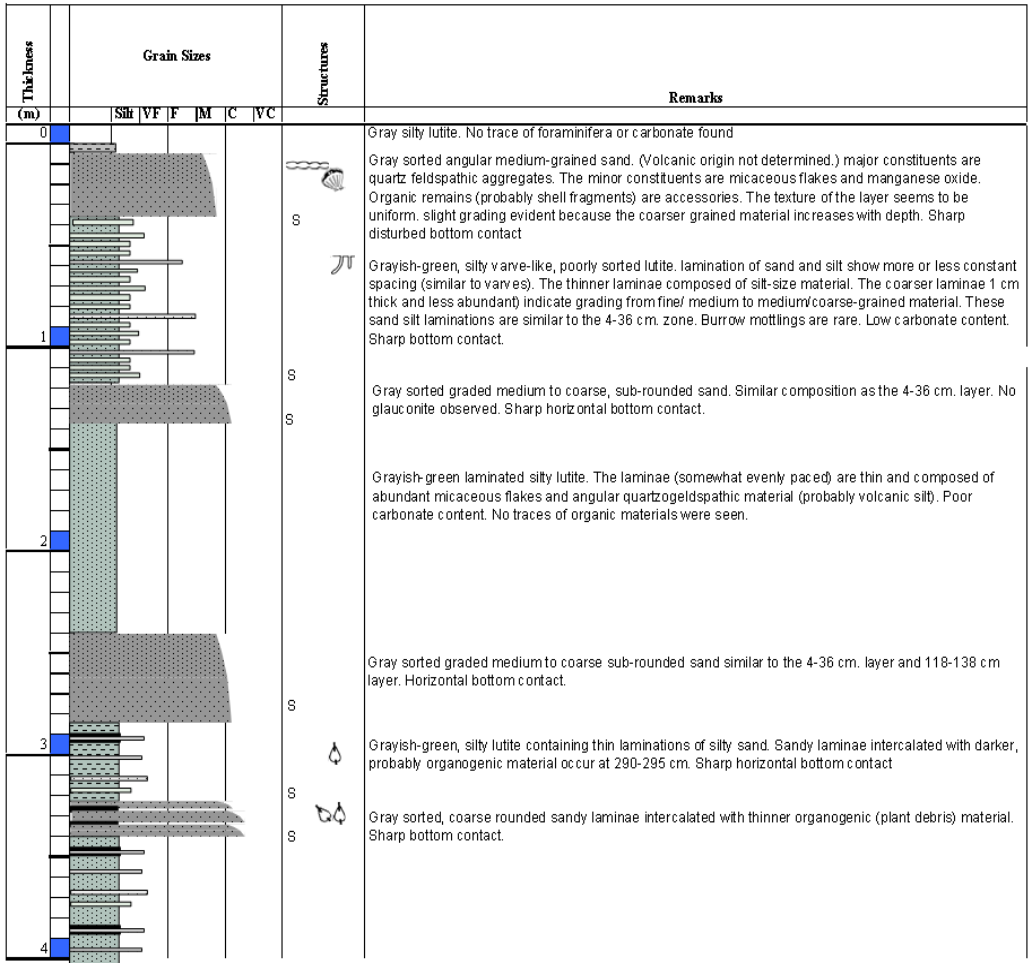
CORE VM12-117 (2)



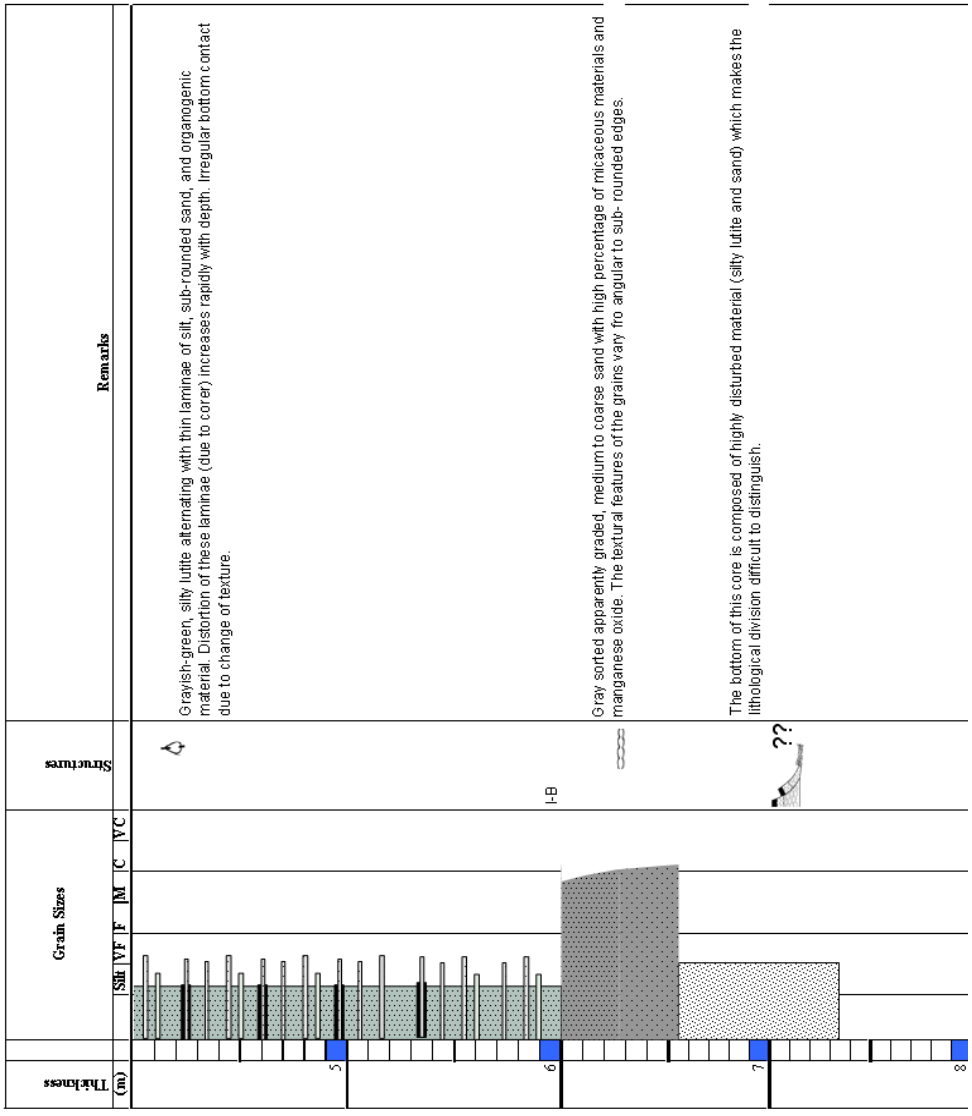
CORE VM12-117 TW



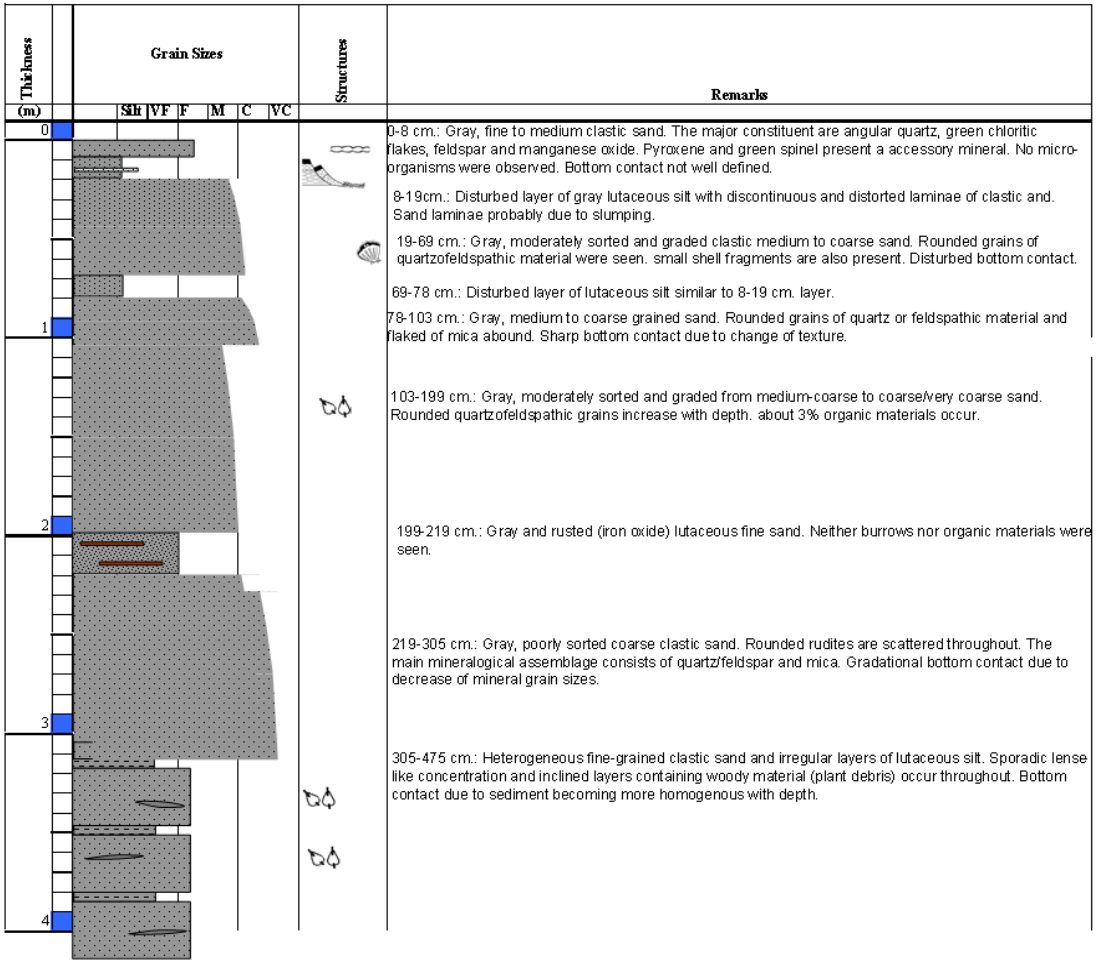
CORE VM12-118 (1)



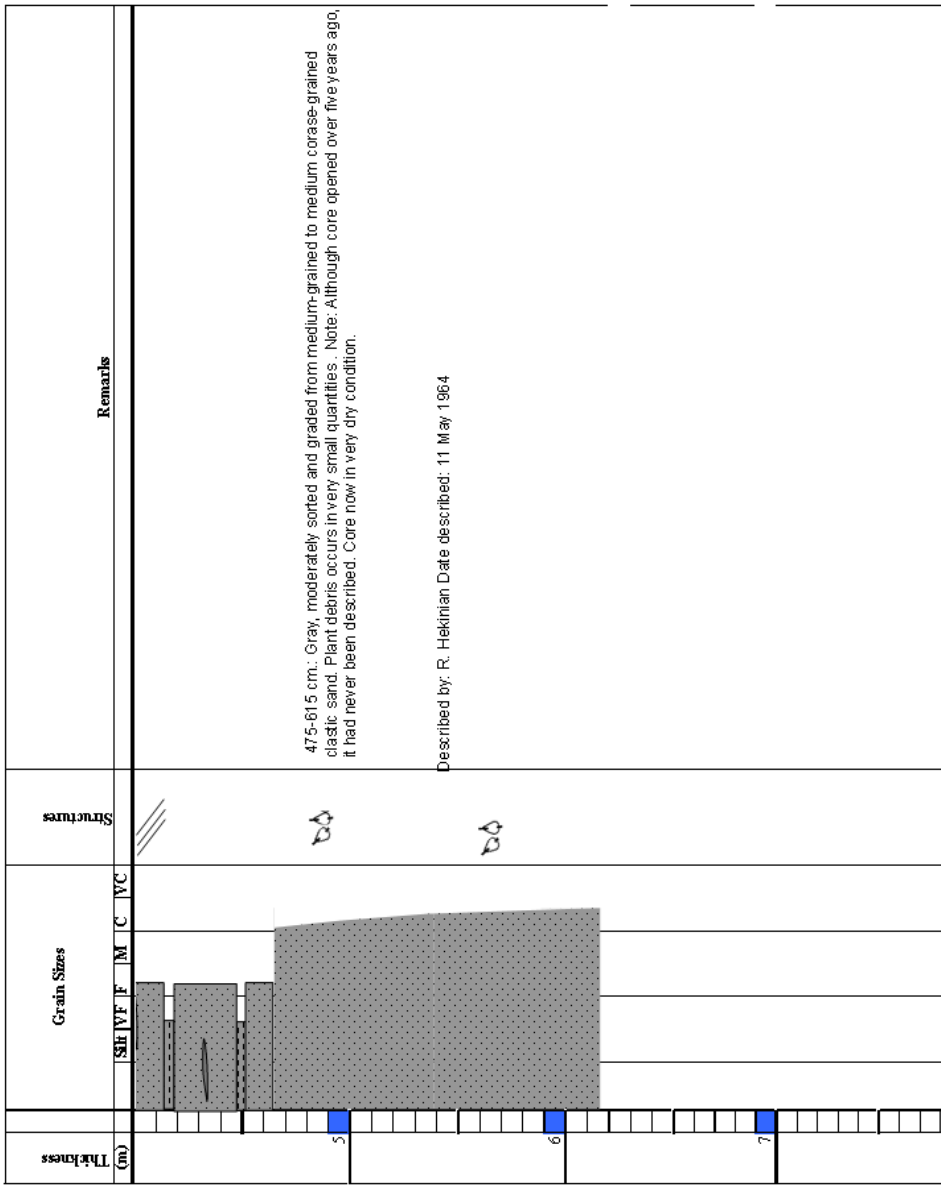
CORE VM12-118 (2)



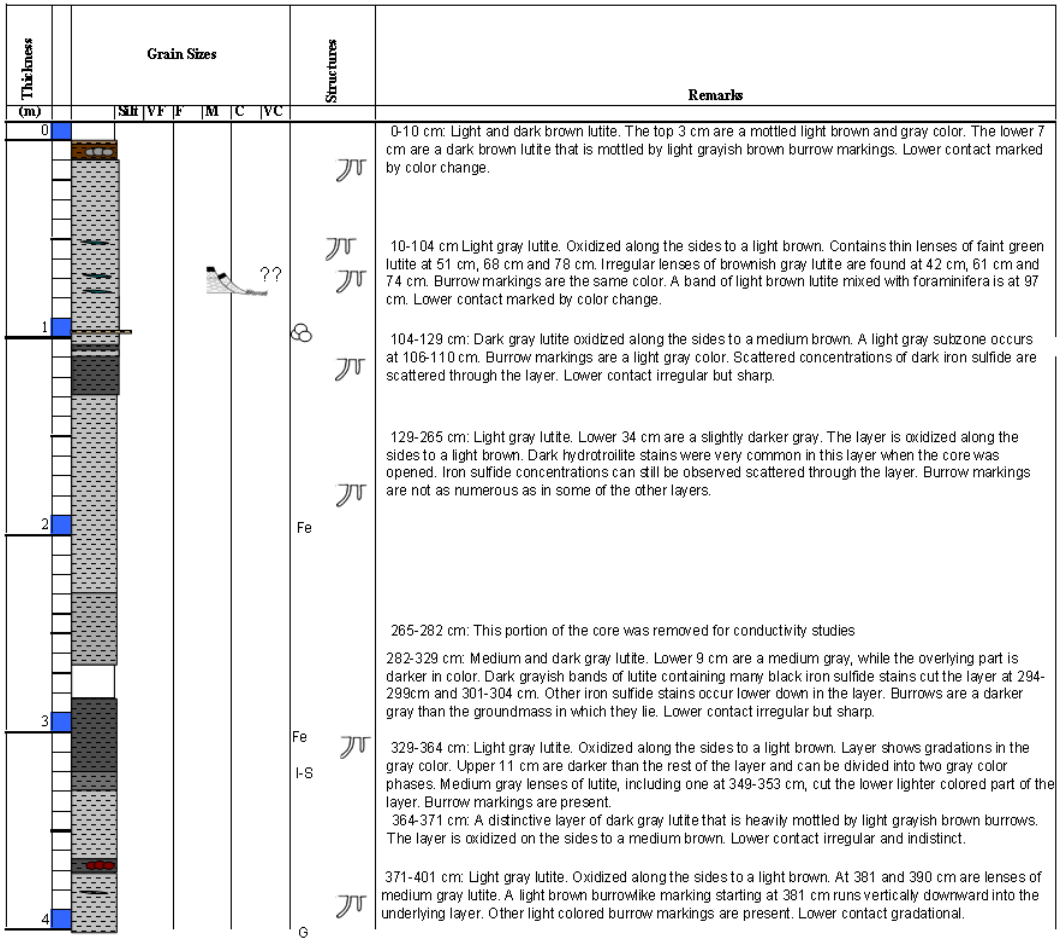
CORE VM12-119 (1)



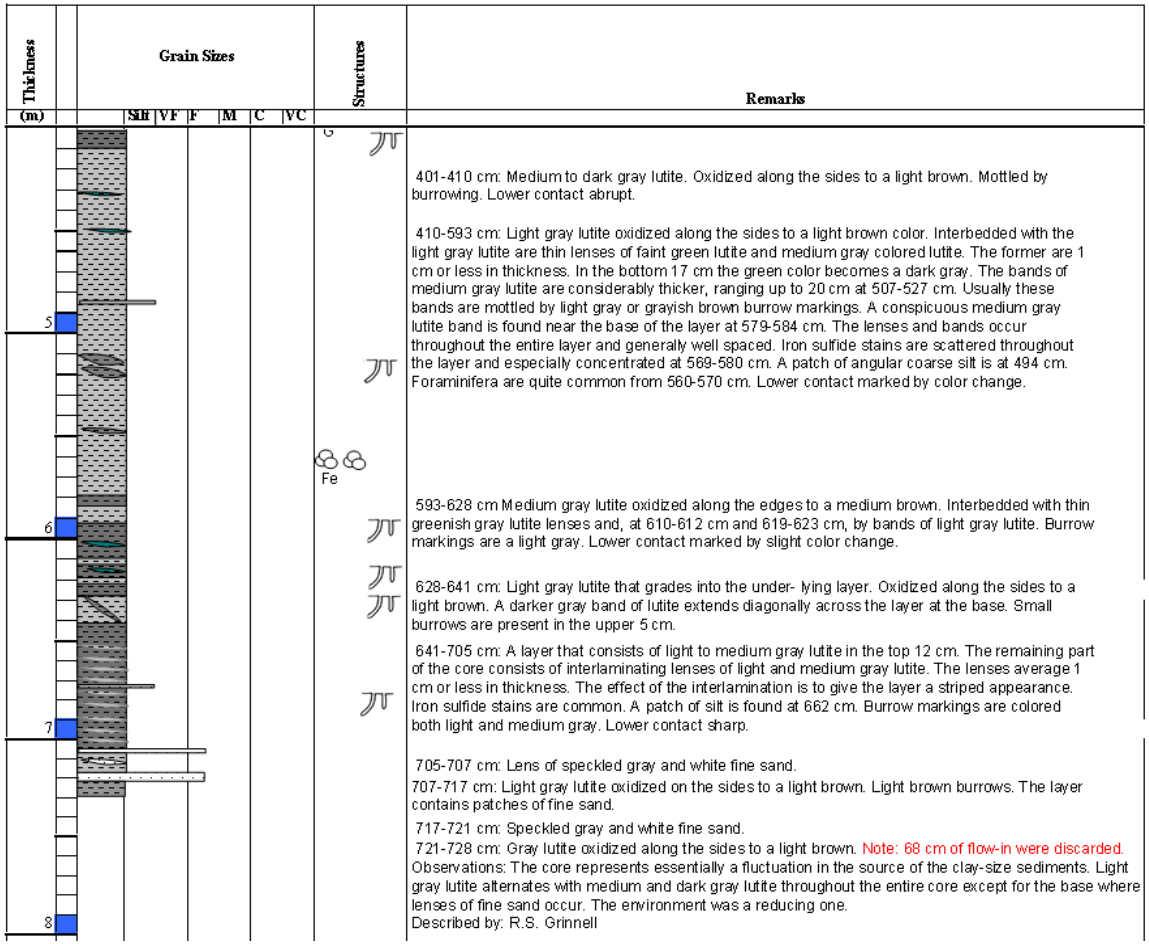
CORE VM12-119 (2)



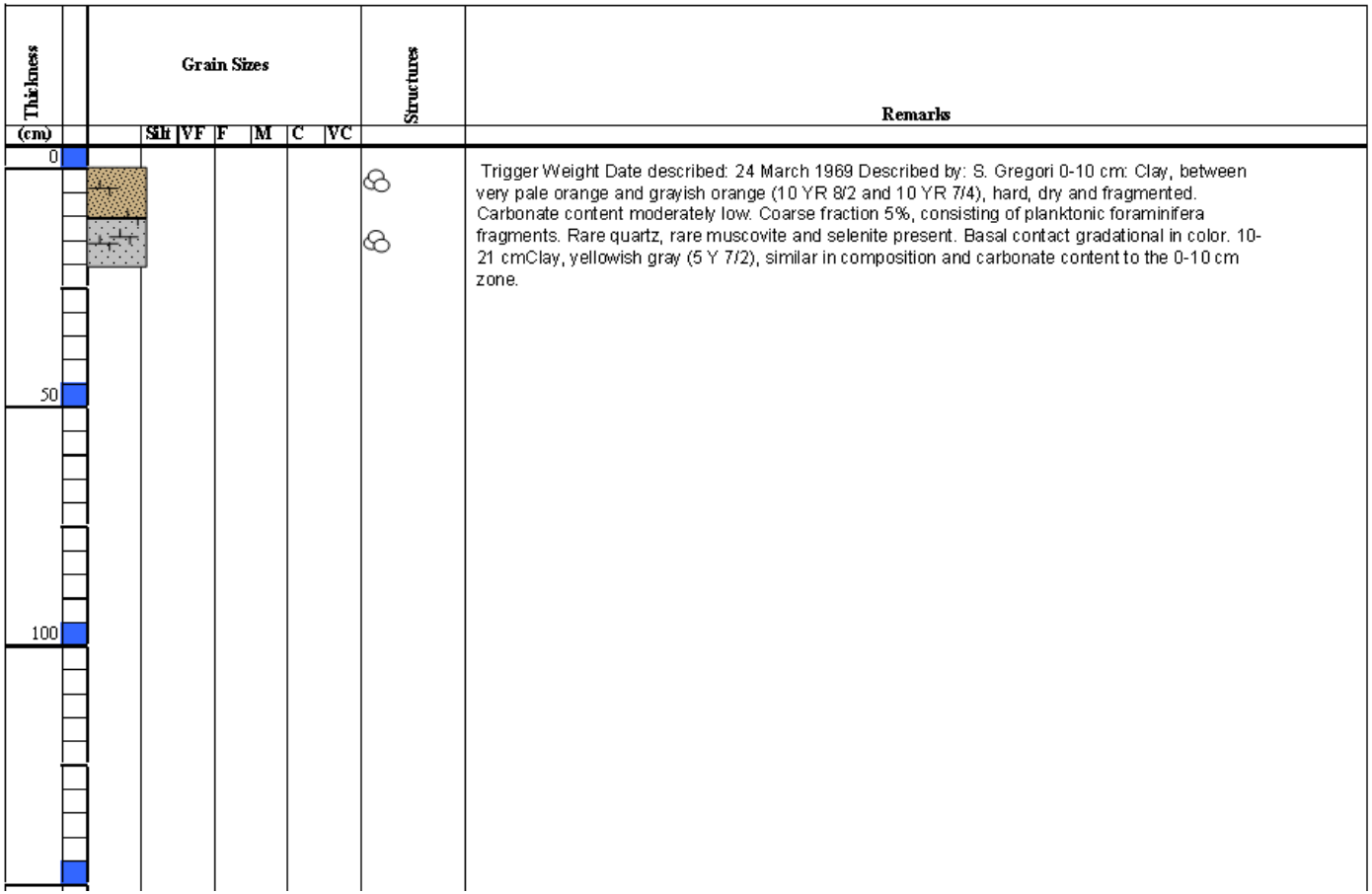
CORE VM15-7 (1)


Thickness
(m)
Grain Sizes
SiH
VF
F
M
C
VC
Structures
Remarks
0
1
2
3
4
??
Fe
Fe
I-S
G
0-10 cm: Light and dark brown lutite. The top 3 cm are a mottled light brown and gray color. The lower 7 cm are a dark brown lutite that is mottled by light grayish brown burrow markings. Lower contact marked by color change.
10-104 cm Light gray lutite. Oxidized along the sides to a light brown. Contains thin lenses of faint green lutite at 51 cm, 68 cm and 78 cm. Irregular lenses of brownish gray lutite are found at 42 cm, 61 cm and 74 cm. Burrow markings are the same color. A band of light brown lutite mixed with foraminifera is at 97 cm. Lower contact marked by color change.
104-129 cm: Dark gray lutite oxidized along the sides to a medium brown. A light gray subzone occurs at 106-110 cm. Burrow markings are a light gray color. Scattered concentrations of dark iron sulfide are scattered through the layer. Lower contact irregular but sharp.
129-265 cm: Light gray lutite. Lower 34 cm are a slightly darker gray. The layer is oxidized along the sides to a light brown. Dark hydrotroilite stains were very common in this layer when the core was opened. Iron sulfide concentrations can still be observed scattered through the layer. Burrow markings are not as numerous as in some of the other layers.
265-282 cm: This portion of the core was removed for conductivity studies
282-329 cm: Medium and dark gray lutite. Lower 9 cm are a medium gray, while the overlying part is darker in color. Dark grayish bands of lutite containing many black iron sulfide stains cut the layer at 294-299cm and 301-304 cm. Other iron sulfide stains occur lower down in the layer. Burrows are a darker gray than the groundmass in which they lie. Lower contact irregular but sharp.
329-364 cm: Light gray lutite. Oxidized along the sides to a light brown. Layer shows gradations in the gray color. Upper 11 cm are darker than the rest of the layer and can be divided into two gray color phases. Medium gray lenses of lutite, including one at 349-353 cm, cut the lower lighter colored part of the layer. Burrow markings are present.
364-371 cm: A distinctive layer of dark gray lutite that is heavily mottled by light grayish brown burrows. The layer is oxidized on the sides to a medium brown. Lower contact irregular and indistinct.
371-401 cm: Light gray lutite. Oxidized along the sides to a light brown. At 381 and 390 cm are lenses of medium gray lutite. A light brown burrowlike marking starting at 381 cm runs vertically downward into the underlying layer. Other light colored burrow markings are present. Lower contact gradational.

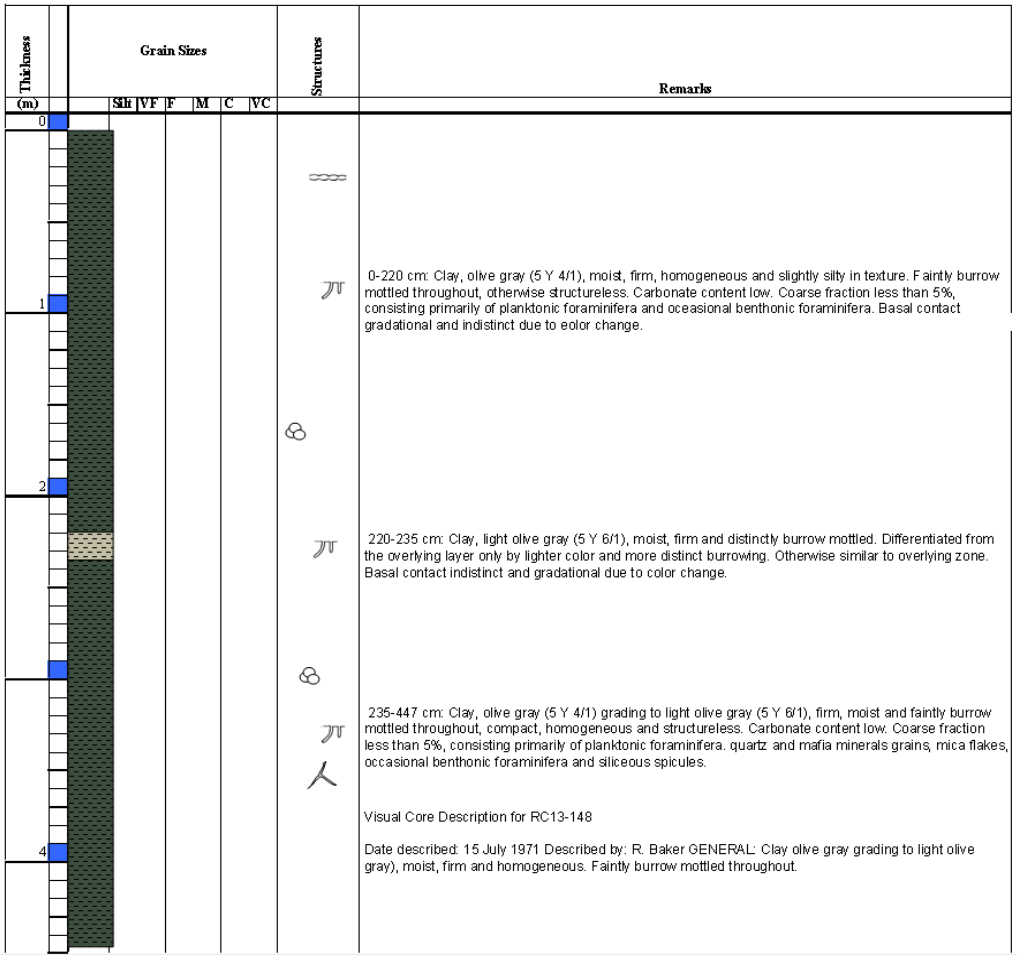
CORE VM15-7 (2)


Thickness
(m)
Grain Sizes
Slt
VF
F
M
C
VC
Structures
Remarks
5
6
7
8
Fe
401-410 cm: Medium to dark gray lutite. Oxidized along the sides to a light brown. Mottled by burrowing. Lower contact abrupt.
410-593 cm: Light gray lutite oxidized along the sides to a light brown color. Interbedded with the light gray lutite are thin lenses of faint green lutite and medium gray colored lutite. The former are 1 cm or less in thickness. In the bottom 17 cm the green color becomes a dark gray. The bands of medium gray lutite are considerably thicker, ranging up to 20 cm at 507-527 cm. Usually these bands are mottled by light gray or grayish brown burrow markings. A conspicuous medium gray lutite band is found near the base of the layer at 579-584 cm. The lenses and bands occur throughout the entire layer and generally well spaced. Iron sulfide stains are scattered throughout the layer and especially concentrated at 569-580 cm. A patch of angular coarse silt is at 494 cm. Foraminifera are quite common from 560-570 cm. Lower contact marked by color change.
593-628 cm Medium gray lutite oxidized along the edges to a medium brown. Interbedded with thin greenish gray lutite lenses and, at 610-612 cm and 619-623 cm, by bands of light gray lutite. Burrow markings are a light gray. Lower contact marked by slight color change.
628-641 cm: Light gray lutite that grades into the under- lying layer. Oxidized along the sides to a light brown. A darker gray band of lutite extends diagonally across the layer at the base. Small burrows are present in the upper 5 cm.
641-705 cm: A layer that consists of light to medium gray lutite in the top 12 cm. The remaining part of the core consists of interlaminating lenses of light and medium gray lutite. The lenses average 1 cm or less in thickness. The effect of the interlamination is to give the layer a striped appearance. Iron sulfide stains are common. A patch of silt is found at 662 cm. Burrow markings are colored both light and medium gray. Lower contact sharp.
705-707 cm: Lens of speckled gray and white fine sand.
707-717 cm: Light gray lutite oxidized on the sides to a light brown. Light brown burrows. The layer contains patches of fine sand.
717-721 cm: Speckled gray and white fine sand.
721-728 cm: Gray lutite oxidized along the sides to a light brown. Note: 68 cm of flow-in were discarded.
Observations: The core represents essentially a fluctuation in the source of the clay-size sediments. Light gray lutite alternates with medium and dark gray lutite throughout the entire core except for the base where lenses of fine sand occur. The environment was a reducing one.
Described by: R.S. Grinnell

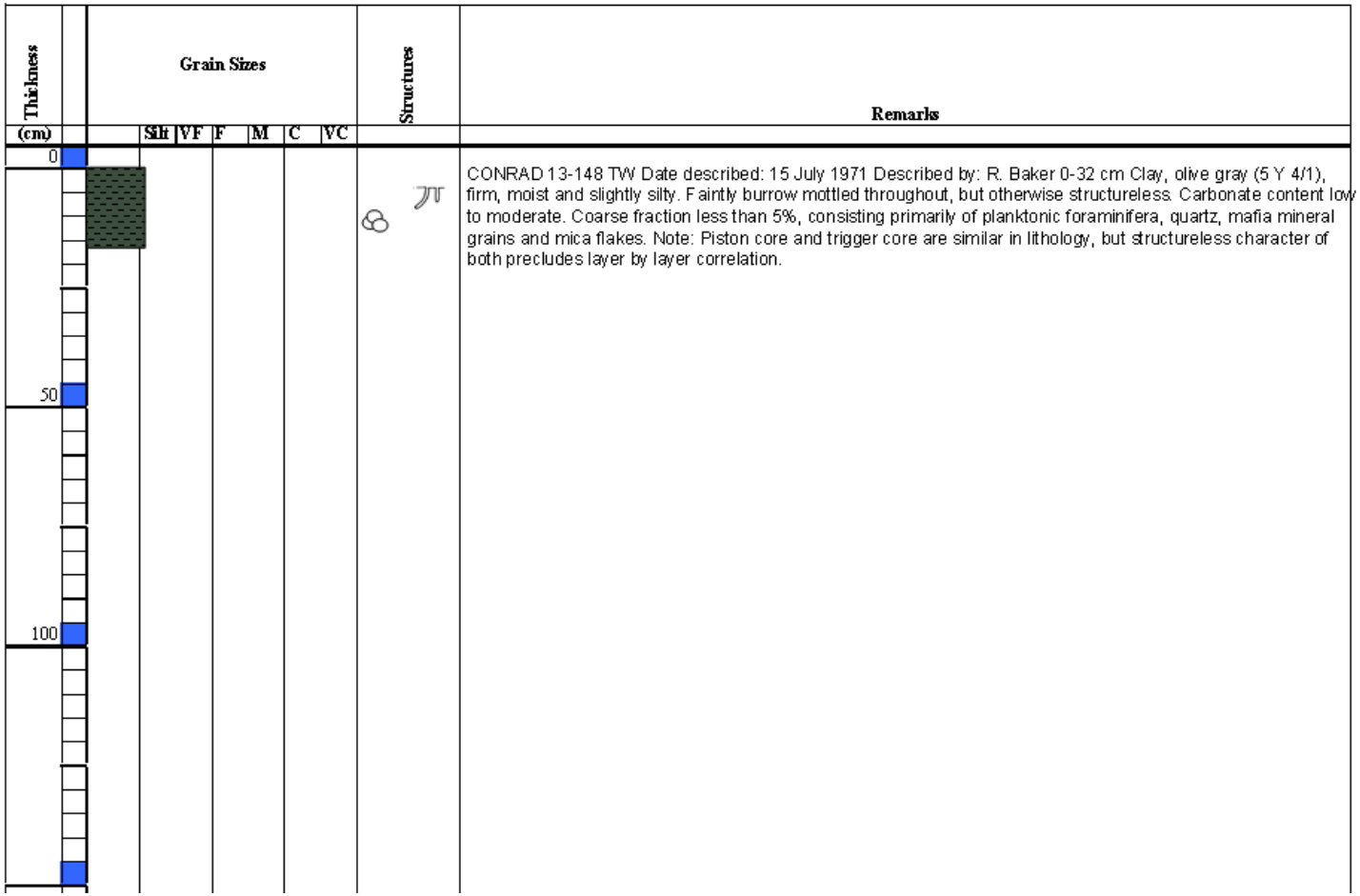
CORE VM15-7 TW



CORE RC13-148



CORE RC13-148 TW



Remarks
CONRAD 13-148 TW Date described: 15 July 1971 Described by: R. Baker 0-32 cm Clay, olive gray (5 Y 4/1), firm, moist and slightly silty. Faintly burrow mottled throughout, but otherwise structureless. Carbonate content low to moderate. Coarse fraction less than 5%, consisting primarily of planktonic foraminifera, quartz, mafia mineral grains and mica flakes. Note: Piston core and trigger core are similar in lithology, but structureless character of both precludes layer by layer correlation.

APPENDIX 2

Flows calculations following Mulder and Syvitski (1995) methodology.

Cc = 36.25 kg m^{-3}. Average critical sediment concentration (sediment density 2650 kg m^{-3}) to overcome difference between fresh and salt water. At equatorial latitudes. (from Kennish, 1989)

Q Mean annual water discharge Units m^3s^{-1}

Qs Mean annual sediment discharge Units m^3s^{-1}

Q_{flood} is calculated by the power function (Mattahai 1990) . Units m^3s^{-1}

$$\log Qflood = \text{-}\ .07(\log A)^2 +).865\log A + :.084$$

$$forA <)^6 km^2, r^2 =).99$$

A Basin area in km^2

-
- Concentration of suspended sediment

$$Css = \frac{Qs}{Q}$$

- Maximum flood discharge

$$C_{flood} = Css\left(\frac{Qflood}{Q}\right)^{\cdot}$$

b Exponent varied until C_{flood} > Cc, b=2

APPENDIX 3

Curvature on Seafloor bathymetry

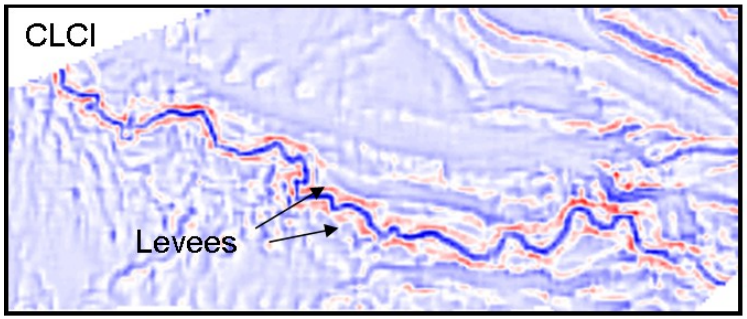
This appendix contains images of curvature attributes generated for one of the bathymetry surveys. For relatively flat surfaces, curvature approximates the second derivative of a surface, and is more accurately defined as the reciprocal of the radius of a circle that is tangent to the given curve at a point. (Chopra and Marfurt, 2007). Curvature will be large for a tightly folded surface and zero for a plane. Different measurements of curvature highlight different features of the seafloor surface as is shown in the following figures. (For definition of curvature types see Chopra and Marfurt, 2007).

Variations of the surface cell size act as spatial filter and will change the curvature results, highlighting different features. Calculations of curvature were implemented for six cell sizes in order to observe the variation of curvature and its different measurements.

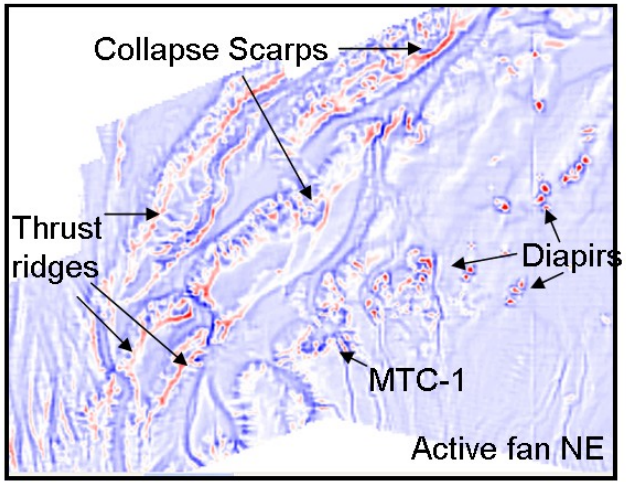
Chopra S., Marfurt K., 2007, Curvature attributes applications to 3D surface seismic data, The *Leading Edge*, 26(4):404-414

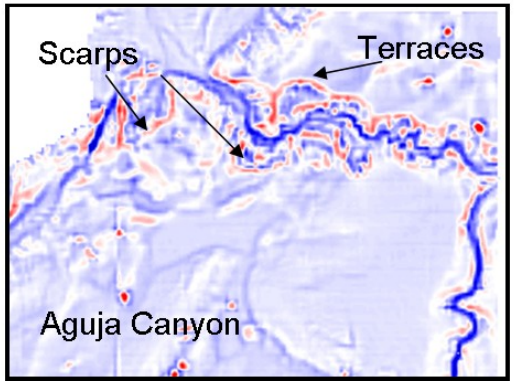
MAIN FEATURES

Concave up features in blue
Convex up features in red



Channel thalweg in blue (concave up). Levees in red (convex up)

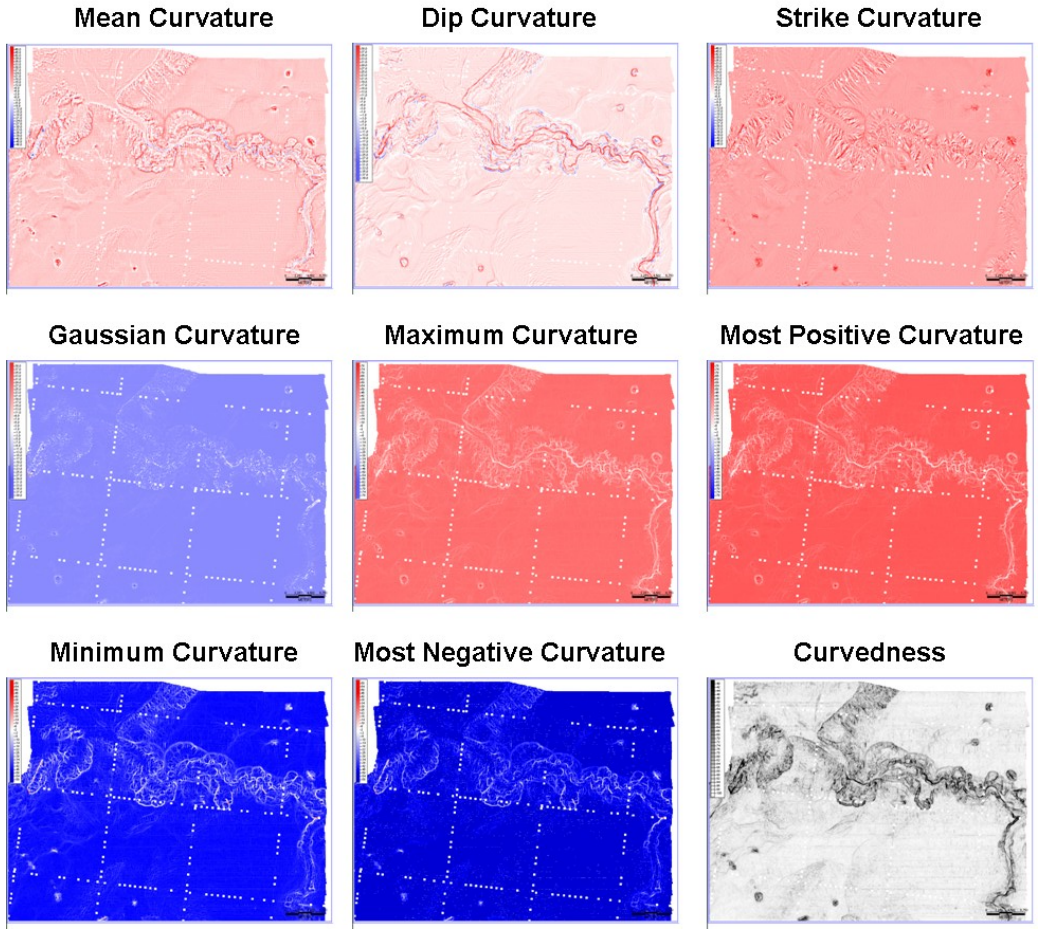




Mean Curvature

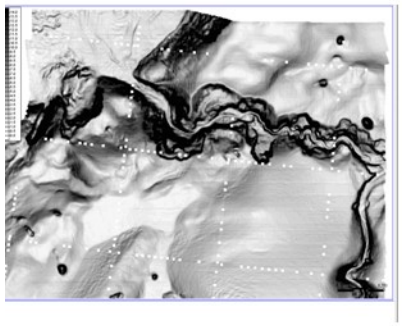
(grid cell 400m)

CURVATURE TYPES – AGUJA CANYON (100M)

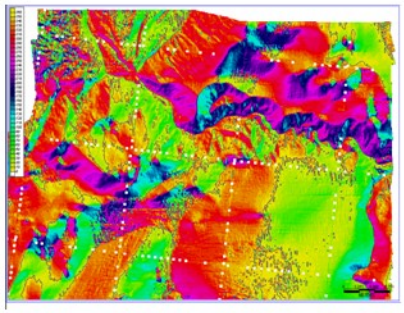


OTHER ATTRIBUTES – AGUJA CANYON (100M)

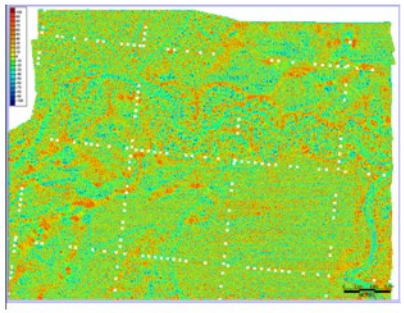
Slope



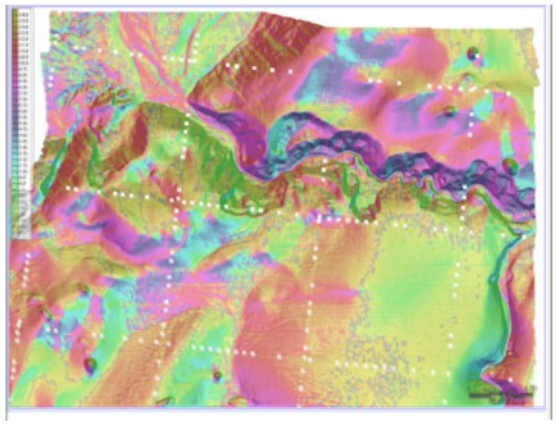
Azimuth



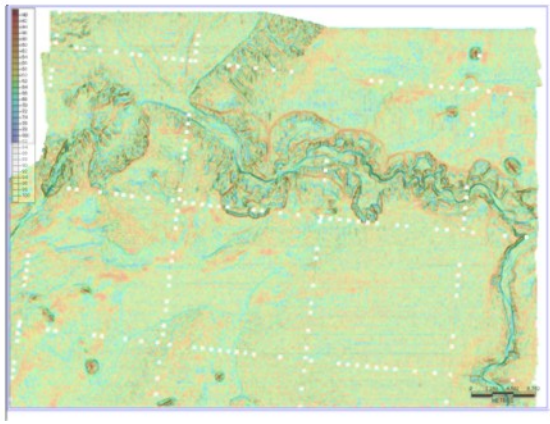
Shape



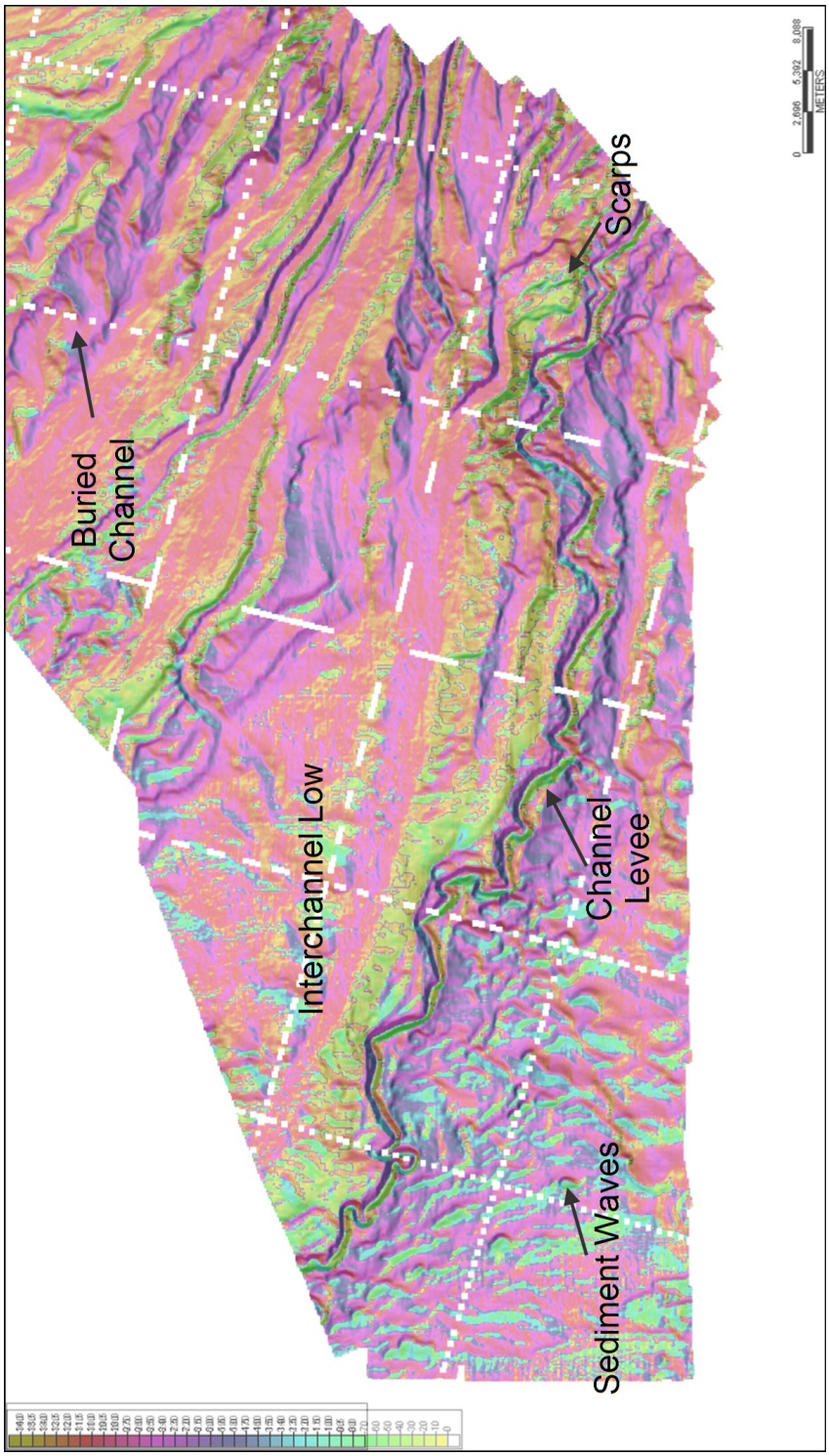
Azimuth +Slope



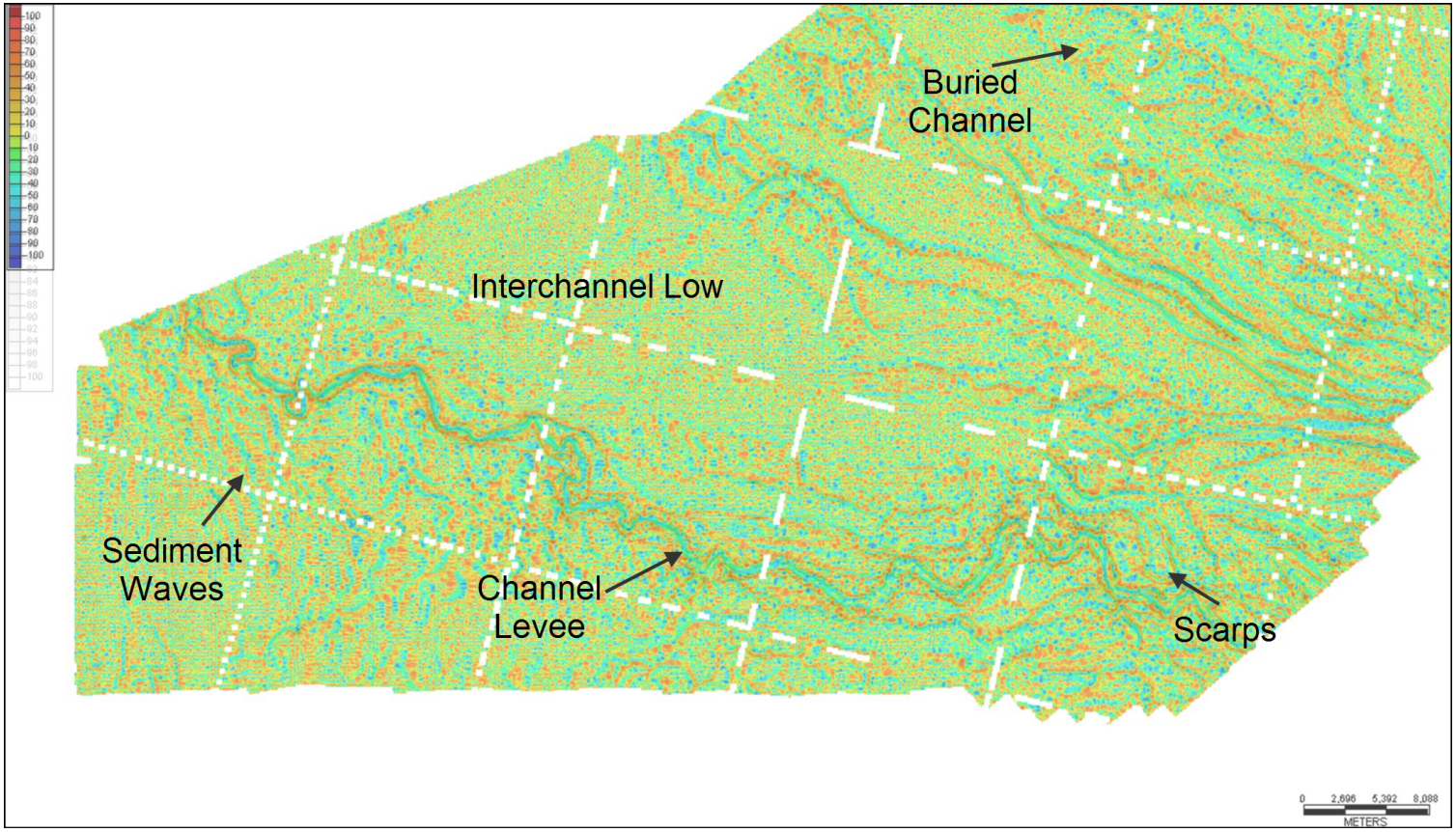
Shape +Curvedness



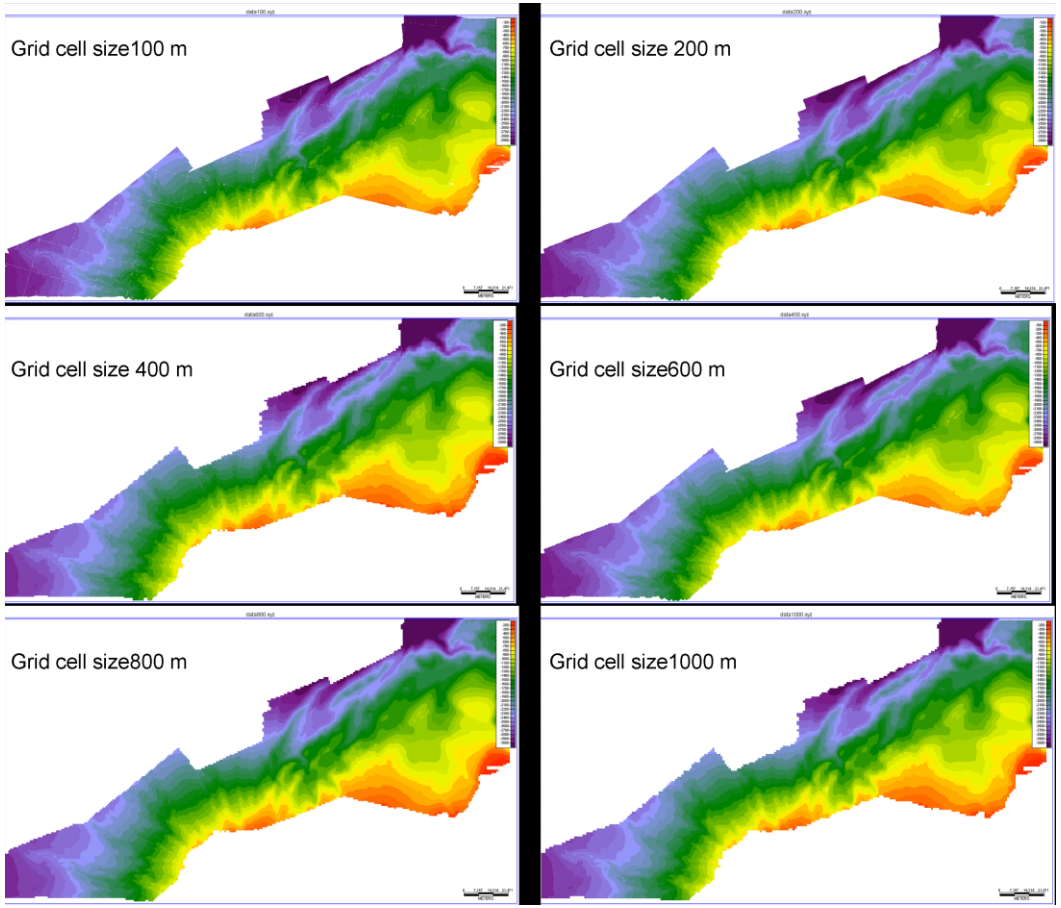
AZIMUTH AND SLOPE BLEND



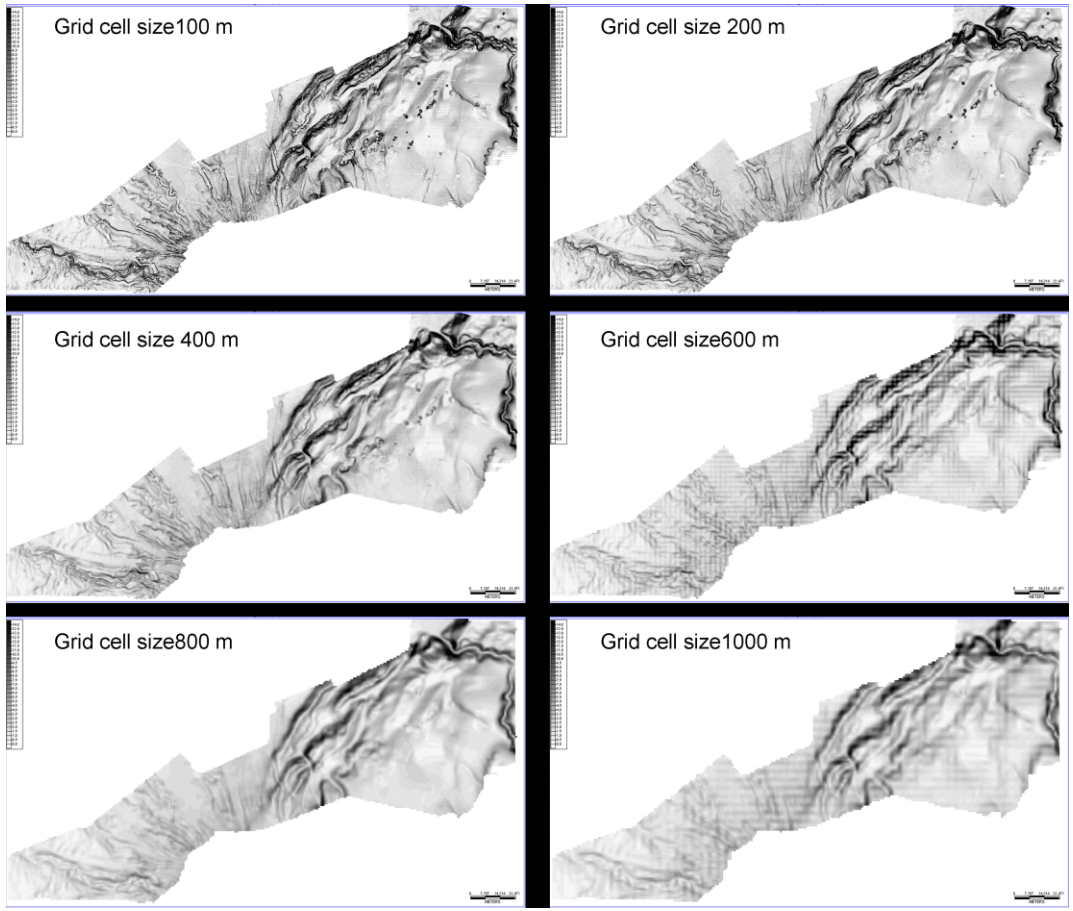
SHAPE AND CURVEDNESS BLEND



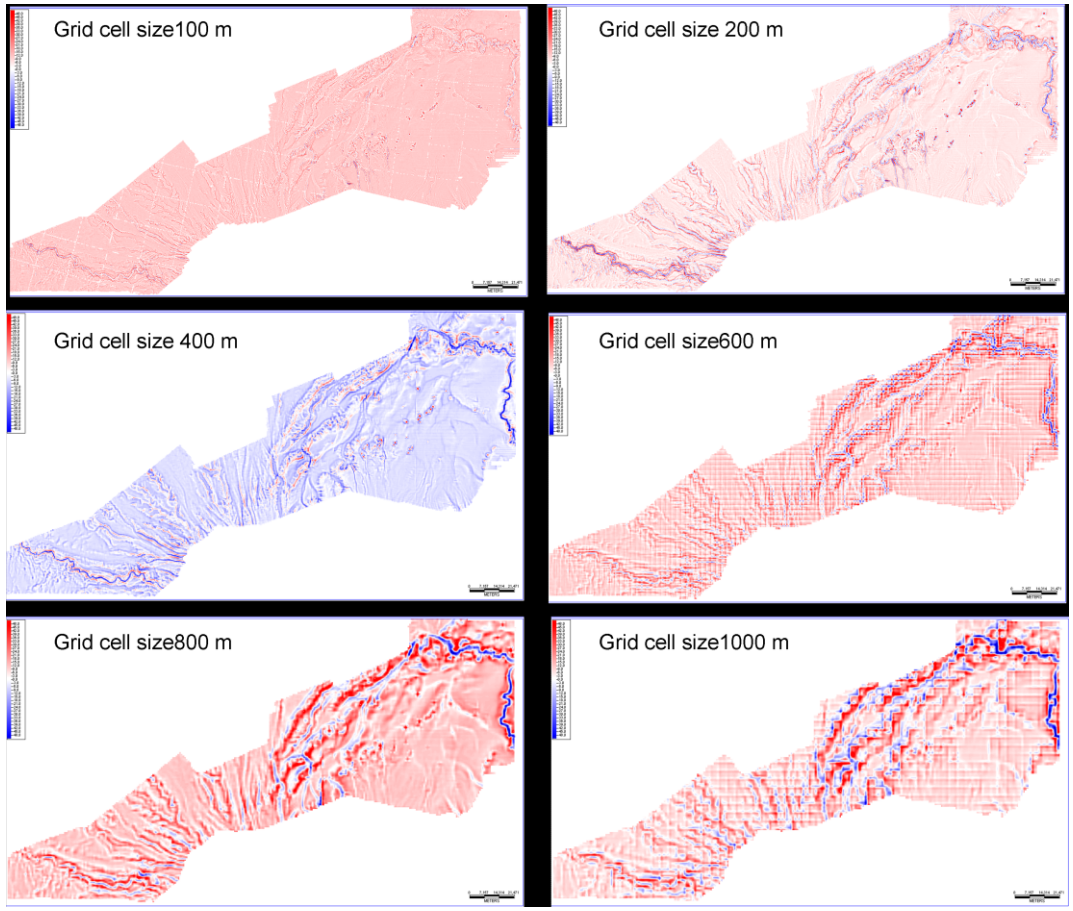
BATHYMETRY MAPS



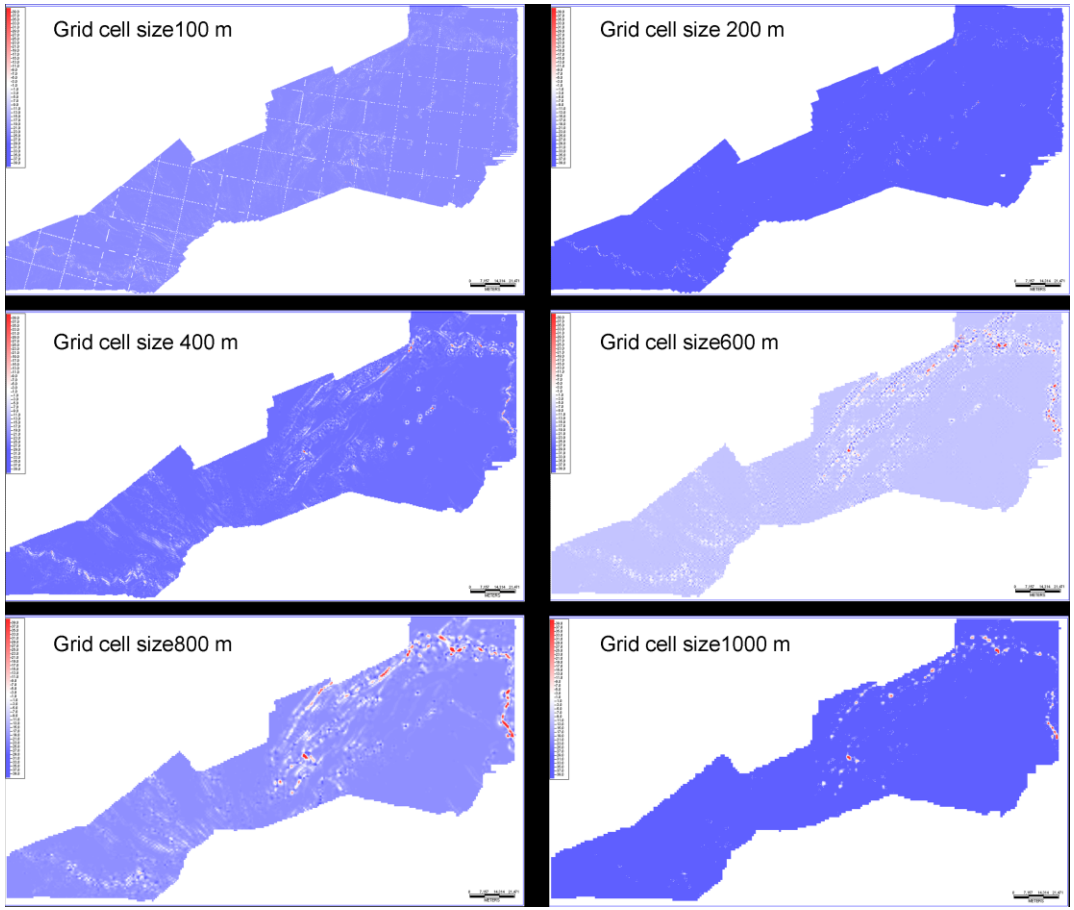
SLOPE MAPS


Grid cell size100 m
Grid cell size 200 m
Grid cell size 400 m
Grid cell size600 m
Grid cell size800 m
Grid cell size1000 m

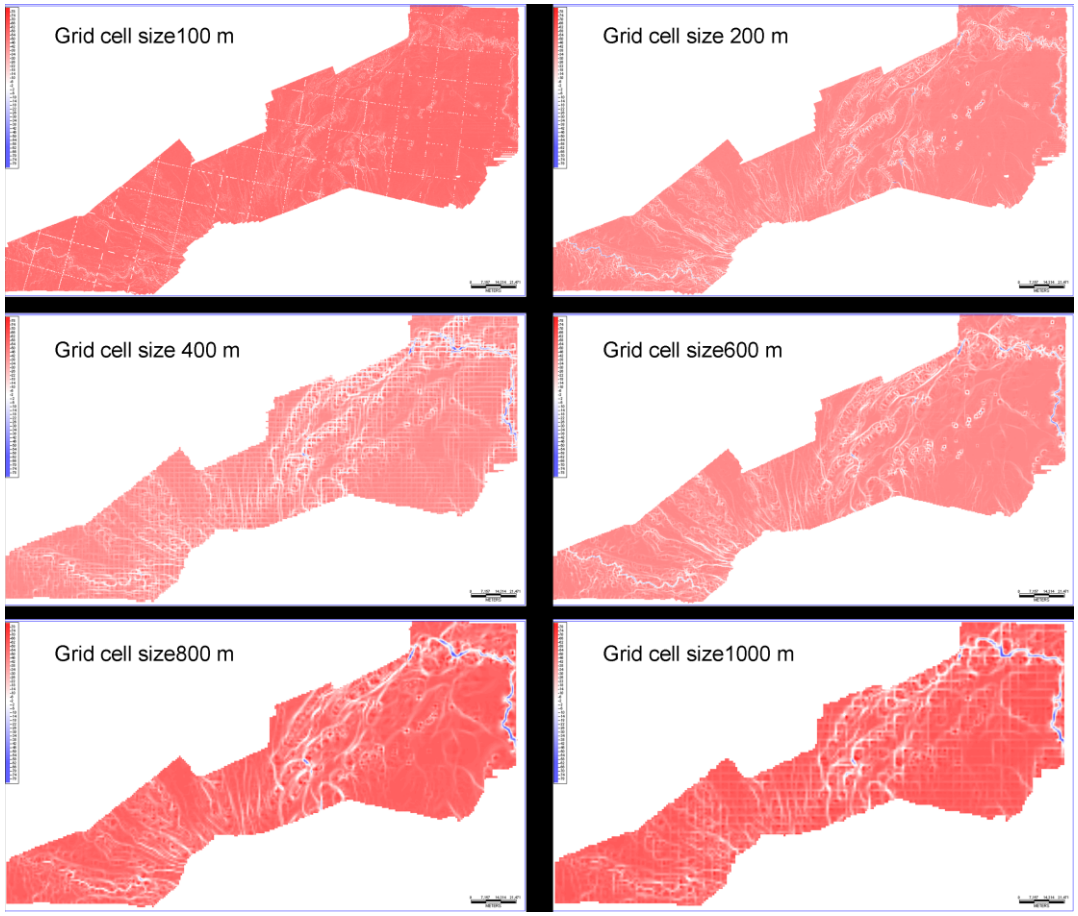
MEAN CURVATURE MAPS



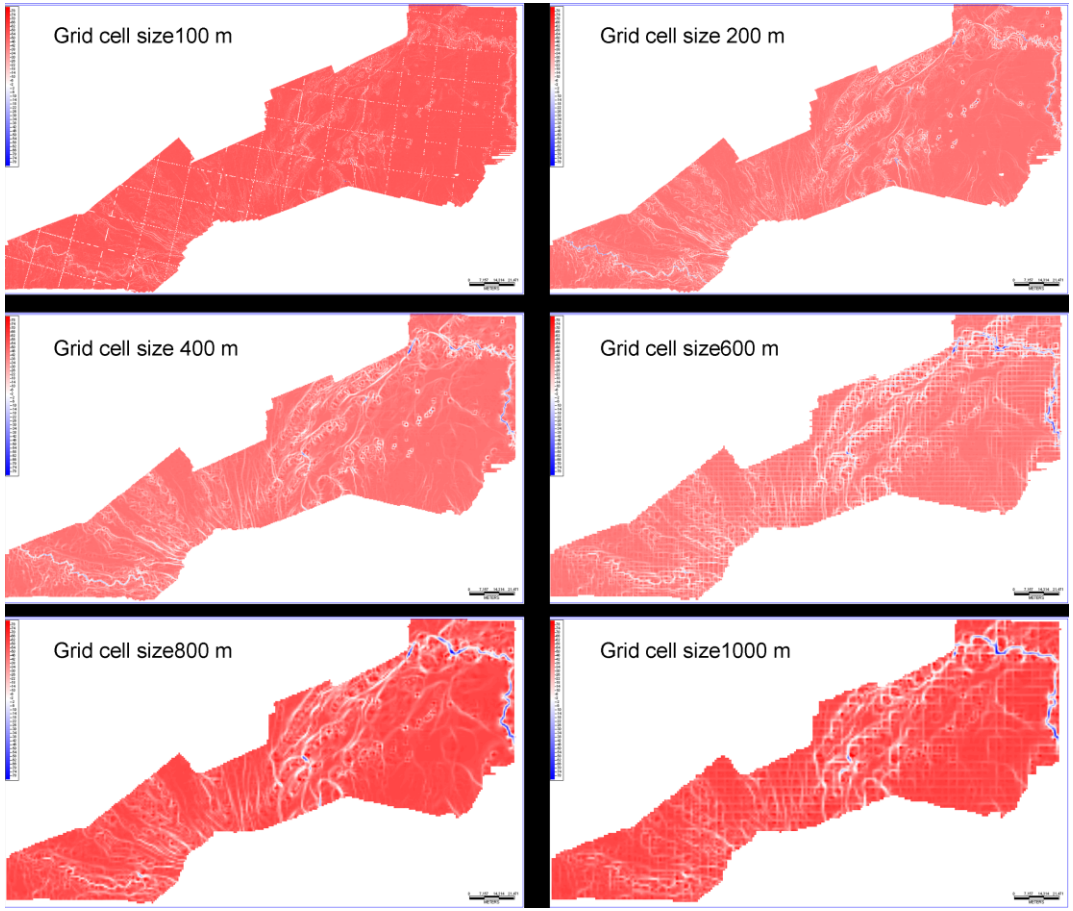
GAUSSIAN CURVATURE MAPS



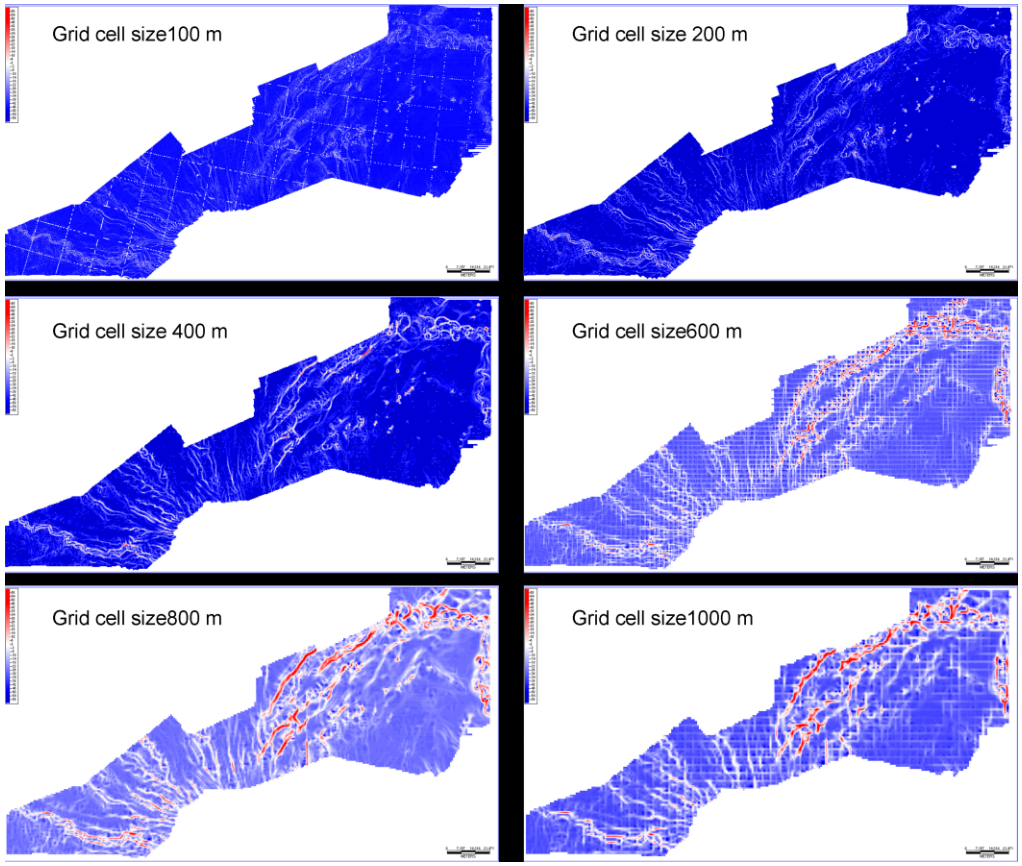
MAXIMUM CURVATURE MAPS



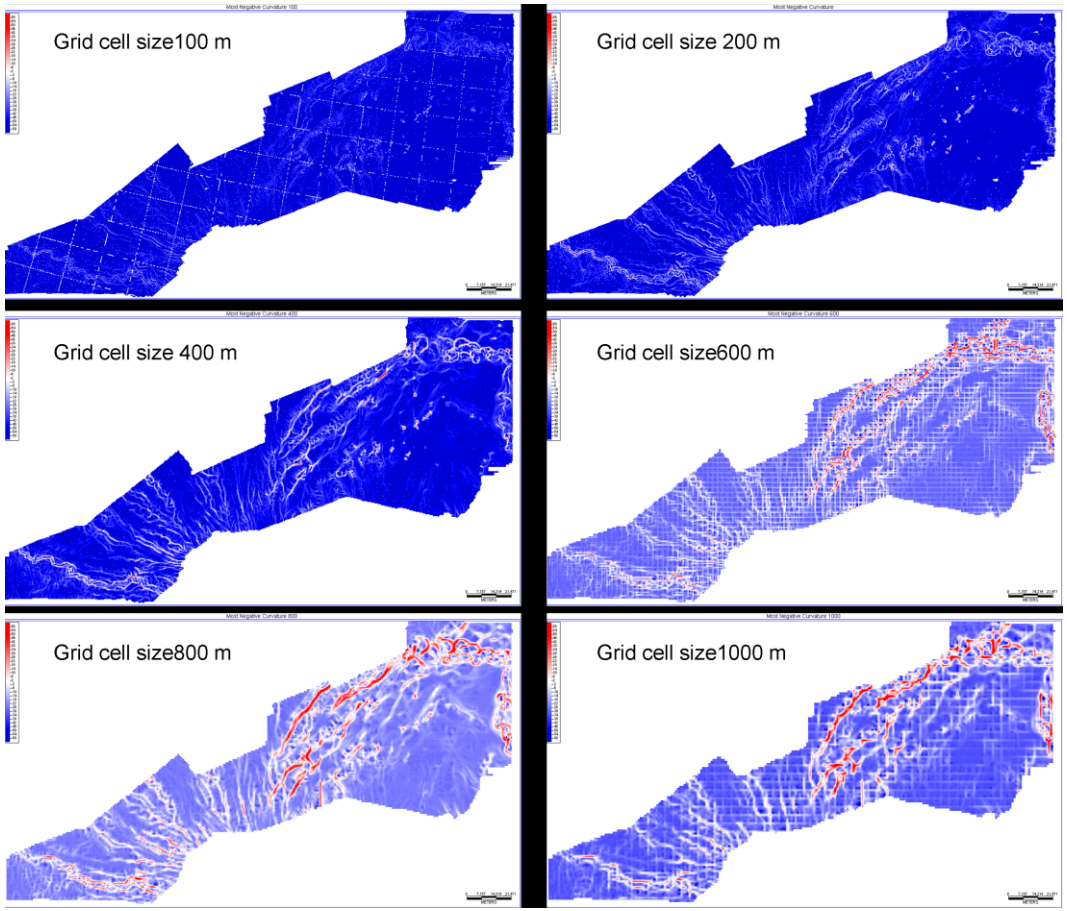
MOST POSITIVE CURVATURE MAPS



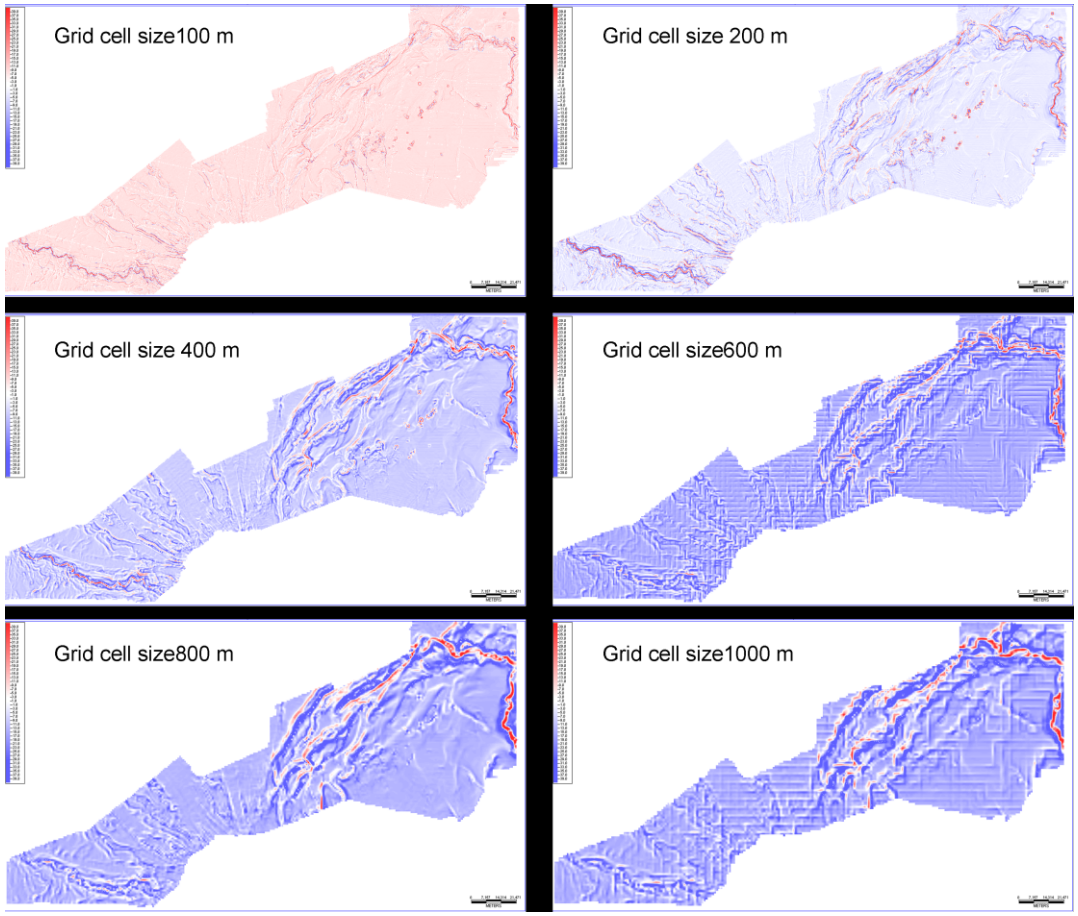
MINIMUM CURVATURE MAPS



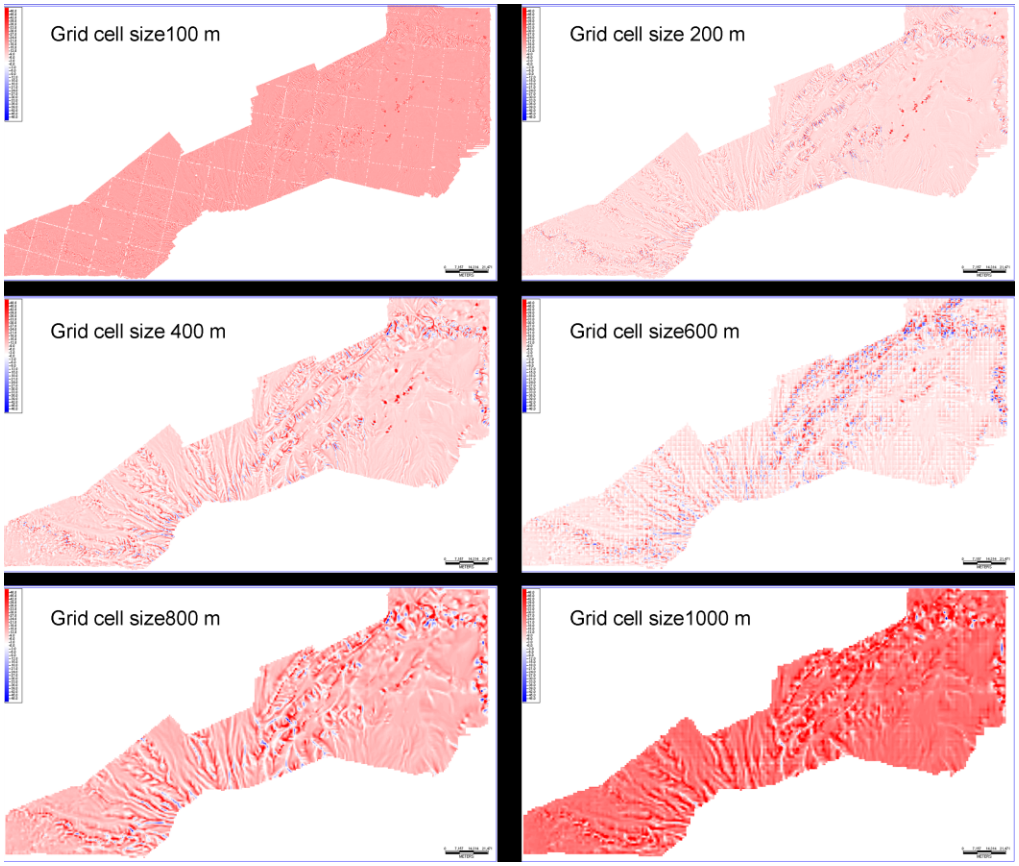
MOST NEGATIVE CURVATURE MAPS



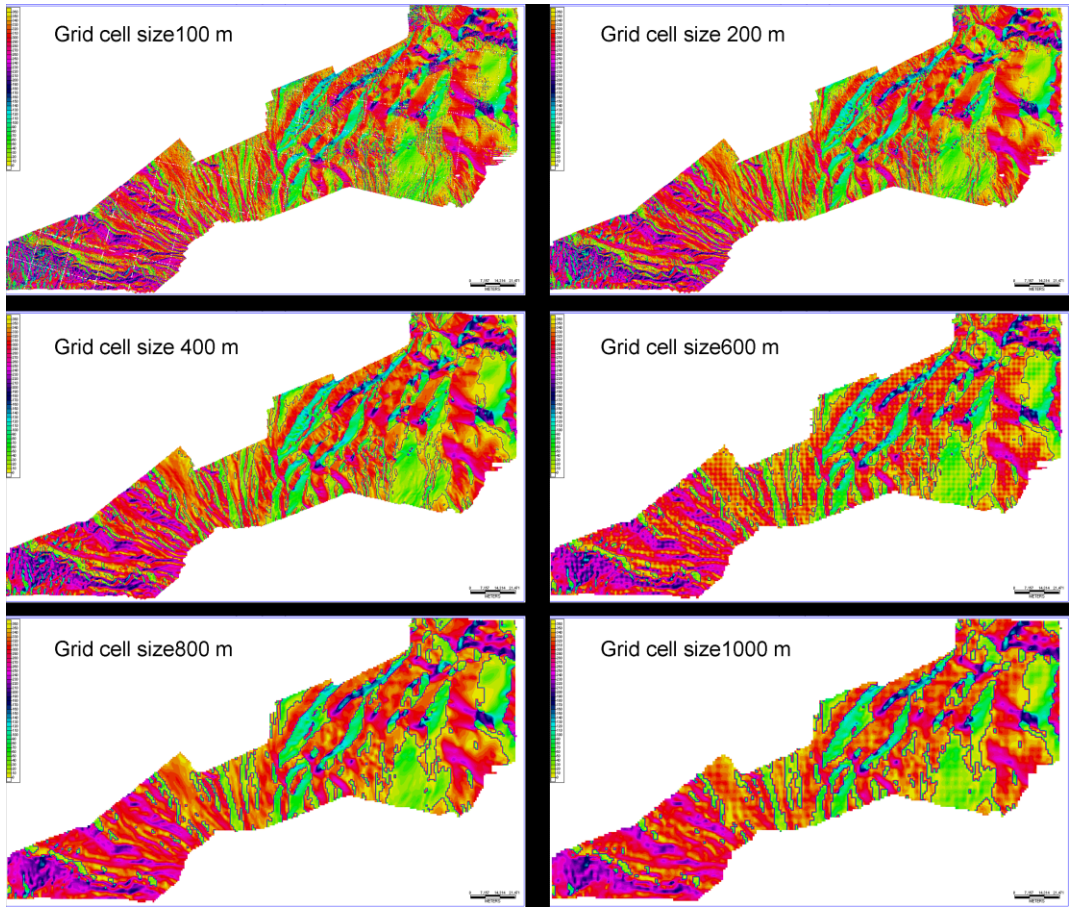
DIP CURVATURE MAPS



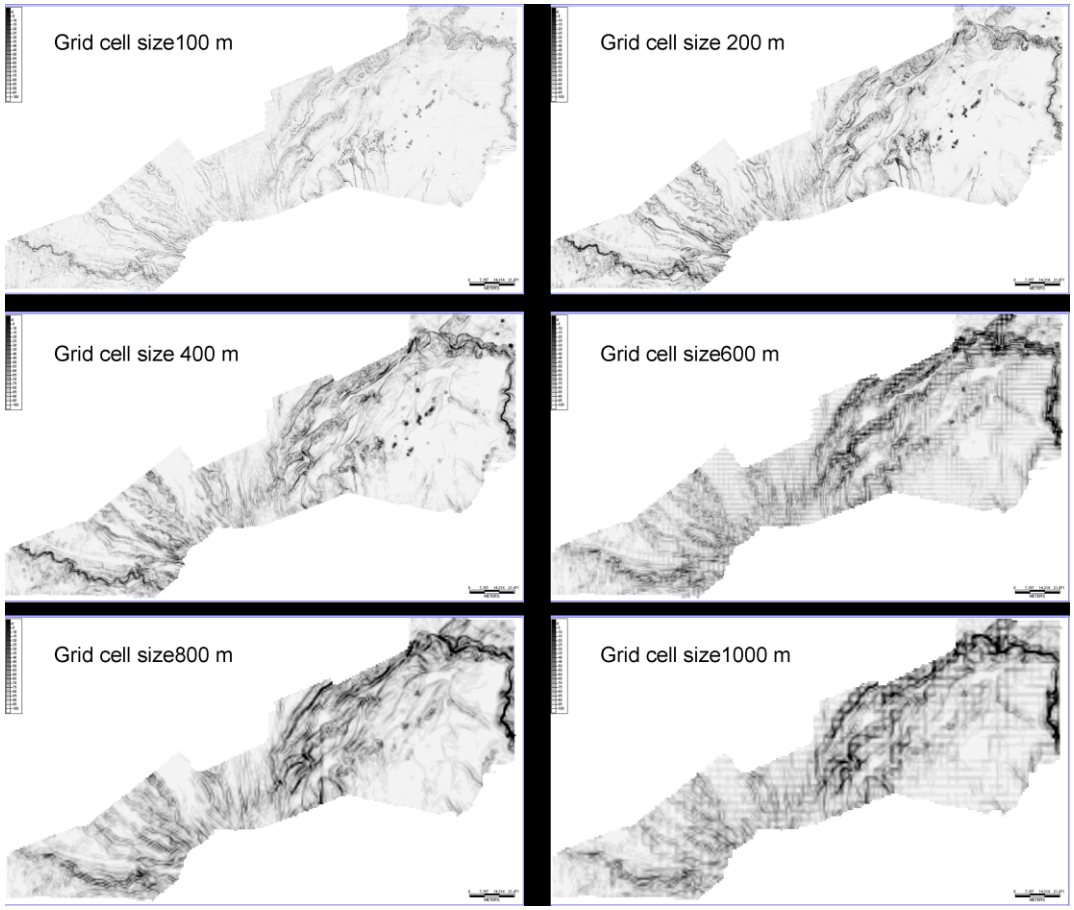
STRIKE CURVATURE MAPS



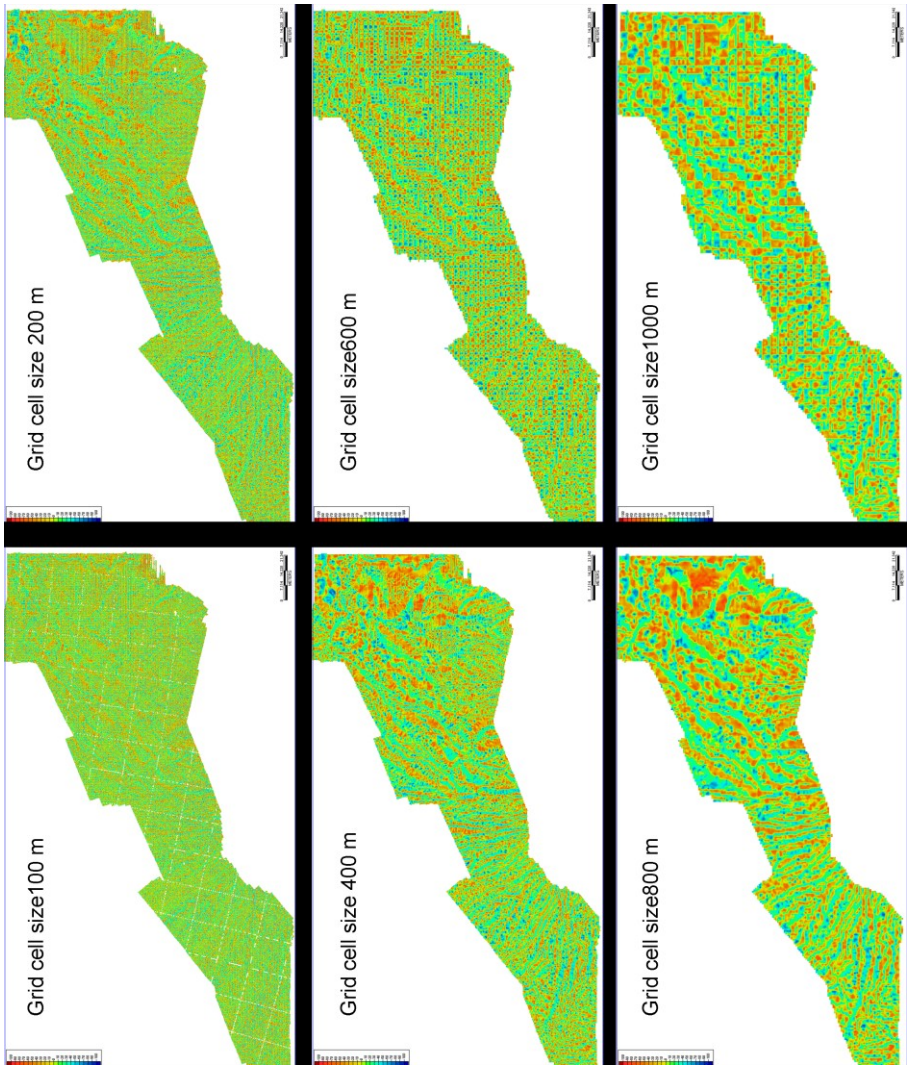
AZIMUTH MAPS



CURVEDNESS MAPS



SHAPE MAPS


Grid cell size 200 m
Grid cell size600 m
Grid cell size1000 m
Grid cell size100 m
Grid cell size 400 m
Grid cell size800 m